University of Alberta

The Role of MUC1/ICAM-1 Interaction in Breast Cancer Cell Motility

by

Qiang Shen 

A thesis submitted to the Faculty of Graduate Studies and Research

in partial fulfillment of the requirements for the degree of

Doctor of Philosophy

Medical Sciences – Laboratory Medicine and Pathology

Edmonton, Alberta
Spring 2007

Your file Votre référence
ISBN: 978-0-494-29741-4
Our file Notre référence
ISBN: 978-0-494-29741-4

Abstract

MUC1, a transmembrane glycoprotein of the mucin family, is normally restricted to the apical surface of mammary epithelial cells (reviewed in [1-3]). However, the apical polarization is frequently lost in breast cancer, substituted by highly overexpressed MUC1 throughout the cytosol or circumferentially around the plasma membrane [4-6]. Clinically, this aberrant expression of MUC1 on breast cancer cells is associated with a poor prognosis and increased lymph node metastases [5]. Previous *in vitro* studies in our laboratory found that MUC1 binds intercellular adhesion molecule-1 (ICAM-1) [7,8], an adhesion molecule present throughout the entire expected migratory track of a transiting tumor cell, and involved in the firm arrest of leukocytes on the vascular endothelium at the site of inflammation and subsequent extravasation [9]. Strengthening the clinical relevance of MUC1, it was demonstrated that the MUC1/ICAM-1 ligation-mediated cell adhesion can withstand the shear stresses equivalent to physical blood flow [10], and the most recent data showed that MUC1, by ligating ICAM-1, also facilitates transendothelial migration (TEM) of MUC1-bearing cells through a monolayer of ICAM-1-expressing cells [11]. These findings suggest a significant role for the MUC1/ICAM-1 ligation in promoting tumor cell migration and extravasation.

The work in this thesis explored the underlying mechanism(s) of the MUC1/ICAM-1 interaction in promoting breast cancer cell migration, and found that (i) MUC1 initiates calcium oscillations after ligation by ICAM-1, and this calcium signaling involves Src family kinase, phosphoinositol 3-kinas (PI3K), and phospholipase C (PLC), but not mitogen activated kinase (MAPK) [12]. (ii) MUC1, by ligating ICAM-1, triggers dramatic actin cytoskeletal rearrangements and rapid formation of motile protrusions

preferentially at the heterotypic cell-cell contact sites. This MUC1-initiated cytoskeletal dynamics are β1 integrin-dependent, and mediated by cascades involving Src family kinase, PI3K, and PLC. Moreover, the MUC1-induced protrusive motility can be abrogated by coexpression of dominant negative Rac1-T17N, Cdc42-T17N, but not by RhoA-T19N. (iii) Also consistant with previous transendothelial migration assays, the MUC1/ICAM-1 ligation potentiates cell invasion. This study provides evidence of a crucial mechanism by which MUC1 may modulate tumor cell motility during breast cancer metastasis.

Acknowledgements

I would like to express my heartfelt thanks to my supervisors, Dr. Judith Hugh and Dr. Andrew Shaw, for all their guidance and patient instruction, which made it possible to accomplish this research project. My appreciation also goes to Dr. Michael Hendzel of my supervisory committee, Dr. Xuejun Sun, and Dr. Jennifer Rahn for their intellectual and moral support on the overall direction of this thesis. Also, I would like to acknowledge Dr. Sandra Gendler and Dr. Ken Dimock for sharing reagents and cell lines, without which this work would not have been possible. I am also grateful to Dr. Gordon Chan, Dr. Roseline Godbout, Dr. Greg Tyrell, Dr. Jason Acker, Ms. Mandy Mah, Dr. Bo Sun, Dr. Jianxun Han, Mr. Jeffrey Chow, Mr. Ming Ye, and Mr. Danny Au for helping me with valuable technical advice and moral support. Last, but not the least, I would like to thank all the academic and non-academic staff in the Department of Laboratory Medicine and Pathology and the Cross Cancer Institute, who have supported me during my graduate program.

Table of Contents

Table of Contents Continued

Table of Contents Continued

Table of Contents Continued

Table of Contents Continued

Table of Contents Continued

List of Tables

List of Figures

List of Figures Continued

List of Figures Continued

List of Figures Continued

List of Abbreviations

2-APB	2-aminoethoxydiphenylborane
3-D	3-dimensional
ABP	Actin binding protein
ACRF	Actin cytoskeletal reorganization factor
ADAM	A disintegrin and metalloprotease
AP	Alkaline phosphatase
APC	Adenomatous polyposis coli
Arp2/3	Actin related protein 2/3
Asn	Asparagine
ATP	Adenosine triphosphate
ATCC	American Type Culture Collection
BCIP	5-Bromo-4-chloro-3-indolyl phosphate
BCR	B cell receptor
bFGF	Basic fibroblast growth factor
BM	Basement membrane
BRCA	Breast Cancer Gene
BSA	Bovine serum albumin
BTP	2% BSA, 0.02% Tween-20 in PBS
Ca^{2+}	Calcium
CaM	Calmodulin
CaMKII	Calmodulin-dependent protein kinase II
CAS	Crk-associated substrate
C_c	Critical concentration
CCK-R	Cholecystokinin-receptor
CBP	CREB binding protein
CD	Cytoplasmic domain
Cdc42	Cell division cycle 42

List of Abbreviations Continued

CICR	Calcium-induced calcium release
CSF	Colony stimulating factor
CTB	Cholera toxin B
CTL	Cytotoxic T lymphocyte
DAPI	Diamidinophenylindole
DCIS	Ductal carcinoma *in situ*
DIC	Differential interference contrast
DMEM	Dulbecco's Modified Eagle Media
DMSO	Dimethyl sulfoxide
ECD	Extracellular domain
ECL	Enhanced chemiluminescence
ECM	Extracellular matrix
EDTA	Ethylenediaminetetraacetic acid
EGF	Epidermal growth factor
EGFP	Enhanced green fluorescent protein
EGFR	Epidermal growth factor receptor
EMA	Epithelial membrane antigen
EMT	Epithelial-mesenchymal transition
EPO-R	Erythropoietin receptor
ER	Endoplasmic reticulum
ERK	Extracellular-signal-regulated kinase
ETA	Epithelial tumor antigen
FAK	Focal adhesion kinase
FAT	Focal adhesion targeting
FBS	Fetal bovine serum
FCB	Flow cytometry buffer
FcγR	Receptor for IgG

List of Abbreviations Continued

FcεR	Receptor for IgE
FERM	Protein 4.1, ezrin, radixin, moesin homology
FITC	Fluorescein isothiocyanate
FMLP-R	Formyl peptide receptor
FRT	Flp recombinase target
Gal	Galactose
GalNAc	N-acetyl galactosamine
GEF	Guanine exchange factor
GlcNAc	N-acetyl glucosamine
GPCR	G-protein coupled receptor
GPI	Glycosylphosphatidylinositol
Grb2	Growth receptor binding protein 2
GSK3β	Glycogen synthase kinase 3 β
HDAC	Histone deacetylase
HGF	Hepatocyte growth factor
HRP	Horseradish peroxidase
ICAM-1	Intercellular adhesion molecule-1
IDC	Invasive ductal carcinoma
IFNγ	Interferon-γ
IGF	Insulin-like growth factor
IGFR	Insulin-like growth factor receptor
IL-1/6	Interleukin-1/6
ILC	Invasive lobular carcinoma
IP3	Inositol (1,4,5) triphosphate
IP3R	Inositol triphosphate receptor
IQGAP1	IQ motif containing GTPase activating protein-1
IRR	Insulin receptor-related receptor

List of Abbreviations Continued

JAM	Junctional adhesion molecule
JNK	Jun N-terminal kinase
LCIS	Lobular carcinoma *in situ*
LEF	Leukocyte enhancer factor
LFA-1	Lymphocyte function-associated antigen-1
LPA-R	Lysophosphatidic acid receptor
Mac-1	Membrane-activated complex-1
MAPK	Mitogen activated protein kinase
MBCD	Methyl-β-cyclodextrin
MCA	Membrane carcinoma antigen
MEA	Membrane epithelial antigen
MH	Mad homology
MLC	Myosin regulatory light chain
MLCK	Myosin light chain kinase
MMP	Matrix metalloprotease
MSG1	Melanocyte-specific gene 1
MT1-MMP	Membrane-type1 matrix metalloprotease
MW	Molecular weight
NBT	Nitro blue tetrazolium chloride
NGFR	Nerve growth factor receptor
NIH	National Institute of Health
PAFR	Platelet-activating factor receptor
PAGE	Polyacrylamide gel electrophoresis
PBS	Phosphate buffered saline
PCNA	Proliferative cell nuclear antigen
PDGF	Platelet derived growth factor
PECAM-1	Platelet endothelial cell adhesion molecule-1

List of Abbreviations Continued

PEM	Polymorphic epithelial mucin
PH	Pleckstrin homology
PI3K	Phosphoinositol 3-kinase
PtdIns(4,5)P2	Phosphoinositol (4,5) diphosphate
PtdIns(3,4,5)P3	Phosphoinositol (3,4,5) triphosphate
PIP5KI	Type I phosphatidylinositol phosphate 5-kinase
PKCδ	Protein kinase Cδ
PLC	Phospholipase C
PP2	3-(-4-chlorephenyl) 1-(1,1-dimethylethyl)-1 H-pyrazolo[3,4-d] pyrinidin-4-amine
PP2A	Protein phosphatase 2A
PUM	Peanut-reactive urinary mucin
Pro	Proline
PTEN	Phosphatase and tensin homology deleted on chromosome 10
Rb	Retinoblastoma
RIPA	Radioimmunoprecipitation assay
ROI	Region of interest
RTK	Receptor tyrosine kinase
RyR	Ryanodine receptor
SBE	Smad binding element
SDS	Sodium dodecyl sulfate
SEA	Sea urchin sperm protein, enterokinase, agrin
Ser	Serine
SH	Src homology
SHC	Src homology 2 domain containing
SHIP	SH2 containing inositol phosphatase
SHP-1/2	Src homology phosphatase-1/2

List of Abbreviations Continued

sLe	Sialylated Lewis antigen
Sos	Son of sevenless
SR	Sarcoplasmic reticulum
STAT	Signal transducer and activator of transcription
SYM	Signal sequence YFP MUC1
TACE	Tumor necrosis factor-alpha converting enzyme
TAE	TGF-β activated element
TBS	Tris-buffered saline
TCF	T-cell specific transcription factor
TCR	T cell receptor
TDLU	Terminal duct lobular unit
TEM	Transendothelial migration
TGF-β	Transforming growth factor-β
TIE	TGF-β inhibitory element
TMD	Transmembrane domain
TNF-α	Tumor necrosis factor-α
Thr	Threonine
TR	Tandem repeat
TβR	TGF-β receptor
Tris-HCl	Trizma hydrochloride
uPA	Urokinase-like plasminogen activator
uPAR	Urokinase-like plasminogen activator receptor
VCAM-1	Vascular cell adhesion molecule-1
VEGF	Vascular endothelial growth factor
VNTR	Variable number of tandem repeats

List of Cell Lines

293T	Human embryonic kidney epithelium
DH5α	E. Coli
Flp-In T-REx 293	293 cells transfected with pFRT/*lac*Zeo and pcDNA6/TR plasmids
Hs578T	Human mammary carcinoma
MCF-7	Human mammary adenocarcinoma; pleural effusion
NIH3T3	Murine embryonic fibroblast
NIH3T3-ICAM-1	NIH3T3 cells transfected with the pBOS-ICAM-1 plasmid
NIH3T3-Mock	NIH3T3 cells transfected with the pBOS plasmid
SYM	293T cells transfected with YFP-MUC1
T47D	Human mammary ductal carcinoma; pleural effusion

List of Antibodies

Antibody	Binding Specificity	Host Species	Detection Concentration	Blockade Concentration	Supplier
B27.29	MUC1-ECD	Mouse	1 μg/ml	N/A	Biomira Inc.
CT2	MUC1-CD	Armenian Hamster	5 μg/ml	N/A	Dr. Sandra Gendler
18E3D	ICAM-1	Mouse	5 μg/ml	20μg/ml	ICOS
164B	ICAM-1	Mouse	5 μg/ml	20μg/ml	ICOS
AP-138	β1 integrin	Mouse	5 μg/ml	20μg/ml	Dr. Andrew Shaw
MOPC 31C	IgG1 isotype control	mouse	5 μg/ml	60-120μg/ml	Sigma Aldrich
B-5-1-2	tubulin	mouse	5 μg/ml	N/A	Sigma Aldrich
GD11	c-Src	mouse	5 μg/ml	N/A	Upstate
anti-MAPK	MAPK	mouse (polyclonal)	5 μg/ml	N/A	Sigma Aldrich

Chapter 1: Introduction

1.0. Thesis Overview

Breast cancer is the most frequently diagnosed malignancy and the second leading cause of cancer deaths in Canadian women with an expected mortality of 5,300 in 2006 [13]. The development of metastases in distant vital organs such as lungs, brain, and liver, is the principle cause of death from breast cancer [14-16]. Metastasis requires increased cell motility, which is a tightly orchestrated process of numerous molecular events with the dynamic reorganization of the actin cytoskeleton playing a decisive role [17-20]. Thus, clarifying the mechanism(s) underlying the aberrantly activated pro-migratory signaling and cytoskeletal rearrangements in tumor cells may allow the development of effective therapeutic strategies to reduce breast cancer mortality.

The MUC1 transmembrane glycoprotein was initially cloned from mammary and pancreatic carcinomas as a tumor antigen [21-23]. In the breast, histopathologic studies found that this mucin, which is normally restricted to the apical surface of mammary epithelium [1,2,4,24], is aberrantly overexpressed in most breast cancers [4,5,25-27]. Clinically, this aberrant expression of MUC1 on breast cancer cells is correlated with a poor prognosis and increased lymph node metastases [5]. As MUC1 contains a long, rigid and negatively charged extracellular domain (200-500nm, compared with 10-50nm for the remainder of the glycocalyx [24,27-30]), it has been suggested that MUC1 contributes to tumor progression by functioning as an anti-adhesive molecule, sterically interfering with E-cadherin and integrin mediated cell-cell and cell-matrix interactions, thereby facilitating dissemination of tumor cells from the primary lesion [27,31-34]. However, despite the anti-adhesive theory about MUC1, our laboratory was the first to demonstrate that MUC1 also has a pro-adhesive function and mediates heterotypic cell-

cell adhesion by binding ICAM-1 on adjacent accessory cells [7,8]. This MUC1/ICAM-1 interaction has since been confirmed by other laboratories [35-37]. Supporting the clinical significance of MUC1 in tumor progression, it was found that underglycosylated MUC1, simulating the variant found in tumors, showed an increased binding propensity for ICAM-1 [36], and this MUC1/ICAM-1 interaction was capable of withstanding the shear stresses equivalent to physiologic blood flow [10]. Most recently, the *in vitro* transwell studies by Rahn et al. [11,38] have shown that MUC1 promotes transendothelial migration (TEM) of breast cancer cells through a monolayer of ICAM-1-expressing cells, indicating MUC1 may not only function as an adhesion molecule, but also promote cell migration by ligating ICAM-1.

Existing evidence in the literature suggests that MUC1 may actively participate in pro-migratory signaling. This includes reports which indicate that MUC1 localizes in lipid rafts and is concentrated at the leading edge of migrating cells [39-41] and MUC1's cytoplasmic domain (CD) co-distributes with ezrin, a known linker of membrane proteins to the actin cytoskeleton [42]. Moreover, MUC1-CD contains seven highly conserved tyrosine (Tyr) residues, four of which are confirmed phosphorylation sites and construct potential binding motifs for PI3K, PLCγ, Src and Grb2 [43,44], all of which are critical for cell motility. The present thesis study explored the underlying mechanisms of MUC1/ICAM-1 ligation-mediated cell motility. We examined the potential role of MUC1 in (i) pro-migratory signaling, (ii) cytoskeletal rearrangements and (iii) cell invasive motility in response to ICAM-1 stimulaiton.

Results provided in this study demonstrated that the MUC1/ICAM-1 interaction initiates calcium oscillations, which are mediated by pathways involving a Src family

kinase, PI3K, PLC, but not MAPK [12], and are accompanied by redistribution of Src into lipid rafts and increased association of Src with MUC1. Additionally, we found MUC1 induces β1 integrin-dependent cytoskeletal rearrangements and protrusive motility; abolition of Src family kinase, PI3K, and PLC activities could also reduce this cytoskeletal migratory responses. Further, we demonstrated that the MUC1-induced cytoskeletal rearrangements require Rho family GTPases Rac1, Cdc42, but not RhoA. Lastly, MUC1/ICAM-1 interaction-potentiated cell invasion was demonstrated in a novel transmigration model. These data offer functional evidence that implicates MUC1 overexpression as a key molecular event in the aggressive tumor phenotype, and provides an insight into the mechanisms tumor cells may utilize to facilitate cell metastasis.

1.1. Breast Cancer and Metastasis

1.1.1. Structure and Development of the Mammary Gland

The mammary gland is a structurally dynamic organ, varying with age, menstrual and reproductive status. It begins to develop in the embryo from the sixth week of conception, as an epidermal thickening or "mammary ridge" on both sides of the anterior thoracic region. This undergoes sequential branching divisions with the formation of fundamental ducts by the end of gestation [45-47]. The mammary gland is comprised of various cell types, including epithelial cells and stromal cells which include fibroblasts, adipocytes and endothelial cells. The epithethial bilayer of luminal epithelial and basal myoepithelial cells forms a network of lobuloaveolar architecture that branches its way through the collagen-enriched stromal scaffold of the mammary gland fat pad [46,48] (Fig. 1.1 A and B). The luminal epithelial cells form a continuous lining of the

lactiferous duct, interlobular ducts and intralobular ducts, that end in a collection of spherical secretory units referred to as acini or alveoli [46,49].

At the time of puberty, the female breast increases in size mainly due to the deposition of interlobular fat. Also, under the influence of ovarian estrogen (E2) in each menstrual cycle, the mammary epithelium proliferates and branches into multiple ducts with terminal alveoli, known as terminal ductal lobular units (TDLU) [48,50]. The mammary gland experiences the most rapid phase of proliferation at the time of pregnancy, when the level of estrogen is increased and directly results in ductal elongation [48,51]. Placental-derived progesterone induces ductal side branching and pituitary-derived prolactin initiates alveolar development [51]. These hormonal stimuli not only lead to the epithelial expansion of pre-existing alveoli, but also confer the secretory capacity of the gland. After parturition, the mammary gland starts to lose its sensitivity to E2 [50]. With the onset of menopause and the fall of circulating ovarian hormones, the mammary gland starts to involute resulting in the degeneration of ductal elements and the replacement by connective tissue [50,52].

1.1.2. Background Knowledge of Breast Cancer

1.1.2.1. Molecular Basis of Breast Carcinogenesis

Breast carcinoma is an epithelial-derived malignancy thought to arise through a multi-step process with sequential accumulation of distinct mutations in genes or disregulation of hormones and growth factor signaling pathways [53-57]. Hereditary breast cancer (5-10% of all breast cancer) is characterized by inherited genetic mutations, in specific genes such as BRCA1, BRCA2, p53 or PTEN [53,55,56,58,59]. Inherited mutations leading to BRCA1 inactivation are correlated with a lifetime risk of 55-85%

for breast cancer development. The normal BRCA1 protein is implicated in repair mechanisms of DNA double-strand breaks, as well as in cell cycle control involving dephosphorylation of the retinoblastoma (Rb) protein and in the transcriptional regulation of tumor suppressor proteins, p53 and p21 [60,61]. Thus, mutations in BRCA1 may result in release of cell cycle control and compromise the repair of accumulated genetic muations that ultimately lead to oncogenic transformation. Sporadic breast cancers are thought to occur from the accumulation of acquired mutations in somatic genes. Mutational activation and/or amplification of oncogenes (e.g. c-Myc, Cyclin D1, and ErbB-2) has been reported to play a critical role in early sporadic tumorigenesis [62-64]. This is frequently accompanied by non-mutational/functional inactivation of tumor suppressor genes (e.g. BRCA1) through epigenetic regulation [65,66].

Breast carcinogenesis also involves growth factor signaling, including epidermal growth factor (EGF), transforming growth factor-β (TGF-β), insulin-like growth factor (IGF), and hepatocyte growth factor (HGF). These normally contribute to the ductal-lobuloaveolar development of the mammary gland. However, when abnormally activated, they are frequently implicated in tumor cell proliferation, epithelial-mesenchymal transition (EMT), and anti-apoptotic properties [67-70]. The relationship between growth factor signaling in breast oncogenic transformation and progression is proving to be incredibly complex at the molecular level.

Recently, with advances in understanding the biological nature of breast cancer, the mucin family glycoproteins also appear to be tumorigenic in cellular growth, immune surveillance, adhesion, and invasion [71]. As the fundamental member of this family, MUC1 and its structure and function will be introduced in section 1.2.

1.1.2.2. Breast Cancer Progression and Metastatsis

Breast cancer originates in the epithelial cells of the ducts (ductal carcinoma) or lobules (lobular carcinoma). Carcinoma ***in situ*** refers to cancers where the abnormal proliferation of tumor cells stay confined to ducts (DCIS) or lobules (LCIS), and have not penetrated the basement membrane (BM) (Fig. 1.1 C and D) [72,73]. As *in situ* carcinoma progresses, the tumor cells break through the BM and invade the surrounding stromal tissue. The cancers at this stage are referred to as **invasive** ductal carcinoma (IDC) or invasive lobular carcinoma (ILC) (Fig. 1.1 E and F) [72,73]. IDC is the most common (~80%) form of breast cancer. Clinically, it is a poorly defined mass of stony consistency. Microscopically, this is represented by round to polygonal tumor cells which form nests or cords scattered widely in dense fibrous stroma [72,74]. ILC, which accounts for ~15% of invasive breast cancers, is characterized by small, uniform tumor cells with little cytoplasm, often containing intracytoplasmic mucinous vacuoles [72,74]. Subsequently, the tumor cells can spread through the blood/lymphatic-circulatory systems to distant vital organs, called **metastasis**. The excessive growth of tumor cells at the secondary sites, such as brain, liver, bone and lungs, generally causes functional failure and results in mortality [75-77].

1.1.3. Metastasis and Cell Motility

1.1.3.1. Overview of Metastatic Cascade

Metastasis of tumor cells to distant sites is a complex, multi-step consequence of tumor progression (Fig. 1.2). The "Metastatic cascade" can be described as a series of events: (1) detaching from the primary tumor mass; (2) penetrating the BM and invading

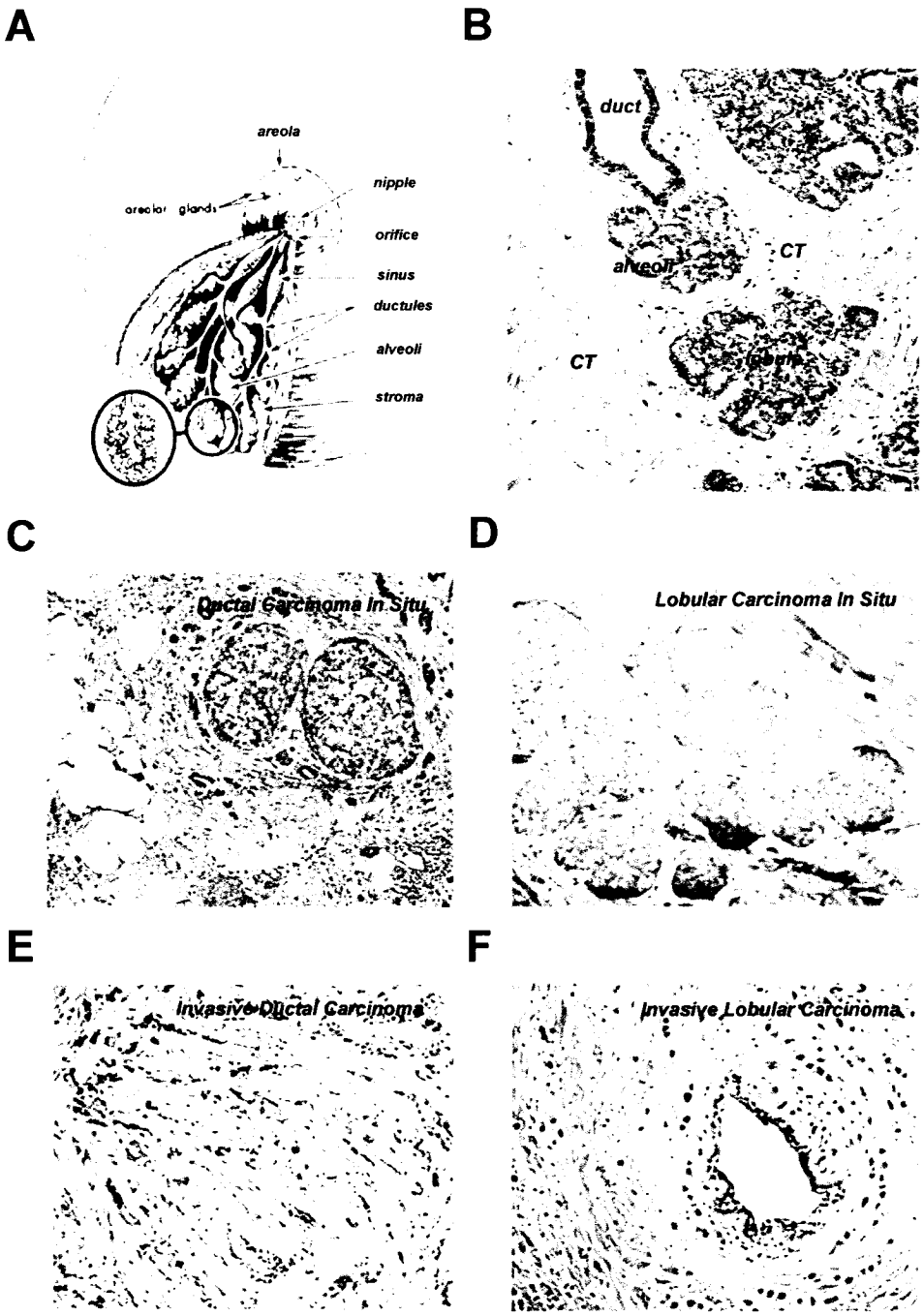

Figure 1.1: The normal mammary gland and breast carcinoma subtypes. (A) Normal breast architecture. The pathological microscopic images of (B) normal mammary gland, (C) ductal carcinoma in situ, (D) lobular carcinoma in situ, (E) invasive ductal carcinoma, and (F) invasive lobular carcinoma. Adapted from http://www.ucihs.uci.edu/anatomy CT – connective tissue stroma

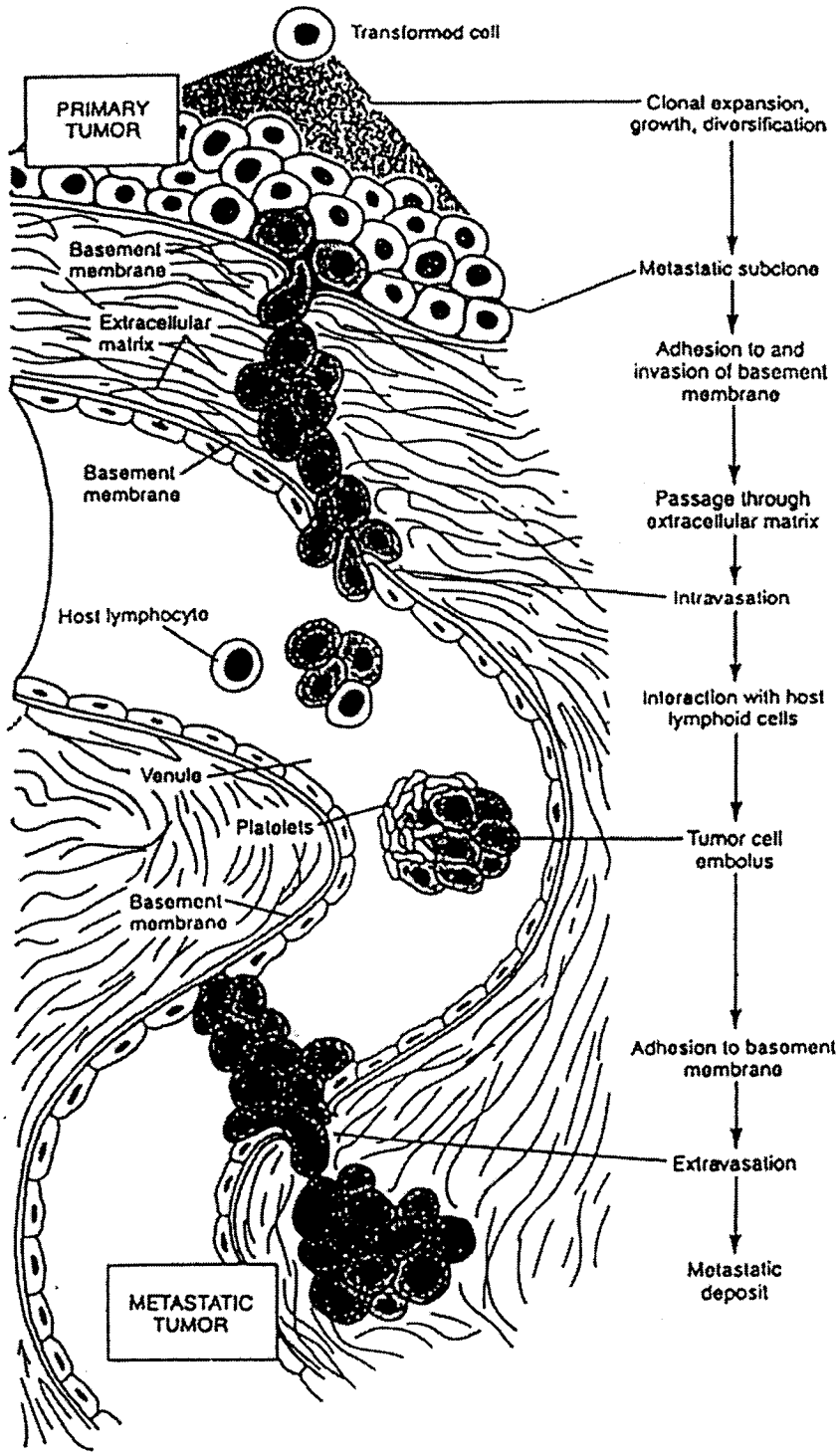

Figure 1.2: The cascade of blood-borne metastasis. Adapted from [78]

the surrounding stroma; (3) intravasation, transportation in the vascular system, and evasion of the host immune surveillance; (4) Attachment to the vascular endothelium of target organs and extravasation; (5) establishment of new growth. Each step in this cascade is rate-limiting, and failure of completing any of these steps will prevent a tumor cell from producing a metastasis.

The first two steps, of detaching from the original site of growth and invading the surrounding stroma, are effectively one process characterized by cellular movement. It is generally an active cell migration in response to motility factors, and is partially assisted by passive cell translocation due to the rapid tumor growth-augmented mechanical pressures [79,80]. In some epithelial-derived tumors including invasive lobular carcinoma of the breast, downregulation of the cellular adhesion molecule E-cadherin is frequently observed and leads to reduced cell-cell adherent junctions, thereby facilitating tumor cell scattering [81,82]. These early stages of carcinogenesis are also usually accompanied by active expression of proteases, such as matrix metalloproteases (MMPs) and urokinase-type plasminogen activator (uPA), which not only degrade the BM and stromal extracellular matrix (ECM) but also cleave and activate cytokines/growth factors (e.g. HGF and TGF-β) to promote tumor cell invasion and migration [83-86]. The requirement for augmented blood supply increases in parallel with tumor growth and progression. Angiogenesis occurs in the early stages of carcinogenesis in response to vascular endothelial growth factor (VEGF) and basic fibroblast growth factor (bFGF) produced by the tumor or stromal cells [87]. However, when compared to normal vessels, this tumor-induced neovasculature possesses a more fenestrated endothelium [88]. Thus, they are more permeable and possibly more susceptible to tumor cell intravasation. Upon

penetrating the blood-lymphatic vasculature wall, it is estimated that less than 0.1% tumor cells can survive this process of transport due to the mechanical trauma, anoikis, and immune attack by natural killer cells or cytotoxic T lymphocytes (CTL) [78,89,90]. One of the mechanism(s) that tumor cells may utilize to evade these attacks is to increase the sialylation and fucosylation of the carbohydrates on cell membrane, masking surface antigens and enhancing the survival rate for subsequent arrest at the target organs [90].

Metastatic breast cancer cells exhibit a preferential pattern of metastases and tend to metastasize to specific organs, such as liver, lung, bone and brain [14-16]. However, the mechanism(s) underlying this bias is still largely unkown. Several theories have been put forward to elucidate this phenomenon. The classical "seed and soil" theory in Stephen Paget's 1889 proposal, suggests that although the same amount of tumor cells are carried within the circulating system to all organs, they proliferate only in those organs providing the appropriate microenviroment [89,91]. Alternatively, there is the "chemoattraction" theory based on the pleiotropic effects of chemoattractants. Müller *et al.* (2001) demonstrated that surface expression of the chemokine receptor CXCR4 was upregulated in most breast malignancies, and correspondingly, its chemokine ligand-CXCL12 was also synthesized at high levels at the preferential metastatic sites, such as lung, liver, and bone marrow [91,92]. Thus, it is possible that the circulating breast cancer cells will be attracted and arrested when they are passing through these organs, so that the distribution of chemokines in different organs will determine the relative risk of tumor metastasis. Another widely accepted theory is that, the development of firm adhesion and subsequent extravasation of tumor cells requires the expression of adhesion molecules by vascular endothelial cells [91,93]. In this model, the mechanisms involved

in tumor cell metastatic extravasation seem to be comparable with those for leukocyte extravasation during inflammation [78,94] (Fig. 1.3).

Inflammation-triggered leukocyte extravasation is characterized by successive formation and breakage of heterotypic cell-cell interactions between leukocytes and endothelial cells lining the blood vessel [94,95]. Briefly, in respose to inflammatory signals, endothelial cells upregulate E-selectin on their luminal surface, which can subsequently "trap" circulating leukocytes by binding to sialylated Lewis ($sLe^{a/x}$) carbohydrate-containing ligands on leukocytes [9,94,95]. Since this interaction is weak, the leukocyte appears to roll along the endothelium. During this process, the leukocyte β2-integrins (LFA-1 and Mac-1) become activated and then bind endothelial adhesion molecule ICAM-1, resulting in firm adhesion of leukocytes to the endothelium [9,94-96]. The leukocytes are preferentially arrested at the tri-endothelial cellular junctions. This is followed by cell spreading, invadopodia formation, and crawling through the endothelium, i.e. transendothelial migration [94,97,98].

Parallel to the leukocyte extravasation, compelling evidence suggests that the tumor cell starts the extravasation process by initially binding to the endothelium [93,99]. Further, it was found that several of endothelial adhesion molecules (e.g. E-selectin, integrins and ICAM-1), involved in the adhesion of leukocyte, have been implicated in the interactions with tumor cells [93], and agents that inhibit inflammation also abrogated tumor metastasis [100-102]. Particularly noteworthy is that MUC1 may initiate tumor cell adhesion to the activated endothelium through the MUC1 O-glycan side chain $sLe^{a/x}$ antigens [103,104], which are known to bind endothelial selectins and are implicated in leukocyte extravasation. Previous studies in our laboratory have demonstrated that

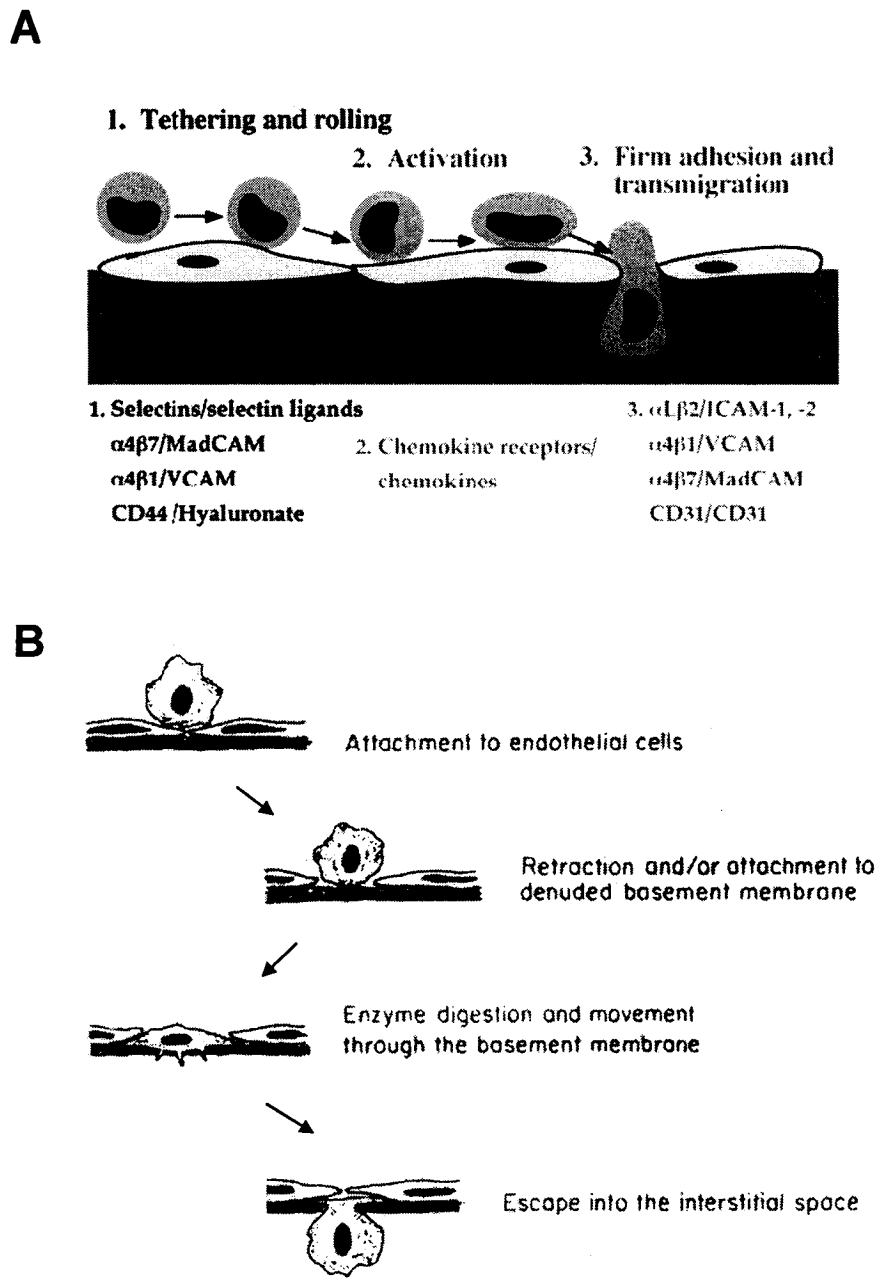

Figure 1.3: Tumor cells are analogous to leukocytes in the process of extravasation. (A) Leukocyte extravasation into sites of inflammation is a multiple-step process mediated by a variety of intercellular adhesion molecules. Adapted from [94] (B) The tumor cell exhibits similarities to the leukocyte in the process of extravasation. Adapted from [78]

MUC1 binds the endothelial ICAM-1 [7,8,10], which subsequently results in increased tumor cell transendothelial migration [105] (see details in section 1.2). These findings strongly suggest that tumor cells may utilize the mechanisms of leukocyte transendothelial migration for metastatic spread.

1.1.3.2. Cell Migration: Orchestrated Molecular Events

Metastasis requires increased cell motility, which is a tightly orchestrated process of multiple molecular events, resulting in attachment at the leading edge, cytoskeletal protrusive motility, cellular contraction, and detachment at the rear [18,106]. Of the numerous molecules involved in cell migration, the Src non-receptor tyrosine kinase family is a particularly crucial one, and has been implicated in the signals downstream of a variety of transmembrane receptors including integrins (Table 1.1) [18,107].

Integrins are transmembrane heterodimeric receptors composed of non-covalently associated α and β subunits [95]. Depending on the combination of the α and β subunits, integrins can bind different components present in the ECM (Table 1.2) [95,108,109]. These interactions not only mediate cell adhesion by constructing **focal contacts** but also recruit Src to the plasma membrane, which together with focal adhesion kinase (FAK) form a "dual-activated Src-FAK signaling complex" (Fig. 1.4) [18]. Within this complex, the preferential binding of the Src SH2 domain to the autophosphorylated Tyr-397 site on FAK releases the intramolecular inhibition of Src and leads to Src activation [18,107]. Thus, Src can further phosphorylate the FAK Tyr-861 and FAK-associated p130CAS and/or paxillin, which sequentially recruit the scaffolding protein Crk to activate the Rho-family GTPases (e.g. Rac1, Cdc42), resulting in dramatic membrane lamellipodial and/or filopodial **protrusions** [18,107,110,111]. Since the signaling mediators p130CAS,

Table 1.1: Signaling substrates and activating receptors for Src.

Src signaling substrates	Src-activating receptors
Focal contact and structural proteins	
FAK	Integrins, PDGFR, IGFR, EGFR, NGFR, FcεRI, bombesin-R, thrombin-R, bradykinin-R, endothelin-R, LPA-R, CCK-R, FMLP-R, gastrin-R, c-Met
paxillin	Integrins, PDGFR, IGFR, NGFR, bombesin-R, PAFR, ICAM, bradykinin-R, FMLP-R, gastrin-R, endothelin-R, CCK-R, IL-3-R
p130CAS	Integrins, NGFR, c-Met, bradykinin-R, IL-8-R
talin	Thrombin-R, PDGFR
ezrin	Integrins, c-Met, CD4, TCR
catenins (β, γ and p120)	CSF-1R, EGFR, PDGFR, c-Met
connexin	PDGFR
caveolin	IGFR
tubulin	TCR, NGFR
Protein tyrosine/serine/threonine kinases	
Syk/ZAP	IRRs, integrins, muscarinic-R, IL-2-R,
FAK	Same as above
PKCδ	PDGFR, EGFR, FcεRI
Enzymes involved in phospholipid metabolism	
PLC-γ	NGFR, PDGFR, EGFR
p85-PI3K	RTKs, thrombin-R, Integrins, IRRs, MUC1
SHIP	FcγRI, BCR, CSF-R
Phosphatases	
SHP-1/2	Thrombin-R, NGFR, IGFR, PDGFR, EGFR, prolactin-R
PP2A	EGFR
Small GTP-regulatory enzyme	
$p190^{RhoGAP}$	RTKs, FcγRIIIA, BCR, TCR
$p120^{RasGAP}$	RTKs, EGFR, EPO-R, prolactin-R
Scaffold proteins	
Shc	RTKs, Class I cytokine-receptors, IRRs, CD4, GiPCRs
Cbl	TCR, BCR, EGFR, FcRs

Aapted from [18,107,112]

Table 1.2: Integrin family glycoproteins and their affinities for ECM ligands.

Integrins		Extracellular Matrix (ECM) Ligands	Binding sites
β1	α1	Native collagen, laminin	
	α2	Native collagen, laminin	DGEA
	α3	Fibronectin, laminin, native collagen	
	α4	Fibronectin (splicing domain)	EILDV
	α5	Fibronectin (RGD-containing domain)	RGD
	α6	Laminin	
	α7	Laminin	
	α8	Fibronectin, vitronectin	RGD
	α9	Tenascin	
	α10	Collagen	
	α11	Collagen	
	αv	Vitronectin, fibronectin, osteopontin	
β2	αL	ICAM-1, ICAM-2, ICAM-3	
	αM	C3b, fibrinogen, ICAM-1, VCAM-1	
	αX	C3b, fibrinogen	
	αD	ICAM-3, VCAM-1	
β3	αIIb	Fibrinogen, fibronectin, von Willebrand factor, vitronectin, thrombospondin	RGD KQAGDV
	αv	Vitronectin, denatured collagen, von Willebrand factor, fibrinogen, thrombospondin, fibulin, osteopontin	RGD
β4	α6	Laminin, desmin	
β5	αv	Vitronectin	
β6	αv	Fibronectin	
β7	α4	Fibronectin (splicing domain), VCAM-1, MAdCAM-1	EILDV
β8	αE	E-cadherin	
	αv	Vitronectin	RGD

Adapted from [95,108,109]

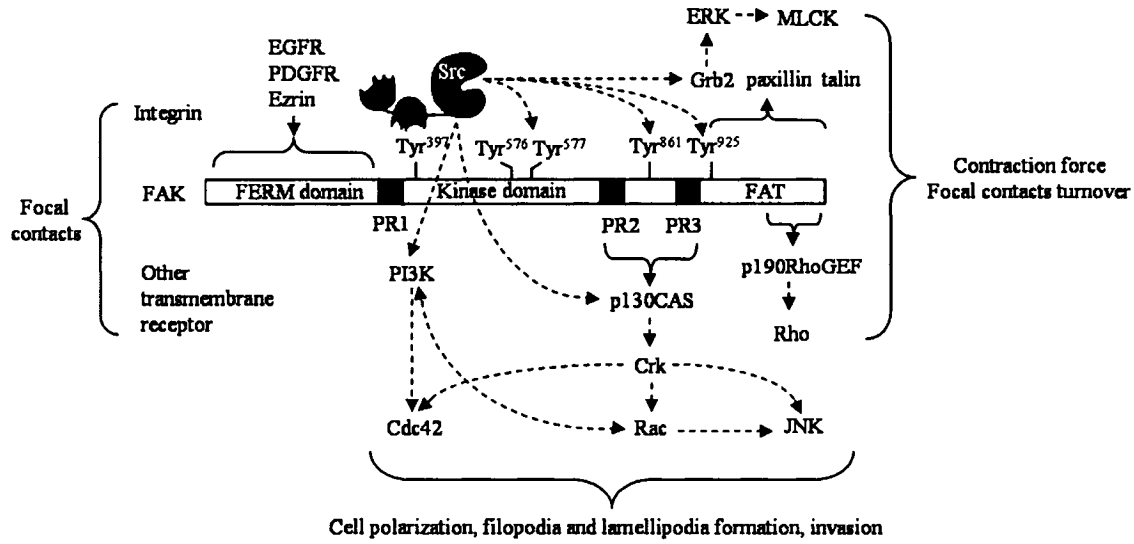

Figure 1.4: Src-FAK signaling complex orchestrated migratory signaling.
Structurally, Src is composed of an N-terminal SH3 domain, a central SH2 domain, and a C-terminal tyrosine kinase domain. FAK consists of an N-terminal FERM domain, a central kinase domain, proline-rich (PR2/PR3) regions and a C-terminal FAT domain. Major tyrosine phosphorylation sites, binding partners and initiated signaling cascades are indicated. Functionally, in response to newly formed focal contacts or growth factor stimulation, Src can form a signaling complex with FAK (i) to initiate cell polarization and membrane protrusion through PI3K and p130CAS/Crk/Dock180/Rac-Cdc42 cascades; (ii) to promote cell invasion through p130CAS/Crk/Rac/JNK cascade; and (iii) to promote cell movement and focal contact turnover through the p190RhoGEF/Rho cascade, Grb2/ERK/MLCK and calpain cascades. Collectively, the Src-FAK complex can co-ordinately initiate cell migration. Based on [18,95,107,111,113-115].

paxillin, and p85-PI3K also contain SH3 domain binding motifs, Src may recruit these molecules directly to its SH3 domain and activate these mediators to initiate cell protrusive motility through PI3K or p130CAS-paxillin/Crk/Dock/Rac1-Cdc42 cascades [107,115]. In addition, Src can phosphorylate FAK at Tyr-925 to create a SH2-domain binding site for Grb2, which in turn activates the Ras/ERK cascade to initiate cell-ECM dissociation and **cellular contraction** through the activation of myosin light chain kinase (MLCK)/myosin light chain (MLC)/myosin cascade [18,95,114]. The Src-FAK signaling-induced **focal contact turnover** is primarily mediated by the ERK cascade. ERK activation at matured focal contacts promotes FAK phosphorylation at Ser-910, which results in decreased paxillin binding to FAK and focal contact disassembly [113]. Also, the ERK cascade can promote focal contact turnover through upregulation of both extracellular (MMPs) and intracellular (calpain) protease activities [18,113], which can degrade the ECM adhesive components and intracellular FAK respectively.

Collectively, cell migration can be described as a spatial-temporally coordinated cyclical event, which is precisely regulated in normal cells but frequently dysregulated in tumor cells. In breast cancers, there is increased Src activity and this is associated with tumor metastasis [116,117]. Since Src oncogenic mutations are seldomly observed in breast cancers [117], exploring the mechanism(s) that activate Src so as to increase the motility of breast cancer cells is significant.

1.1.3.3. Calcium Related Signaling and Cell Motility

Cell motility depends mainly on directional actin cytoskeletal rearrangements [106,118]. Intensive studies over the past decade suggest that calcium (Ca^{2+}) and Ca^{2+}-related signaling play crucial roles in the cytoskeletal "treadmilling" dynamics and the

subsequent cell migration [95,119,120] (Fig. 1.5). For instance, normal migrating cells, such as leukocytes and immature neurons, migrate in a Ca^{2+} sensitive manner [121,122]. The presence of the Ca^{2+} oscillation is mandatory [122,123] and the frequency of oscillations is directly related to the rate of cellular migration [121].

Intracellular Ca^{2+} signaling initiated by transmembrane receptors (e.g. RTKs, GPCRs, and integrins) is generally mediated via PI3K and PLC. PI3K, which is frequently activated in lipid rafts [124,125], can phosphorylate inositol on the D3-position of phosphoinositides to generate PtdIns(3,4)P2 and PtdIns(3,4,5)P3, providing docking sites to activate the pleckstrin homology (PH) domain-containing proteins, such as PLC [126,127].

In resting cells, the actin cytoskeleton is usually in a steady state characterized by a dynamic equilibrium between globular-actin (G-actin) polymerization at the barbed (+) end and depolymerization at the pointed (-) end of actin filaments (F-actin) [95]. Generally, the physiological concentration of free G-actin is above the critical concentration (C_c, 0.1μM) and favors polymerization [95]. One of the mechanisms by which the cells retain this balance is through the presence of the actin binding protein (ABP) thymosin-β_4, which binds to the free G-actins and prevents them from adding to the barbed end of F-actins [95]. However, upon activation of PLC by upstream signaling, it can hydrolyze PtdIns(4,5)P2 and release profilin into the cytosol, where profilin can sequentially displace thymosin-β_4, facilitate G-actin ADP/ATP exchange and incorporate G-actin to the barbed end of F-actin through binding to the proline rich proteins at the leading edge of the cells [95,120]. Further, following PLC activation, the PtdIns(4,5)P2-bound gelsolin and cofilin will also be released from membrane. These proteins can

sever the F-actin and cap the newly created barbed end, at the cleavage sites, to promote depolymerization of F-actin from the pointed end [95,120]. As a result, the cyotosolic concentration of free G-actin is increased, resulting in directional actin polymerization and membrane protrusion at the leading edge [95,120].

The actin cytoskeleton "treadmilling" process can be extensively enhanced by Ca^{2+} signals. The inositol (1,4,5) triphosphate (IP3), generated by PLC-mediated cleavage of PtdIns(4,5)P2, can induce intracellular Ca^{2+} release through activation of the IP3R on the endoplasmic reticulum (ER), which usually appears as Ca^{2+} oscillations with a 20-30 seconds period [128,129]. The Ca^{2+} flux can directly activate gelsolin, thereby inducing directional actin cytoskeletal rearrangements [95,130]. Moreover, increased intracellular Ca^{2+} concentration facilitates its binding to calmodulin (CaM) to form a Ca^{2+}/CaM complex, which can directly activate calmodulin-dependent protein kinase II (CaMKII) or MLCK to phosphorylate MLC so as to promote myosin-mediated cellular contraction [95,131,132]. Furthermore, it was reported that Ca^{2+} can also activate calpain, a Ca^{2+} sensitive protease, which can digest the intracellular components of focal contacts (e.g. FAK and talin) to release the anchors of cells [18,133]. Particularly noteworthy is a significant finding by Brundage *et al.* showing that migrating cells exhibit a cytosolic Ca^{2+} gradient with the lower concentration at the leading edge and higher concentration at the rear [134]. This suggests that gelsolin-mediated actin cytoskeleton depolymerization, myosin-induced cellular contraction, as well as calpain-mediated focal contacts dissembly may preferentially occur at the rear of migrating cell, with the actin cytoskeletal polymerization and focal contact formation preferentially taking place at the leading edge. Thus, polarized cell motility can be enhanced by Ca^{2+}

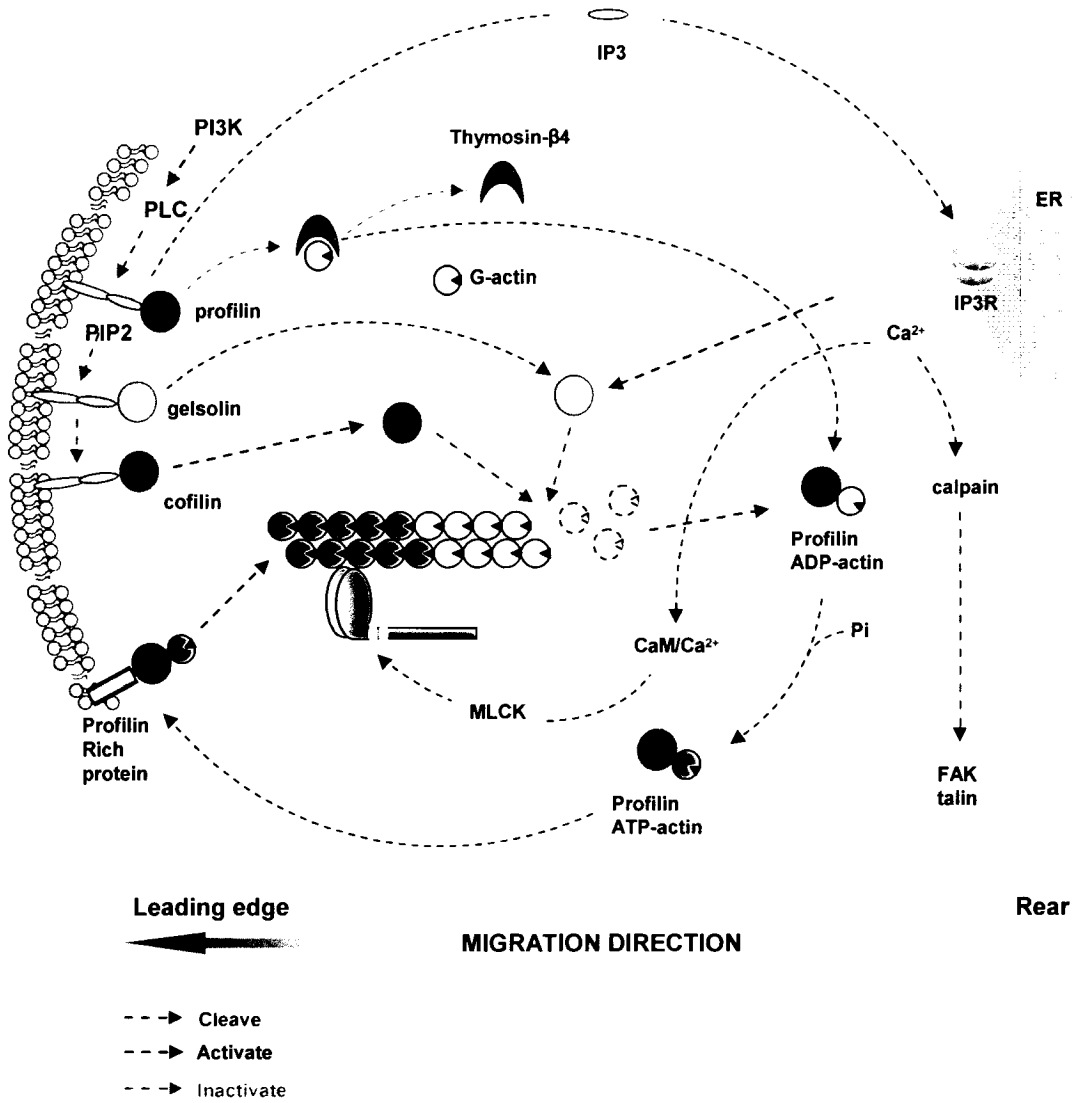

Figure 1.5: Actin cytoskeleton treadmilling regulated by PLC and Ca^{2+} signaling.
Based on [18,95,120]

and Ca^{2+}-based signals.

1.1.3.4. Protrusive Machinery and Cell Migration

As described above, the polarized actin cytoskeletal rearrangements result directly in membrane protrusions. However, for cell migration to occur, cells generally organize their protrusive actin filaments into different constructions: **lamellipodia** and **filopodia**. Lamellipodia appear as thin, but broad "brush-like" membrane projections, which push forward along the edge of plasma membrane and provide the basis for directional migration [135]. Structurally, lamellipodia are branched "dendritic" networks of actin filaments, characterized by Arp2/3 complex-mediated actin polymerization [136]. The Arp2/3 complex consists of two actin-related proteins, Arp2 and Arp3, along with five other small proteins. When activated by WAVE/WASP family members on the membrane, the Arp2/3 complexes bind to the sides or tip of an existing actin filament and nucleate assembly of new actin filaments that branch off the parental filament, with their barbed ends oriented toward the plasma membrane [135,136]. The actin cross-linking proteins, cortactin and actinin, by stabilizing the branches and actin filaments are also implicated in the dendritic system [135,136]. In contrast to lamellipodia, filopodia (also called microspikes) are organized as bundles of parallel actin filaments and reinforced by fascin-mediated cross-linking, appearing as long thin processes that extend out from the plasma membrane [95,136]. Filopodial protrusions are thought to develop through an actin filament treadmilling mechanism, characterized by actin polymerizing preferentially at barbed ends of F-actin, without dentritic branches [136]. Previous studies suggest critical roles for Ena/Vasp proteins in this process, where they can bind barbed ends of F-actin to prevent both actin filament capping and branching [136].

Rho family GTPases are central regulators of actin cytoskeleton lamellipodial and filopodial protrusions [137] (Fig. 1.6). Of the Rho family members, Rac1, Cdc42 and RhoA are the most thoroughly understood ones. They function as "molecular switches", depending on their active GTP-bound or the inactive GDP-bound status, to control the cellular protrusive mechinery [137,138]. The WAVE/WASP family of Arp2/3 complex activators are the major substrates for Rac and Cdc42 [136,139]. Thus, when activated to a GTP-bound state, Rac can initiate lamellipodial protrusive motility through the Scar/WAVE/Arp2/3 cascade [139], whereas Cdc42 can induce filopodia via the N-WASP cascade [139-141]. Although this paradigm has been challenged by recent studies showing that cells without WASP successfully formed filopodia and WAVE was also found to be localized in filopodia [142,143], the decisive role of Rho family GTPase in cell protrusive motility is entrenched.

Notably, in response to migratory cues, PI3K is instantly polarized and activated at the leading edge [125,144,145], which generally leads to the activation of Rho family GTPases, Rac and Cdc42, at the leading edge through the PI3K product PtdIns(3,4,5)P3 [145,146]. This may be triggered by guanine exchange factor (GEF) mediated GTP-loading on Rac and Cdc42, since all of Dbl family GEFs, such as Tiam and Vav2, contain PH domains and can be recruited to the PI3K activation sites by targeting PtdIns(3,4,5)P3 [147,148]. Moreover, activation of PI3K, Rac and Cdc42 at the leading edge is implicated in the exclusion of RhoA and the PtdIns(3,4,5)P3 phosphatase PTEN from protrusions [106,149]. Although the mechanism underlying the negative feedback loop is still elusive, this polarized distribution of Rac, Cdc42, and RhoA may facilitate synchronizing directional protrusive motility.

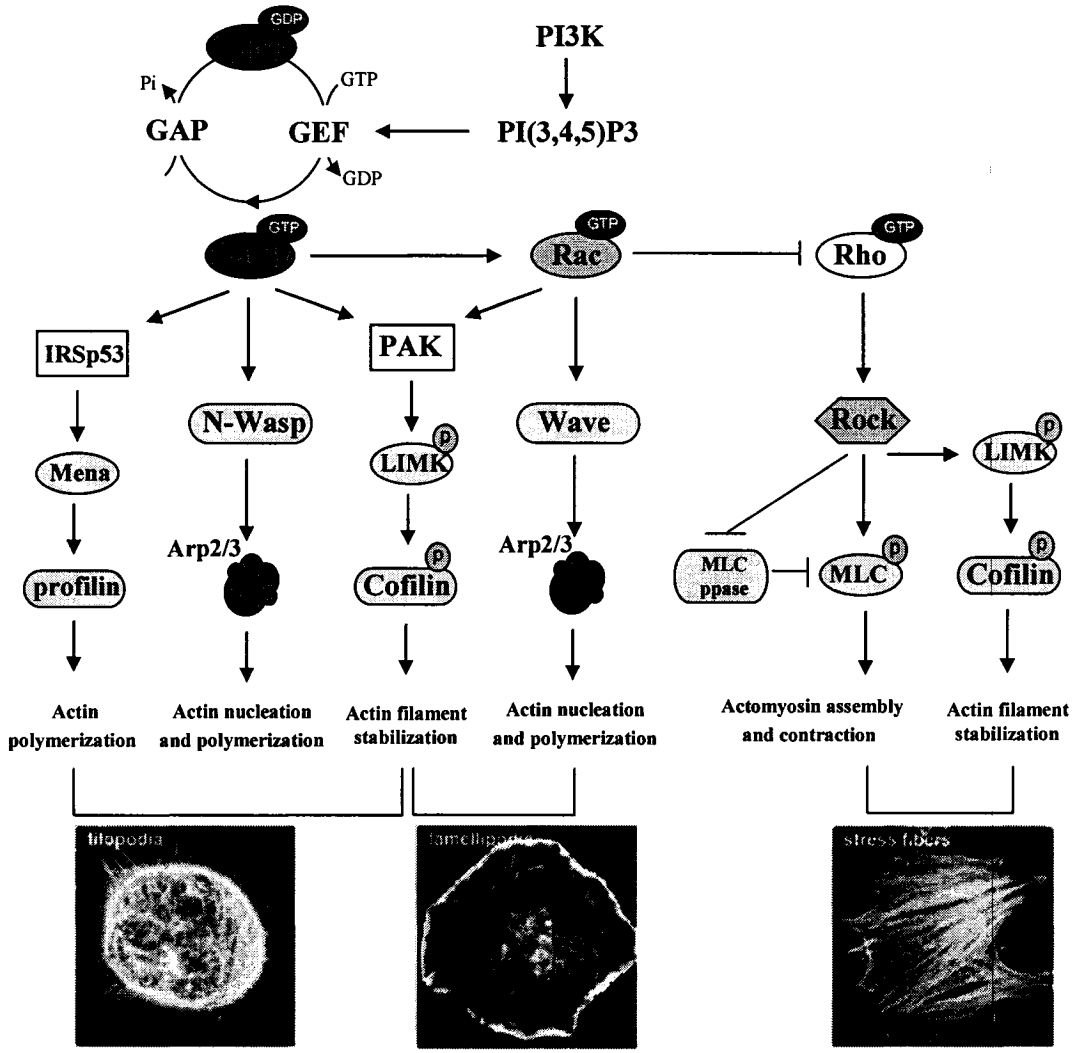

Figure 1.6: Rho GTPases and their effects on actin cytoskeletal reorganization. Cdc42 and Rac regulate filopodial and lamellipodial protrusions via the WASP/WAVE family proteins acting on the Arp2/3 complex, and via the PAK/LIMK cascade acting on cofilin. Rho promotes actin stress fiber formation and cellular contraction through the p160Rock-mediated MLC and LIMK cascades. Based on [136-138,140-147,150]

1.1.3.5. Lipid Rafts, Pro-migratory Signaling and Cell Motility

Lipid rafts are liquid-ordered membrane microdomains with elevated cholesterol and glycosphingolipid content in the exoplasmic leaflet of plasma membrane [151]. The inner leaflet of the raft is believed to be composed of saturated phospholipids and cholesterol, thereby coupling to the outer leaflet with saturated fatty acid-mediated interdigitation, which is further stabilized by transmembrane proteins [151]. In addition, due to the unique lipid composition, lipid rafts are also characterized by the insolubility in cold non-ionic detergent (e.g. Triton X-100, Brij 58, and CHAPS) and a low buoyant density in a sucrose gradient [152].

There is increasing evidence suggesting that lipid rafts serve as the membrane "signaling centers" to modulate signal transduction [152]. By recruiting certain signaling molecules such as glycosylphosphatidylinositol (GPI)-achored proteins, doubly acylated proteins (e.g. Src family kinases), PH domain-containing proteins (e.g. PLC isoforms), α-subunit of trimeric G-proteins, cholesterol-linked/palmitoylated transmembrane proteins (e.g. integrins) within a membrane compartment, lipid rafts could facilitate efficient and specific signal transduction in response to stimuli [151]. Signaling cross-talk can also be initiated if the molecules involved in different pathways are co-localized in the same lipid raft [152]. Subsequently, through redistribution of signaling mediators in and out of rafts following stimuli, these signaling events could also be spatial-temporally regulated [152]. Most significantly, since most of the signaling mediators crucial for cell motility (e.g. Src family kinases, Ras, PI3K, PLC, integrins and etc.) are usually activated in lipid rafts, it has been suggested that polarized or migrating cells by clustering one or more types of lipid rafts in response to pro-migratory cues, could form highly-organized and efficient

signaling complexes to co-ordinate cell motility [152]. There are also several lines of circumstantial evidence supporting the critical role of lipid rafts in pro-migratory signaling and cell motility: (1) it has been found that lipid rafts are concentrated at the leading edge of migrating cells [153,154]; (2) PtdIns(3,4,5)P3 which has been implicated in actin cytoskeletal protrusive motility through Rho family small GTPases as previously described in section 1.1.3.4, is highly concentrated in lipid rafts; (3) PtdIns(4,5)P2 which synergizes with Cdc42 in actin polymerization by activating the signaling cascade involving WASP and Arp2/3 is also located in lipid rafts [155,156]. The crucial role of PtdIns(4,5)P2 in cell motility is further supported by the finding that overexpression of type I phosphatidylinositol phosphate 5-kinase (PIP5KI), which synthesizes PtdIns(4,5)P2, promoted actin polymerization from membrane-bound vesicles to form motile actin comets [157]. Moreover, the PtdIns(4,5)P2-dependent raft assemblies also capture microtubules through IQ motif containing GTPase activating protein-1 (IQGAP1), thereby stabilizing microtubules at the leading edge and polarizing cell protrusive motility [158].

There is also considerable evidence suggesting that intracellular calcium signaling is spatial-temporally regulated by lipid rafts. Lipid rafts are the sites from which the PtdIns(4,5)P2-derived second messenger, IP3, is released from membrane through PLC activation [155,159]. Subsequently, as previously described in section 1.1.3.3, IP3 binds to the IP3R resulting in intracellular calcium release from nearby segments of ER [128,129]. Further, it has been suggested that the caveolae subtype of lipid rafts may play a direct role in loading the ER with calcium through a process of protocytosis [160].

1.2. Structure and Function of the MUC1 and ICAM-1 Molecules

1.2.1. Overview of Mucins

Mucins are a family of large, heavily glycosylated proteins which can be divided into two main classes: secreted mucins and membrane-associated mucins [71] (Fig. 1.7). The secreted mucins (e.g. MUC2 and MUC5) can form a gel-type steric barrier through core protein-mediated oligomerization to protect the secretory epithelial surface from harmful components [71]. They may also sequester growth factors or cytokines, such as IL-1 and TNF-α, for subsequent release in response to local inflammation [71]. The membrane-associated mucins (e.g. MUC1 and MUC4) are normally composed of a large extracellular domain, a single-span transmembrane doman, and a relatively short cytoplasmic domain [71]. Intensive studies in the past decade have demonstrated that these transmembrane mucins are crucial in signal transduction and involved in normal cell proliferation, differentiation, and morphology by functioning as cell surface receptors [71,161]. Mucin expression and glycosylation are frequently dysregulated in cancer cells, and are thought to contribute to malignant progression [71,162], generally by promoting tumor cell transformation, proliferation, and survival [71,162]. Moreover, emerging evidence suggests that they are also involved in tumor cell invasion, immune surveillance and extravasation in the process of metastasis [5,71]. Of those mucins implicated in malignancies, MUC1 is most thoroughly understood, especially in breast cancer.

1.2.2. The Structure and Expression of MUC1

The human MUC1 (also called CA15-3, CD227, episialin, EMA, ETA, DF3, MEA, MCA, PEM and PUM), first isolated from human breast milk, is encoded on

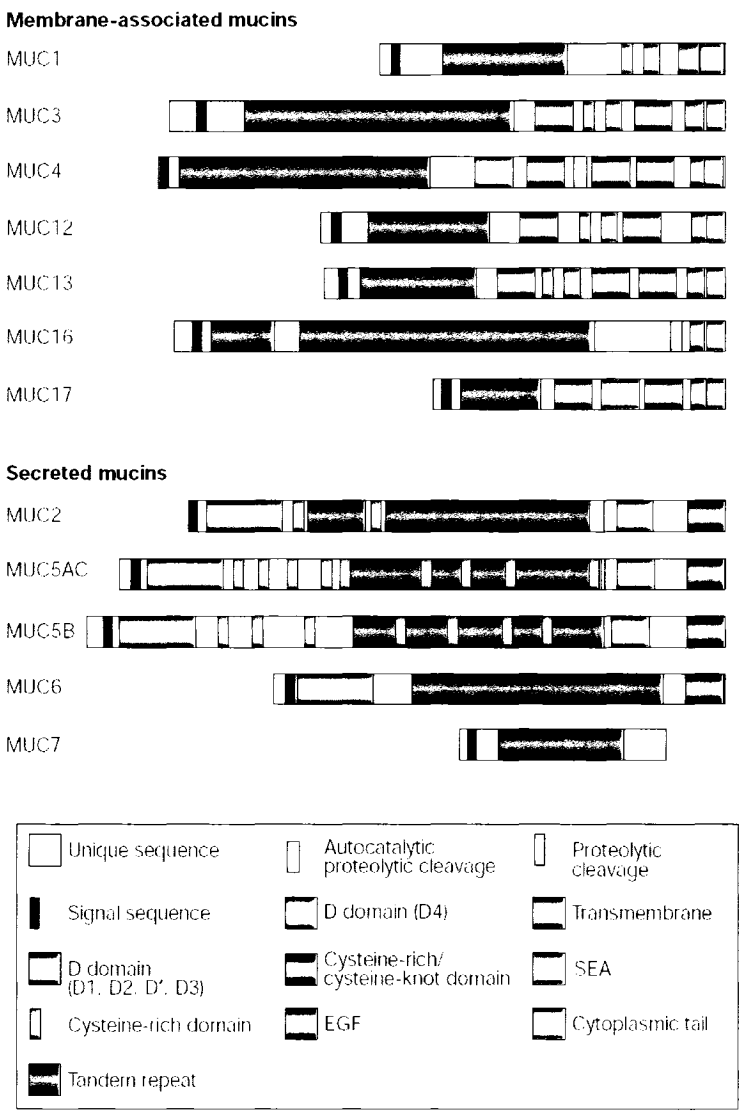

Figure 1.7: The structure of mucin family glycoproteins. Adapted from [71]

chromosome 1q21 [163,164]. The transcribed MUC1 pro-peptide undergoes cleavage in the endoplasmic reticulum (ER), reassociation prior to transport in the Golgi complex, and then targeting to the cell surface as a transmembrane heterodimeric glycoprotein with the large N-terminal subunit tethered to the plasma membrane through a noncovalent interaction with the extracellular region of its C-terminal subunit, which contains the transmembrane domain and a highly conserved cytoplasmic domain [24,162,165] (Fig. 1.8).

1.2.2.1. The MUC1 Extracellular Domain

The MUC1 extracellular domain (ECD), consists of the N-terminal subunit and the extracellular region of the C-terminal subunit. It has a variable (20 to 120) number of tandem repeats (VNTR) of a 20 amino acid sequence, which is enriched with serine, threonine and proline (STP-rich region), that is flanked by non-repetitive sequences [24,166]. The two serine and three threonine residues in each tandem repeat represent the potential sites for O-glycosylation (Fig 1.9), which generally starts with the GalNAc and then branches off by Gal and/or GlcNAc at the positions C3 and C6 to form a "core region" proximal to the STP-rich region [167]. The "core region" is elongated by repetitive Galβ1-3 or 4 GlcNAc disaccharides to construct the "backbone region" , which is followed by the "peripheral regions" characterized by fucose and sialic acid terminal structures [167]. It is believed that the MUC1 O-glycosylation is initiated in *cis* Golgi and matured in *trans* Golgi after several rounds of recycling from the membrane [165,168]. In addition, the MUC1-ECD may be also post-translationally modified by N-glycosylation at five potential asparagine residues in the ER (Fig. 1.9) [23,165]. Both the O- and N-glycosylation of MUC1 may be significant for its biological functions, as

emerging evidence suggests that it is implicated in MUC1 intracellular trafficking and adhesive properties [36,169,170].

The MUC1-ECD is rigid and extends up to 200-500 nm from the cell surface, considerably more extended when compared with the ~30 nm glycocalyx on the membrane [27]. The rigidity of MUC1 is partially due to the negative charge confered by the O-linked glycans [24,171,172]. Also, there are abundant proline residues in the MUC1 tandem repeats, where the rigid ring-structure of proline prevent the protein from "close packing" and contribute to the stiffness of rod-shaped MUC1-ECD by forming a polyproline β-turn helix [173]. Thus, the MUC1-ECD was generally believed to serve as a barrier to pathogens, cytotoxic lymphocytes and have an anti-adhesive role by interfering with E-cadherin and integrin mediated cell-cell and cell-matrix adhesion [27,31-34,174,175]. The MUC1-ECD also contains a SEA (sea urchin sperm protein, enterokinase, agrin) module, which is a 120 amino acid juxtamembrane region next to the N-terminal tandem repeats section [176,177]. The SEA module is the site at which the MUC1 pro-peptide is cleaved in the ER, and subsequently undergoes a tight heterodimeric reassociation before trafficking to the plasma membrane [165,177,178]. Although the exact function of the SEA module is still not elucidated, it is postulated that the N-terminal motif of the SEA may bind to the ECM components, such as laminin [176]. Further, as a region close to SEA module exhibits a high similarity with the ligand binding site of cytokine receptors for IL-3, IL-7, and GH, it may also be implicated in intracellular signaling events [44].

1.2.2.2. The MUC1 Transmembrane Domain

MUC1 has a single-span transmembrane domain (TMD), which is 28 amino acids

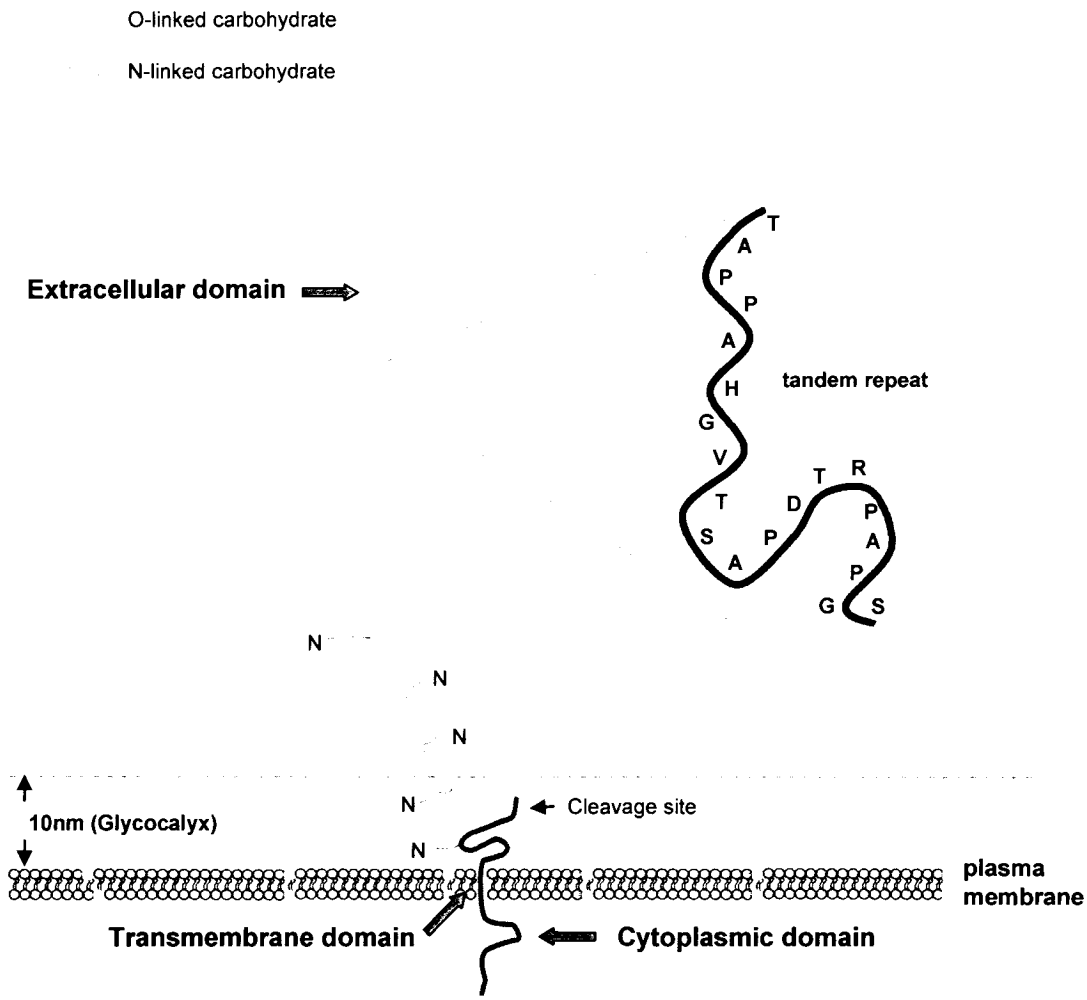

Figure 1.8: Molecular structure of human MUC1. MUC1 contains a short cytoplasmic domain, a highly hydrophobic transmembrane domain, and a large (200-500nm) extracellular domain, which consists of variable number of tandem repeats of a 20 amino acid sequence that is heavily O-glycosylated. Based on [24,27,32,162,166]

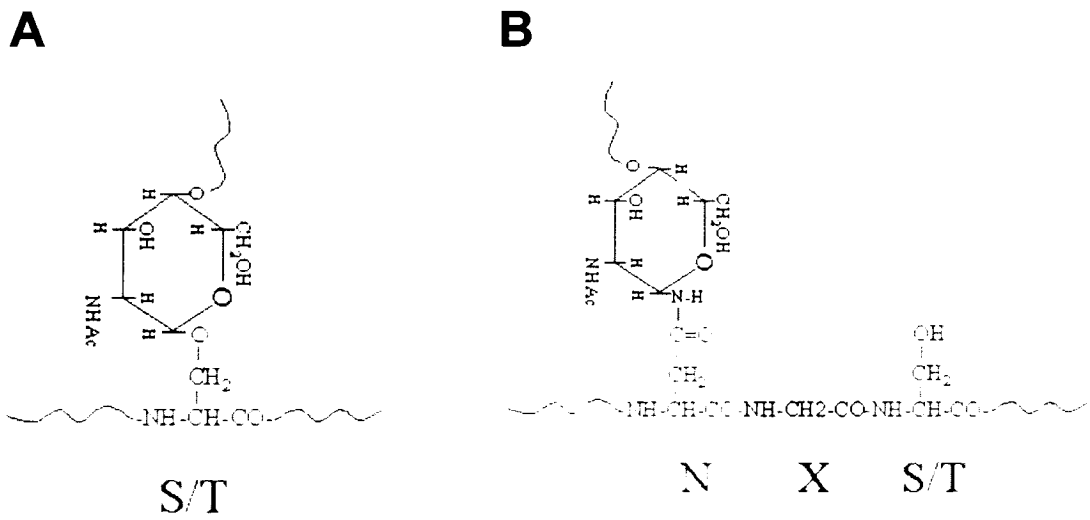

Figure 1.9: O- and N-linked protein glycosylation. O-linked carbohydrates link through N-acetylgalactosamine (GalNAc) to a serine (S) or threonine (T) residue. However, no amino acid consensus sequence has been defined for O-glycosylation. N-linked carbohydrates link through N-acetylglucosamine (GlcNAc) to an asparagine (N) residue. The N-linked amino acid consensus sequence is Asn-any AA- Ser or Thr. The middle amino acid can not be proline (Pro). Adapted from http://www.ionsource.com/Card/carbo/nolink.htm.

long and highly hydrophobic [167]. Since MUC1 has been reported to be localized in lipid rafts [39,40], the "membrane centers" crucial for spatial-temporal regulation of signaling molecules, it is postulated that the MUC1-TMD is critical for MUC1 lipid raft distribution thereby contributing to its biological activities. Supporting this, it is reported that deletion of the MUC1 cytosplasmic domain did not influence its membrane localization [3]. However, alteration of the C-Q-C motif at the junction between the transmembrane and cytoplasmic domain resulted in failure of MUC1 membrane targeting and localization [3], suggesting that cysteine-mediated palmitoylation and/or farnesylation may play a crucial role in MUC1 lipid raft localization.

Recent studies in our laboratory have found that MUC1 homodimerizes in lipid rafts (unpublished data) which may also be conferred by the cysteine residues in the MUC1-TMD. Evidence from other proteins, such as synaptobrevin and tetraspanin, suggests that either the cysteine-mediated disulfide bonds or the fatty acyl modification of the TMD could contribute to the dimerization and clustering of transmembrane proteins [179-182].

1.2.2.3. The MUC1 Cytoplasmic Domain

MUC1 contains a relatively short 72 amino acid cytoplasmic domain (Fig. 1.10). Although the MUC1-CD is enriched with serine and threonine residues, up to 90% of the phosphates present in ^{32}P-labelled MUC1-CD are conferred by tyrosine phosphorylation [44]. The MUC1-CD contains seven highly conserved tyrosine residues, four of which are confirmed phosphorylation sites and construct potential binding motifs for the SH2 or SH3 domains of signaling mediators, such as PI3K (Y^{20}HPM), PLCγ1 (Y^{35}VPP), Src family kinase (Y^{46}EKV) and Grb2 (Y^{60}TNP) [43,44]. It has been reported that the EGFR

family of receptor tyrosine kinases [183,184], PKCδ [185], and Src [183,186] can physically associate with and phosphorylate the MUC1-CD. Other signaling and/or structural molecules such as Grb2/Sos [187], GSK3β [186,188], β-catenin [183,185,188-190], γ-catenin [191], p120-catenin [192], and APC [193] have also been reported in association with the MUC1-CD. These findings strongly suggest that MUC1 plays a significant role in signaling, although MUC1 itself does not have an intrinsic kinase acitivity [174]. Since cytochalasin D-mediated disruption of the actin cytoskeleton also disrupted the polarized localization of MUC1, it is believed that MUC1-CD binds to the actin cytoskeleton [194]. More recently, MUC1 has been found to co-distribute with ezrin [42], a known linker of membrane proteins to the actin cytoskeleton, suggesting that the linkage of MUC1 to cytoskeleton may be indirect.

1.2.2.4. The MUC1 Splice Isoforms

Although the full length MUC1, as described above, represents the major form of MUC1 expressed on the cell surface, alternative splice variants of MUC1 mRNA encode several other MUC1 isoforms with distinct functions. The first described variant, MUC1/Y, is a 42-45 KDa transmembrane protein which lacks the entire tandem repeat region and part of the SEA module [195]. Therefore, it has no mucin-like characteristics and does not undergo cleavage in the ER. MUC1/Y serves as a binding partner for the secreted MUC1/SEC, another MUC1 splice isoform which lacks both the TMD and CD. Binding of MUC1/SEC results in phosphorylation of the MUC1/Y cytoplasmic domain [162,196]. Since MUC1/Y is preferentially expressed in breast carcinomas and faciliates oncogenic transformation of mouse DA3 mammary epithelial cells [196,197], a tumorigenic activity was suggested for MUC1/Y in human breast cancer. The MUC1/X

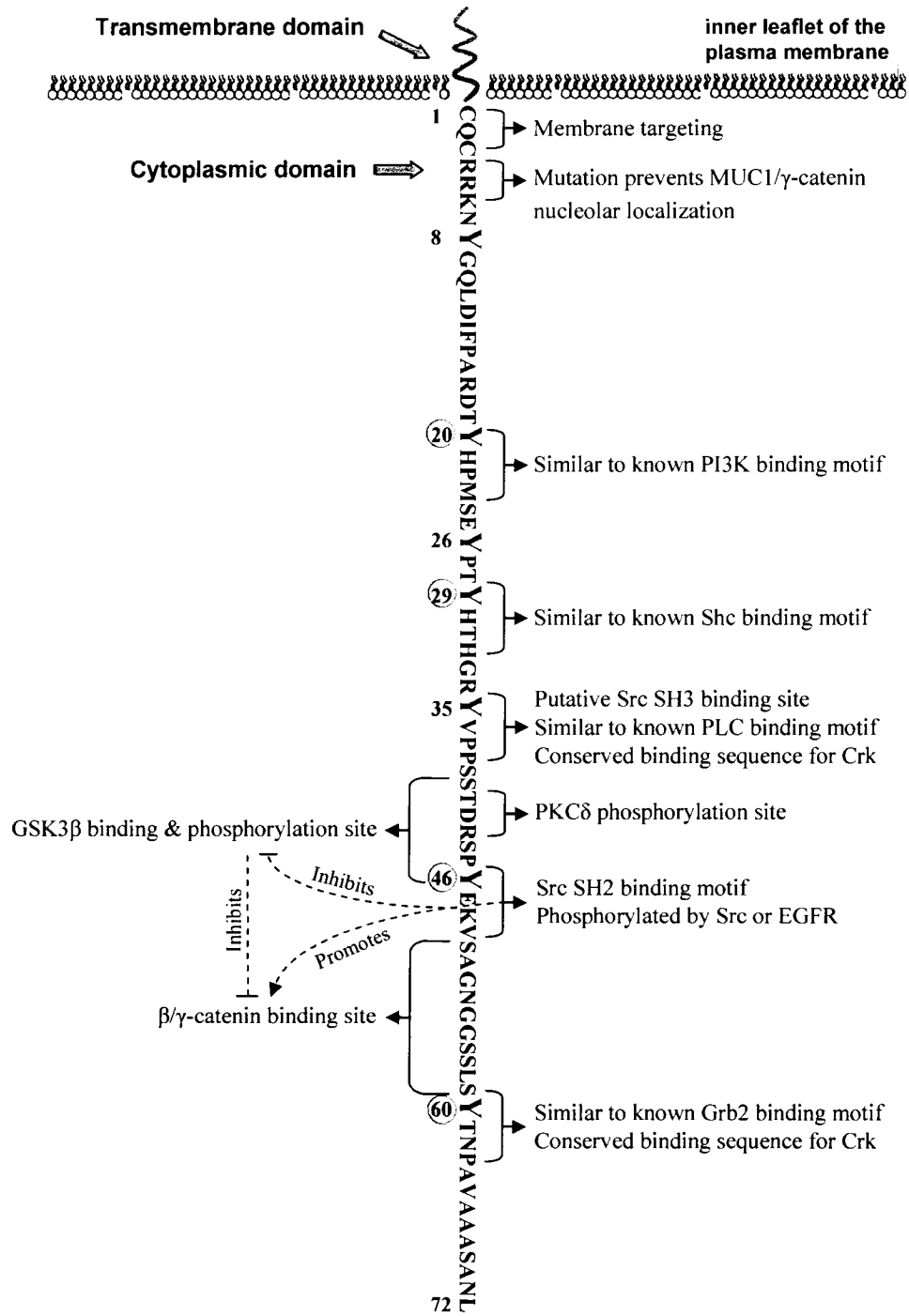

Figure 1.10: Main characteristics of MUC1 cytoplasmic domain. MUC1 has a 72 amino acid cytoplasmic domain. Major tyrosine phosphorylation sites (Y) and associated signaling partners are indicated. Based on [3,43,183-191,198]

isoform (also named MUC1/Z), similar to MUC1/Y, also lacks the tandem repeats region but contains 18 more amino acid in its extracellular domain than MUC1/Y [197,199]. In addition to the pre-translational regulation, the N-terminal mucin-like subunit of full length MUC1 can also be shed from the membrane by TACE/ADAM17 or MT1-MMP mediated cleavage of the MUC1-ECD [200,201].

1.2.2.5. MUC1 Expression

MUC1 is normally heavily glycosylated and expressed exclusively on the apical surface of most secretory epithelial cells of the mammary gland, respiratory, gastrointestinal, and reproductive tracts, as well as on activated hematopoietic cells [41,162,167,202,203]. However, the apical polarized-expression of MUC1 is frequently lost in breast cancers and other malignancies, and replaced by highly overexpressed MUC1 either throughout the cytosol or circumferentially around the plasma membrane [4,5,25-27,204-207] (Figure 1.11). The proliferation of mammary tumor cells was reported to be decreased in MUC1 knock-out mice, although they behaved normally in development and reproduction [208], indicating MUC1 expression is correlated with breast tumorigenesis and progression. Significantly, several correlative clinical studies have shown that this aberrant expression of MUC1 is correlated with a higher tendency for metastasis and a poor prognosis [5,209-214]. It is generally supposed that the upregulation of MUC1 is caused by a higher gene dosage effect and increased transcription [162,215]. In addition, several cases of B-cell lymphomas showed a *MUC1* gene translocation t(1;14)(q21;q32) downstream of the Ig heavy chain enhancer [216,217], suggesting that increased MUC1 expression in some cases could be a consequence of a strong enhancer-induced transcription. Transcriptional regulatory

effects have also been demonstrated by several cytokines, including TNF-α, IFN-γ and IL-6 [218-220]. The STAT (signal transducer and activator of transcription) molecule is a proposed mediator for this process [220]. Moreover, neutrophil elastase was reported to stimulate MUC1 expression through increased Sp1 binding to the *MUC1* promoter [221]. In addition to the STAT and Sp1 binding sites, the *MUC1* gene promoter region also contains numerous potential response elements for other transcriptional regulators, such as NF-*k*B, NF-1, Smad and AP1-4 [162], indicating that the expression of MUC1 may be regulated in a multi-factorial fashion. In addition, the underglycosylation of MUC1 would also be implicated in MUC1 overexpression, as it directly causes defects in MUC1 trafficking, resulting in its cellular accumulation [169].

MUC1 glycosylation levels vary depending on the tissues in which it is expressed, from ~50% of MW in normal breast gland to 80% in pancreas [162,222]. This is largely dependent on the glycosyltransferase profile expressed in these tissues. Notably, MUC1 is also aberrantly glycosylated in breast cancers, as well as other tumors, due to the dysregulation of glycosyltransferases governing extension and termination of O-glycans [223]. Breast cancer cells show a reduction (MCF-7) or loss (T47D) of core-2 β6-GlcNAc-transferase activity and an increase in sialyltransferase acitivities, which result in short, linear O-glycan side chains in tumor cells and reveal the tumor-specific peptide epitopes on the VNTR which are normally masked by glycosylation [223,224]. Paradoxically, T47D cells exhibit a higher density of O-glycosylation, with O-linked glycans attached to 95% of available sites as compared with the ~50% O-glycosylation of MUC1 in normal mammary tissues [225]. Tumor-derived MUC1 shows an increased affinity for antibodies against the peptide core of the MUC1-ECD, such as SM-3 and

Figure 1.11: MUC1 expression in normal and malignant breast epithelia. Immunohistochemical detection of MUC1 which is stained brown (DAB), with cell nuclei counterstained blue (alkaline hematoxylin). MUC1 appears on the apical luminal surfaces of normal breast epithelial cells (A). In breast cancer, MUC1 is overexpressed throughout the cytosol (B) or circumferentially around the plasma membrane (C).

DF-3P [207,226]. Emerging evidence suggests that this aberrant glycosylation may confer the adhesive property of MUC1, which we will discuss later in section 1.2.3.

1.2.3. The Biological Functions of MUC1

1.2.3.1. Evidence for a Signaling Function of MUC1

There is increasing evidence implicating MUC1 in signal transduction. Tyrosine phosphorylation is a fundamental mechanism initiating intracellular signaling, and this has been reported on the MUC1-CD following culturing at low density (lacking cell-cell contact) [227], phosphatase inhibition [44,187], stimulation of a CD8-MUC1 chimera with anti-CD8 antibodies [228], and binding of the bacterium *Pseudomonas aeruginosa* [229]. Further, EGFR has been found to physically interact with and phosphorylated MUC1 in reponse to EGF stimulation. EGFR is frequently upregulated and correlates with an aggressive phenotype in breast cancers [184,230] and the EGF-induced ERK/MAPK pathway is significantly enhanced in the presence of MUC1 [184,190]. Since MUC1 interacts directly with the Grb2/Sos complex [187] and ERK/MAPK is generally activated via EGFR/Grb2/Sos/Raf/Ras/MEK cascade to promote cell proliferation, survival and cell motility [95,231], this may be the pathway whereby MUC1 potentiates EGFR signaling. As well, subsequent to MUC1-CD phosphorylation, activation of ERK/MAPK cascade was also observed after binding of *Pseudomonas aeruginosa* to MUC1 [229,232,233]. Recent work by Li *et al.* found that MUC1 associates constitutively with EGFR in breast cancer ZR-75-1 cells, and EGFR-mediated phosphorylation at $Y^{46}EKV$ motif of MUC1-CD creates a binding site for the Src SH2 domain [183], suggesting MUC1 may play a crucial role in Src signaling, which has been implicated in almost all processes of tumorigenesis and metastasis.

MUC1 also associates with β-catenin [183,185,188-190], a structural protein bridging E-cadherin and the actin cytoskeleton. This MUC1/β-catenin interaction is mediated by a conserved $S^{50}XXXXXSSL^{58}$ site on the MUC1-CD, and is regulated by several signaling mediators such as glycogen synthase kinase 3β (GSK3β), Src, and PKCδ [183,185,188,189]. GSK3β binds directly to MUC1-CD $S^{40}TDRS^{44}PYE$ motif and phosphorylate S^{44}, resulting in decreased interaction between MUC1 and β-catenin [188]. Thus, an augmented cytosolic β-catenin pool may lead to E-cadherin/β-catenin complex restoration at sites of intercellular adhesion, or result in β-catenin/TCF-LEF transcriptional complex formation to modulate transcription of genes such as c-myc and cyclin D1 [234,235]. In contrast, it was found that the EGFR/Src-mediated MUC1-CD $Y^{46}EKV$ phosphorylation and subsequent Src binding can dissociate GSK3β from MUC1-CD, thereby promoting the interaction of MUC1-CD with β-catenin [183,186]. A similar effect occurs with PKCδ, which can phosphorylate the $T^{41}DR$ motif within the MUC1-CD GSK3β binding site and thus increase binding of MUC1 and β-catenin both *in vivo* and *in vitro* [185].

MUC1-CD binds directly to p120(ctn), and subsequently induces p120(ctn) nuclear localization [192], suggesting a critical role of MUC1 in membrane-to-nuclear signaling. Recent work by Li *et al.* demonstrated that treatment of breast cancer cells with heregulin/neuregulin (HRG) promotes MUC1/ErbB-2 interaction, which results in MUC1-γ-catenin complex formation and targeting of this complex to the nucleolus, thereby participating in cross-talk between the ErbB-2 and Wnt cascades [191]. Significantly, this MUC1-γ-catenin nucleolar transportation was only observed in carcinoma cells, but not in normal cells [191], highlighting the tumorigenic potential of

MUC1 in breast cancer. Overexpression of MUC1 has also been found to transform 3Y1 fibroblast cells via signaling cascades involving PI3K, Akt, Bad, and Bcl-(x)L, resulting in attenuation of the mitochondrial apoptotic signaling and gemcitabine-induced apoptosis [236]. Most recently, Wei *et al.* found that the C-terminal subunit of MUC1 also associates with and stabilizes estrogen receptor-α (ER-α) in response to 17β-estradiol (E2) stimulation, thereby promoting E2/ER-α-mediated gene transcription [237].

Taken together, the evidence presented above suggests that MUC1 is a signaling molecule crucial for the regulation of gene transcription, cell proliferation, and survival. Thus, MUC1 overexpression is proposed as one of the vital mechanisms in tumorigenesis.

1.2.3.2. Evidence for MUC1 as a Pro-migratory Molecule

MUC1 has long been associated with tumor progression, including the processes of invasion and metastasis [5,211,212]. Suwa *et al.* using the gastric cancer cell line MKN74 demonstrated that MUC1 contributes to increased cell motility in a gold particle phagokinetic track assay and increased invasiveness of tumor cells into Matrigel and the muscle layer after subcutaneous injection [238]. They suggested that this increase in cell motility might be due to the large and extended ECD of MUC1, which destabilizes the cell-matrix connections [238]. Also, since MUC1 can competitively bind β-catenin, which bridges E-cadherin and actin filaments in constructing cell-cell adherent junctions [95], MUC1 may actively abrogate E-cadherin mediated cell-cell connections and thus promote cell dissemination from their orginial site.

Emerging evidence suggests that MUC1 is also functioning as a surface adhesion molecule. The sialyl Lewis $^{a/x}$ carbohydrates present on the O-linked glycans of MUC1-ECD were demonstrated to serve as a ligand for selectin-like molecules on endothelial

cells, thereby promoting cell adhesion and metastatic dissemination [239-242]. Further, cell imaging studies showed that MUC1 is concentrated at the tips of filopodial protrusions in breast cancer MCF-7 cells, where MUC1 is co-distributed with ezrin, a linker of membrane proteins to the actin cytoskeleton [42]. Again, in activated T cells, MUC1 is also found highly concentrated at the leading edge rather than on the uropod [41]. Taken together, these findings strongly support the previous findings from our lab which showed that MUC1 is a pro-adhesive molecule, and we have indentified ICAM-1, an immunoglobulin family member, as the ligand [7,8].

1.2.4. The Structure and Function of ICAM-1

1.2.4.1. The Structure and Expression of ICAM-1

The human ICAM-1 (also known as CD54), encoded on chromosome 19p13, is a transmembrane glycoprotein of the immunoglobulin (Ig) superfamily [243,244] (Figure 1.12). Structurally, the "rod shaped" extracellular domain of ICAM-1 is around 19nm (453 amino acids) long and contains five Ig-like domains, each of which is folded into anti-parallel β strands and stabilized by disulfide bridge(s) between conserved cysteine residues with the exception of Domain-4 [245,246]. The majority of ICAM-1 is expressed on the cell surface in a homodimeric form, which is supposed to be mediated by the juxtamembrane cysteine residue and assisted by a"dimerisation interface" on Domain-1 [247,248]. Moreover, the ICAM-1 extracellular domain contains eight N-linked glycosylation sites and the cell type-dependent glycosylation results in variations of its molecular weight between 60-114 kDa [245,249,250]. The transmembrane domain of ICAM-1 consists of 24 amino acids that may contribute to its distribution in lipid rafts in response to ligation induced clustering [243,251]. Lastly, ICAM-1 contains a highly

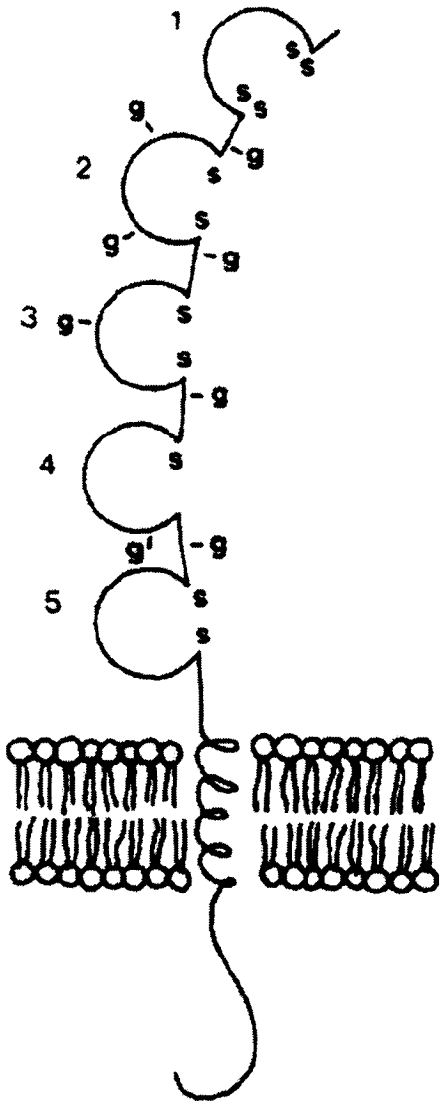

Figure 1.12: Molecular structure of ICAM-1. Intercellular adhesion molecule-1 (ICAM-1) is composed of a 453 amino acid extracellular domain, a 24 amino acid transmembrane domain, and a 28 amino acid cytoplasmic tail. The extracellular domain contains five Ig-like domains, where disulfide bonds are formed between B and F strands in each domain to stabilize the rod-like structure, except for the fourth domain. The "g" represents N-glycosylation sites. Adapted from [243]

conserved 28 amino acid cytoplasmic domain [243], which has been demonstrated to associated with the actin cytoskeleton binding proteins, such as α-actinin [252] and ezrin [253,254], suggesting a critical role of ICAM-1 in cell motility.

ICAM-1 is constitutively expressed on endothelial and epithelial cells, as well as on hematopoietic cells [243,247]. On the activated endothelium, ICAM-1 is located exclusively along the luminal membrane [255,256]. The expression level of ICAM-1 can be transcriptionally up-regulated by inflammatory cytokines, such as TNF-α, IL-1β and IFN-γ [243,257-259]. Also, its expression on endothelial cells can be increased by non-inflammatory stimuli, such as shear stress, reperfusion injury and ischemia [96,243,260]. In contrast, glucocorticoids have been shown to repress the gene transcription of ICAM-1 [261,262]. Angiogenic factors (e.g. bFGF) also downregulate ICAM-1 expression, thereby reducing the sensitivity of endothelial cells to inflammatory cytokines and possibly serving to inhibit leukocyte recruitment to tumors [263].

1.2.4.2. The Function of ICAM-1

ICAM-1 is a critical molecule for the induction of heterotypic cell-cell adhesive interactions and subsequent signaling [243,264]. One of the major families of ligands for ICAM-1 are the β2 integrins, such as LFA-1 (CD11a/CD18) and Mac-1 (CD11b/CD18), which can recongize the N-teminal first and third Ig-like domains of ICAM-1 respectively [95,245,265]. In addition, ICAM-1 also binds to CD43 on leukocytes and platelets, extracellular components such as fibrinogen and hyaluronan [243,266,267], and MUC1 on tumor cells [7,8]. Binding to LFA-1 induces ICAM-1 clustering at the point of cell-cell contact and the homodimerized ICAM-1 exhibits a higher level of avidity for the LFA-1 ligand than the monomer [248,268-270]. Further, it has been suggested that the

binding affinity of ICAM-1 is also influenced by the glycosylation patterns and levels on its extracellular domain, as the binding site for Mac-1 can be shielded by carbohydrate chains [265].

During inflammation, accumulating evidence suggests that ICAM-1 plays a more complex role than simply facilitating firm anchorage for leukocytes on the vascular endothelium. The ligation of ICAM-1 also triggers an intracellular calcium flux [96,271] and activation of several signaling mediators, including Src, PKC, FAK, paxillin, Rho, p130CAS and MLCK [264,272-274], all of which (as described in section 1.1.3.2-4) have been implicated in cytoskeletal reorganization and focal contact dynamics. As a result, the endothelial cells dissociate preferentially at the "tricellular corners" where three endothelial cells share cell-cell junctions [97,264,272,275]. Several mechanisms may facilitate the ICAM-1-induced endothelial cell dissociation in response to the ligation of cross-linking antibodies or activated leukocytes. First, the endothelial tight junctions are discontinuous at these "tricellular corners" [97,275]. Further, it has been shown that ICAM-1, which is normally distributed evenly across the apical membrane of endothelial cells, is redistributed to the cell-cell junctions after 24 hours of cytokine stimulation [258]. Other endothelial proteins, such as platelet endothelial cell adhesion molecule-1 (PECAM-1), CD99, vascular cell adhesion molecule-1 (VCAM-1), and junctional adhesion molecule (JAM) also act in concert with ICAM-1 to direct activated leukocytes towards tricellular corners and subsequent extravasation [264,276]. Significantly, breast cancer cells (MCF-7), but not normal mammary epithelial cells, are capable of initiating the intracellular calcium signal [277] and retraction of human umbilical vein endothelial cells (HUVECs) [278]. This suggests that tumor cells may utilize similar strategies as

activated leukocytes in cell-endothelium interaction and subsequent extravasation, and that possession or overexpression of an appropriate ligand for ICAM-1 by tumor cells may represent a critical mechanism in metastasis.

1.2.5. MUC1/ICAM-1 Interaction and Cell Migration

Our laboratory was the first to report that tumor-associated MUC1 had pro-adhesive properties and identified ICAM-1 as the ligand [7,8]. The MUC1/ICAM-1 interaction is mediated by the highly immunogenic knob-like protrusion on the VNTR tandem repeat of MUC1-ECD, and can be abrogated by purified tumor MUC1 and antibodies against either the MUC1-PDTRPAP epitope (B27.29) or ICAM-1 (18E3D) [7,8]. Hayashi *et al.* has since demonstrated that a minimum of two tandem repeats of MUC1-ECD is required for its binding to ICAM-1 on the extracellular Ig-like domain-1 [35]. Further, Horne *et al.* in our lab showed that this MUC1/ICAM-1 interaction is strong enough to withstand the shear stresses equivalent to physiologic blood flow [10], suggesting a crucial role for MUC1 in the adhesion of metastatic tumor cells to the vascular endothelium. Supporting this, recent work by McDermott *et al.* found that treatment with benzyl-α-GalNAc, an inhibitor of O-glycan extension, increases MUC1 binding to ICAM-1 [36]. This is significant since MUC1 generated by breast cancer cells (e.g. T47D and MCF-7) generally exhibit short, linear, less bulky sugar side chains due to the dysregulation of glycosyltransferases governing extension and termination of O-glycans [223,224]. Significantly, the most recent data by Rahn *et al.* in our laboratory found that MUC1 promotes transendothelial migration of MUC1-bearing cells through a simulated blood vessel wall in response to the ligation of ICAM-1 expressed on endothelial cells [11]. The potentiated migration can be inhibited by preincubation with

antibodies that block interaction sites on either the MUC1 or ICAM-1 molecules [11]. Further, by upregulating ICAM-1 on the accessory cells, the MUC1/ICAM-1-mediated transendothelial migration is also increased [11]. These findings strongly support the potential role of MUC1/ICAM-1 ligation in promoting cell migration.

1.3. Hypothesis and Objectives

This thesis is focused on investigating the underlying mechanism(s) by which MUC1/ICAM-1 ligation promotes breast cancer cell migration. It is based on our previous work showing that MUC1 binds ICAM-1, mediating adhesion of breast cancer cells to accessory cells [7,8] and facilitating transendothelial migration of MUC1-bearing cells through a monolayer of ICAM-1-expressing cells [11]. Further, since (1) MUC1 has been reported to be localized in lipid rafts and concentrated at the leading edge of migrating cells [39-41]; (2) MUC1-CD co-distributes with components, such as p120-ctn and ezrin, which are known linkers of membrane proteins to the actin cytoskeleton [42,192]; (3) MUC1-CD contains seven highly conserved tyrosine residues, four of which are confirmed phosphorylation sites and construct potential binding motifs for PI3K, PLCγ, Grb2 and Src family kinase [43,44], all of which are critical in cell motility; we hypothesize that by ligating ICAM-1, MUC1 may not only function as an adhesion molecule, but also initiate pro-migratory signaling and cytoskeletal reorganization resulting in increased tumor cell motility. To test this hypothesis, three specific objectives are proposed in this study:

1. To investigate MUC1-initiated pro-migratory signaling following ICAM-1 ligation.
2. To investigate MUC1/ICAM-1 interaction-initiated actin cytoskeletal reorganization.
3. To investigate MUC1/ICAM-1 interaction-potentiated cell invasion.

1.4. References

1. Braga VM, Pemberton LF, Duhig T, Gendler SJ: **Spatial and temporal expression of an epithelial mucin, Muc-1, during mouse development.** *Development* 1992, **115**:427-437.
2. Gendler SJ, Spicer AP: **Epithelial mucin genes.** *Annu Rev Physiol* 1995, **57**:607-634.
3. Pemberton LF, Rughetti A, Taylor-Papadimitriou J, Gendler SJ: **The epithelial mucin MUC1 contains at least two discrete signals specifying membrane localization in cells.** *J Biol Chem* 1996, **271**:2332-2340.
4. Kufe D, Inghirami G, Abe M, Hayes D, Justi-Wheeler H, Schlom J: **Differential reactivity of a novel monoclonal antibody (DF3) with human malignant versus benign breast tumors.** *Hybridoma* 1984, **3**:223-232.
5. Rahn JJ, Dabbagh L, Pasdar M, Hugh JC: **The importance of MUC1 cellular localization in patients with breast carcinoma: an immunohistologic study of 71 patients and review of the literature.** *Cancer* 2001, **91**:1973-1982.
6. Apostolopoulos V, McKenzie IF, Pietersz GA: **Breast cancer immunotherapy: current status and future prospects.** *Immunol Cell Biol* 1996, **74**:457-464.
7. Kam JL, Regimbald LH, Hilgers JH, Hoffman P, Krantz MJ, Longenecker BM, Hugh JC: **MUC1 synthetic peptide inhibition of intercellular adhesion molecule-1 and MUC1 binding requires six tandem repeats.** *Cancer Res* 1998, **58**:5577-5581.
8. Regimbald LH, Pilarski LM, Longenecker BM, Reddish MA, Zimmermann G, Hugh JC: **The breast mucin MUCI as a novel adhesion ligand for endothelial intercellular adhesion molecule 1 in breast cancer.** *Cancer Res* 1996, **56**:4244-4249.
9. Kuby J: *Immunology* edn 3rd. New York: W.H. Freeman; 1997.
10. Horne GJ, University of Alberta. Dept. of Laboratory Medicine and Pathology.: **The role of breast cancer associated with MUC1 in tumor cell recruitment to vascular endothelium during physiological fluid flow**: 1999.
11. Rahn JJ, Chow JW, Horne GJ, Mah BK, Emerman JT, Hoffman P, Hugh JC: **MUC1 mediates transendothelial migration in vitro by ligating endothelial cell ICAM-1.** *Clin Exp Metastasis* 2005, **22**:475-483.
12. Rahn JJ, Shen Q, Mah BK, Hugh JC: **MUC1 initiates a calcium signal after ligation by intercellular adhesion molecule-1.** *J Biol Chem* 2004, **279**:29386-29390.
13. **Breast Cancer Stats on World Wide Web URL: http://www.cancer.ca/ccs/internet/standard/0,3182,3172_14435_371399_langId-en,00.html.**
14. Kamby C, Ejlertsen B, Andersen J, Birkler NE, Rytter L, Zedeler K, Rose C: **The pattern of metastases in human breast cancer. Influence of systemic adjuvant therapy and impact on survival.** *Acta Oncol* 1988, **27**:715-719.
15. Patanaphan V, Salazar OM, Risco R: **Breast cancer: metastatic patterns and their prognosis.** *South Med J* 1988, **81**:1109-1112.
16. Fidler IJ: **Critical factors in the biology of human cancer metastasis: twenty-eighth G.H.A. Clowes memorial award lecture.** *Cancer Res* 1990, **50**:6130-6138.

17. Friedl P, Brocker EB, Zanker KS: **Integrins, cell matrix interactions and cell migration strategies: fundamental differences in leukocytes and tumor cells.** *Cell Adhes Commun* 1998, **6**:225-236.
18. Playford MP, Schaller MD: **The interplay between Src and integrins in normal and tumor biology.** *Oncogene* 2004, **23**:7928-7946.
19. Suetsugu S, Takenawa T: **Regulation of cortical actin networks in cell migration.** *Int Rev Cytol* 2003, **229**:245-286.
20. Ridley AJ: **Rho proteins and cancer.** *Breast Cancer Res Treat* 2004, **84**:13-19.
21. Gendler SJ, Burchell JM, Duhig T, Lamport D, White R, Parker M, Taylor-Papadimitriou J: **Cloning of partial cDNA encoding differentiation and tumor-associated mucin glycoproteins expressed by human mammary epithelium.** *Proc Natl Acad Sci U S A* 1987, **84**:6060-6064.
22. Gendler SJ, Lancaster CA, Taylor-Papadimitriou J, Duhig T, Peat N, Burchell J, Pemberton L, Lalani EN, Wilson D: **Molecular cloning and expression of human tumor-associated polymorphic epithelial mucin.** *J Biol Chem* 1990, **265**:15286-15293.
23. Lan MS, Batra SK, Qi WN, Metzgar RS, Hollingsworth MA: **Cloning and sequencing of a human pancreatic tumor mucin cDNA.** *J Biol Chem* 1990, **265**:15294-15299.
24. Patton S, Gendler SJ, Spicer AP: **The epithelial mucin, MUC1, of milk, mammary gland and other tissues.** *Biochim Biophys Acta* 1995, **1241**:407-423.
25. Szpak CA, Johnston WW, Lottich SC, Kufe D, Thor A, Schlom J: **Patterns of reactivity of four novel monoclonal antibodies (B72.3, DF3, B1.1 and B6.2) with cells in human malignant and benign effusions.** *Acta Cytol* 1984, **28**:356-367.
26. Gendler SJ, Spicer AP, Lalani EN, Duhig T, Peat N, Burchell J, Pemberton L, Boshell M, Taylor-Papadimitriou J: **Structure and biology of a carcinoma-associated mucin, MUC1.** *Am Rev Respir Dis* 1991, **144**:S42-47.
27. Hilkens J, Vos HL, Wesseling J, Boer M, Storm J, van der Valk S, Calafat J, Patriarca C: **Is episialin/MUC1 involved in breast cancer progression?** *Cancer Lett* 1995, **90**:27-33.
28. Spicer AP, Duhig T, Chilton BS, Gendler SJ: **Analysis of mammalian MUC1 genes reveals potential functionally important domains.** *Mamm Genome* 1995, **6**:885-888.
29. Soler M, Desplat-Jego S, Vacher B, Ponsonnet L, Fraterno M, Bongrand P, Martin JM, Foa C: **Adhesion-related glycocalyx study: quantitative approach with imaging-spectrum in the energy filtering transmission electron microscope (EFTEM).** *FEBS Lett* 1998, **429**:89-94.
30. Hilkens J: **Episialin/CA15-3: its structure and involvement in breast cancer progression.** *Ned Tijdschr Klin Chem* 1995:293-298.
31. Wesseling J, van der Valk SW, Hilkens J: **A mechanism for inhibition of E-cadherin-mediated cell-cell adhesion by the membrane-associated mucin episialin/MUC1.** *Mol Biol Cell* 1996, **7**:565-577.
32. Wesseling J, van der Valk SW, Vos HL, Sonnenberg A, Hilkens J: **Episialin (MUC1) overexpression inhibits integrin-mediated cell adhesion to extracellular matrix components.** *J Cell Biol* 1995, **129**:255-265.

33. Hayes DF, Silberstein DS, Rodrique SW, Kufe DW: **DF3 antigen, a human epithelial cell mucin, inhibits adhesion of eosinophils to antibody-coated targets.** *J Immunol* 1990, **145**:962-970.
34. Kondo K, Kohno N, Yokoyama A, Hiwada K: **Decreased MUC1 expression induces E-cadherin-mediated cell adhesion of breast cancer cell lines.** *Cancer Res* 1998, **58**:2014-2019.
35. Hayashi T, Takahashi T, Motoya S, Ishida T, Itoh F, Adachi M, Hinoda Y, Imai K: **MUC1 mucin core protein binds to the domain 1 of ICAM-1.** *Digestion* 2001, **63 Suppl 1**:87-92.
36. McDermott KM, Crocker PR, Harris A, Burdick MD, Hinoda Y, Hayashi T, Imai K, Hollingsworth MA: **Overexpression of MUC1 reconfigures the binding properties of tumor cells.** *Int J Cancer* 2001, **94**:783-791.
37. Treon SP, Raje, N., Ti, Y.T., Hideshima, T., Shima, Y., Davies, F.E., Hilgers, J., Hoffman, P., Anderson, K.C.: **Expression of MUC1 core protein on multiple myeloma plasma cells permits binding to ICAM-1.** *41st Annual Meeting of the American Society of Hematology* 1999.
38. Rahn JJ, Hugh JC: **The MUC1/ICAM-1 signal: its potential to trigger tumor cell migration.** *Six Conference on Signaling in Normal and Cancer Cells, IRCM* 2004.
39. Handa K, Jacobs F, Longenecker BM, Hakomori SI: **Association of MUC-1 and SPGL-1 with low-density microdomain in T-lymphocytes: a preliminary note.** *Biochem Biophys Res Commun* 2001, **285**:788-794.
40. Foster LJ, De Hoog CL, Mann M: **Unbiased quantitative proteomics of lipid rafts reveals high specificity for signaling factors.** *Proc Natl Acad Sci U S A* 2003, **100**:5813-5818.
41. Correa I, Plunkett T, Vlad A, Mungul A, Candelora-Kettel J, Burchell JM, Taylor-Papadimitriou J, Finn OJ: **Form and pattern of MUC1 expression on T cells activated in vivo or in vitro suggests a function in T-cell migration.** *Immunology* 2003, **108**:32-41.
42. Bennett R, Jr., Jarvela T, Engelhardt P, Kostamovaara L, Sparks P, Carpen O, Turunen O, Vaheri A: **Mucin MUC1 is seen in cell surface protrusions together with ezrin in immunoelectron tomography and is concentrated at tips of filopodial protrusions in MCF-7 breast carcinoma cells.** *J Histochem Cytochem* 2001, **49**:67-77.
43. Wang H, Lillehoj EP, Kim KC: **Identification of four sites of stimulated tyrosine phosphorylation in the MUC1 cytoplasmic tail.** *Biochem Biophys Res Commun* 2003, **310**:341-346.
44. Zrihan-Licht S, Baruch A, Elroy-Stein O, Keydar I, Wreschner DH: **Tyrosine phosphorylation of the MUC1 breast cancer membrane proteins. Cytokine receptor-like molecules.** *FEBS Lett* 1994, **356**:130-136.
45. Black R, Jarman L, Simpson J: **The Science and Breastfeeding.** *Jones and Bartlett, london* 1998.
46. Hovey RC, Trott JF, Vonderhaar BK: **Establishing a framework for the functional mammary gland: from endocrinology to morphology.** *J Mammary Gland Biol Neoplasia* 2002, **7**:17-38.
47. Hu MC, Rosenblum ND: **Genetic regulation of branching morphogenesis: lessons learned from loss-of-function phenotypes.** *Pediatr Res* 2003, **54**:433-438.

48. Parmar H, Cunha GR: **Epithelial-stromal interactions in the mouse and human mammary gland in vivo.** *Endocr Relat Cancer* 2004, **11**:437-458.
49. **Structure of mammary gland in mature female on World Wide Web URL: http://courseweb.edteched.uottawa.ca/medicine-histology/English/Reproduction/Mammary/Mammary_repro.htm.**
50. Hansen RK, Bissell MJ: **Tissue architecture and breast cancer: the role of extracellular matrix and steroid hormones.** *Endocr Relat Cancer* 2000, **7**:95-113.
51. Shillingford JM, Hennighausen L: **Experimental mouse genetics-- answering fundamental questions about mammary gland biology.** *Trends Endocrinol Metab* 2001, **12**:402-408.
52. Russo J, Hu YF, Silva ID, Russo IH: **Cancer risk related to mammary gland structure and development.** *Microsc Res Tech* 2001, **52**:204-223.
53. Yang X, Lippman ME: **BRCA1 and BRCA2 in breast cancer.** *Breast Cancer Res Treat* 1999, **54**:1-10.
54. Byers S, Park M, Sommers C, Seslar S: **Breast carcinoma: a collective disorder.** *Breast Cancer Res Treat* 1994, **31**:203-215.
55. Edlich RF, Winters KL, Lin KY: **Breast cancer and ovarian cancer genetics.** *J Long Term Eff Med Implants* 2005, **15**:533-545.
56. Ingvarsson S: **Molecular genetics of breast cancer progression.** *Semin Cancer Biol* 1999, **9**:277-288.
57. Nicolini A, Carpi A, Tarro G: **Biomolecular markers of breast cancer.** *Front Biosci* 2006, **11**:1818-1843.
58. Ellisen LW, Haber DA: **Hereditary breast cancer.** *Annu Rev Med* 1998, **49**:425-436.
59. Hampl M, Chang-Claude J, Schwarz P, Saeger HD, Schackert HK: **[Molecular genetics of hereditary breast carcinoma].** *Zentralbl Chir* 1997, **122**:67-73.
60. Pavelic K, Gall-Troselj K: **Recent advances in molecular genetics of breast cancer.** *J Mol Med* 2001, **79**:566-573.
61. Schuyer M, Berns EM: **Is TP53 dysfunction required for BRCA1-associated carcinogenesis?** *Mol Cell Endocrinol* 1999, **155**:143-152.
62. Bieche I, Olivi M, Nogues C, Vidaud M, Lidereau R: **Prognostic value of CCND1 gene status in sporadic breast tumours, as determined by real-time quantitative PCR assays.** *Br J Cancer* 2002, **86**:580-586.
63. Desai KV, Kavanaugh CJ, Calvo A, Green JE: **Chipping away at breast cancer: insights from microarray studies of human and mouse mammary cancer.** *Endocr Relat Cancer* 2002, **9**:207-220.
64. Miyakis S, Spandidos DA: **Allelic loss in breast cancer.** *Cancer Detect Prev* 2002, **26**:426-434.
65. Bianco T, Chenevix-Trench G, Walsh DC, Cooper JE, Dobrovic A: **Tumour-specific distribution of BRCA1 promoter region methylation supports a pathogenetic role in breast and ovarian cancer.** *Carcinogenesis* 2000, **21**:147-151.
66. Birgisdottir V, Stefansson OA, Bodvarsdottir SK, Hilmarsdottir H, Jonasson JG, Eyfjord JE: **Epigenetic silencing and deletion of the BRCA1 gene in sporadic breast cancer.** *Breast Cancer Res* 2006, **8**:R38.
67. Ross JS, Fletcher JA: **The HER-2/neu oncogene in breast cancer: prognostic factor, predictive factor, and target for therapy.** *Stem Cells* 1998, **16**:413-428.

68. Camirand A, Zakikhani M, Young F, Pollak M: **Inhibition of insulin-like growth factor-1 receptor signaling enhances growth-inhibitory and proapoptotic effects of gefitinib (Iressa) in human breast cancer cells.** *Breast Cancer Res* 2005, **7**:R570-579.
69. Kretzschmar M: **Transforming growth factor-beta and breast cancer: Transforming growth factor-beta/SMAD signaling defects and cancer.** *Breast Cancer Res* 2000, **2**:107-115.
70. Elliott BE, Hung WL, Boag AH, Tuck AB: **The role of hepatocyte growth factor (scatter factor) in epithelial-mesenchymal transition and breast cancer.** *Can J Physiol Pharmacol* 2002, **80**:91-102.
71. Hollingsworth MA, Swanson BJ: **Mucins in cancer: protection and control of the cell surface.** *Nat Rev Cancer* 2004, **4**:45-60.
72. Lanyi M: *Mammography : diagnosis and pathological analysis.* Berlin ; New York: Springer-Verlag; 2003.
73. Page DL, Anderson TJ: *Diagnostic histopathology of the breast.* Edinburgh ; New York: Churchill Livingstone; 1987.
74. Robbins SL, Kumar V: *Basic pathology* edn 4th. Philadelphia: Saunders; 1987.
75. Mayne PD, Thakrar S, Rosalki SB, Foo AY, Parbhoo S: **Identification of bone and liver metastases from breast cancer by measurement of plasma alkaline phosphatase isoenzyme activity.** *J Clin Pathol* 1987, **40**:398-403.
76. Ohno S, Ishida M, Kataoka A, Murakami S: **Brain metastasis of breast cancer.** *Breast Cancer* 2004, **11**:27-29.
77. Ozlem ER, Coskun HS, Soyuer I, Altinbas M: **Late onset of distant meastases from breast cancer.** *Turk J Cancer* 2001, **31**:125-130.
78. Tannock I, Hill RP: *The basic science of oncology* edn 3rd. New York: McGraw-Hill, Health Professions Division; 1998.
79. Hood JD, Cheresh DA: **Role of integrins in cell invasion and migration.** *Nat Rev Cancer* 2002, **2**:91-100.
80. Gordon VD, Valentine MT, Gardel ML, Andor-Ardo D, Dennison S, Bogdanov AA, Weitz DA, Deisboeck TS: **Measuring the mechanical stress induced by an expanding multicellular tumor system: a case study.** *Exp Cell Res* 2003, **289**:58-66.
81. Berx G, Van Roy F: **The E-cadherin/catenin complex: an important gatekeeper in breast cancer tumorigenesis and malignant progression.** *Breast Cancer Res* 2001, **3**:289-293.
82. Sarrio D, Perez-Mies B, Hardisson D, Moreno-Bueno G, Suarez A, Cano A, Martin-Perez J, Gamallo C, Palacios J: **Cytoplasmic localization of p120ctn and E-cadherin loss characterize lobular breast carcinoma from preinvasive to metastatic lesions.** *Oncogene* 2004, **23**:3272-3283.
83. Yu Q, Stamenkovic I: **Cell surface-localized matrix metalloproteinase-9 proteolytically activates TGF-beta and promotes tumor invasion and angiogenesis.** *Genes Dev* 2000, **14**:163-176.
84. Duffy MJ, Maguire TM, Hill A, McDermott E, O'Higgins N: **Metalloproteinases: role in breast carcinogenesis, invasion and metastasis.** *Breast Cancer Res* 2000, **2**:252-257.

85. Rabbani SA, Xing RH: **Role of urokinase (uPA) and its receptor (uPAR) in invasion and metastasis of hormone-dependent malignancies.** *Int J Oncol* 1998, **12**:911-920.
86. Okusa Y, Ichikura T, Mochizuki H, Shinomiya N: **Urokinase type plasminogen activator and its receptor regulate the invasive potential of gastric cancer cell lines.** *Int J Oncol* 2000, **17**:1001-1005.
87. Lutsenko SV, Kiselev SM, Severin SE: **Molecular mechanisms of tumor angiogenesis.** *Biochemistry (Mosc)* 2003, **68**:286-300.
88. Hoeben A, Landuyt B, Highley MS, Wildiers H, Van Oosterom AT, De Bruijn EA: **Vascular endothelial growth factor and angiogenesis.** *Pharmacol Rev* 2004, **56**:549-580.
89. Fidler IJ: **The pathogenesis of cancer metastasis: the 'seed and soil' hypothesis revisited.** *Nat Rev Cancer* 2003, **3**:453-458.
90. Bohle AS, Kalthoff H: **Molecular mechanisms of tumor metastasis and angiogenesis.** *Langenbecks Arch Surg* 1999, **384**:133-140.
91. Liotta LA: **An attractive force in metastasis.** *Nature* 2001, **410**:24-25.
92. Muller A, Homey B, Soto H, Ge N, Catron D, Buchanan ME, McClanahan T, Murphy E, Yuan W, Wagner SN, et al.: **Involvement of chemokine receptors in breast cancer metastasis.** *Nature* 2001, **410**:50-56.
93. Orr FW, Wang HH, Lafrenie RM, Scherbarth S, Nance DM: **Interactions between cancer cells and the endothelium in metastasis.** *J Pathol* 2000, **190**:310-329.
94. Fabbri M, Bianchi E, Fumagalli L, Pardi R: **Regulation of lymphocyte traffic by adhesion molecules.** *Inflamm Res* 1999, **48**:239-246.
95. Lodish HF: *Molecular cell biology* edn 4th. New York: W.H. Freeman; 2000.
96. Clayton A, Evans RA, Pettit E, Hallett M, Williams JD, Steadman R: **Cellular activation through the ligation of intercellular adhesion molecule-1.** *J Cell Sci* 1998, **111 (Pt 4)**:443-453.
97. Burns AR, Walker DC, Brown ES, Thurmon LT, Bowden RA, Keese CR, Simon SI, Entman ML, Smith CW: **Neutrophil transendothelial migration is independent of tight junctions and occurs preferentially at tricellular corners.** *J Immunol.* 1997, **159**:2893-2903.
98. Bianchi E, Bender JR, Blasi F, Pardi R: **Through and beyond the wall: late steps in leukocyte transendothelial migration.** *Immunol Today* 1997, **18**:586-591.
99. Glinskii OV, Huxley VH, Glinsky GV, Pienta KJ, Raz A, Glinsky VV: **Mechanical entrapment is insufficient and intercellular adhesion is essential for metastatic cell arrest in distant organs.** *Neoplasia* 2005, **7**:522-527.
100. Akhmedkhanov A, Toniolo P, Zeleniuch-Jacquotte A, Kato I, Koenig KL, Shore RE: **Aspirin and epithelial ovarian cancer.** *Prev Med* 2001, **33**:682-687.
101. Wong BC, Jiang X, Fan XM, Lin MC, Jiang SH, Lam SK, Kung HF: **Suppression of RelA/p65 nuclear translocation independent of IkappaB-alpha degradation by cyclooxygenase-2 inhibitor in gastric cancer.** *Oncogene* 2003, **22**:1189-1197.
102. Moyad MA: **An introduction to aspirin, NSAIDs, and COX-2 inhibitors for the primary prevention of cardiovascular events and cancer and their potential preventive role in bladder carcinogenesis: part I.** *Semin Urol Oncol* 2001, **19**:294-305.

103. Kannagi R: **Carbohydrate-mediated cell adhesion involved in hematogenous metastasis of cancer.** *Glycoconj J* 1997, **14**:577-584.
104. Thurin M, Kieber-Emmons T: **SA-Lea and tumor metastasis: the old prediction and recent findings.** *Hybrid Hybridomics* 2002, **21**:111-116.
105. Rahn JJ, University of Alberta. Dept. of Medical Sciences.: **The role of the MUC1/ICAM-1 interaction in promoting breast cancer cell migration**: 2004.
106. Ridley AJ, Schwartz MA, Burridge K, Firtel RA, Ginsberg MH, Borisy G, Parsons JT, Horwitz AR: **Cell migration: integrating signals from front to back.** *Science* 2003, **302**:1704-1709.
107. Thomas SM, Brugge JS: **Cellular functions regulated by Src family kinases.** *Annu Rev Cell Dev Biol* 1997, **13**:513-609.
108. Brakebusch C, Fassler R: **beta 1 integrin function in vivo: adhesion, migration and more.** *Cancer Metastasis Rev* 2005, **24**:403-411.
109. Berman AE, Kozlova NI, Morozevich GE: **Integrins: structure and signaling.** *Biochemistry (Mosc)* 2003, **68**:1284-1299.
110. Chodniewicz D, Klemke RL: **Regulation of integrin-mediated cellular responses through assembly of a CAS/Crk scaffold.** *Biochim Biophys Acta* 2004, **1692**:63-76.
111. Hanks SK, Ryzhova L, Shin NY, Brabek J: **Focal adhesion kinase signaling activities and their implications in the control of cell survival and motility.** *Front Biosci* 2003, **8**:d982-996.
112. Al Masri A, Gendler SJ: **Muc1 affects c-Src signaling in PyV MT-induced mammary tumorigenesis.** *Oncogene* 2005, **24**:5799-5808.
113. Mitra SK, Hanson DA, Schlaepfer DD: **Focal adhesion kinase: in command and control of cell motility.** *Nat Rev Mol Cell Biol* 2005, **6**:56-68.
114. Klemke RL, Cai S, Giannini AL, Gallagher PJ, de Lanerolle P, Cheresh DA: **Regulation of cell motility by mitogen-activated protein kinase.** *J Cell Biol* 1997, **137**:481-492.
115. Reiske HR, Kao SC, Cary LA, Guan JL, Lai JF, Chen HC: **Requirement of phosphatidylinositol 3-kinase in focal adhesion kinase-promoted cell migration.** *J Biol Chem* 1999, **274**:12361-12366.
116. Hiscox S, Morgan L, Green TP, Barrow D, Gee J, Nicholson RI: **Elevated Src activity promotes cellular invasion and motility in tamoxifen resistant breast cancer cells.** *Breast Cancer Res Treat* 2006, **97**:263-274.
117. Russello SV, Shore SK: **Src in human carcinogenesis.** *Front Biosci* 2003, **8**:s1068-1073.
118. Horwitz R, Webb D: **Cell migration.** *Curr Biol* 2003, **13**:R756-759.
119. Selve N, Wegner A: **Rate of treadmilling of actin filaments in vitro.** *J Mol Biol* 1986, **187**:627-631.
120. Feldner JC, Brandt BH: **Cancer cell motility--on the road from c-erbB-2 receptor steered signaling to actin reorganization.** *Exp Cell Res* 2002, **272**:93-108.
121. Kumada T, Komuro H: **Completion of neuronal migration regulated by loss of Ca(2+) transients.** *Proc Natl Acad Sci U S A* 2004, **101**:8479-8484.
122. Marks PW, Hendey B, Maxfield FR: **Attachment to fibronectin or vitronectin makes human neutrophil migration sensitive to alterations in cytosolic free calcium concentration.** *J Cell Biol* 1991, **112**:149-158.

123. Berridge MJ, Lipp P, Bootman MD: **The versatility and universality of calcium signalling.** *Nat Rev Mol Cell Biol* 2000, **1**:11-21.
124. Peres C, Yart A, Perret B, Salles JP, Raynal P: **Modulation of phosphoinositide 3-kinase activation by cholesterol level suggests a novel positive role for lipid rafts in lysophosphatidic acid signalling.** *FEBS Lett* 2003, **534**:164-168.
125. Gomez-Mouton C, Lacalle RA, Mira E, Jimenez-Baranda S, Barber DF, Carrera AC, Martinez AC, Manes S: **Dynamic redistribution of raft domains as an organizing platform for signaling during cell chemotaxis.** *J Cell Biol* 2004, **164**:759-768.
126. Bobe R, Wilde JI, Maschberger P, Venkateswarlu K, Cullen PJ, Siess W, Watson SP: **Phosphatidylinositol 3-kinase-dependent translocation of phospholipase Cgamma2 in mouse megakaryocytes is independent of Bruton tyrosine kinase translocation.** *Blood* 2001, **97**:678-684.
127. Wymann MP, Pirola L: **Structure and function of phosphoinositide 3-kinases.** *Biochim Biophys Acta* 1998, **1436**:127-150.
128. Harootunian AT, Kao JP, Paranjape S, Tsien RY: **Generation of calcium oscillations in fibroblasts by positive feedback between calcium and IP3.** *Science* 1991, **251**:75-78.
129. Keizer J, De Young GW: **Two roles of Ca2+ in agonist stimulated Ca2+ oscillations.** *Biophys J* 1992, **61**:649-660.
130. Kwiatkowski DJ: **Functions of gelsolin: motility, signaling, apoptosis, cancer.** *Curr Opin Cell Biol* 1999, **11**:103-108.
131. Harnett KM, Cao W, Kim N, Sohn UD, Rich H, Behar J, Biancani P: **Signal transduction in esophageal and LES circular muscle contraction.** *Yale J Biol Med* 1999, **72**:153-168.
132. Means AR: **Regulatory cascades involving calmodulin-dependent protein kinases.** *Mol Endocrinol* 2000, **14**:4-13.
133. Franco SJ, Huttenlocher A: **Regulating cell migration: calpains make the cut.** *J Cell Sci* 2005, **118**:3829-3838.
134. Fay FS, Gilbert SH, Brundage RA: **Calcium signalling during chemotaxis.** *Ciba Found Symp* 1995, **188**:121-135; discussion 136-140.
135. Pollard TD, Borisy GG: **Cellular motility driven by assembly and disassembly of actin filaments.** *Cell* 2003, **112**:453-465.
136. Welch MD, Mullins RD: **Cellular control of actin nucleation.** *Annu Rev Cell Dev Biol* 2002, **18**:247-288.
137. Raftopoulou M, Hall A: **Cell migration: Rho GTPases lead the way.** *Dev Biol* 2004, **265**:23-32.
138. Ridley AJ: **Rho GTPases and cell migration.** *J Cell Sci* 2001, **114**:2713-2722.
139. Miki H, Takenawa T: **Regulation of actin dynamics by WASP family proteins.** *J Biochem (Tokyo)* 2003, **134**:309-313.
140. Miki H, Sasaki T, Takai Y, Takenawa T: **Induction of filopodium formation by a WASP-related actin-depolymerizing protein N-WASP.** *Nature* 1998, **391**:93-96.
141. Carlier MF, Ducruix A, Pantaloni D: **Signalling to actin: the Cdc42-N-WASP-Arp2/3 connection.** *Chem Biol* 1999, **6**:R235-240.

142. Snapper SB, Takeshima F, Anton I, Liu CH, Thomas SM, Nguyen D, Dudley D, Fraser H, Purich D, Lopez-Ilasaca M, et al.: **N-WASP deficiency reveals distinct pathways for cell surface projections and microbial actin-based motility.** *Nat Cell Biol* 2001, **3**:897-904.
143. Nozumi M, Nakagawa H, Miki H, Takenawa T, Miyamoto S: **Differential localization of WAVE isoforms in filopodia and lamellipodia of the neuronal growth cone.** *J Cell Sci* 2003, **116**:239-246.
144. Funamoto S, Meili R, Lee S, Parry L, Firtel RA: **Spatial and temporal regulation of 3-phosphoinositides by PI 3-kinase and PTEN mediates chemotaxis.** *Cell* 2002, **109**:611-623.
145. Hawkins PT, Eguinoa A, Qiu RG, Stokoe D, Cooke FT, Walters R, Wennstrom S, Claesson-Welsh L, Evans T, Symons M, et al.: **PDGF stimulates an increase in GTP-Rac via activation of phosphoinositide 3-kinase.** *Curr Biol* 1995, **5**:393-403.
146. Li Z, Hannigan M, Mo Z, Liu B, Lu W, Wu Y, Smrcka AV, Wu G, Li L, Liu M, et al.: **Directional sensing requires G beta gamma-mediated PAK1 and PIX alpha-dependent activation of Cdc42.** *Cell* 2003, **114**:215-227.
147. Welch HC, Coadwell WJ, Stephens LR, Hawkins PT: **Phosphoinositide 3-kinase-dependent activation of Rac.** *FEBS Lett* 2003, **546**:93-97.
148. Srinivasan S, Wang F, Glavas S, Ott A, Hofmann F, Aktories K, Kalman D, Bourne HR: **Rac and Cdc42 play distinct roles in regulating PI(3,4,5)P3 and polarity during neutrophil chemotaxis.** *J Cell Biol* 2003, **160**:375-385.
149. Devreotes P, Janetopoulos C: **Eukaryotic chemotaxis: distinctions between directional sensing and polarization.** *J Biol Chem* 2003, **278**:20445-20448.
150. Hall A: **Rho GTPases and the actin cytoskeleton.** *Science* 1998, **279**:509-514.
151. Simons K, Toomre D: **Lipid rafts and signal transduction.** *Nat Rev Mol Cell Biol* 2000, **1**:31-39.
152. Zajchowski LD, Robbins SM: **Lipid rafts and little caves. Compartmentalized signalling in membrane microdomains.** *Eur J Biochem* 2002, **269**:737-752.
153. Manes S, Mira E, Gomez-Mouton C, Lacalle RA, Keller P, Labrador JP, Martinez AC: **Membrane raft microdomains mediate front-rear polarity in migrating cells.** *Embo J* 1999, **18**:6211-6220.
154. Heijnen HF, Van Lier M, Waaijenborg S, Ohno-Iwashita Y, Waheed AA, Inomata M, Gorter G, Mobius W, Akkerman JW, Slot JW: **Concentration of rafts in platelet filopodia correlates with recruitment of c-Src and CD63 to these domains.** *J Thromb Haemost* 2003, **1**:1161-1173.
155. van Rheenen J, Achame EM, Janssen H, Calafat J, Jalink K: **PIP2 signaling in lipid domains: a critical re-evaluation.** *Embo J* 2005, **24**:1664-1673.
156. Higgs HN, Pollard TD: **Activation by Cdc42 and PIP(2) of Wiskott-Aldrich syndrome protein (WASp) stimulates actin nucleation by Arp2/3 complex.** *J Cell Biol* 2000, **150**:1311-1320.
157. Rozelle AL, Machesky LM, Yamamoto M, Driessens MH, Insall RH, Roth MG, Luby-Phelps K, Marriott G, Hall A, Yin HL: **Phosphatidylinositol 4,5-bisphosphate induces actin-based movement of raft-enriched vesicles through WASP-Arp2/3.** *Curr Biol* 2000, **10**:311-320.

158. Golub T, Caroni P: **PI(4,5)P2-dependent microdomain assemblies capture microtubules to promote and control leading edge motility.** *J Cell Biol* 2005, **169**:151-165.
159. Sato K, Fukami Y, Stith BJ: **Signal transduction pathways leading to Ca(2+) release in a vertebrate model system: Lessons from Xenopus eggs.** *Semin Cell Dev Biol* 2006, **17**:285-292.
160. Isshiki M, Anderson RG: **Calcium signal transduction from caveolae.** *Cell Calcium* 1999, **26**:201-208.
161. Carraway KL, Ramsauer VP, Haq B, Carothers Carraway CA: **Cell signaling through membrane mucins.** *Bioessays* 2003, **25**:66-71.
162. Gendler SJ: **MUC1, the renaissance molecule.** *J Mammary Gland Biol Neoplasia* 2001, **6**:339-353.
163. Gendler SJ, Cohen EP, Craston A, Duhig T, Johnstone G, Barnes D: **The locus of the polymorphic epithelial mucin (PEM) tumour antigen on chromosome 1q21 shows a high frequency of alteration in primary human breast tumours.** *Int J Cancer* 1990, **45**:431-435.
164. Kobylka D, Carraway KL: **Proteins and glycoproteins of the milk fat globule membrane.** *Biochim Biophys Acta* 1972, **288**:282-295.
165. Hilkens J, Buijs F: **Biosynthesis of MAM-6, an epithelial sialomucin. Evidence for involvement of a rare proteolytic cleavage step in the endoplasmic reticulum.** *J Biol Chem* 1988, **263**:4215-4222.
166. Gendler S, Taylor-Papadimitriou J, Duhig T, Rothbard J, Burchell J: **A highly immunogenic region of a human polymorphic epithelial mucin expressed by carcinomas is made up of tandem repeats.** *J Biol Chem* 1988, **263**:12820-12823.
167. Baldus SE, Engelmann K, Hanisch FG: **MUC1 and the MUCs: a family of human mucins with impact in cancer biology.** *Crit Rev Clin Lab Sci* 2004, **41**:189-231.
168. Litvinov SV, Hilkens J: **The epithelial sialomucin, episialin, is sialylated during recycling.** *J Biol Chem* 1993, **268**:21364-21371.
169. Altschuler Y, Kinlough CL, Poland PA, Bruns JB, Apodaca G, Weisz OA, Hughey RP: **Clathrin-mediated endocytosis of MUC1 is modulated by its glycosylation state.** *Mol Biol Cell* 2000, **11**:819-831.
170. Scheiffele P, Peranen J, Simons K: **N-glycans as apical sorting signals in epithelial cells.** *Nature* 1995, **378**:96-98.
171. Fukuda M: **Possible roles of tumor-associated carbohydrate antigens.** *Cancer Res* 1996, **56**:2237-2244.
172. Jentoft N: **Why are proteins O-glycosylated?** *Trends Biochem Sci* 1990, **15**:291-294.
173. Fontenot JD, Tjandra N, Bu D, Ho C, Montelaro RC, Finn OJ: **Biophysical characterization of one-, two-, and three-tandem repeats of human mucin (muc-1) protein core.** *Cancer Res* 1993, **53**:5386-5394.
174. Hilkens J, Wesseling J, Vos HL, Storm J, Boer B, van der Valk SW, Maas MC: **Involvement of the cell surface-bound mucin, episialin/MUC1, in progression of human carcinomas.** *Biochem Soc Trans* 1995, **23**:822-826.
175. van de Wiel-van Kemenade E, Ligtenberg MJ, de Boer AJ, Buijs F, Vos HL, Melief CJ, Hilkens J, Figdor CG: **Episialin (MUC1) inhibits cytotoxic lymphocyte-target cell interaction.** *J Immunol* 1993, **151**:767-776.

176. Bork P, Patthy L: **The SEA module: a new extracellular domain associated with O-glycosylation.** *Protein Sci* 1995, **4**:1421-1425.
177. Wreschner DH, McGuckin MA, Williams SJ, Baruch A, Yoeli M, Ziv R, Okun L, Zaretsky J, Smorodinsky N, Keydar I, et al.: **Generation of ligand-receptor alliances by "SEA" module-mediated cleavage of membrane-associated mucin proteins.** *Protein Sci* 2002, **11**:698-706.
178. Parry S, Silverman HS, McDermott K, Willis A, Hollingsworth MA, Harris A: **Identification of MUC1 proteolytic cleavage sites in vivo.** *Biochem Biophys Res Commun* 2001, **283**:715-720.
179. Roy R, Laage R, Langosch D: **Synaptobrevin transmembrane domain dimerization-revisited.** *Biochemistry* 2004, **43**:4964-4970.
180. Stipp CS, Kolesnikova TV, Hemler ME: **Functional domains in tetraspanin proteins.** *Trends Biochem Sci* 2003, **28**:106-112.
181. Liu D, Sy MS: **Phorbol myristate acetate stimulates the dimerization of CD44 involving a cysteine in the transmembrane domain.** *J Immunol* 1997, **159**:2702-2711.
182. Macdonald J, Li Z, Su W, Pike LJ: **The membrane proximal disulfides of the EGF receptor extracellular domain are required for high affinity binding and signal transduction but do not play a role in the localization of the receptor to lipid rafts.** *Biochim Biophys Acta* 2006.
183. Li Y, Ren J, Yu W, Li Q, Kuwahara H, Yin L, Carraway KL, 3rd, Kufe D: **The epidermal growth factor receptor regulates interaction of the human DF3/MUC1 carcinoma antigen with c-Src and beta-catenin.** *J Biol Chem* 2001, **276**:35239-35242.
184. Schroeder JA, Thompson MC, Gardner MM, Gendler SJ: **Transgenic MUC1 interacts with epidermal growth factor receptor and correlates with mitogen-activated protein kinase activation in the mouse mammary gland.** *J Biol Chem* 2001, **276**:13057-13064.
185. Ren J, Li Y, Kufe D: **Protein kinase C delta regulates function of the DF3/MUC1 carcinoma antigen in beta-catenin signaling.** *J Biol Chem* 2002, **277**:17616-17622.
186. Li Y, Kuwahara H, Ren J, Wen G, Kufe D: **The c-Src tyrosine kinase regulates signaling of the human DF3/MUC1 carcinoma-associated antigen with GSK3 beta and beta-catenin.** *J Biol Chem* 2001, **276**:6061-6064.
187. Pandey P, Kharbanda S, Kufe D: **Association of the DF3/MUC1 breast cancer antigen with Grb2 and the Sos/Ras exchange protein.** *Cancer Res* 1995, **55**:4000-4003.
188. Li Y, Bharti A, Chen D, Gong J, Kufe D: **Interaction of glycogen synthase kinase 3beta with the DF3/MUC1 carcinoma-associated antigen and beta-catenin.** *Mol Cell Biol* 1998, **18**:7216-7224.
189. Yamamoto M, Bharti A, Li Y, Kufe D: **Interaction of the DF3/MUC1 breast carcinoma-associated antigen and beta-catenin in cell adhesion.** *J Biol Chem* 1997, **272**:12492-12494.
190. Schroeder JA, Adriance MC, Thompson MC, Camenisch TD, Gendler SJ: **MUC1 alters beta-catenin-dependent tumor formation and promotes cellular invasion.** *Oncogene* 2003, **22**:1324-1332.

191. Li Y, Yu WH, Ren J, Chen W, Huang L, Kharbanda S, Loda M, Kufe D: **Heregulin targets gamma-catenin to the nucleolus by a mechanism dependent on the DF3/MUC1 oncoprotein.** *Mol Cancer Res* 2003, **1**:765-775.
192. Li Y, Kufe D: **The Human DF3/MUC1 carcinoma-associated antigen signals nuclear localization of the catenin p120(ctn).** *Biochem Biophys Res Commun* 2001, **281**:440-443.
193. Hattrup CL, Fernandez-Rodriguez J, Schroeder JA, Hansson GC, Gendler SJ: **MUC1 can interact with adenomatous polyposis coli in breast cancer.** *Biochem Biophys Res Commun* 2004, **316**:364-369.
194. Parry G, Beck JC, Moss L, Bartley J, Ojakian GK: **Determination of apical membrane polarity in mammary epithelial cell cultures: the role of cell-cell, cell-substratum, and membrane-cytoskeleton interactions.** *Exp Cell Res* 1990, **188**:302-311.
195. Williams CJ, Wreschner DH, Tanaka A, Tsarfaty I, Keydar I, Dion AS: **Multiple protein forms of the human breast tumor-associated epithelial membrane antigen (EMA) are generated by alternative splicing and induced by hormonal stimulation.** *Biochem Biophys Res Commun* 1990, **170**:1331-1338.
196. Baruch A, Hartmann M, Yoeli M, Adereth Y, Greenstein S, Stadler Y, Skornik Y, Zaretsky J, Smorodinsky NI, Keydar I, et al.: **The breast cancer-associated MUC1 gene generates both a receptor and its cognate binding protein.** *Cancer Res* 1999, **59**:1552-1561.
197. Baruch A, Hartmann M, Zrihan-Licht S, Greenstein S, Burstein M, Keydar I, Weiss M, Smorodinsky N, Wreschner DH: **Preferential expression of novel MUC1 tumor antigen isoforms in human epithelial tumors and their tumor-potentiating function.** *Int J Cancer* 1997, **71**:741-749.
198. Schaller MD, Parsons JT: **pp125FAK-dependent tyrosine phosphorylation of paxillin creates a high-affinity binding site for Crk.** *Mol Cell Biol* 1995, **15**:2635-2645.
199. Oosterkamp HM, Scheiner L, Stefanova MC, Lloyd KO, Finstad CL: **Comparison of MUC-1 mucin expression in epithelial and non-epithelial cancer cell lines and demonstration of a new short variant form (MUC-1/Z).** *Int J Cancer* 1997, **72**:87-94.
200. Thathiah A, Blobel CP, Carson DD: **Tumor necrosis factor-alpha converting enzyme/ADAM 17 mediates MUC1 shedding.** *J Biol Chem* 2003, **278**:3386-3394.
201. Thathiah A, Carson DD: **MT1-MMP mediates MUC1 shedding independent of TACE/ADAM17.** *Biochem J* 2004, **382**:363-373.
202. Kohlgraf KG, Gawron AJ, Higashi M, Meza JL, Burdick MD, Kitajima S, Kelly DL, Caffrey TC, Hollingsworth MA: **Contribution of the MUC1 tandem repeat and cytoplasmic tail to invasive and metastatic properties of a pancreatic cancer cell line.** *Cancer Res* 2003, **63**:5011-5020.
203. Park H, Hyun SW, Kim KC: **Expression of MUC1 mucin gene by hamster tracheal surface epithelial cells in primary culture.** *Am J Respir Cell Mol Biol* 1996, **15**:237-244.
204. Zaretsky JZ, Weiss M, Tsarfaty I, Hareuveni M, Wreschner DH, Keydar I: **Expression of genes coding for pS2, c-erbB2, estrogen receptor and the H23**

breast tumor-associated antigen. A comparative analysis in breast cancer. *FEBS Lett* 1990, **265**:46-50.

205. Hilkens J, Buijs F, Hilgers J, Hageman P, Calafat J, Sonnenberg A, van der Valk M: **Monoclonal antibodies against human milk-fat globule membranes detecting differentiation antigens of the mammary gland and its tumors.** *Int J Cancer* 1984, **34**:197-206.
206. Girling A, Bartkova J, Burchell J, Gendler S, Gillett C, Taylor-Papadimitriou J: **A core protein epitope of the polymorphic epithelial mucin detected by the monoclonal antibody SM-3 is selectively exposed in a range of primary carcinomas.** *Int J Cancer* 1989, **43**:1072-1076.
207. Burchell J, Gendler S, Taylor-Papadimitriou J, Girling A, Lewis A, Millis R, Lamport D: **Development and characterization of breast cancer reactive monoclonal antibodies directed to the core protein of the human milk mucin.** *Cancer Res* 1987, **47**:5476-5482.
208. Spicer AP, Rowse GJ, Lidner TK, Gendler SJ: **Delayed mammary tumor progression in Muc-1 null mice.** *J Biol Chem* 1995, **270**:30093-30101.
209. Takao S, Uchikura K, Yonezawa S, Shinchi H, Aikou T: **Mucin core protein expression in extrahepatic bile duct carcinoma is associated with metastases to the liver and poor prognosis.** *Cancer* 1999, **86**:1966-1975.
210. Guddo F, Giatromanolaki A, Koukourakis MI, Reina C, Vignola AM, Chlouverakis G, Hilkens J, Gatter KC, Harris AL, Bonsignore G: **MUC1 (episialin) expression in non-small cell lung cancer is independent of EGFR and c-erbB-2 expression and correlates with poor survival in node positive patients.** *J Clin Pathol* 1998, **51**:667-671.
211. Nakamori S, Ota DM, Cleary KR, Shirotani K, Irimura T: **MUC1 mucin expression as a marker of progression and metastasis of human colorectal carcinoma.** *Gastroenterology* 1994, **106**:353-361.
212. McGuckin MA, Walsh MD, Hohn BG, Ward BG, Wright RG: **Prognostic significance of MUC1 epithelial mucin expression in breast cancer.** *Hum Pathol* 1995, **26**:432-439.
213. Dong Y, Walsh MD, Cummings MC, Wright RG, Khoo SK, Parsons PG, McGuckin MA: **Expression of MUC1 and MUC2 mucins in epithelial ovarian tumours.** *J Pathol* 1997, **183**:311-317.
214. Sagara M, Yonezawa S, Nagata K, Tezuka Y, Natsugoe S, Xing PX, McKenzie IF, Aikou T, Sato E: **Expression of mucin 1 (MUC1) in esophageal squamous-cell carcinoma: its relationship with prognosis.** *Int J Cancer* 1999, **84**:251-257.
215. Bieche I, Lidereau R: **A gene dosage effect is responsible for high overexpression of the MUC1 gene observed in human breast tumors.** *Cancer Genet Cytogenet* 1997, **98**:75-80.
216. Dyomin VG, Palanisamy N, Lloyd KO, Dyomina K, Jhanwar SC, Houldsworth J, Chaganti RS: **MUC1 is activated in a B-cell lymphoma by the t(1;14)(q21;q32) translocation and is rearranged and amplified in B-cell lymphoma subsets.** *Blood* 2000, **95**:2666-2671.
217. Gilles F, Goy A, Remache Y, Shue P, Zelenetz AD: **MUC1 dysregulation as the consequence of a t(1;14)(q21;q32) translocation in an extranodal lymphoma.** *Blood* 2000, **95**:2930-2936.

218. Clark S, McGuckin MA, Hurst T, Ward BG: **Effect of interferon-gamma and TNF-alpha on MUC1 mucin expression in ovarian carcinoma cell lines.** *Dis Markers* 1994, **12**:43-50.
219. Lagow EL, Carson DD: **Synergistic stimulation of MUC1 expression in normal breast epithelia and breast cancer cells by interferon-gamma and tumor necrosis factor-alpha.** *J Cell Biochem* 2002, **86**:759-772.
220. Gaemers IC, Vos HL, Volders HH, van der Valk SW, Hilkens J: **A stat-responsive element in the promoter of the episialin/MUC1 gene is involved in its overexpression in carcinoma cells.** *J Biol Chem* 2001, **276**:6191-6199.
221. Kuwahara I, Lillehoj EP, Hisatsune A, Lu W, Isohama Y, Miyata T, Kim KC: **Neutrophil elastase stimulates MUC1 gene expression through increased Sp1 binding to the MUC1 promoter.** *Am J Physiol Lung Cell Mol Physiol* 2005, **289**:L355-362.
222. Baeckstrom D, Hansson GC, Nilsson O, Johansson C, Gendler SJ, Lindholm L: **Purification and characterization of a membrane-bound and a secreted mucin-type glycoprotein carrying the carcinoma-associated sialyl-Lea epitope on distinct core proteins.** *J Biol Chem* 1991, **266**:21537-21547.
223. Brockhausen I, Yang JM, Burchell J, Whitehouse C, Taylor-Papadimitriou J: **Mechanisms underlying aberrant glycosylation of MUC1 mucin in breast cancer cells.** *Eur J Biochem* 1995, **233**:607-617.
224. Karsten U, Serttas N, Paulsen H, Danielczyk A, Goletz S: **Binding patterns of DTR-specific antibodies reveal a glycosylation-conditioned tumor-specific epitope of the epithelial mucin (MUC1).** *Glycobiology* 2004, **14**:681-692.
225. Muller S, Alving K, Peter-Katalinic J, Zachara N, Gooley AA, Hanisch FG: **High density O-glycosylation on tandem repeat peptide from secretory MUC1 of T47D breast cancer cells.** *J Biol Chem* 1999, **274**:18165-18172.
226. Perey L, Hayes DF, Kufe D: **Effects of differentiating agents on cell surface expression of the breast carcinoma-associated DF3-P epitope.** *Cancer Res* 1992, **52**:6365-6370.
227. Quin RJ, McGuckin MA: **Phosphorylation of the cytoplasmic domain of the MUC1 mucin correlates with changes in cell-cell adhesion.** *Int J Cancer* 2000, **87**:499-506.
228. Meerzaman D, Xing PX, Kim KC: **Construction and characterization of a chimeric receptor containing the cytoplasmic domain of MUC1 mucin.** *Am J Physiol Lung Cell Mol Physiol* 2000, **278**:L625-629.
229. Lillehoj EP, Kim H, Chun EY, Kim KC: **Pseudomonas aeruginosa stimulates phosphorylation of the airway epithelial membrane glycoprotein Muc1 and activates MAP kinase.** *Am J Physiol Lung Cell Mol Physiol* 2004, **287**:L809-815.
230. Cianga C, Cianga P, Cozma L, Diaconu C, Carasevici E: **[Overexpression of c-erbB-2 gene product is associated with poor prognosis factors in breast carcinoma].** *Rev Med Chir Soc Med Nat Iasi* 2003, **107**:349-353.
231. Arteaga CL: **Epidermal growth factor receptor dependence in human tumors: more than just expression?** *Oncologist* 2002, **7 Suppl 4**:31-39.
232. Lillehoj EP, Hyun SW, Kim BT, Zhang XG, Lee DI, Rowland S, Kim KC: **Muc1 mucins on the cell surface are adhesion sites for Pseudomonas aeruginosa.** *Am J Physiol Lung Cell Mol Physiol* 2001, **280**:L181-187.

233. Lillehoj EP, Kim BT, Kim KC: **Identification of Pseudomonas aeruginosa flagellin as an adhesin for Muc1 mucin.** *Am J Physiol Lung Cell Mol Physiol* 2002, **282**:L751-756.
234. He TC, Sparks AB, Rago C, Hermeking H, Zawel L, da Costa LT, Morin PJ, Vogelstein B, Kinzler KW: **Identification of c-MYC as a target of the APC pathway.** *Science* 1998, **281**:1509-1512.
235. Tetsu O, McCormick F: **Beta-catenin regulates expression of cyclin D1 in colon carcinoma cells.** *Nature* 1999, **398**:422-426.
236. Raina D, Kharbanda S, Kufe D: **The MUC1 oncoprotein activates the anti-apoptotic phosphoinositide 3-kinase/Akt and Bcl-xL pathways in rat 3Y1 fibroblasts.** *J Biol Chem* 2004, **279**:20607-20612.
237. Wei X, Xu H, Kufe D: **MUC1 oncoprotein stabilizes and activates estrogen receptor alpha.** *Mol Cell* 2006, **21**:295-305.
238. Suwa T, Hinoda Y, Makiguchi Y, Takahashi T, Itoh F, Adachi M, Hareyama M, Imai K: **Increased invasiveness of MUC1 and cDNA-transfected human gastric cancer MKN74 cells.** *Int J Cancer* 1998, **76**:377-382.
239. Zhang K, Baeckstrom D, Brevinge H, Hansson GC: **Secreted MUC1 mucins lacking their cytoplasmic part and carrying sialyl-Lewis a and x epitopes from a tumor cell line and sera of colon carcinoma patients can inhibit HL-60 leukocyte adhesion to E-selectin-expressing endothelial cells.** *J Cell Biochem* 1996, **60**:538-549.
240. Hanski C, Drechsler K, Hanisch FG, Sheehan J, Manske M, Ogorek D, Klussmann E, Hanski ML, Blank M, Xing PX, et al.: **Altered glycosylation of the MUC-1 protein core contributes to the colon carcinoma-associated increase of mucin-bound sialyl-Lewis(x) expression.** *Cancer Res* 1993, **53**:4082-4088.
241. Fernandez-Rodriguez J, Dwir O, Alon R, Hansson GC: **Tumor cell MUC1 and CD43 are glycosylated differently with sialyl-Lewis a and x epitopes and show variable interactions with E-selectin under physiological flow conditions.** *Glycoconj J* 2001, **18**:925-930.
242. Sikut R, Zhang K, Baeckstrom D, Hansson GC: **Distinct sub-populations of carcinoma-associated MUC1 mucins as detected by the monoclonal antibody 9H8 and antibodies against the sialyl-Lewis a and sialyl-Lewis x epitopes in the circulation of breast-cancer patients.** *Int J Cancer* 1996, **66**:617-623.
243. van de Stolpe A, van der Saag PT: **Intercellular adhesion molecule-1.** *J Mol Med* 1996, **74**:13-33.
244. Rosette C, Roth RB, Oeth P, Braun A, Kammerer S, Ekblom J, Denissenko MF: **Role of ICAM1 in invasion of human breast cancer cells.** *Carcinogenesis* 2005, **26**:943-950.
245. Staunton DE, Dustin ML, Erickson HP, Springer TA: **The arrangement of the immunoglobulin-like domains of ICAM-1 and the binding sites for LFA-1 and rhinovirus.** *Cell* 1990, **61**:243-254.
246. Staunton DE, Marlin SD, Stratowa C, Dustin ML, Springer TA: **Primary structure of ICAM-1 demonstrates interaction between members of the immunoglobulin and integrin supergene families.** *Cell* 1988, **52**:925-933.

247. Anderson ME, Siahaan TJ: **Targeting ICAM-1/LFA-1 interaction for controlling autoimmune diseases: designing peptide and small molecule inhibitors.** *Peptides* 2003, **24**:487-501.
248. Jun CD, Shimaoka M, Carman CV, Takagi J, Springer TA: **Dimerization and the effectiveness of ICAM-1 in mediating LFA-1-dependent adhesion.** *Proc Natl Acad Sci U S A* 2001, **98**:6830-6835.
249. Dustin ML, Rothlein R, Bhan AK, Dinarello CA, Springer TA: **Induction by IL 1 and interferon-gamma: tissue distribution, biochemistry, and function of a natural adherence molecule (ICAM-1).** *J Immunol* 1986, **137**:245-254.
250. Rothlein R, Dustin ML, Marlin SD, Springer TA: **A human intercellular adhesion molecule (ICAM-1) distinct from LFA-1.** *J Immunol* 1986, **137**:1270-1274.
251. Tilghman RW, Hoover RL: **E-selectin and ICAM-1 are incorporated into detergent-insoluble membrane domains following clustering in endothelial cells.** *FEBS Lett* 2002, **525**:83-87.
252. Carpen O, Pallai P, Staunton DE, Springer TA: **Association of intercellular adhesion molecule-1 (ICAM-1) with actin-containing cytoskeleton and alpha-actinin.** *J Cell Biol* 1992, **118**:1223-1234.
253. Romero IA, Amos CL, Greenwood J, Adamson P: **Ezrin and moesin co-localise with ICAM-1 in brain endothelial cells but are not directly associated.** *Brain Res Mol Brain Res* 2002, **105**:47-59.
254. Barreiro O, Yanez-Mo M, Serrador JM, Montoya MC, Vicente-Manzanares M, Tejedor R, Furthmayr H, Sanchez-Madrid F: **Dynamic interaction of VCAM-1 and ICAM-1 with moesin and ezrin in a novel endothelial docking structure for adherent leukocytes.** *J Cell Biol* 2002, **157**:1233-1245.
255. Albelda SM: **Endothelial and epithelial cell adhesion molecules.** *Am J Respir Cell Mol Biol* 1991, **4**:195-203.
256. Fabry Z, Waldschmidt MM, Hendrickson D, Keiner J, Love-Homan L, Takei F, Hart MN: **Adhesion molecules on murine brain microvascular endothelial cells: expression and regulation of ICAM-1 and Lgp 55.** *J Neuroimmunol* 1992, **36**:1-11.
257. Wyble CW, Desai TR, Clark ET, Hynes KL, Gewertz BL: **Physiologic concentrations of TNFalpha and IL-1beta released from reperfused human intestine upregulate E-selectin and ICAM-1.** *J Surg Res* 1996, **63**:333-338.
258. Bradley JR, Pober JS: **Prolonged cytokine exposure causes a dynamic redistribution of endothelial cell adhesion molecules to intercellular junctions.** *Lab Invest* 1996, **75**:463-472.
259. Ledebur HC, Parks TP: **Transcriptional regulation of the intercellular adhesion molecule-1 gene by inflammatory cytokines in human endothelial cells. Essential roles of a variant NF-kappa B site and p65 homodimers.** *J Biol Chem* 1995, **270**:933-943.
260. Braddock M, Schwachtgen JL, Houston P, Dickson MC, Lee MJ, Campbell CJ: **Fluid Shear Stress Modulation of Gene Expression in Endothelial Cells.** *News Physiol Sci* 1998, **13**:241-246.
261. van de Stolpe A, Caldenhoven E, Raaijmakers JA, van der Saag PT, Koenderman L: **Glucocorticoid-mediated repression of intercellular adhesion molecule-1**

expression in human monocytic and bronchial epithelial cell lines. *Am J Respir Cell Mol Biol* 1993, **8**:340-347.
262. van de Stolpe A, Caldenhoven E, Stade BG, Koenderman L, Raaijmakers JA, Johnson JP, van der Saag PT: **12-O-tetradecanoylphorbol-13-acetate- and tumor necrosis factor alpha-mediated induction of intercellular adhesion molecule-1 is inhibited by dexamethasone. Functional analysis of the human intercellular adhesion molecular-1 promoter.** *J Biol Chem* 1994, **269**:6185-6192.
263. Griffioen AW, Relou IA, Gallardo Torres HI, Damen CA, Martinotti S, De Graaf JC, Zwaginga JJ, Groenewegen G: **The angiogenic factor bFGF impairs leukocyte adhesion and rolling under flow conditions.** *Angiogenesis* 1998, **2**:235-243.
264. Cook-Mills JM, Deem TL: **Active participation of endothelial cells in inflammation.** *J Leukoc Biol* 2005, **77**:487-495.
265. Diamond MS, Staunton DE, Marlin SD, Springer TA: **Binding of the integrin Mac-1 (CD11b/CD18) to the third immunoglobulin-like domain of ICAM-1 (CD54) and its regulation by glycosylation.** *Cell* 1991, **65**:961-971.
266. Rosenstein Y, Park JK, Hahn WC, Rosen FS, Bierer BE, Burakoff SJ: **CD43, a molecule defective in Wiskott-Aldrich syndrome, binds ICAM-1.** *Nature* 1991, **354**:233-235.
267. Tiisala S, Majuri ML, Carpen O, Renkonen R: **Enhanced ICAM-1-dependent adhesion of myelomonocytic cells expressing increased levels of beta 2-integrins and CD43.** *Scand J Immunol* 1994, **39**:249-256.
268. Jun CD, Carman CV, Redick SD, Shimaoka M, Erickson HP, Springer TA: **Ultrastructure and function of dimeric, soluble intercellular adhesion molecule-1 (ICAM-1).** *J Biol Chem* 2001, **276**:29019-29027.
269. Reilly PL, Woska JR, Jr., Jeanfavre DD, McNally E, Rothlein R, Bormann BJ: **The native structure of intercellular adhesion molecule-1 (ICAM-1) is a dimer. Correlation with binding to LFA-1.** *J Immunol* 1995, **155**:529-532.
270. Sanders VM, Vitetta ES: **B cell-associated LFA-1 and T cell-associated ICAM-1 transiently cluster in the area of contact between interacting cells.** *Cell Immunol* 1991, **132**:45-55.
271. Etienne-Manneville S, Manneville JB, Adamson P, Wilbourn B, Greenwood J, Couraud PO: **ICAM-1-coupled cytoskeletal rearrangements and transendothelial lymphocyte migration involve intracellular calcium signaling in brain endothelial cell lines.** *J Immunol* 2000, **165**:3375-3383.
272. Etienne S, Adamson P, Greenwood J, Strosberg AD, Cazaubon S, Couraud PO: **ICAM-1 signaling pathways associated with Rho activation in microvascular brain endothelial cells.** *J Immunol* 1998, **161**:5755-5761.
273. Tilghman RW, Hoover RL: **The Src-cortactin pathway is required for clustering of E-selectin and ICAM-1 in endothelial cells.** *Faseb J* 2002, **16**:1257-1259.
274. Smith A, Bracke M, Leitinger B, Porter JC, Hogg N: **LFA-1-induced T cell migration on ICAM-1 involves regulation of MLCK-mediated attachment and ROCK-dependent detachment.** *J Cell Sci* 2003, **116**:3123-3133.
275. Burns AR, Bowden RA, MacDonell SD, Walker DC, Odebunmi TO, Donnachie EM, Simon SI, Entman ML, Smith CW: **Analysis of tight junctions during neutrophil transendothelial migration.** *J Cell Sci* 2000, **113(Pt1)**:45-57.

276. Ozaki H, Ishii K, Horiuchi H, Arai H, Kawamoto T, Okawa K, Iwamatsu A, Kita T: **Cutting edge: combined treatment of TNF-alpha and IFN-gamma causes redistribution of junctional adhesion molecule in human endothelial cells.** *J Immunol* 1999, **163**:553-557.
277. Lewalle JM, Cataldo D, Bajou K, Lambert CA, Foidart JM: **Endothelial cell intracellular Ca2+ concentration is increased upon breast tumor cell contact and mediates tumor cell transendothelial migration.** *Clin Exp Metastasis* 1998, **16**:21-29.
278. Lewalle JM, Bajou K, Desreux J, Mareel M, Dejana E, Noel A, Foidart JM: **Alteration of interendothelial adherens junctions following tumor cell-endothelial cell interaction in vitro.** *Exp Cell Res* 1997, **237**:347-356.

Chapter 2: MUC1/ICAM-1 Ligation Induced Signaling[1]

[1]Part of this chapter has been published in the J Biol Chem. 2004 279:29386-90 by Qiang Shen as co-first author. Work present in this chapter of the thesis is data directly generated by Qiang Shen.

2.0. Introduction

MUC1, as described in Chapter 1, when aberrantly expressed on breast cancer cells is crucial for mammary tumorigenesis and metastasis [1-3]. We and others have previously demonstrated that MUC1 can function as an adhesion receptor for ICAM-1 expressed on accessory cells [4-8] and facilitate transendothelial migration of MUC1-bearing cells through a monolayer of ICAM-1-expressing cells [9,10]. Also, accumulating evidence has demonstrated that MUC1-CD is associated with signaling mediators, such as Src, Grb2 and β-catenin [11-17], all of which have been implicated in cell motility. Therefore, it is possible that MUC1 may initiate a pro-migratory signaling cascade in response to ICAM-1 ligation.

Calcium-based signaling has long been associated with cell migration. It is well known that calcium can activate actin binding proteins, such as gelsolin and myosin, to facilitate actin cytoskeletal rearrangements and cellular contraction [18,19]. Further, calcium can also activate calpain and PKC, the calcium-dependent proteins, to promote focal contact dynamics and cell motility [18,20-22]. Significantly, compelling studies based on normal migrating cells, such as immature neurons and neutrophils, have demonstrated that transient intracellular calcium elevations or oscillations are obligatory events in migration and the frequency of the oscillations is directly related to the rate of cellular migration [23-25]. Since MUC1 was reported to interact directly with Src [12,13], which has been implicated in the calcium signaling [19,26], it seemed worthwhile to determine if any such signal might be initiated by the MUC1/ICAM-1 interaction. Thus, the specific questions asked in this chapter were: 1) Was the hypothesized MUC1/ICAM-1 ligation-induced signal calcium-based? If so, 2) what is

the underlying molecular mechanism(s)? Addressing these issues represents a crucial step in understanding the role of MUC1 in tumor malignant progression and metastasis.

2.1. Materials and Methods

2.1.1. Reagents

The B27.29 mouse monoclonal antibody (mAb) against the MUC1-ECD PDTRPAP epitope was kindly provided by Biomira, Inc (Edmonton, AB, Canada). The CT2 Armenian hamster mAb specific for the last 17 amino acids (SSLSYTNPAVAAT SANL) of the MUC1-CD was generously provided by Dr. Sandra Gendler (Mayo Clinic, Scottsdale, AZ). The mouse anti-human ICAM-1 mAb was kindly provided by ICOS Corporation (Bothell, WA, USA). The GD11 anti-Src mAb was purchased from Upstate Cell Signaling Solutions (Lake Placid, NY, USA). The goat anti-mouse or anti-Armenian hamster horseradish peroxidase (HRP) conjugated secondary antibodies were purchased from Jackson ImmunoResearch Laboratories, Inc (West Grove, PA, USA). The pC1Neo TR^+ FLAG plasmid carrying the *MUC1* gene was provided by Dr. Sandra Gendler (Mayo Clinic, Scottsdale, AZ). The *MUC1* gene was PCR amplified from the plasmid and inserted into the Clontech pEYFP-N1 plasmid at the BsrG1/Not1 cut sites (work of Jennifer Rahn). A synthetic MUC1-specific MUC1 signal sequence, TCGAC TAGGCCTATGACACCGGGCACCCAGTCTCCTTTCTTCCTGCTGCTGCTCCTC ACAGTGCTTACAGTTGTTACG, made by the DNA Core Services Laboratory, Department of Biochemistry, University of Alberta, was inserted into the multiple cloning site [9]. Fluo-3 AM was purchased from Molecular Probes (Burlington, ON, Canada). ECL Plus Western Blotting detection reagents were purchased from Amersham

Biosciences (England, UK). 35mm glass-bottomed microwell dishes were purchased from MatTek Corporation (Asland, MA, USA). Anti-tubulin B-5-1-2 antibody, Pluronic F-127, U-73122, U-73343, methyl-β-cyclodextrin (MBCD), nystatin, wortmannin, protease inhibitor cocktail, phosphatase inhibitor cocktail II, deoxycholic acid, Trizma hydrochloride (Tris-HCl), Tris-Base, polyoxyethylene-sorbitan monolaurate (Tween-20), potassium chloride (KCl), magnesium chloride ($MgCl_2$), calcium chloride ($CaCl_2$), HEPES, glycine, sucrose, glycerol, Nonidet P-40, 2-mercaptoethanol, and gelatin were purchased from Sigma-Aldrich (Oakville, ON, Canada). PD98059 was from Calbiochem (Mississauga, ON, Canada). PP2 and 2-APB were from Tocris (Ellisville, MO, USA). Sodium dodecyl sulfate (SDS) was from Pierce Biotechnology (Rockford, IL, USA). Sodium chloride (NaCl), ammonium persulfate, 40% (w/v) acrylamide stock solution, methanol and Triton X-100 were purchased from Fisher Scientific International (Nepean, ON, Canada). Bromophenol blue was purchased from Bio-Rad Laboratories Ltd (Hercules, CA, USA). Cholera toxin B-HRP was purchased from List Chemical Laboratories (Campbell, CA, USA). Dulbecco's modified Eagle's medium (DMEM), ethylenediaminetetraacetic acid (EDTA), fetal bovine serum (FBS), trypsin, antibiotic G418, and blasticidin S were purchased from Invitrogen, Inc (Carlsbad, CA, USA). Protein G-agarose was purchased from Roche Diagnostics (Indianapolis, IN, USA).

2.1.2. Cell Culture

293T human embryonic kidney epithelial cells, and breast cancer T47D, MCF-7 and MDA-MB-468 cells were purchased from the American Type Culture Collection (ATCC), and maintained in DMEM supplemented with 10% FBS and 60μg/ml insulin. To generate the MUC1-transfected 293T cells, the 293T cells were transfected with

pEYFP-N1/MUC1 plasmids using lipofectomine^{TM}2000 and Opti-MEM (Invitrogen, Inc.), according to the manufacturer's protocol [9]. The generated transfectants were designated as SYM (Signal sequence-YFP-MUC1), and three suclones SYM1, SYM3 and SYM25 differing in the level of MUC1 expression were selected for future study. Mock and ICAM-1-transfected NIH3T3 mouse fibroblast cells were a generous gift of Dr. Ken Dimock, University of Ottawa, ON., and maintained in DMEM supplemented with 10% FBS and 2μg/ml Blasticidine S. All the cell lines are cultured at 37°C in a humidified incubator containing 5% CO_2 (Water-Jacketed Incubator, Forma Scientific, Marietta, OH, USA)

2.1.3. SDS-PAGE and Western Blot Analysis

Cells were lysed in RIPA buffer (20mM Tris pH 7.5, 150mM NaCl, 1% Nonidet P-40, 5mM EDTA, 0.1% SDS, and 0.5% deoxycholic acid, freshly supplemented with 0.5% (v/v) protease inhibitor cocktail and phosphatase inhibitor cocktail II), homogenized with a 26 gauge needle and the insoluble components pelleted by centrifugation at 14000 xg for 3 minutes (EBA 12R Hettich Zentrifugen, Rose Scientific Ltd, Edmonton, AB, Canada). The supernatants were assessed for protein concentration using the Bio-Rad DC assay kit and then boiled in Laemmli Buffer (0.5 M Tris-HCl pH 6.8, 10% glycerol, 2% SDS, 5% 2-mercaptoethanol, and 0.05% bromophenol blue) for 10 minutes. The generated samples were then either stored at -20°C or subjected to a 4-20% gradient SDS-PAGE.

Electrophoresis was performed using Bio-Rad Mini-PROTEAN II system at 60 mA per gel, 80 V (constant voltage) for the initial 10 minutes followed by 120 V (constant voltage) for the remaining time in Running Buffer (25mM Tris-Base pH 8.3,

192mM glycine, and 0.1% SDS in ddH_2O). The separated proteins were then transferred to an Immobilon-P or PSQ membrane (Millipore Corporation, Billerica, MA, USA) using a Bio-Rad Mini Trans-Blot system on ice for 60 minutes at 100 V (constant voltage) and 350 mA in Transfer Buffer (25mM Tris-Base pH 8.3, 192mM glycine, 0.1% SDS, and 20% methanol in ddH_2O). After transferring, the membranes were blocked in 5% (w/v) fat-free milk in Tris-buffered saline containing 0.05% (v/v) Tween-20 (TBS-T) for 1 hour at room temperature (RT) or overnight at 4°C with rocking. The membranes were then incubated with specific primary antibodies for 1.5 hour at RT at the concentrations recommended by manufacturers, followed by 3 X 10 minutes of washes in TBS-T. Subsequently, the membranes were incubated with HRP-conjugated secondary antibodies for 1 hour at RT in 5% fat-free milk in TBS-T. Following 3X washes in TBS-T, the membranes were then incubated with ECL plus reagent, scanned using a Typhoon Imager-8600 and processed with NIH Scion-Image software for quantification. Membranes were then reprobed for tubulin, as a loading control, in order to correct protein loading differences.

To completely remove the primary and secondary antibodies from the membrane for reprobing other proteins with similar molecular weight or the same protein with another antibody, the membranes were immersed in Stripping Buffer (100mM 2-mecaptoethanol, 2% SDS, 62.5mM Tris-HCl pH 6.7) and incubated at 50°C for 30 minutes with occasional agitation. The membranes were then washed 2 X 10 minutes in TBS-T at RT, followed by membrane-blocking in 5% fat-free milk in TBS-T for 1 hour at RT. Then, the immunoblotting procedures were repeated as described above. After

ECL detection, the membranes were stored wet and wrapped in Saran Wrap in a refrigerator (2-8°C).

2.1.4. Calcium Oscillation Assay

35mm glass-bottomed MatTek microwell dishes were coated with 100µl of FBS (for untransfected cell lines) or 0.1% (w/v) gelatin (for 293T transfectants), and then air-dried for ~1 hour in the culture hood. Then, 100µL of untransfected breast cancer cells or MUC1-transfected 293T cells at 5-10 x 10^4/ml were plated onto the precoated dishes and allowed to equilibrate overnight. This generally resulted in ~60% cell confluency the next day. The culture media was aspirated from plated cells and replaced with loading media, which is freshly generated by mixing 5mM Fluo-3 with 20% (w/v) Pluronic F-127 in DMSO at 1:1 ratio and then diluted 1/500 in DMEM containing 10% FBS. The plated cells were incubated with Fluo-3 for 1 hour at 37°C, 5% CO_2. When indicated, the plated cells were then incubated with 10µM PD98059, 10µM PP2, 10µM U-73122, 10µM U-73343, 15mM methyl-β-cyclodextrin, 75µg/ml nystatin, 2µM wortmannin, or 100µM 2-APB for 30 minutes at 37°C, 5% CO_2. Cells were then washed once in 37°C Imaging Buffer (152mM NaCl, 5.4mM KCl, 0.8mM $MgCl_2$, 1.8mM $CaCl_2$, 5.6 mM glucose, 10mM HEPES pH 7.2 [27]), and then left in Imaging Buffer at 37°C for 30-45 minutes until imaged. In the meantime, NIH3T3-ICAM-1 or -Mock transfectants were trypsinized and resuspended in Imaging Buffer at ~1 x 10^7/ml. Immediately before the experiment, the Imaging Buffer was decanted. Then the MatTek dish was placed in a 37°C microscope stage warmer on a Zeiss Axioscope Digital Imaging Microscope and the cells were imaged using a plan neofluar 20X lens. Using Metamorph software (Universal Imaging Corporation, Downingtown, PA, USA), a differential interference

contrast (DIC) image was recorded (20ms), and then 60 images (200ms exposure) at 3 second intervals were recorded using the fluorescein isothiocyanate (FITC) filter. 100μl of NIH3T3-ICAM-1 or -Mock transfectant suspension was added to the plated cells immediately after the first FITC image was taken, so that the calcium flux response of the plated cells was recorded in the remaining 59 images. A final DIC image was taken at the end of the time course to ensure that all plated cells had been covered by the NIH3T3 cells (Figure 2.1).

2.1.5. Quantitative Analysis of Calcium Oscillation

Using Metamorph software, the images taken under each experimental condition were built into a stack, and 40 random cells per condition were circled (circled areas = regions of interest, or ROI). The changes in average fluorescence intensity for each ROI were graphed over time and exported to MS Excel. Each condition was repeated at least 3 times, n = a minimum of 120 cells observed.

MS Excel was used to plot the data and calculate the "Oscillation Factor" which is defined as the number of oscillation cycles multiplied by the "amplitude factor" for each ROI (Figure 2.2). The number of oscillation cycles was counted manually from the plotted data. The "amplitude factors" were calculated by plotting an Excel "LOGEST" trend line ($y = \text{intercept} \cdot \text{slope}^x$) from the start of the oscillatory portion of the data to the last recorded data point, then calculating the absolute value of the difference between the actual plotted data and the trend line and for each data point; the sum of these differences was defined as the amplitude factor.

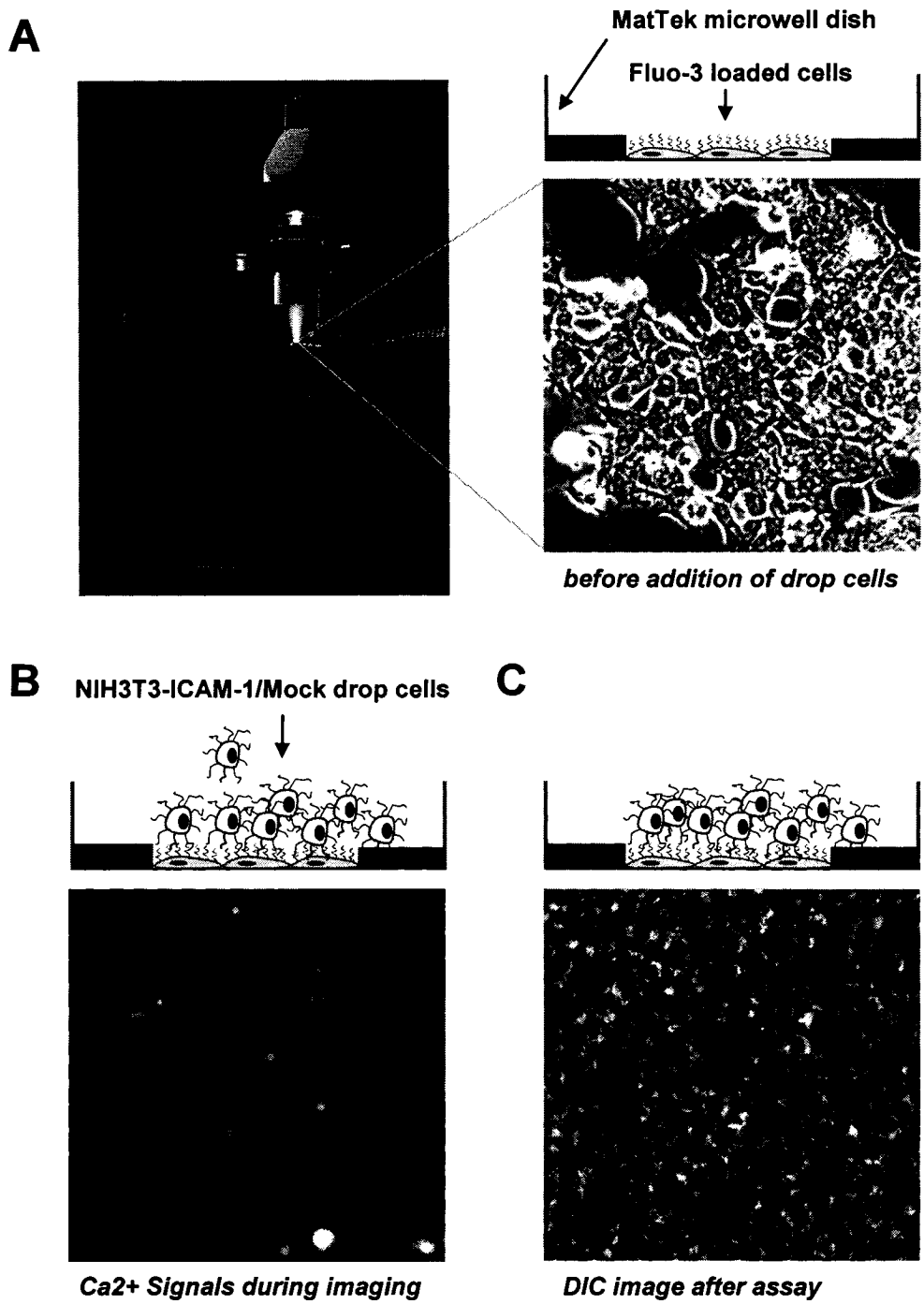

Figure 2.1: The calcium oscillation assay. (A) The 35mm MatTek glass-bottomed dish, containing Fluo-3 loaded adherent cells, was placed on a Zeiss Axiovert 200 digital microscope. A DIC image was taken before adding the NIH3T3 tranfectant. (B) FITC images (gray-scaled) of the adherent cells were recorded every 3 seconds. (C) A DIC image of the dropped NIH3T3 transfectants was taken after the time course.

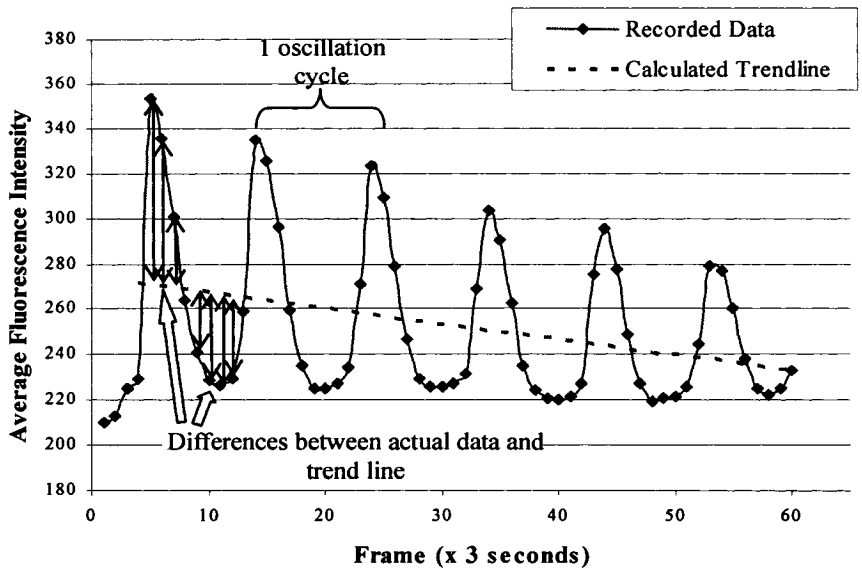

Trendline ➔ pre-programmed "LOGEST" function in Excel ➔ $y= b \bullet m^x$

Figure 2.2: Quantitative analysis of calcium oscillation. As a representive result to be shown here, the number of oscillation cycles (NOC) was counted manually after tracing the average fluorescence intensity for each ROI over time. Single peaks with no obvious secondary intracellular calcium increase were scored as zero. The amplitude factor (AF) was calculated by drawing an Excel LOGEST trendline through the data, beginning with the first oscillation, then summing the absolute values of the differences between the actual data points and the trendline. The NOC was then multiplied by the AF, resulting in the oscillation factor (oscillation factor = NOC x AF) [28].

2.1.6. Lipid Raft Extraction

Breast cancer cells and MUC1-transfected 293T cells were cultured on 10cm cell culture dishes (Corning Inc.) until ~60% confluent. When indicated, the plated cells were then stimulated with NIH3T3-ICAM-1 or -Mock transfectants for various periods, or incubated with 15mM methyl-β-cyclodextrin or 75μg/ml nystatin for 30 minutes at 37°C. After that, the cell culture dishes were placed on ice and the plated cells were washed twice with ice-cold PBS, then scraped into 500μl lipid raft lysis buffer (25mM Tris-HCl pH 7.5, 1% Triton X-100, 150mM NaCl, 5mM EDTA, freshly supplemented with 0.5% protease inhibitor cocktail and phosphatase inhibitor cocktail II), homogenized with a 26 gauge needle and then the insoluble components pelleted by centrifugation at 14000 xg for 3 minutes. The supernatants were then tranferred to ultra-centrifuge tubes (Sorvall Instruments) and mixed thoroughly with 1ml of ice-cold 80% sucrose in lipid raft isolation buffer (25mM Tris-HCl pH 7.5, 150mM NaCl, 5mM EDTA, freshly supplemented with 0.5% protease inhibitor cocktail and phosphatase inhibitor cocktail II), then sequentially overlaied with 2ml of 30% sucrose, and 2ml of 5% sucrose in lipid rafts isolation buffer (Figure 2.3). After the tubes were balanced, the gradients were centrifuged at 40,000 rpm for 18 hours at 4°C in a SW41Ti rotor (Beckman Instruments, Palo Alto, CA, USA). Following centrifugation, lipid rafts appeared as a cloudy band near the top of the gradient. A total of 10 fractions (600μl/each) were collected from the top for the subsequent dot blot analysis (Figure 2.3).

2.1.7. Dot Blot Analysis

To determine the lipid raft fractions, the 10 fractions were tested for GM1

ganglioside localization using a dot-blot analysis as follows. An Immobilon-P membrane (soaked sequentially in methanol and in TBS) was placed between the sample template and the sealing gasket of the 96 well dot-blot apparatus (Bio-Rad Laboratories), and a "Blot-Sandwich" was assembled. After loading 100µl of TBS into each well of sample template, 5µl of sample from each of the collected fractions was loaded sequentially into the wells (Figure 2.3). Then, a vacuum was applied to allow the samples to filter through the membrane, followed by addition of another 100µl TBS into each well and reapplication of the vacuum. The membrane was then taken from the dot-blot apparatus and blocked in 5% fat-free milk in TBS-T for 1 hour at RT. Subsequently, the membrane was incubated with 0.1µg/ml cholera toxin B-HRP, which binds the lipid raft marker GM1, for 1.5 hour at RT. This was followed by 2 X 10 minutes of washes with TBS-T and 1 X 10 minutes of wash with TBS. Finally, the membranes were incubated with ECL plus reagent, scanned, and analyzed as described in section 2.1.3.

2.1.8. Co-immunoprecipitation

Breast cancer cells or MUC1-transfected 293T cells were cultured on 10cm cell culture plates until ~60% confluent. When indicated, the plated cells were stimulated with NIH3T3-ICAM-1 or -Mock transfectants for various periods, and then lysed in Co-IP lysis buffer (50mM Tris pH 7.6, 0.5% Nonidet P-40, 100mM NaCl, 0.5mM EDTA, freshly supplemented with 0.5% protease inhibitor cocktail and phosphatase cocktail II). The lysates were homogenized with a 26 gauge needle and insoluble components pelleted by centrifugation at 14000 xg for 1 minute. Following centrifugation, the supernatants were adjusted to final volumes of 1ml with lysis buffer in 1.5ml eppendorff tubes. If necessary, 30µl of each cell extract was spared, mixed with 10µl of 4X Laemmli Buffer

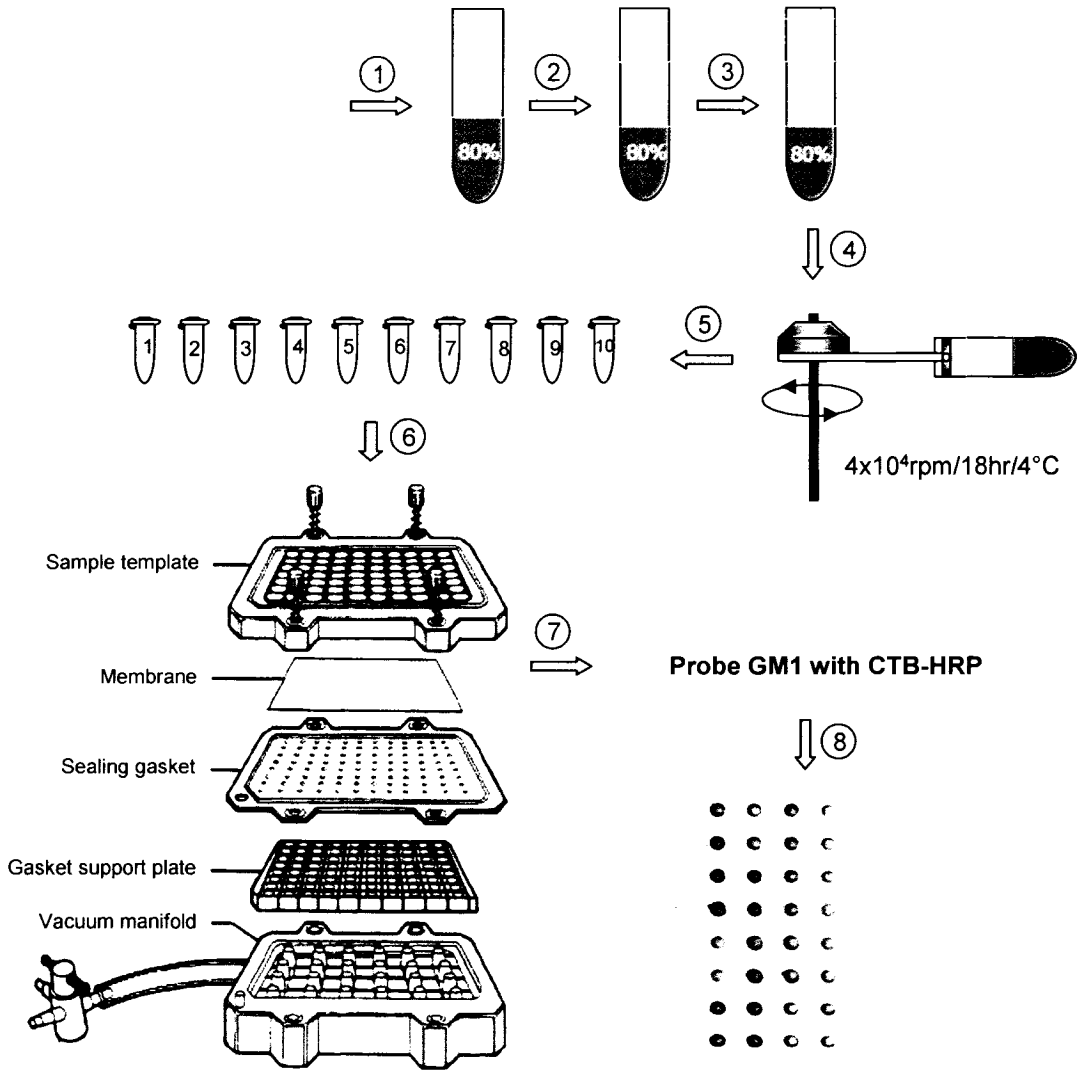

Figure 2.3: Procedures for dot blot analysis. (1) The plated cells were lysed and mixed with 80% sucrose. (2) 30% sucrose was overlaied. (3) 5% sucrose was overlaied. (4) The gradients underwent centrifugation at 40,000 rpm for 18 hours at 4°C. (5) Ten fractions were collected sequentially from the top to the bottom of gradient. (6) Equal amounts of sample from each fraction was loaded into the dot blot apparatus, followed by application of a vacuum. (7) The lipid raft marker GM1 was probed using cholera toxin B-HRP (CTB-HRP). (8) The membrane was subjected to ECL reagent and scanned using a Typhoon Imager-8600.

and boiled for 10 minutes for later usage as crude lysate controls. The remaining cell lysates were incubated with 10μg/ml of B27.29 or CT2 mAb for 2 hours at 4°C with gentle agitation. Incubation continued with the addition of 50μl of Protein G-agarose, rinsed once with lysis buffer, for 7 hours at 4°C with end-to-end agitation. The immunocomplexes were then pelleted and washed 3X with 1 ml of lysis buffer. This was followed by resuspension of the immunocomplexes, boiling in 60μl laemmli buffer for 10 minutes, and centrifugation at 14000 xg for 1 minute. The supernatants collected were either analyzed immediately or stored at -20°C. As a negative control, a Mock IP condition, which consisted of lysis buffer, immunoprecipitating antibody (B27.29 or CT2) and protein G-agarose was also included to allow for identification of non-specific bands in the subsequent Western blots.

2.1.9. Statistical Analysis

The calcium signals generated under different experimental conditions were represented by their average oscillation factor ± S.E. (Standard Error), using MS Excel software. Statistical significance was determined using the Student's t-test, $p<0.05$. The Newman-Keuls multiple range comparision was used to determine statistical differences in data sets where there were more than two conditions.

2.2. Results

2.2.1. MUC1 Induces Intracellular Calcium Oscillations by Ligating ICAM-1

To investigate if MUC1 can initiate intracellular calcium dynamics in response to ICAM-1 stimulation, the MUC1 construct was transfected into 293T cells, and a series of subclones were isolated which differed in their MUC1 expression levels (Fig. 2.4 A [28]. By conducting calcium oscillation assays under a Zeiss Axioscope Digital Imaging Microscope (see details in section 2.1.4), we found that the calcium-based signal in Fluo-3-loaded MUC1-positive 293T SYM1 cells was more intense and oscillatory when these cells came into contact with ICAM-1-transfected NIH3T3 cells, as compared with mock-transfected cells (Fig. 2.4 B and Fig. 2.5 A and B). Although these calcium oscillations were asynchronous between cells, they appeared to last at least 3 minutes and have a relatively constant oscillation period of ~30 seconds (Fig. 2.6 A). However, the 293T SYM3 cells, which have no MUC1 expression, exhibited only minor levels of calcium oscillatory responses regardless of the presence or absence of ICAM-1 on the dropped NIH3T3 transfectants. A single moderate calcium spike was frequently observed in both 293T SYM1 and SYM3 cells under conditions lacking either MUC1 on the 293T cells or ICAM-1 on the NIH3T3 transfectants (Fig. 2.6 B – D), indicating that the calcium oscillations provoked in the MUC1-positive 293T transfectants are specifically initiated in the presence of ICAM-1. Similar results were also observed in breast cancer MCF-7 cells, where significantly higher intracellular calcium oscillations were initiated in response to NIH3T3-ICAM-1 stimulation, as compared with their counterparts stimulated with NIH3T3-Mock transfectants.

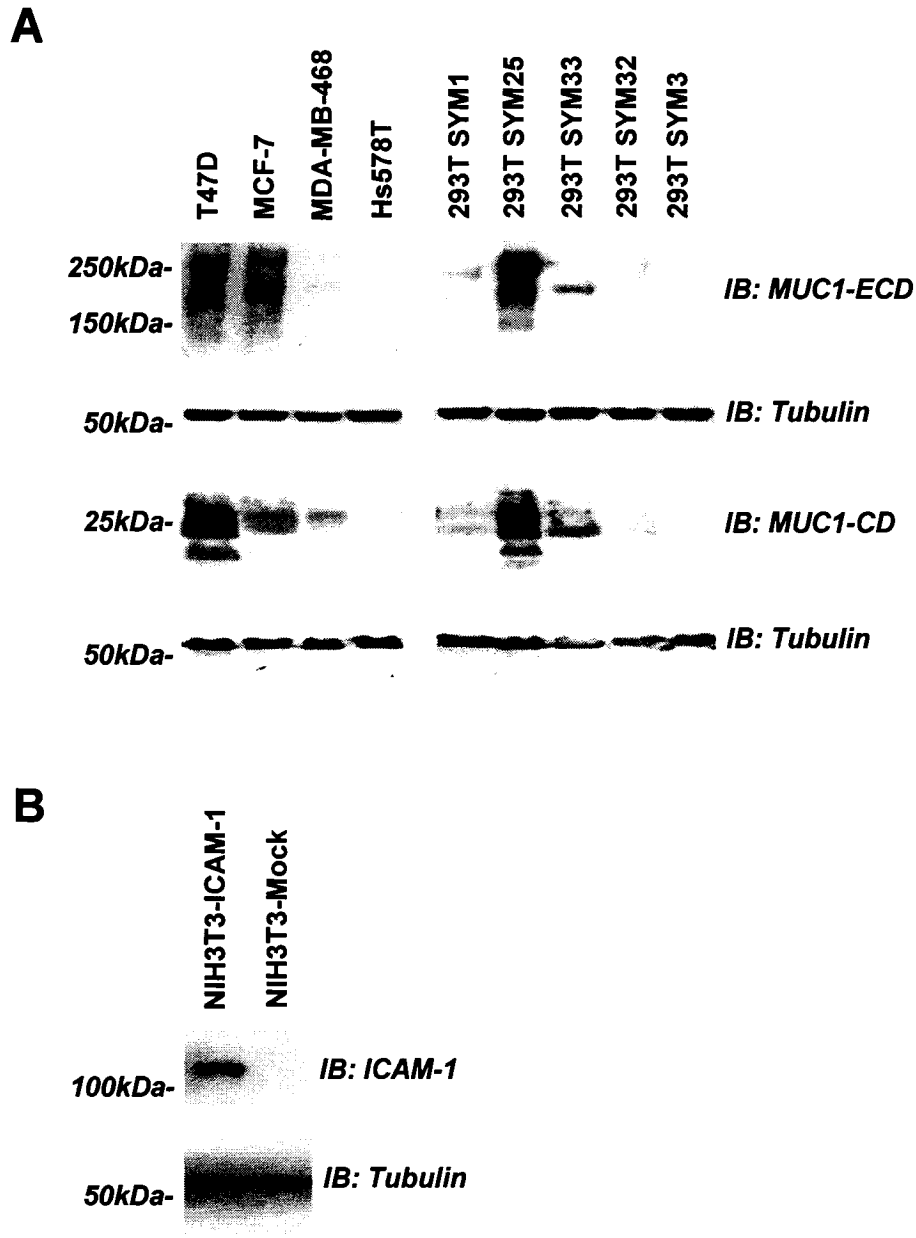

Figure 2.4: Western blots for the cellular expression of MUC1 and ICAM-1. (A) MUC1 expression levels were examined in breast cancer cell lines (T47D, MCF-7, MDA-MB-468, and Hs578T) and MUC1-transfected 293T subclones (SYM1, SYM25, SYM33, SYM32, and SYM3) with antibodies against MUC1-ECD and MUC1-CD. Tubulin was used as a loading control [28]. (B) ICAM-1 expression levels were examined in NIH3T3-ICAM-1 and NIH3T3-Mock transfectants, using tubulin as a loading control.

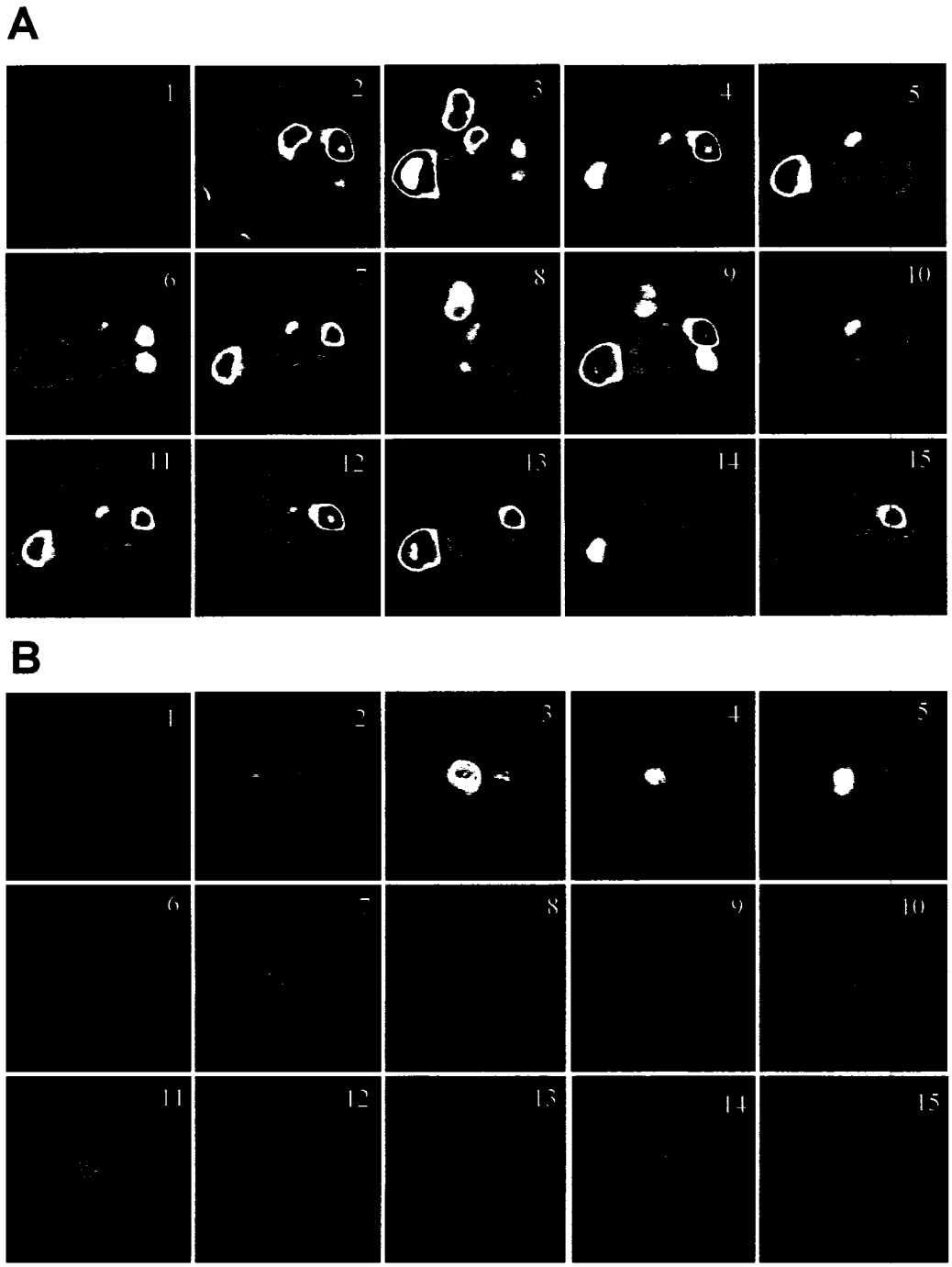

Figure 2.5: Contact with ICAM-1-expressing cells induces intracellular calcium oscillations in the MUC1-expressing cells. MUC1-positive 293T SYM1 cells were preloaded with the fluorescent calcium indicator, Fluo-3, before undergoing a calcium oscillation assay in response to (A) NIH3T3-ICAM-1 or (B) NIH3T3-Mock stimulation.

Figure 2.5 Continued: Using Metamorph software, 60 images at 3 second intervals were recorded under the FITC filter (see details in section 2.1.4). As representatives to be shown here, the numbered pictures represent the pseudocolored images that were sequentially taken every 12 seconds, showing that the SYM1 cells exhibited calcium-based oscillatory signals in the presence of ICAM-1 (A), as compared with the Mock stimulated controls (B).

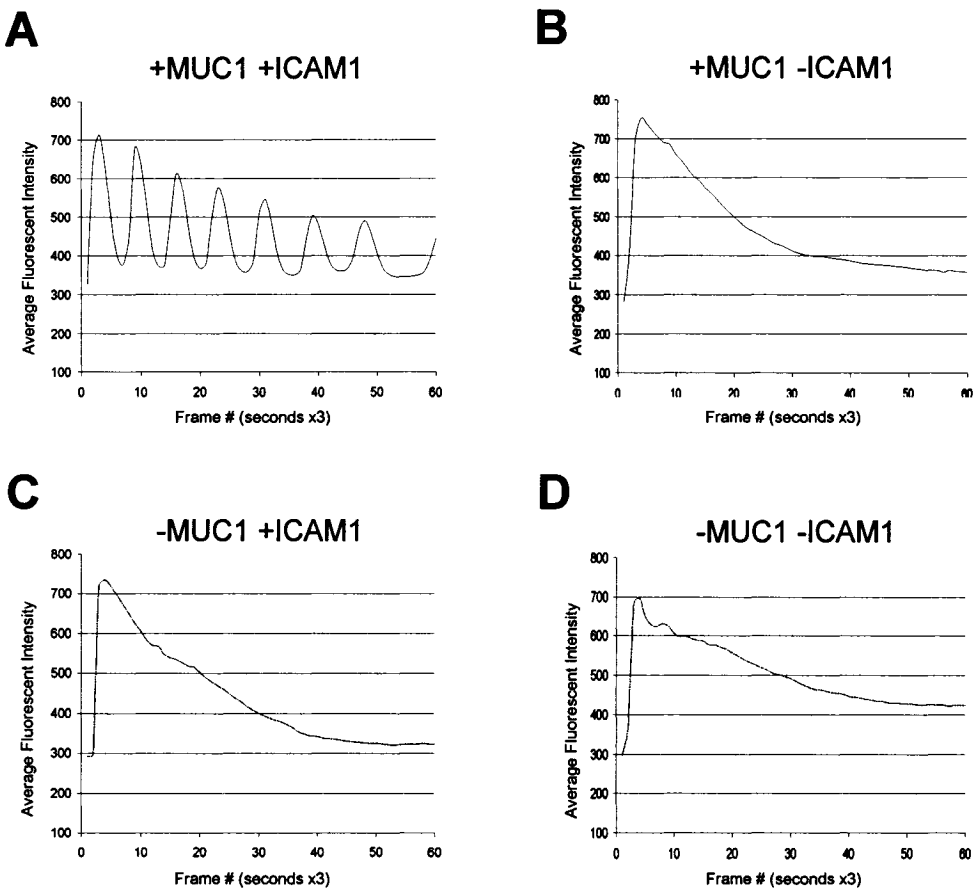

Figure 2.6: Representative calcium dynamics in the MUC1-transfected 293T subclones in the presence or absence of ICAM-1 stimulation. Time courses of Fluo-3 fluorescent intensities detected in individual MUC1-positive 293T SYM1 cell in response to (A) NIH3T3-ICAM-1 or (B) NIH3T3-Mock stimulation, as well as in individual MUC1-negative 293T SYM3 cell in response to (C) NIH3T3-ICAM-1 or (D) NIH3T3-Mock stimulation.

To quantitatively analyze and compare the calcium oscillatory signals between experimental conditions, we have developed a method to average the signals into oscillation factors (see details in section 2.1.5). Based on results from at least three independent experiments of a total of 120 individual cells under each condition, we found that the oscillatory response in the MUC1-postive 293T SYM1 cells was significantly increased in response to NIH3T3-ICAM-1 stimulation, as compared with NIH3T3-Mock stimulation, as well as the MUC1-negative 293T SYM3 cells stimulated with either NIH3T3-ICAM-1 or -Mock transfectants (Fig. 2.7 A, t-test, $p<0.001$ [28]). Further, as shown in Fig. 2.7 B, breast cancer MCF-7 cells also exhibited statistically significant increase in the oscillatory response when exposed to ICAM-1 as compared with Mock transfectants (t-test, $p<0.01$).

Other work in our laboratory (thesis project of Jennifer J. Rahn) has confirmed the results above and extended the calcium oscillation assays to a panel of other breast cancer cell lines (T47D, MDA-MB-468, and Hs578T) and MUC1-transfected 293T subclones (SYM25, SYM33, and SYM32), which exhibited various expression levels of MUC1 (Fig. 2.4 A [28]). The results showed that only the MUC1-positive cells (breast cancer T47D cells, 293T SYM25 and SYM33 cells) exhibited a significantly increased calcium oscillatory responses in response to NIH3T3-ICAM-1 stimulation, as compared with the NIH3T3-Mock stimulated controls (t-test, $p<0.05$) [28]. Moreover, this calcium oscillatory reponse was correlated with the surface expression levels of MUC1 [28]. In response to ICAM-1 stimulation, T47D cells showed higher calcium-based signals than MCF-7 cells, and both of these MUC1-positive breast cancer cell lines exhibited significantly increased calcium-based signals as compared with MUC1-low/negative

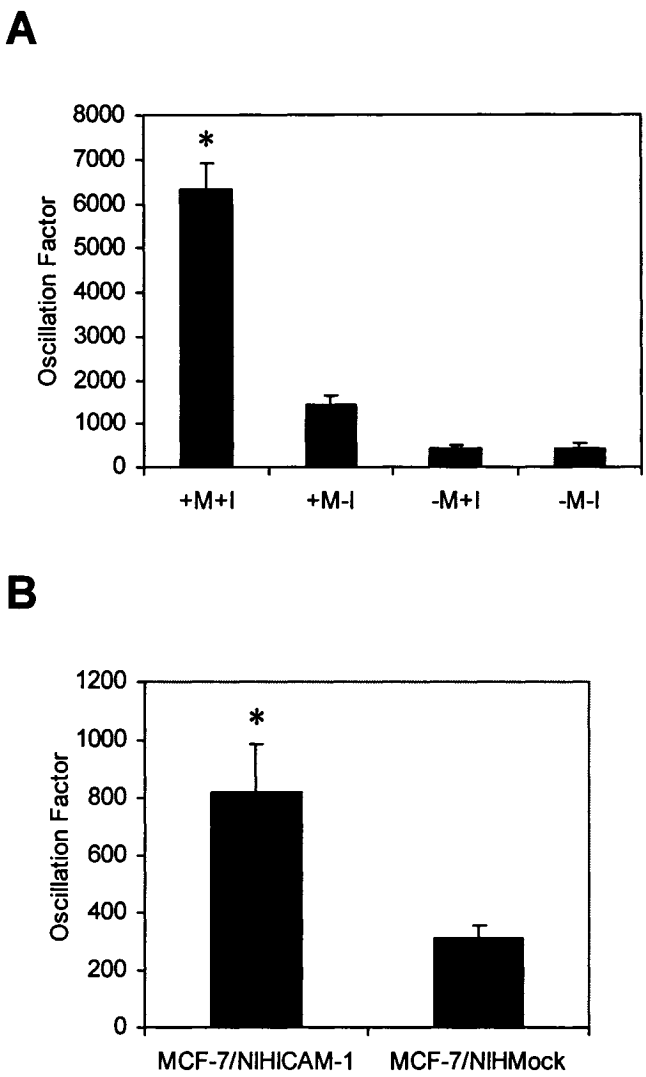

Figure 2.7: Calcium oscillation is initiated in the MUC1-positive cells in the presence of ICAM-1. (A) Data represent the average oscillation factor ± S.E. for MUC1-positive SYM1 (+M) and MUC1-negative SYM3 (-M) from at least three independent experiments with a total of 120 cells, in the presence (+I) or absence (-I) of ICAM-1 stimulation [28]. (B) Data represent the average oscillation factor ± S.E. for MUC1-positive breast cancer MCF-7 cells from at least three independent experiments of 120 cells, in the presence or absence of ICAM-1 stimulation.

MDA-MB-468 and Hs578T cells [28]. Also, 293T SYM25 cells showed increased calcium oscillatory responses relative to the intermediate MUC1-expressing SYM33 cells. Both of these sublines exhibited higher calcium-based signals than MUC1-negative SYM32 and SYM3 cells [28]. Significantly, the anti-MUC1-ECD antibody B27.29 that are known to block the interaction with ICAM-1 could abrogate the calcium oscillatory response in MUC1-positive cells in reponse to ICAM-1 stimulation (work of Jennifer J. Rahn [28]). Taken together, these results demonstrate that MUC1 can initiate intracellular calcium oscillatory signals by ligating ICAM-1.

2.2.2. Role of Src Family Kinase, PI3K and PLC in MUC1/ICAM-1 Ligation Induced Calcium Oscillation

Mechanisms underlying intracellular calcium signals are quite complex. Since the calcium concentration outside of cells (1mM) and in some intracellular organelles (~0.1mM), such as the endoplasmic reticulum (ER) and sacroplasmic reticulum (SR) is much higher than the resting cytosolic calcium concentration (~0.1μM), the calcium flux can be divided into extracellular calcium entry and intracellular calcium release [23]. The extracellular calcium entry can be mediated by several mechanisms including the voltage-gated calcium channels, receptor-operated calcium channels, store-operated calcium channel and passive calcium leak through the plasma membrane [23,29,30]. The intracellular calcium release, as described previously in section 1.1.3.3, is generally initiated by transmembrane receptors, such as RTK and GPCR that can activate PI-PLC to generate IP3 by cleaving PtdIns(4,5)P2 on membrane, leading to intracellular calcium release through the IP3 receptor on the ER [23,31]. The intracellular calcium release can also occur through calcium-induced calcium release (CICR) involving the ryanodine

receptor (RyR) on the SR [23,31]. Significantly, of the mechanisms mediating intracellular calium signals, the calcium flux induced by the PLC/IP3/IP3R cascade appears as calcium oscillations due to the positive feedback between calcium and IP3 [32,33]. Since MUC1-CD is associated with Grb2 [16] and Src [12], which can activate PI3K and PLC to initiate calcium signals through IP3R [26,34], and the MUC1-CD contains potential binding motifs for PI3K and PLC [35,36], we speculated that the MUC1/ICAM-1 interaction-induced calcium oscillations are mediated by signaling cascade(s) through IP3R.

To test that hypothesis, 293T SYM1 cells and SYM3 cells were pretreated with one of the following pharmaceutical inhibitors 2-APB (inhibits IP3-induced calcium release from the ER), U-73122 (inhibits PLC), or U-73343 (inactive analogue of U-73122) and compared with untreated cells in the calcium oscillation assays (see details in section 2.1.4). As shown in Fig. 2.8, we found that U-73122 and 2-APB, but not the inactive analogue U-73343, significantly abrogated the MUC1-induced calcium oscillations in response to ICAM-1 ligation [28]. Further, the selective inhibitory experiments were also conducted using PD98059 (inhibits MAPK), wortmannin (inhibits PI3K), or PP2 (inhibits Src family kinases) and compared with an untreated control in the calcium oscillation assays (see details in section 2.1.4). We found that wortmannin and PP2, but not PD98059, could also reduce the level of calcium oscillations seen in the presence of both MUC1 and ICAM-1 to the levels seen when one or both of the molecules were absent (Fig. 2.9) [28]. Taken together, these findings suggest that MUC1 by ligating ICAM-1, can initiate intracellular calcium oscillations through signaling(s) involving a Src family kinase, PI3K, PLC, IP3R, but not MAPK [28].

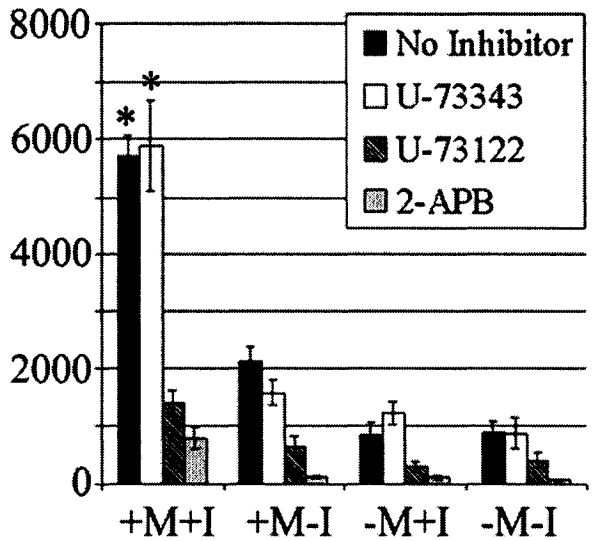

Figure 2.8: Role of PLC and IP3 receptor in the MUC1/ICAM-1 induced calcium oscillations. Data represent the average oscillation factor ± S.E. from at least three independent experiments for a total of 120 individual 293T SYM1 cells (+M) or SYM3 cells (-M) that came into contact with NIH3T3-ICAM-1 (+I) or NIH3T3-Mock (-I) transfectants. Prior to testing in the calcium oscillation assay, the SYM cells were pretreated with inhibitors of PLC (U-73122), IP3 receptor (2-APB) or an inactive analogue (U-73343) [28].

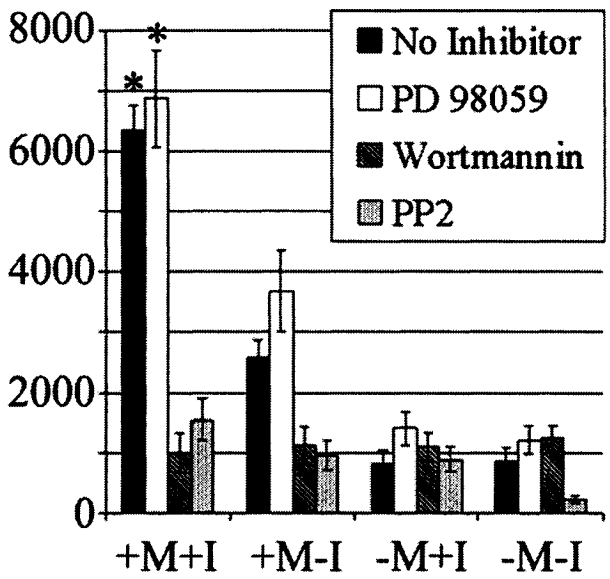

Figure 2.9: Role of MAPK, PI3K, and Src family kinase in the MUC1/ICAM-1 induced calcium oscillations. Data represent the average oscillation factor ± S.E. from at least three independent experiments for a total of 120 individual 293T SYM1 cells (+M) or SYM3 cells (-M) that came into contact with NIH3T3-ICAM-1 (+I) or NIH3T3-Mock (-I) transfectants. Prior to testing in the calcium oscillation assay, the SYM cells were pretreated with inhibitors of MAPK (PD 98059), PI3K (wortmannin) or Src family kinase (PP2) [28].

2.2.3. MUC1/ICAM-1 Ligation Induced Calcium Oscillation is Lipid Raft Dependent

Lipid rafts are cholesterol and glycosphingolipid enriched membrane domains where cholesterol intercalates tightly between saturated fatty acid chains of sphingolipids, thereby forming liquid-ordered microdomains approximately 50nm in diameter [37]. Accumulating evidence suggests that lipid rafts serve as a nexus for the spatial clustering of signaling molecules. Signaling mediators such as Src family kinases, PI3K, PLCγ/β, Gab1 and Ras are generally activated in lipid rafts [37,38]. As well, transmembrane receptors especially if palmitoylated (e.g. tetraspanins) are also capable of partitioning into rafts [37,38]. Thus, by localizing all the components of a specific signaling pathway within a raft compartment, specific and efficient signaling can be initiated in response to an appropriate stimulus [38]. Recent studies have reported finding MUC1 in lipid rafts on T-lymphocytes [39], which is significant since lipid rafts are crucial for calcium-related signals [40]. This has led to the following questions: Is MUC1 localized in lipid rafts in breast cancer cells? Further, are lipid rafts required for the MUC1/ICAM-1 ligation-induced calcium oscillation?

To address that, breast cancer cell lines T47D and MCF-7, as well as MUC1-transfected 293T SYM1 cells were subjected to the lipid raft extraction using a discontinuous sucrose gradient (see details in section 2.1.6-7). Following centrifugation, lipid rafts were successfully isolated in fractions 4 and 5. MUC1 was shown to be localized and highly concentrated (~50%) in the lipid rafts in both T47D and MCF-7 cells (Fig. 2.10). Similar results were also obtained in 293T SYM1 cells (Fig. 2.11), indicating MUC1 as a transmembrane mucin has a naturally high affinity for raft localization.

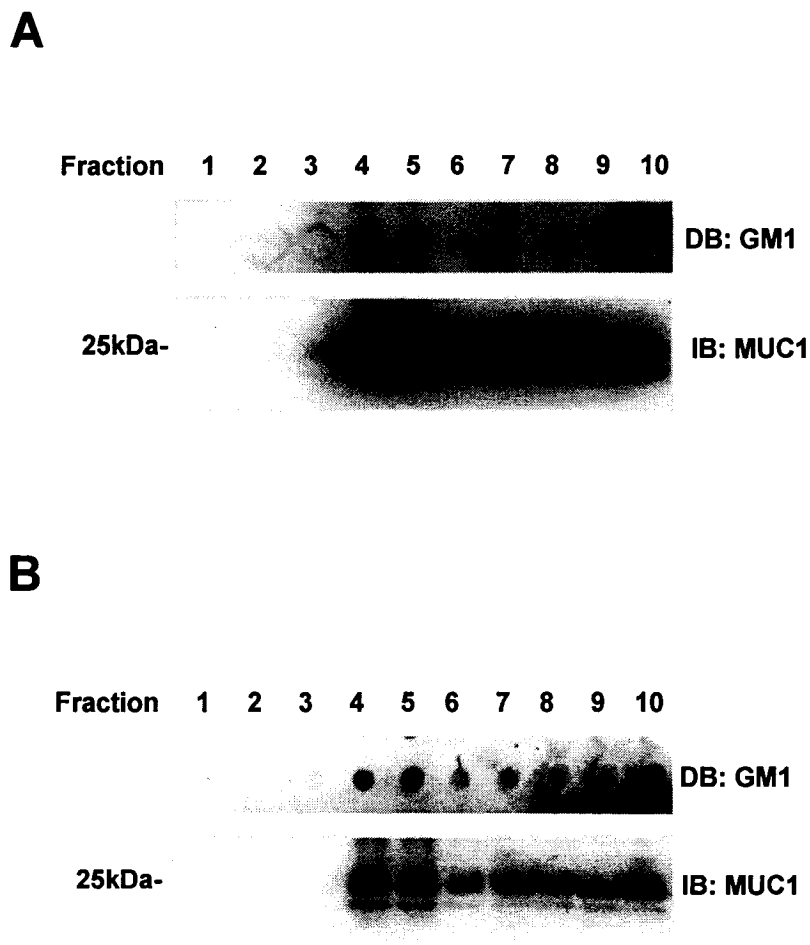

Figure 2.10: MUC1 localizes in lipid rafts in breast cancer cells. (A) Upper lane: The extracted lipid raft fractions of breast cancer T47D cells were identified by dot blot (*DB*) using CTB-HRP. Bottom lane: Equal volumes of samples from each fraction were subjected to SDS-PAGE and Western blot for the MUC1-CD. (B) Upper lane: The extracted lipid raft fractions of breast cancer MCF-7 cells were identified by dot blot (*DB*) using CTB-HRP. Bottom lane: Equal volumes of samples from each fraction were subjected to SDS-PAGE and Western blot for the MUC1-CD.

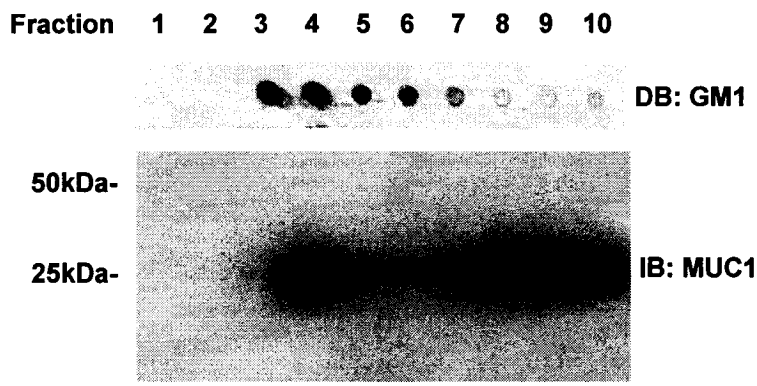

Figure 2.11: MUC1 localizes in lipid rafts in MUC1-transfected 293T cells. Upper lane: The extracted lipid raft fractions of 293T SYM1 cells were identified by dot blot (*DB*) using CTB-HRP. Bottom lane: Equal volumes of samples from each fraction were subjected to SDS-PAGE and Western blot for the MUC1-CD.

Further, we investigated the dependency of the MUC1/ICAM-1 ligation-induced calcium signals on lipid raft integrity. The plated MCF-7 and 293T SYM1 cells were preincubated with either 15mM methyl-β-cyclodextrin (MBCD) or 75μg/ml nystatin for 30 minutes at 37°C, 5% CO_2, before lipid raft extraction. MBCD disrupts lipid rafts by depleting cholesterol from the membrane, whereas nystatin sequesters membrane cholesterol to disrupt lipid rafts [37]. As shown in Fig. 2.12, lipid rafts in both MCF-7 and 293T SYM1 cells were disrupted by MBCD and nystatin. As a result, the lipid raft marker GM1 was redistributed to the high density fractions (Fig. 2.12). Calcium oscillation assays were conducted on 293T SYM1 and SYM3 cells following MBCD or nystatin treatment. The oscillation factors calculated from at least three independent experiments with a total of 120 cells under each condition showed that both MBCD and nystatin-mediated lipid rafts disruption significantly abrogated MUC1-induced calcium oscillatory signals in 293T SYM1 cells in response to ICAM-1 stimulation, as compared with their untreated 293T SYM1 counterparts (Fig. 2.13, t-test, $p<0.001$ [28]). However, the MUC1-negative 293T SYM3 cells showed no significant difference when compared the MBCD or nystatin-pretreated cells with their untreated counterparts (Fig 2.13 [28]). These findings collectively suggest that the integrity of lipid rafts is required for the MUC1/ICAM-1 ligation-induced calcium oscillations.

2.2.4. MUC1/ICAM-1 Ligation Induces Redistribution of Src into Lipid Rafts

Since MUC1 is localized in lipid rafts and most of the downstream molecules of MUC1 (e.g. Src and Grb2) are usually activated in lipid rafts, we propose that MUC1 by interacting with human ICAM-1 on the accessary cells, may function as an adaptor protein to induce this calcium oscillatory signaling by recruiting downstream signaling

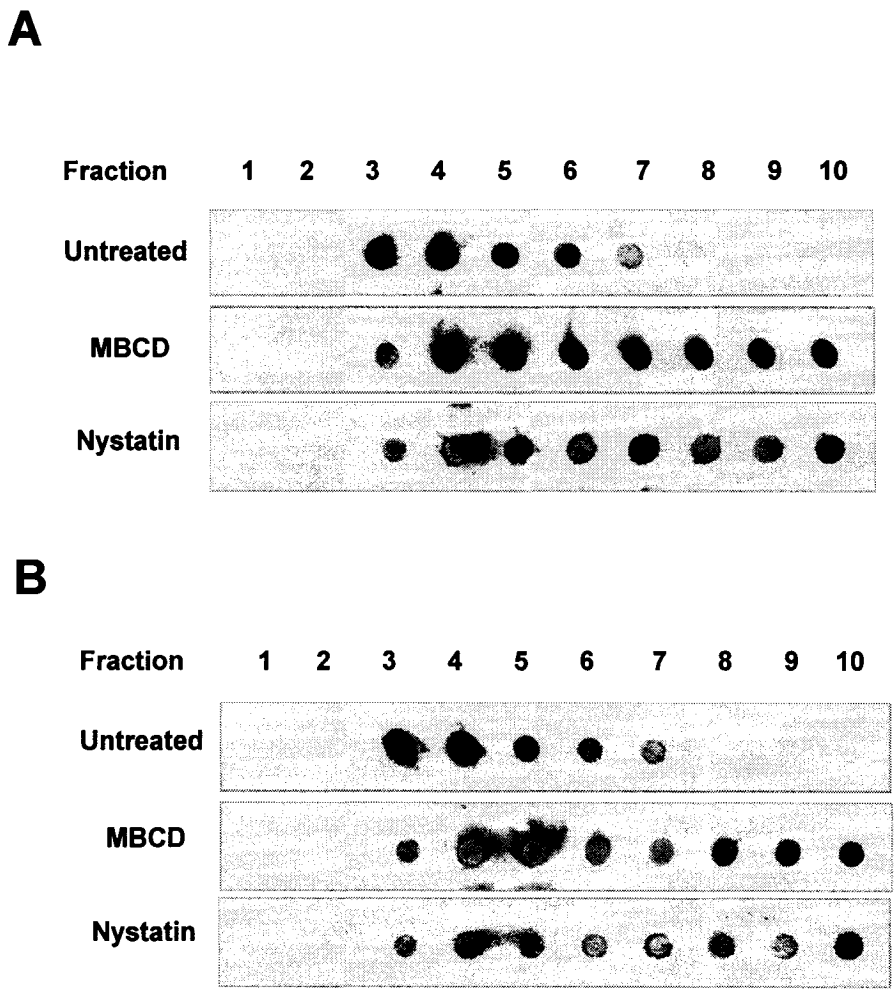

Figure 2.12: Dot blot examination of methyl-β-cyclodextrin and nystatin-mediated lipid rafts disruption. (A) The extracted lipid raft fractions of untreated MCF-7 cells were identified (upper lane) using CTB-HRP. Following treatment with methyl-β-cyclodextrin (MBCD, middle lane) and nystatin (bottom lane), the disruption of lipid rafts was confirmed by redistribution of GM1 to the bottom high density fractions. (B) The extracted lipid raft fractions of untreated 293T SYM1 cells were identified (upper lane) using CTB-HRP. Following treatment with methyl-β-cyclodextrin (MBCD, middle lane) and nystatin (bottom lane), the disruption of lipid rafts was confirmed by the spreading of GM1 to the bottom high density fractions.

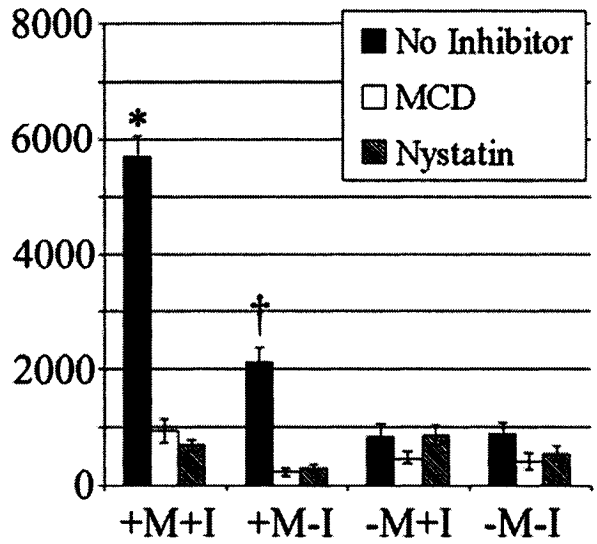

Figure 2.13: The MUC1/ICAM-1 induced calcium oscillations is lipid raft dependent. Data represent the average oscillation factor ± S.E. from at least three independent experiments for a total of 120 individual 293T SYM1 cells (+M) or SYM3 cells (-M) that came into contact with NIH3T3-ICAM-1 (+I) or NIH3T3-Mock (-I) transfectants. Prior to testing in the calcium oscillation assay, the 293T SYM cells were pretreated with MBCD or nystatin [28].

mediators into lipid rafts through the binding motifs on its cytoplasmic domain. Therefore, we investigated the potential cellular redistribution of Src in both breast cancer MCF-7 cells and 293T SYM1 cells in response to MUC1/ICAM-1 interaction. Identical to the protocol used in the calcium oscillation assay, the cells were plated, serum starved, and then stimulated with either NIH3T3-ICAM-1 or -Mock transfectants. In this study, the plated cells were collected after 10 seconds and 1 minute of stimulation with NIH3T3 cells and then lysed prior to lipid raft extraction and subsequent analysis for Src distribution, using the cells collected in culture media and in Imaging Buffer (serum starved) as controls. As shown in Fig. 2.14 A and B, in culture media Src was constitutively found in lipid rafts as well as in non-rafts fractions of MCF-7. Following serum starvation in Imaging Buffer, Src was redistributed into the non-raft fractions (Fig. 2.14 C), which was not altered following NIH3T3-Mock stimulation for 10 seconds and 1 minute (Fig. 2.14 D and E). However, there is a significant shift of Src into lipid rafts after 10 seconds of contact with NIH3T3-ICAM-1 transfectants (Fig. 2.14 F) and this lipid raft localization of Src was increased at 1 minute (Fig. 2.14 G). The same membranes were stripped and reprobed for the distribution of p44/42 MAPK as controls, as we had previously demonstrated that MAPK was not involved in the MUC1/ICAM-1-induced calcium oscillatory signaling. In marked contrast to Src, we found no obvious MAPK redistribution in serum starved MCF-7 cells in response to stimulation by either NIH3T3-ICAM-1 or -Mock transfectants (Fig. 2.15). Similar results were also observed in 293T SYM1 cells, where src (Fig. 2.16), but not MAPK (Fig. 2.17) was shifted into lipid rafts following ICAM-1 stimulation. Taken together, these results suggest that the MUC1/ICAM-1 interaction may specifically induce redistribution of Src into lipid rafts.

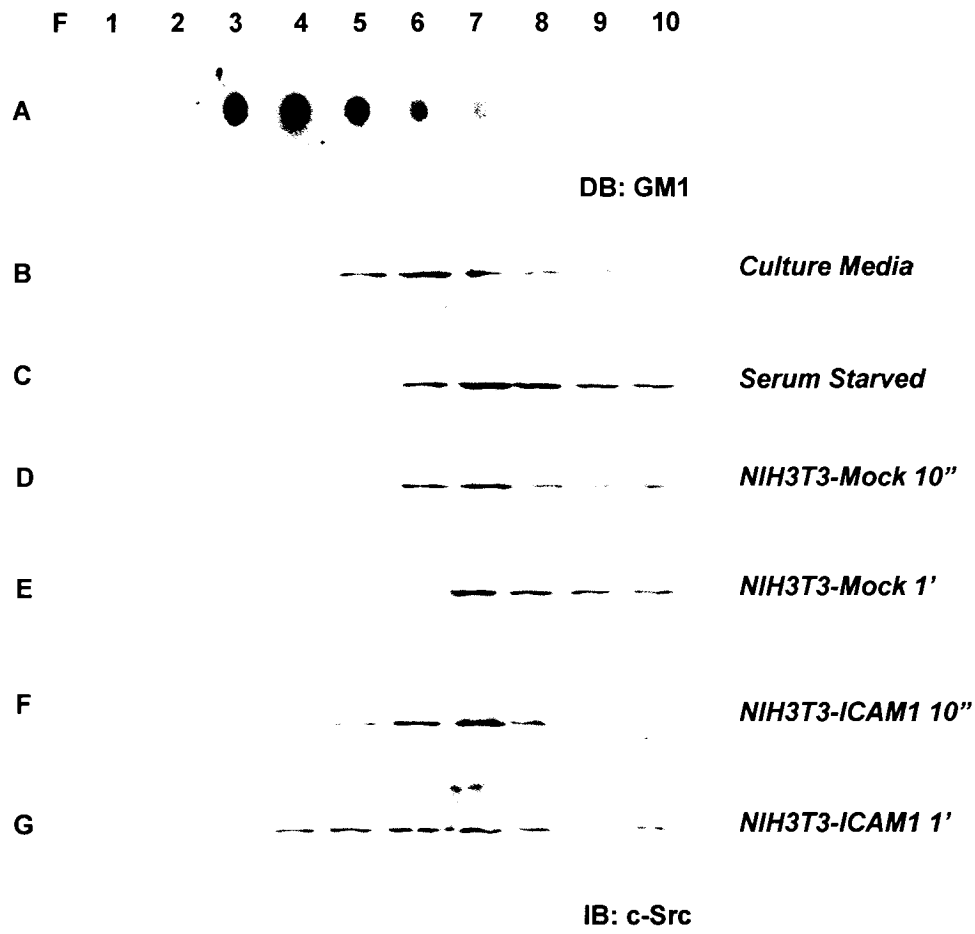

Figure 2.14: Redistribution of Src into lipid rafts in MCF-7 cells in response to ICAM-1 stimulation. (A) The extracted lipid raft fractions of MCF-7 cells were identified by dot blot (*DB*) using CTB-HRP. Src distribution was examined in MCF-7 cells (B) in culture media; (C) after serum starvation in Imaging Buffer; (D) after 10 second of stimulation with NIH3T3-Mock transfectants; (E) after 1 minute of stimulation with NIH3T3-Mock transfectants; (F) after 10 second of stimulation with NIH3T3-ICAM-1 transfectants; (G) after 1 minute of stimulation with NIH3T3-ICAM-1 transfectants.

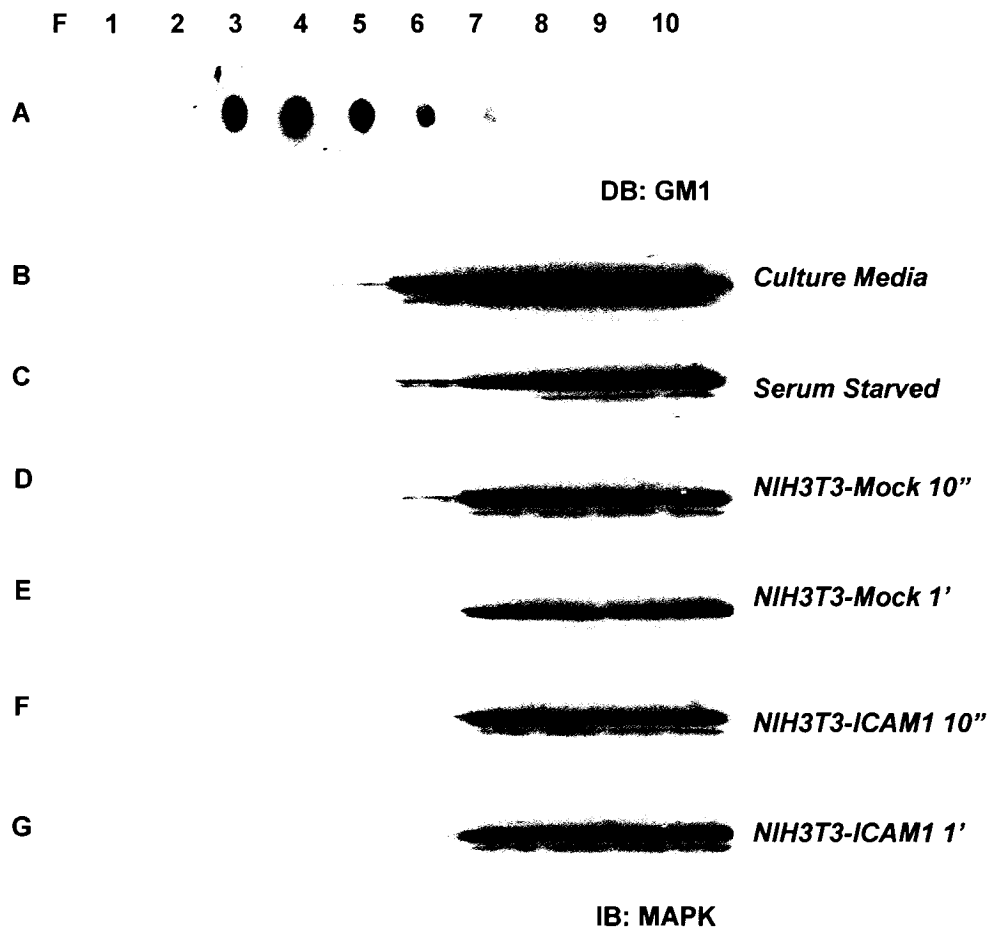

Figure 2.15: MAPK distribution in MCF-7 cells in response to ICAM-1 stimulation. (A) The extracted lipid raft fractions of MCF-7 cells were identified by dot blot (*DB*) using CTB-HRP. MAPK distribution was examined in MCF-7 cells (B) in culture media; (C) after serum starvation in Imaging Buffer; (D) after 10 second of stimulation with NIH3T3-Mock transfectants; (E) after 1 minute of stimulation with NIH3T3-Mock transfectants; (F) after 10 second of stimulation with NIH3T3-ICAM-1 transfectants; (G) after 1 minute of stimulation with NIH3T3-ICAM-1 transfectants.

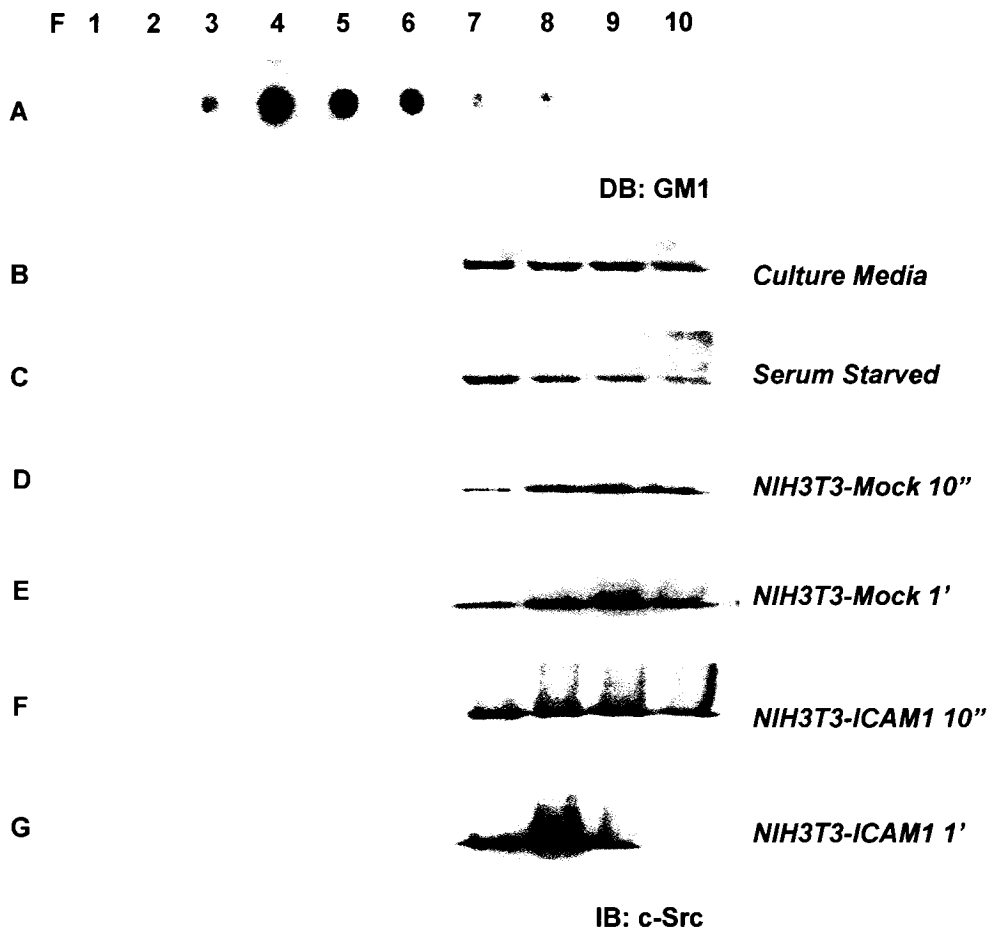

Figure 2.16: Redistribution of Src into lipid rafts in 293T SYM1 cells in response to ICAM-1 stimulation. (A) The extracted lipid raft fractions of 293T SYM1 cells were identified by dot blot (*DB*) using CTB-HRP. Src distribution was examined in 293T SYM1 cells (B) in culture media; (C) after serum starvation in Imaging Buffer; (D) after 10 second of stimulation with NIH3T3-Mock transfectants; (E) after 1 minute of stimulation with NIH3T3-Mock transfectants; (F) after 10 second of stimulation with NIH3T3-ICAM-1 transfectants; (G) after 1 minute of stimulation with NIH3T3-ICAM-1 transfectants.

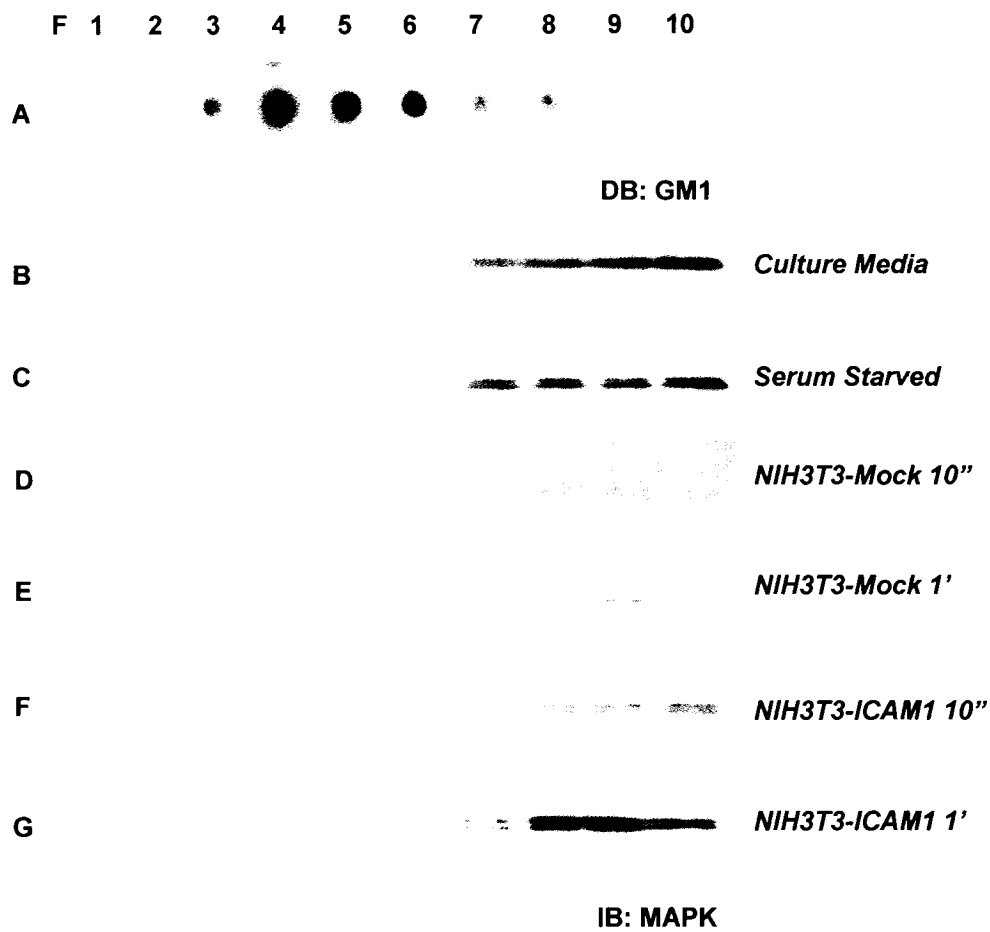

Figure 2.17: MAPK distribution in 293T SYM1 cells in response to ICAM-1 stimulation. (A) The extracted lipid raft fractions of 293T SYM1 cells were identified by dot blot (*DB*) using CTB-HRP. MAPK distribution was examined in 293T SYM1 cells (B) in culture media; (C) after serum starvation in Imaging Buffer; (D) after 10 second of stimulation with NIH3T3-Mock transfectants; (E) after 1 minute of stimulation with NIH3T3-Mock transfectants; (F) after 10 second of stimulation with NIH3T3-ICAM-1 transfectants; (G) after 1 minute of stimulation with NIH3T3-ICAM-1 transfectants.

2.2.5. ICAM-1 Promotes the Association of MUC1 and Src

Since the MUC1-CD can directly associate with Src [12,13], and Src has been implicated in the MUC1/ICAM-1 ligation-induced calcium oscillatory signaling, we further investigated the interaction between Src and MUC1 in response to ICAM-1 ligation. For the purpose of this study, Breast cancer cells T47D cells and MUC1-transfected 293T SYM25 cells were serum starved and then stimulated with either NIH3T3-ICAM-1 or -Mock transfectants for 10 second or 1 minute, followed by MUC1 immunoprecipitation (IP) using anti-MUC1-CD mAb CT2 or anti-MUC1-ECD mAb B27.29 (see details in section 2.1.8). The immunoprecipitates were then analyzed by sequential immunoblotting for Src, MUC1-CD and MUC1-ECD. The crude cell lysates collected after 1 minute of stimulation with NIH3T3-ICAM-1 were used as positive controls. The "acellular" samples consisting of only protein G-agarose and/or IP antibody were used as negative controls. As shown in Fig. 2.18, we found that there was alway a basal level of association of Src and MUC1 when the cells were grown in culture media, serum starved, or non-specifically stimulated by NIH3T3-Mock transfectants. However, in the T47D cells stimulated with NIH3T3-ICAM-1 transfectants, both anti-MUC1 mAb CT2 and B27.29 can co-immunoprecipitate increased amounts of Src as compared with NIH3T3-Mock stimulated and serum starved controls (Fig. 2.18). This ICAM-1-induced increased association of MUC1 and Src was confirmed in MUC1-positive 293T SYM25 cells (Fig. 2.19), where similar to breast cancer T47D cells, the increased Src association was also observed within 10 seconds of stimulation by ICAM-1 positive cells (this represents prelimilary data from a single experiment).

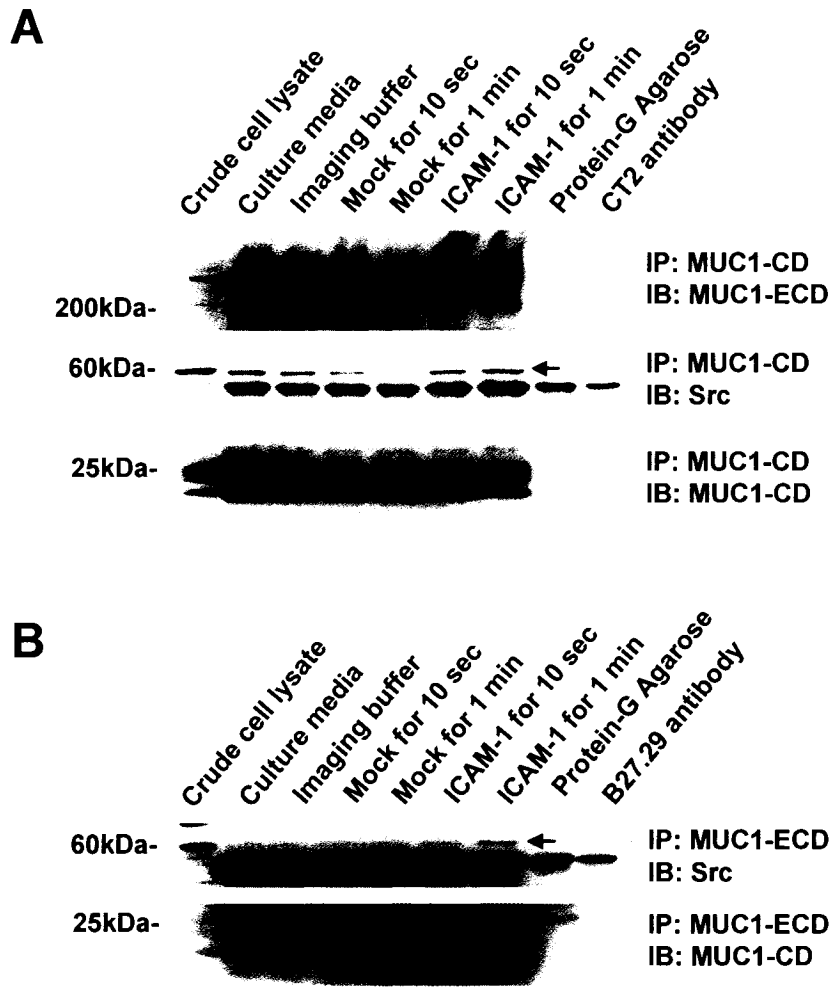

Figure 2.18: ICAM-1 increases the association of Src with MUC1 in breast cancer T47D cells. (A) The anti-MUC1-CD mAb CT2 was used to immunoprecipitate MUC1 from breast cancer T47D cells after co-culturing with NIH3T3-Mock or -ICAM-1 transfectants for 10 seconds and 1 minute. Increased Src (indicated as red arrow) was co-immunoprecipitated with MUC1 after NIH3T3-ICAM-1 stimulation. Crude cell lysate following co-culture of NIH3T3-ICAM-1 for 1 minute was used as a positive control. Protein-G Agarose and CT2 antibody were used as negative controls. (B) The anti-MUC1-ECD mAb B27.29 was used to immunoprecipitate MUC1 from breast cancer T47D cells after co-culturing with NIH3T3-Mock or -ICAM-1 transfectants for 10 seconds and 1 minute. Increased Src (indicated as red arrow) was co-immunoprecipitated with MUC1 after NIH3T3-ICAM-1 stimulation.

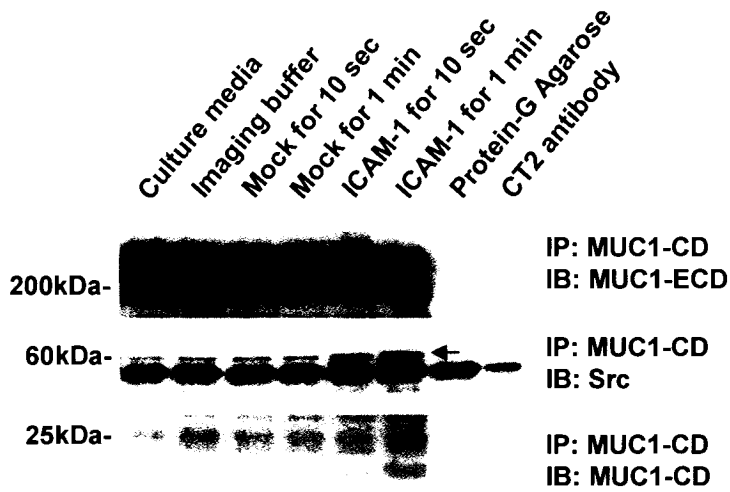

Figure 2.19: ICAM-1 increases the association of Src with MUC1 in 293T SYM25 cells. The anti-MUC1-CD mAb CT2 was used to immunoprecipitate MUC1 from 293T SYM25 cells after co-culturing with NIH3T3-Mock or -ICAM-1 transfectants for 10 seconds and 1 minute. Increased Src (indicated as red arrow) was co-immunoprecipitated with MUC1 after NIH3T3-ICAM-1 stimulation. Protein-G Agarose and CT2 antibody were used as negative controls.

2.3. Discussion

Recent advances in the biology of MUC1 have found that the aberrantly overexpressed MUC1 is critical in carcinogenic activity and tumor metastasis [1-3,41,42]. However, the mechanism(s) underlying the pro-migratory property of MUC1 is still largely unknown. Real-time fluorescent video microscopy studies have shown that adhesion of tumor cells to the vasculature of target organs is an essential and actively mediated step, independent of "mechanical trapping", in the formation of blood-borne metastases [43-47]. This implies that tumor cells may behave similarly to leukocytes in cell-endothelium adhesion and subsequent extravasation. ICAM-1 is present throughout the entire expected migratory track of a transiting cell and is essential in mediating leukocyte migration [48,49]. We and others have previously demonstrated that human breast epithelial cell MUC1, by binding ICAM-1 on the accessory cells, could also mediate tumor cell adhesion [6-8] and transendothelial migration [10,50]. This suggests that both tumor cells and leukocytes may utilize the same signaling mechanism(s) to initiate the orchestrated molecular events for transendothelial migration.

2.3.1. The MUC1/ICAM-1 Interaction Specifically Induces Calcium Oscillatory Signals.

In this study using live imaging fluorescent microscopy, we found that ICAM-1 specifically triggered intracellular calcium oscillatory signals in the MUC1-positive cells, which have been pre-loaded with fluorescent calcium indicator Fluo-3 [28]. Further, since these calcium-based signals were proportional to the surface MUC1 expression levels and could be abrogated by antibodies against either MUC1 or ICAM-1 [28], we conclude that MUC1 can initiate intracellular calcium oscillations by ligating ICAM-1.

This is different from the transient calcium spikes observed when either MUC1 or ICAM-1 was absent in the system. It was reported that the mechanical "poke" can induce calcium responses, which are characterized by a transient intracellular calcium rise without oscillations [51]. Thus, we propose that this transient calcium signal may simply be a result of non-specific cell-cell contact in the absence of MUC1/ICAM-1 ligation.

Further, the calcium oscillatory response is strongly suggestive of a definite signal, as the frequency and amplitude of calcium oscillations can encode instructions to activate particular kinases (e.g. calcium/CaMKII) [52] or transcription factors [53]. This is significant in light of the fact that calcium/CaMKII can directly activate MLCK to promote actomyosin-mediated cytoskeletal contraction and cell motility [18]. In addition, the possible downstream calcium-sensitive targets of this signal, as described above in section 1.1.3 may also include gelsolin [18,54] and calpain [55], both of which are involved in cytoskeletal reorganization and focal adhesion disassembly.

2.3.2. Src Family Kinase, PI3K and PLC are Required for the MUC1/ICAM-1 Induced Calcium Oscillatory Signaling.

This study provides evidence that the MUC1/ICAM-1 interaction-initiated calcium oscillations are mediated by a signaling cascade(s) involving Src family kinase, PI3K, PLC, and IP3R, but not MAPK [28]. This appears to differ from the previously described MUC1-CD phosphotyrosine-based signal(s) [11-13,15,16,36,56-58], as it is independent of the MAPK/ERK pathway. An earlier study by Schroeder *et al.* [15] found enhanced MAPK signaling as a downstream consequence of EGFR-mediated MUC1-CD phosphorylation following EGF stimulation. The activation of MAPK was not associated with proliferation as there was no increase in the activation status of PCNA (proliferative

cell nuclear antigen). The same group subsequently demonstrated that MUC1-CD is implicated in the focal adhesion complex and increased cell transmigration through a transwell membrane [17]. Since the critical role of MAPK/ERK cascade has been well established in cell migration [19,59], the MUC1/ICAM-1-induced calcium signal involving Src/PI3K/PLC may represent a novel MUC1-associated signaling that works in parallel with MUC1-CD-induced MAPK cascade in promoting cell migration.

Of particular significance, this study provides the first evidence that MUC1-associated signaling is dependent on lipid rafts. The present data confirms Handa's previous results that MUC1 was localized in lipid rafts [39], and extends the finding to breast cancer cells, as well as MUC1-transfected 293T cells. Further, we found that disruption of lipid rafts using MBCD or nystatin inhibited the MUC1/ICAM-1-induced calcium signaling [28]. This was expected, given that the signaling components which have been implicated in the MUC1/ICAM-1 ligation-induced calcium signaling, such as Src family kinases, PI3K and PLC are usually activated in lipid rafts [37,38] and cholesterol depletion has been shown to abrogate the function of Src and PLC [60-62]. There are nine members of the human Src family kinases, three of which (Src [13], Lyn [63] and Lck [64]) have been reported to associate with MUC1. Thus far, only Src has been found to interact with MUC1 in breast cancer cells [12,13]. Therefore, we specifically investigated the interaction between Src and MUC1 in response to ICAM-1 ligation. We found that Src was significantly shifted into lipid rafts and increased Src was associated with MUC1 in both breast cancer cells and MUC1-transfected 293T cells following ICAM-1 stimulation. This suggests that Src may play a vital role in the MUC1/ICAM-1-induced calcium signaling, particularly since Src can be upstream of

both PI3K and PLC [26,34,65,66]. As well, since the MUC1-CD contains a potential PI3K binding site and overexpression of MUC1 has been shown to activate the PI3K-mediated signaling [67], PI3K may also facilitate PLC membrane localization and activation by generating the PH domain binding site, PtdIns(3,4)P2 and PtdIns(3,4,5)P3, on the plasma membrane [68,69].

Taken together, these findings suggest that MUC1, by ligating ICAM-1 initiates a calcium-based pro-migratory signaling, which involves Src, PI3K, PLC and IP3R. This represents a novel MUC1-associated signaling and expands MUC1's repertoire of putative oncogenic functions.

2.4. References

1. Rahn JJ, Dabbagh L, Pasdar M, Hugh JC: **The importance of MUC1 cellular localization in patients with breast carcinoma: an immunohistologic study of 71 patients and review of the literature.** *Cancer* 2001, **91**:1973-1982.
2. Schroeder JA, Masri AA, Adriance MC, Tessier JC, Kotlarczyk KL, Thompson MC, Gendler SJ: **MUC1 overexpression results in mammary gland tumorigenesis and prolonged alveolar differentiation.** *Oncogene* 2004, **23**:5739-5747.
3. Wei X, Xu H, Kufe D: **Human MUC1 oncoprotein regulates p53-responsive gene transcription in the genotoxic stress response.** *Cancer Cell* 2005, **7**:167-178.
4. Hayashi T, Takahashi T, Motoya S, Ishida T, Itoh F, Adachi M, Hinoda Y, Imai K: **MUC1 mucin core protein binds to the domain 1 of ICAM-1.** *Digestion* 2001, **63 Suppl 1**:87-92.
5. Horne GJ, University of Alberta. Dept. of Laboratory Medicine and Pathology.: **The role of breast cancer associated with MUC1 in tumor cell recruitment to vascular endothelium during physiological fluid flow**: 1999.
6. Kam JL, Regimbald LH, Hilgers JH, Hoffman P, Krantz MJ, Longenecker BM, Hugh JC: **MUC1 synthetic peptide inhibition of intercellular adhesion molecule-1 and MUC1 binding requires six tandem repeats.** *Cancer Res* 1998, **58**:5577-5581.
7. McDermott KM, Crocker PR, Harris A, Burdick MD, Hinoda Y, Hayashi T, Imai K, Hollingsworth MA: **Overexpression of MUC1 reconfigures the binding properties of tumor cells.** *Int J Cancer* 2001, **94**:783-791.
8. Regimbald LH, Pilarski LM, Longenecker BM, Reddish MA, Zimmermann G, Hugh JC: **The breast mucin MUCI as a novel adhesion ligand for endothelial intercellular adhesion molecule 1 in breast cancer.** *Cancer Res* 1996, **56**:4244-4249.
9. Rahn JJ, University of Alberta. Dept. of Medical Sciences.: **The role of the MUC1/ICAM-1 interaction in promoting breast cancer cell migration**: 2004.
10. Rahn JJ, Chow JW, Horne GJ, Mah BK, Emerman JT, Hoffman P, Hugh JC: **MUC1 mediates transendothelial migration in vitro by ligating endothelial cell ICAM-1.** *Clin Exp Metastasis* 2005, **22**:475-483.
11. Li Y, Bharti A, Chen D, Gong J, Kufe D: **Interaction of glycogen synthase kinase 3beta with the DF3/MUC1 carcinoma-associated antigen and beta-catenin.** *Mol Cell Biol* 1998, **18**:7216-7224.
12. Li Y, Kuwahara H, Ren J, Wen G, Kufe D: **The c-Src tyrosine kinase regulates signaling of the human DF3/MUC1 carcinoma-associated antigen with GSK3 beta and beta-catenin.** *J Biol Chem* 2001, **276**:6061-6064.
13. Li Y, Ren J, Yu W, Li Q, Kuwahara H, Yin L, Carraway KL, 3rd, Kufe D: **The epidermal growth factor receptor regulates interaction of the human DF3/MUC1 carcinoma antigen with c-Src and beta-catenin.** *J Biol Chem* 2001, **276**:35239-35242.
14. Yamamoto M, Bharti A, Li Y, Kufe D: **Interaction of the DF3/MUC1 breast carcinoma-associated antigen and beta-catenin in cell adhesion.** *J Biol Chem* 1997, **272**:12492-12494.

15. Schroeder JA, Thompson MC, Gardner MM, Gendler SJ: **Transgenic MUC1 interacts with epidermal growth factor receptor and correlates with mitogen-activated protein kinase activation in the mouse mammary gland.** *J Biol Chem* 2001, **276**:13057-13064.
16. Pandey P, Kharbanda S, Kufe D: **Association of the DF3/MUC1 breast cancer antigen with Grb2 and the Sos/Ras exchange protein.** *Cancer Res* 1995, **55**:4000-4003.
17. Schroeder JA, Adriance MC, Thompson MC, Camenisch TD, Gendler SJ: **MUC1 alters beta-catenin-dependent tumor formation and promotes cellular invasion.** *Oncogene* 2003, **22**:1324-1332.
18. Lodish HF: *Molecular cell biology* edn 4th. New York: W.H. Freeman; 2000.
19. Feldner JC, Brandt BH: **Cancer cell motility--on the road from c-erbB-2 receptor steered signaling to actin reorganization.** *Exp Cell Res* 2002, **272**:93-108.
20. Pontremoli S, Melloni E: **The role of calpain and protein kinase C in activation of human neutrophils.** *Prog Clin Biol Res* 1988, **282**:195-208.
21. Pontremoli S, Melloni E: **The role of intracellular proteinases in human neutrophil activation.** *Revis Biol Celular* 1989, **20**:161-177.
22. Playford MP, Schaller MD: **The interplay between Src and integrins in normal and tumor biology.** *Oncogene* 2004, **23**:7928-7946.
23. Berridge MJ, Lipp P, Bootman MD: **The versatility and universality of calcium signalling.** *Nat Rev Mol Cell Biol* 2000, **1**:11-21.
24. Kumada T, Komuro H: **Completion of neuronal migration regulated by loss of Ca(2+) transients.** *Proc Natl Acad Sci U S A* 2004, **101**:8479-8484.
25. Marks PW, Hendey B, Maxfield FR: **Attachment to fibronectin or vitronectin makes human neutrophil migration sensitive to alterations in cytosolic free calcium concentration.** *J Cell Biol* 1991, **112**:149-158.
26. Thomas SM, Brugge JS: **Cellular functions regulated by Src family kinases.** *Annu Rev Cell Dev Biol* 1997, **13**:513-609.
27. Oosawa Y, Imada C, Furuya K: **Temperature dependency of calcium responses in mammary tumour cells.** *Cell Biochem Funct* 1997, **15**:113-117.
28. Rahn JJ, Shen Q, Mah BK, Hugh JC: **MUC1 initiates a calcium signal after ligation by intercellular adhesion molecule-1.** *J Biol Chem* 2004, **279**:29386-29390.
29. Montano LM, Bazan-Perkins B: **Resting calcium influx in airway smooth muscle.** *Can J Physiol Pharmacol* 2005, **83**:717-723.
30. Barritt GJ: **Receptor-activated Ca2+ inflow in animal cells: a variety of pathways tailored to meet different intracellular Ca2+ signalling requirements.** *Biochem J* 1999, **337 (Pt 2)**:153-169.
31. Marks AR: **Intracellular calcium-release channels: regulators of cell life and death.** *Am J Physiol* 1997, **272**:H597-605.
32. Harootunian AT, Kao JP, Paranjape S, Tsien RY: **Generation of calcium oscillations in fibroblasts by positive feedback between calcium and IP3.** *Science* 1991, **251**:75-78.
33. Keizer J, De Young GW: **Two roles of Ca2+ in agonist stimulated Ca2+ oscillations.** *Biophys J* 1992, **61**:649-660.

34. Tokmakov AA, Sato KI, Iwasaki T, Fukami Y: **Src kinase induces calcium release in Xenopus egg extracts via PLCgamma and IP3-dependent mechanism.** *Cell Calcium* 2002, **32**:11-20.
35. Zrihan-Licht S, Baruch A, Elroy-Stein O, Keydar I, Wreschner DH: **Tyrosine phosphorylation of the MUC1 breast cancer membrane proteins. Cytokine receptor-like molecules.** *FEBS Lett* 1994, **356**:130-136.
36. Wang H, Lillehoj EP, Kim KC: **Identification of four sites of stimulated tyrosine phosphorylation in the MUC1 cytoplasmic tail.** *Biochem Biophys Res Commun* 2003, **310**:341-346.
37. Simons K, Toomre D: **Lipid rafts and signal transduction.** *Nat Rev Mol Cell Biol* 2000, **1**:31-39.
38. Zajchowski LD, Robbins SM: **Lipid rafts and little caves. Compartmentalized signalling in membrane microdomains.** *Eur J Biochem* 2002, **269**:737-752.
39. Handa K, Jacobs F, Longenecker BM, Hakomori SI: **Association of MUC-1 and SPGL-1 with low-density microdomain in T-lymphocytes: a preliminary note.** *Biochem Biophys Res Commun* 2001, **285**:788-794.
40. Isshiki M, Anderson RG: **Calcium signal transduction from caveolae.** *Cell Calcium* 1999, **26**:201-208.
41. Al Masri A, Gendler SJ: **Muc1 affects c-Src signaling in PyV MT-induced mammary tumorigenesis.** *Oncogene* 2005, **24**:5799-5808.
42. Cozzi PJ, Wang J, Delprado W, Perkins AC, Allen BJ, Russell PJ, Li Y: **MUC1, MUC2, MUC4, MUC5AC and MUC6 expression in the progression of prostate cancer.** *Clin Exp Metastasis* 2005, **22**:565-573.
43. Al-Mehdi AB, Tozawa K, Fisher AB, Shientag L, Lee A, Muschel RJ: **Intravascular origin of metastasis from the proliferation of endothelium-attached tumor cells: a new model for metastasis.** *Nat Med* 2000, **6**:100-102.
44. Glinskii OV, Huxley VH, Glinsky GV, Pienta KJ, Raz A, Glinsky VV: **Mechanical entrapment is insufficient and intercellular adhesion is essential for metastatic cell arrest in distant organs.** *Neoplasia* 2005, **7**:522-527.
45. Glinskii OV, Huxley VH, Turk JR, Deutscher SL, Quinn TP, Pienta KJ, Glinsky VV: **Continuous real time ex vivo epifluorescent video microscopy for the study of metastatic cancer cell interactions with microvascular endothelium.** *Clin Exp Metastasis* 2003, **20**:451-458.
46. Glinsky VV, Glinsky GV, Glinskii OV, Huxley VH, Turk JR, Mossine VV, Deutscher SL, Pienta KJ, Quinn TP: **Intravascular metastatic cancer cell homotypic aggregation at the sites of primary attachment to the endothelium.** *Cancer Res* 2003, **63**:3805-3811.
47. Vlems FA, Ruers TJ, Punt CJ, Wobbes T, van Muijen GN: **Relevance of disseminated tumour cells in blood and bone marrow of patients with solid epithelial tumours in perspective.** *Eur J Surg Oncol* 2003, **29**:289-302.
48. Kuby J: *Immunology* edn 3rd. New York: W.H. Freeman; 1997.
49. Luscinskas FW, Gimbrone MA, Jr.: **Endothelial-dependent mechanisms in chronic inflammatory leukocyte recruitment.** *Annu Rev Med* 1996, **47**:413-421.
50. Rahn JJ, Hugh JC: **The MUC1/ICAM-1 signal: its potential to trigger tumor cell migration.** *Six Conference on Signaling in Normal and Cancer Cells, IRCM* 2004.

51. Sigurdson WJ, Sachs F, Diamond SL: **Mechanical perturbation of cultured human endothelial cells causes rapid increases of intracellular calcium.** *Am J Physiol* 1993, **264**:H1745-1752.
52. Putney JW, Jr.: **Calcium signaling: up, down, up, down...what's the point?** *Science* 1998, **279**:191-192.
53. Dolmetsch RE, Xu K, Lewis RS: **Calcium oscillations increase the efficiency and specificity of gene expression.** *Nature* 1998, **392**:933-936.
54. Sun HQ, Yamamoto M, Mejillano M, Yin HL: **Gelsolin, a multifunctional actin regulatory protein.** *J Biol Chem* 1999, **274**:33179-33182.
55. Perrin BJ, Huttenlocher A: **Calpain.** *Int J Biochem Cell Biol* 2002, **34**:722-725.
56. Quin RJ, McGuckin MA: **Phosphorylation of the cytoplasmic domain of the MUC1 mucin correlates with changes in cell-cell adhesion.** *Int J Cancer* 2000, **87**:499-506.
57. Ren J, Li Y, Kufe D: **Protein kinase C delta regulates function of the DF3/MUC1 carcinoma antigen in beta-catenin signaling.** *J Biol Chem* 2002, **277**:17616-17622.
58. Meerzaman D, Shapiro PS, Kim KC: **Involvement of the MAP kinase ERK2 in MUC1 mucin signaling.** *Am J Physiol Lung Cell Mol Physiol* 2001, **281**:L86-91.
59. Kim MS, Lee EJ, Kim HR, Moon A: **p38 kinase is a key signaling molecule for H-Ras-induced cell motility and invasive phenotype in human breast epithelial cells.** *Cancer Res* 2003, **63**:5454-5461.
60. Hur EM, Park YS, Lee BD, Jang IH, Kim HS, Kim TD, Suh PG, Ryu SH, Kim KT: **Sensitization of epidermal growth factor-induced signaling by bradykinin is mediated by c-Src. Implications for a role of lipid microdomains.** *J Biol Chem* 2004, **279**:5852-5860.
61. Bodin S, Viala C, Ragab A, Payrastre B: **A critical role of lipid rafts in the organization of a key FcgammaRIIa-mediated signaling pathway in human platelets.** *Thromb Haemost* 2003, **89**:318-330.
62. Kiely JM, Hu Y, Garcia-Cardena G, Gimbrone MA, Jr.: **Lipid raft localization of cell surface E-selectin is required for ligation-induced activation of phospholipase C gamma.** *J Immunol* 2003, **171**:3216-3224.
63. Li Y, Chen W, Ren J, Yu WH, Li Q, Yoshida K, Kufe D: **DF3/MUC1 signaling in multiple myeloma cells is regulated by interleukin-7.** *Cancer Biol Ther* 2003, **2**:187-193.
64. Li Q, Ren J, Kufe D: **Interaction of human MUC1 and beta-catenin is regulated by Lck and ZAP-70 in activated Jurkat T cells.** *Biochem Biophys Res Commun* 2004, **315**:471-476.
65. Shu L, Shayman JA: **Src kinase mediates the regulation of phospholipase C-gamma activity by glycosphingolipids.** *J Biol Chem* 2003, **278**:31419-31425.
66. Ozdener F, Dangelmaier C, Ashby B, Kunapuli SP, Daniel JL: **Activation of phospholipase Cgamma2 by tyrosine phosphorylation.** *Mol Pharmacol* 2002, **62**:672-679.
67. Raina D, Kharbanda S, Kufe D: **The MUC1 oncoprotein activates the anti-apoptotic phosphoinositide 3-kinase/Akt and Bcl-xL pathways in rat 3Y1 fibroblasts.** *J Biol Chem* 2004, **279**:20607-20612.

68. Bobe R, Wilde JI, Maschberger P, Venkateswarlu K, Cullen PJ, Siess W, Watson SP: **Phosphatidylinositol 3-kinase-dependent translocation of phospholipase Cgamma2 in mouse megakaryocytes is independent of Bruton tyrosine kinase translocation**. *Blood* 2001, **97**:678-684.
69. Wymann MP, Pirola L: **Structure and function of phosphoinositide 3-kinases**. *Biochim Biophys Acta* 1998, **1436**:127-150.

Chapter 3: MUC1 Initiates Cytoskeletal Reorganization and Increased Protrusive Motility by Ligating ICAM-1[2]

[2]A manuscript based on the data of this chapter has been submitted to the Journal of Biological Chemistry.

3.0. Introduction

The results presented in chapter 2, together with our previous findings that MUC1 binds ICAM-1 on accessory cells [1-3] and facilitates transendothelial migration of MUC1-bearing cells through a monolayer of ICAM-1 expressing cells [4,5], indicates that MUC1 may not only function as an adhesion molecule but also initiate calcium-based pro-migratory signaling during cell migration. The signaling mediators involved in MUC1/ICAM-1-induced calcium oscillations, such as Src family kinase, PI3K, and PLC are critical intermediaries in the regulation of actin cytoskeletal rearrangements and cell migration [6-8]. As well, calcium-based signaling is frequently implicated in actin cytoskeletal reorganization [9], with the frequency of the calcium oscillations directly related to the rate of cell migration [10]. Thus, it is worthwhile to investigate the potential role of the MUC1/ICAM-1 interaction in actin cytoskeletal reorganization and cell motility. This is important, since tumor metastasis requires increased cell motility, in which the actin cytoskeletal rearrangements play a decisive role.

Integrin family glycoproteins also play an important role in regulating cell migration. Integrins are preferentially activated and localized at the leading edge, where they relay signals from the extracellular matrix (ECM) to the cytoskeleton, initiating and sustaining cell motility [7,11]. Notably, previous cell imaging studies showed that MUC1 is also concentrated at the leading edge of migrating cells [12] and co-distributes with ezrin [13], a linker of membrane proteins to the actin cytoskeleton. However, the relationship between MUC1 and integrins in cell motility is still uncharacterized.

Rho family small GTPases (Rac, Cdc42, and Rho), as described in chapter 1, are also critical in regulating actin cytoskeletal protrusive motility [14,15]. Generally in

response to migratory cues, Rac and Cdc42 are activated and implicated in membrane ruffling and the formation of membrane lamellipodial and filopodial protrusions, thereby controlling directional migration [16], whereas Rho is frequently involved in cellular contraction and focal adhesion dynamics [17].

Taken together, there were several questions to be addressed in this chapter: i) Does the MUC1/ICAM-1 interaction induce actin cytoskeletal reorganization? If so, ii) what mediates the MUC1/ICAM-1-initiated cytoskeletal reorganization? iii) Is integrin involved in the MUC1/ICAM-1-initiated cytoskeletal reorganization? iv) What role do the Rho GTPases play in this process? These studies represent a further investigation into mechanism(s) by which MUC1 may promote breast cancer metastasis.

3.1. Materials and Methods

3.1.1. Reagents

B27.29 mouse mAb against the MUC1-ECD was a gift from Biomira, Inc (Edmonton, AB, Canada). CT2 Armenian hamster mAb against MUC1-CD was generously provided by Dr. Sandra Gendler, Mayo Clinic, Scottsdale, AZ. The mouse anti-human ICAM-1 mAbs 18E3D and 164B were provided by ICOS Corporation (Bothell, WA, USA). The goat anti-mouse or anti-Armenian hamster horseradish peroxidase (HRP) conjugated secondary antibodies were obtained from Jackson ImmunoResearch (West Grove, PA, USA). NotI, KpnI, and T4 DNA ligase were purchased from New England Biolabs (Ipswich, MA, USA). AP-138, a mouse anti-β1 integrin mAb, was provided by Dr. Andrew R.E. Shaw, University of Alberta, AB. GRGDNP and RGES peptides were purchased from American Peptide Company, Inc

(Sunnyvale, CA, USA). ECL Plus Western Blotting detection reagents were purchased from Amersham Biosciences, England, UK. 35mm glass-bottomed microwell dishes were purchased from MatTek Corporation (Asland, MA, USA). U-73122, U-73343, wortmannin, protease inhibitor cocktail, MOPC 31C mouse IgG1, B-5-1-2 anti-tubulin mAb, L-glutamine and gelatin were from Sigma-Aldrich (Oakville, ON, Canada). PP2 and 2-APB were from Tocris (Ellisville, MO, USA). Dextran-Alexa Fluor 568 (10000 MW, anionic) was purchased from Molecular Probes (Burlington, ON, Canda). Aluminosilicate-filaments (O.D.: 1.0mm, I.D.: 0.68mm, length: 10cm) were purchased from Sutter Instrument (Novato, CA, USA). DMEM, FBS, trypsin, low melting point agarose, lipofectamine^{TM}2000, Opti-MEM, G418, blasticidin S, zeocin, hygromycin B and tetracycline were purchased from Invitrogen, Inc (Carlsbad, CA, USA).

3.1.2. Expression Plasmids

pEGFP-actin plasmid was purchased from Clontech laboratories, Inc. (Mountain View, CA, USA). pC1Neo-hMUC1-TR+ plasmid was kindly provided by Dr. Sandra Gendler, Mayo Clinic, Scottsdale, AZ. The pcDNA5/FRT/TO plasmid and pOG44 Flp recombinase expression plasmid were purchased from Invitrogen, Inc (Carlsbad, CA, USA). Dominant negative Rac1-T17N, Cdc42-T17N, and RhoA-T19N plasmids were kindly provided by cDNA Resource Center, University of Missouri-Rolla, MO, USA.

3.1.3. Plasmid Construction

The Flp-In System from Invitrogen was used to generate conditional MUC1-expressing 293 cells. The main components consist of the pOG44 plasmid, which

encodes Flp-recombinase, the pcDNA5/FRT/TO cassette vector, which is designed to carry the gene of interest, and the Flp-In T-Rex 293 cell line. This cell line is engineered to have a single, stably integrated FRT (Flp Recombinase Target) site placed at a locus that is transcriptionally active. Thus, co-transfection of these cells with pOG44 plasmid and pcDNA5/FRT/TO plasmid carrying the gene of interest is designed to result in fewer subclone artifacts by having targeted, stable integration of the expression vector to the same locus in every cell, giving homogenous expression. In addition, the T-Rex system contains a tetracycline responsive promoter that allows conditional expression of the gene of interest based on the presence or absence of tetracycline in the culture medium.

To create the conditional MUC1-expressing pcDNA5/FRT/TO-MUC1 plasmid (Fig. 3.1), the pC1Neo-hMUC1-TR+ plasmid (kindly provided by Dr. Sandra Gendler, Mayo Clinic, Scottsdale, AZ) and the pcDNA5/FRT/TO plasmid were digested with NotI. The digested pcDNA5/FRT/TO plasmid was also dephosphorylated to prevent religation of the cut ends. Both plasmids were then purified on a 1% low melting point agarose gel, and the pcDNA5/FRT/TO plasmid and 2.8 kB MUC1 insert bands were cut out of the gel. The gel slices were melted at 70°C, and then rapidly frozen in a dry ice/acetone bath for five minutes. After they thawed, they were centrifuged at 14000 xg for ten minutes to remove the precipitated agarose, leaving the DNA fragments in the supernatant. 1 µl of the pcDNA5/FRT/TO supernatant was mixed with 7 µl of the MUC1 insert supernatant, and incubated with T4 ligase and the manufacturer supplied reaction buffer at 16°C overnight. The entire ligation reaction was used to transform DH5α host bacteria. Ampicillin resistant colonies were screened for proper directional insertion of the MUC1 gene, using KpnI, which cuts the cassette vector once, close to the 5' end of

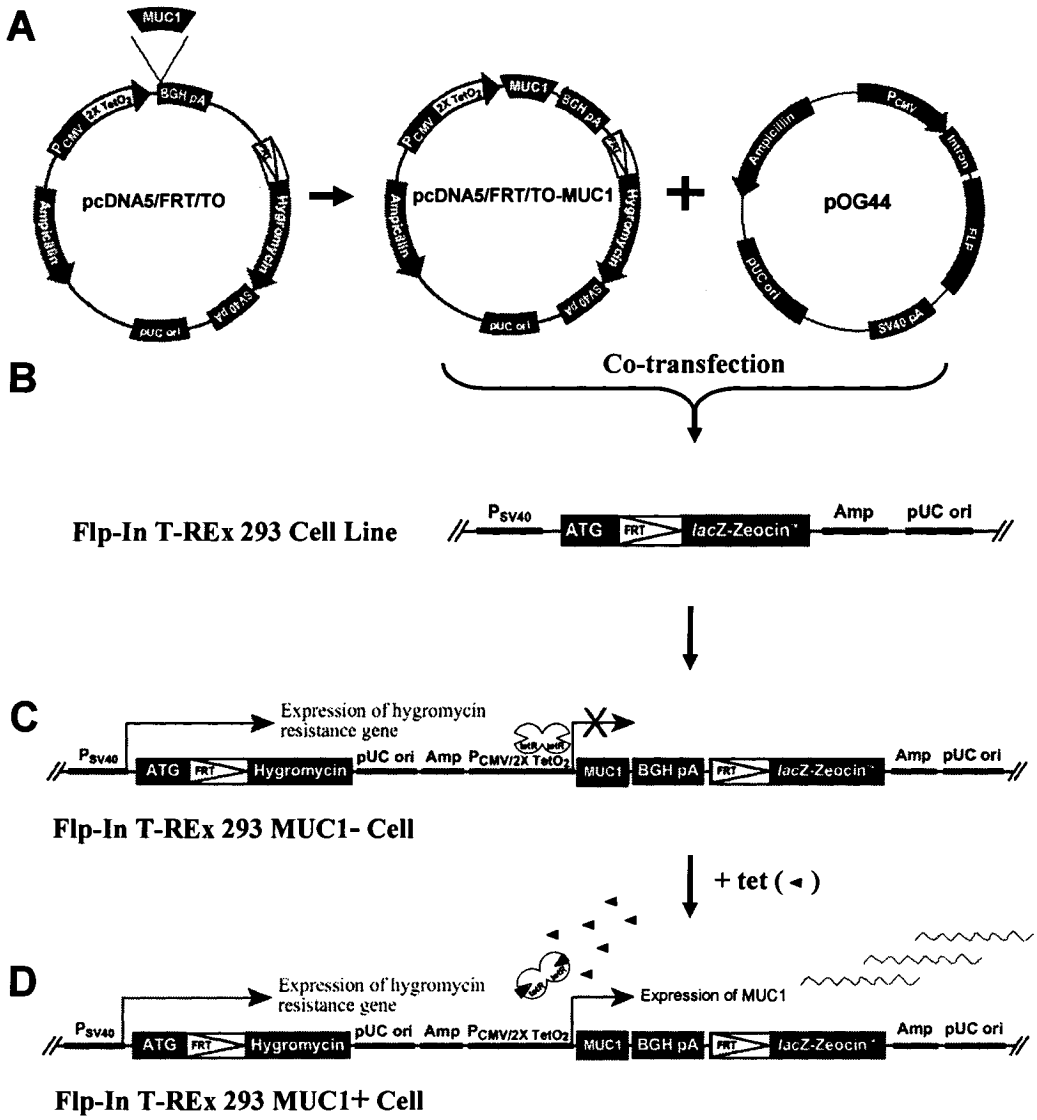

Figure 3.1: Generation of the Flp-In T-REx 293 MUC1 system. (A) pcDNA5/FRT/TO-MUC1 plasmid was created by ligating *MUC1* gene into the pcDNA5/FRT/TO plasmid. (B) pcDNA5/FRT/TO-MUC1 and pOG44 plasmids were co-tranfected into the Flp-In T-REx 293 cells, and hygromycin resistant cells were selected. (C) Expression of MUC1 was repressed by the Tet repressor (TetR) in the generated Flp-In T-REx 293 MUC1 cells. (D) Expression of MUC1 was induced by the adding of tetracycline in culture medium. Adapted from http://www.invitrogen.com/content/sfs/manuals/flpintrexcells_man.pdf

the multiple cloning site, and the MUC1 gene close to the 3' end. Thus, KpnI digests that resulted in a larger insertion fragment had MUC1 inserted in the correct orientation.

3.1.4. Cell Culture

Human breast cancer cells T47D, MCF-7, and Hs578T were from the ATCC, and were maintained in DMEM containing 10% FBS. The MUC1-transfected 293T cells SYM3, SYM25, and SYM33, as previously described [18], were maintained in DMEM containing 10% FBS and 200μg/ml G418. Human ICAM-1-transfected NIH3T3 cells and the mock-transfected counterparts were a generous gift of Dr. Ken Dimock, University of Ottawa, ON, and were maintained in DMEM containing 10% FBS and 2μg/ml blasticidin S. Flp-In T-REx 293 cells (Invitrogen), which contains a single integrated Flp combinase target (FRT) site from pFRT/lacZeo and expresses the Tet repressor from pcDNA6/TR, were maintained in DMEM containing 10% FBS, 2 mM L-glutamine, 200μg/ml zeocin, and 15μg/ml blasticidin S. To establish the Flp-In T-REx 293 MUC1 inducible expression system, the Flp-In T-REx 293 cells were co-transfected with pcDNA5/FRT/TO-MUC1 plasmids and pOG44 plasmids using lipofectamine^{TM} 2000 and Opti-MEM (Fig. 3.1). Forty-eight hours after transfection, the culture medium was replaced with DMEM containing 10% FBS, 15μg/ml blasticidin S, and 150μg/ml hygromycin B for selecting Flp-In T-REx 293 MUC1 cells. Two weeks after transfection, the antibiotic resistant cells were harvested without cloning and tested for MUC1 expression. As expected, MUC1 protein expression can be induced or inhibited in this system by tetracycline-responsive regulation (Fig. 3.1). To generate pEGFP-actin expressing cells, all the cell lines described above (i.e. T47D, MCF-7, Hs578T, 293T SYM25, SYM33, SYM3, and Flp-In T-REx 293 MUC1 cells) were transfected with

pEGFP-actin respectively using lipofectamine^{TM}2000 and Opti-MEM (see section 3.1.5). Forty-eight hours after transfection, 1200μg/ml G418 was added to the culture medium for selection and the resultant pEGFP-actin transfectants were used for the cytoskeletal reorganization analysis as described below in section 3.1.8.

3.1.5. Transfection and Selection of Transfectants

Transfections were carried out in 6-well plates (Corning) using lipofectamine^{TM} 2000 according to the manufacturer's instruction. The day before transfection, 2 ml of cells at ~6 X 10^5/ml were seeded into each well of the plate, and equilibrated overnight in DMEM supplemented with 10% FBS. This generally resulted in ~90% cell confluency the next day. Then, the culture medium was replaced with serum free DMEM medium 4 hours before transfection. For generating the MUC1 inducible-expression Flp-In T-REx 293 cells, eppendorf tubes containing 4μg of pcDNA5/FRT/TO-MUC1 plasmid and 36μg of pOG44 plasmid in a volume of 250μl of Opti-MEM medium were combined with a second set of tubes containing 30μl of lipofectamine^{TM}2000 in a volume of 250μl of Opti-MEM. For generating the pEGFP-actin transfected cells, eppendorf tubes containing 4μg of pEGFP-actin plasmid DNA in a volume of 250μl of Opti-MEM medium were combined with a second set of tubes containing 10μl of lipofectamine^{TM} 2000 in a volume of 250μl of Opti-MEM. After combining the plasmid DNA and lipofectamine^{TM}2000, the mixtures were incubated for 20 minutes at room temperature to allow the DNA-lipofectamine^{TM}2000 complexes to form. Then, 500μl of the DNA-lipofectamine^{TM}2000 complexes were added into each well, which had been washed once and refilled with 1.5ml of Opti-MEM. Following 6 hours of incubation at 37°C and 5% CO_2, the transfection mixture was replaced with 2ml of regular growth medium DMEM.

FBS and sodium butyrate were then subsequently added onto the cells to get the final concentrations of 10% and 2mM respectively for increasing expression of the plasmid. The cells were incubated overnight at 37 °C, 5% CO_2, and then passaged at 1:10 dilution into fresh DMEM medium supplemented with 10% FBS and selecting antibiotics. For pEGFP-actin transfected cells, flow cytometry was used to select the pEGFP-actin expressing cells as described below.

3.1.6. Flow Cytometry

The adherent pEGFP-actin transfected cells, as well as the untransfected control cells, were trypsinized from culture dishes. Then, the cells were washed 3 times in Flow Cytometry Buffer (PBS supplemented with 1% BSA and 1mM EDTA) and resuspended at 1 X 10^6/ml in 15ml Falcon polystyrene tubes (12 X 75mm). Fluorescence-activated cell sorting (FACS) was carried out on a Beckman Coulter EPICS Ultra High-Speed Cell Sorter, equipped with a water-cooled 488nm Argon laser. Forward scatter (FS) and side scatter (SSC) were collected using filters as follows. The EGFP signal was collected in the FL1 channel using a 530 bandpass filter. A light scatter gate was drawn in the SSC versus FS plot to exclude the cell debris. Cells in the gate were displayed in a single parameter histogram for EGFP signal and final gate settings were determined to collect the positive cells. Then, the cells were sorted into a 6 well plate at a concentration of 5 X 10^4/well and, in 24 hours, transferred into a T-75 Flask in fresh culture medium for future analysis.

3.1.7. SDS-PAGE and Western Blot Analysis

Cells were lysed in RIPA buffer, and then analyzed with a Bio-Rad DC assay and Bio-Rad Mini-PROTEIN II gel (4-20% gradient with 4% stacking) electrophoresis. The separated proteins were then transferred to an Immobilon-P membrane using a Bio-Rad Mini Trans-Blot system as described in section 2.1.3. After transferring, membranes were blocked and immunoblotted with subsequent detection using ECL Plus reagent as previously described in section 2.1.3.

3.1.8. Cytoskeletal Reorganization Assays

The 35mm glass-bottomed MatTek microwell dishes were coated with 100 µl of FBS or 0.1% (w/v) gelatin as described previously in section 2.1.4 [18]. 100 µl of pEGFP-actin transfected breast cancer cells (T47D, MCF-7, and Hs578T), 293T SYM subclones (SYM25, SYM33, and SYM3) or Flp-In T-REx 293 MUC1 cells at 5 x 10^4/ml were seeded on the precoated dishes and equilibrated overnight. The plated cells were then washed once with 37°C Imaging Buffer [18,19], and left in Imaging Buffer at 37°C for 30 minutes until imaged. Meanwhile, NIH3T3-ICAM-1 or -Mock transfectants were trypsinized, rinsed once with PBS, and resuspended in Imaging Buffer at ~ 1 x 10^7/ml. Then, the MatTek dish was placed in a 37°C microscope stage warmer on a Zeiss 2-photon confocal microscope (Zeiss NLO 510), and a representative cell was focused with a plan neofluar 40X/1.3 oil immersion lens (Fig. 3.2). The EGFP was excited using a 488 nm laser line of a 25mW Argon laser excitation source (for the dominant negative Rho GTPase microinjected cells, a 543 nm laser line of a 1mW HeNe laser was used for excitation of the Alexa Fluor-568 signal) with the intensity output was set to 25%. 8-bit images were collected with a 1.60µs dwell time per pixel. The pinhole was set to 1 Airy unit and images were collected at 0.11 µm/pixel resolution. The gain and offset were set

to expand the signal from the cell being imaged over the 255 grey value scale of the 8-bit data range. Then, Z stacks (~0.45 μm intervals from cell bottom to top) were acquired every 2 minutes for a total of 45, recorded over the 1.5 hour experiment under both DIC and a 505 nm long pass filter (EGFP). 600 μl of NIH3T3-ICAM-1 or -Mock cell suspension was gently added onto the plated cells immediately after the first image was taken.

For the ICAM-1 blocking experiments, the NIH3T3-ICAM-1 transfectants were preincubated with anti-ICAM-1 mAb 164-B (20μg/ml) or mAb 18E3D (20μg/ml) for 30 minutes at 37°C, 5% CO_2, before adding onto the pEGFP-actin transfected breast cancer cells (T47D and Hs578T) and MUC1-transfected 293T subclones (SYM25 and SYM3) and commencing cell imaging. For the β1 integrin blocking experiments, the pEGFP-actin transfected breast cancer T47D cells, as well as the 293T SYM25 cells were incubated with anti-β1 integrin antibody AP-138 (20μg/ml) or isotype matched mouse IgG1 (20μg/ml) for 30 minutes at 37°C, 5% CO_2, before stimulation by NIH3T3-ICAM-1 or -Mock transfectants. To confirm the results generated by anti-β1 integrin AP-138 antibody, either the β1 integrin blocking GRGDNP (1.0mM) peptide or the control RGES peptide (1.0mM) was used to pretreat the pEGFP-actin transfected T47D cells and 293T SYM25 cells for 30 minutes at 37°C, 5% CO_2, prior to the stimulation by NIH3T3 transfectants. For the pharmaceutical inhibition experiments, the pEGFP-actin transfected breast cancer T47D cells and 293T SYM25 cells were preincubated with wortmannin (2μM), PP2 (10μM), 2-APB (100μM), U-73122 (10μM), or U-73343 (10μM) in Imaging Buffer for 30 minutes at 37°C, 5% CO_2, followed by stimulation with NIH3T3-ICAM-1 or -Mock cells and imaging.

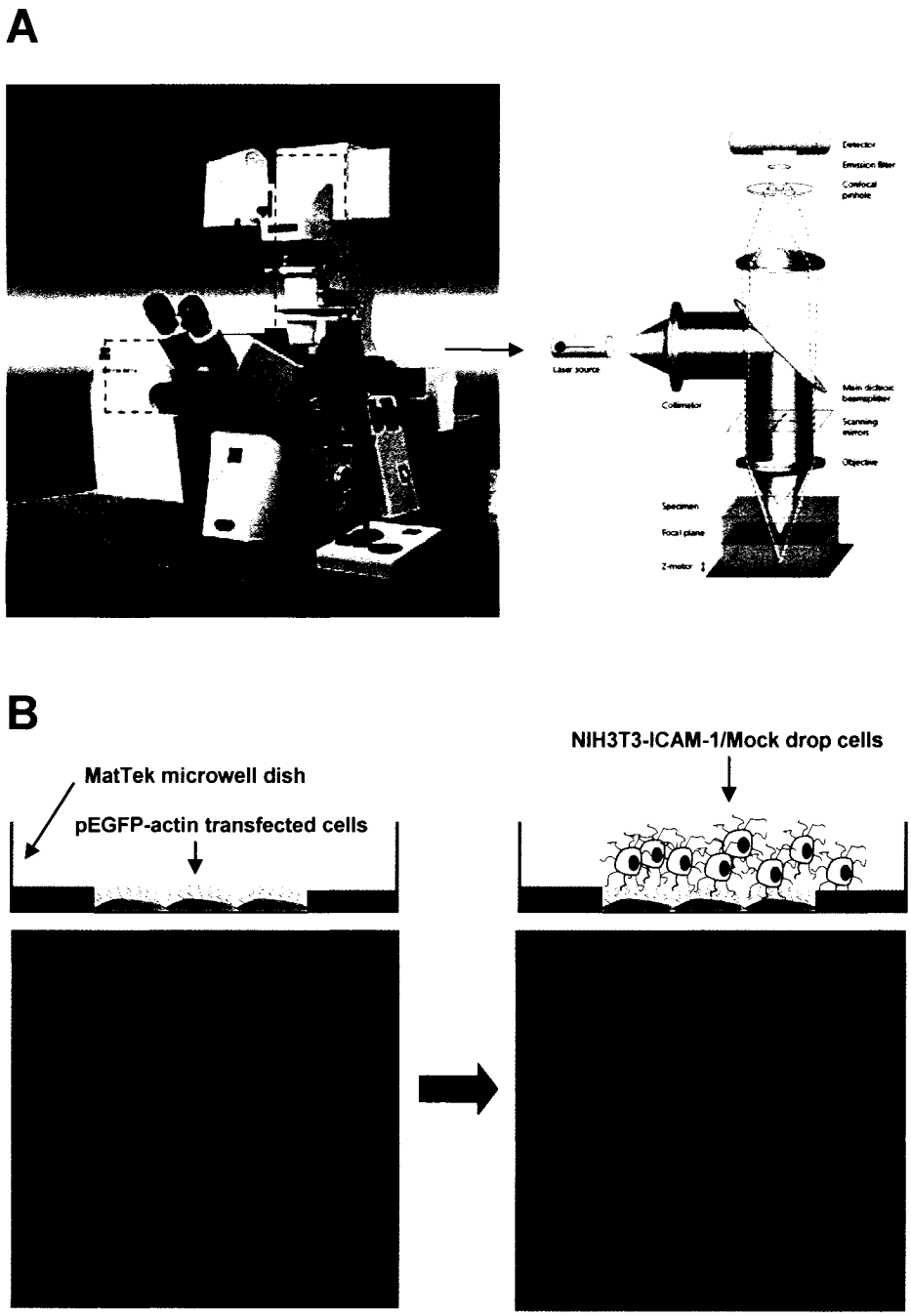

Figure 3.2: The actin cytoskeletal reorganization assay. (A) Zeiss 2-photon confocal microscope (Zeiss NLO 501) and mechanism cartoon. (B) A pEGFP-actin transfected cell was imaged with a plan neofluar 40X/1.3 oil immersion lens (left), and then the cytoskeletal rearrangements were examined following stimulation by NIH3T3 transfectants (right).

3.1.9. Quantitative Analysis of Cytoskeletal Reorganization

Under the Expert Mode of LSM software, the image stacks of Z-series were collected at every 5th time point (i.e. every 10 minutes) from time zero (i.e. the first image Z-stack collected within the first 2 minutes). Thus, in total 9 time points were generated and saved for quantitative analysis.

The analyses of actin cytoskeletal rearrangements were performed using Imaris Software (Bitplane AG, version 4.2) (Fig. 3.3). In the surpass mode of Imaris, the DIC channel was deleted and the 3-D GFP images at each time point were surface rendered by setting a threshold value, which subtracted the non-specific fluorescence intensity values of background. The isosurface was then used to measure the whole cell pEGFP-actin voxel intensity sum (AVIS) at each time point and the resultant data was exported to MS Excel. Then, the cell body was contoured manually in each slice of the imaging stacks. Further, by masking channel with the contoured surface and setting the voxels inside of the contoured surface to zero, the AVIS in the protrusions was obtained. Thus, the cytoskeletal rearrangements can be tracked by tracing the proportion (%) of AVIS in the protrusions as compared with that in the whole cell over time. The actin cytoskeletal reorganization factor (ACRF) was calculated as the average of the AVIS changes in protrusions, during the course of the entire cytoskeletal reorganization assay. The ACRF thus numerically represents the level of cytoskeletal dynamics under each experimental condition (Fig. 3.4).

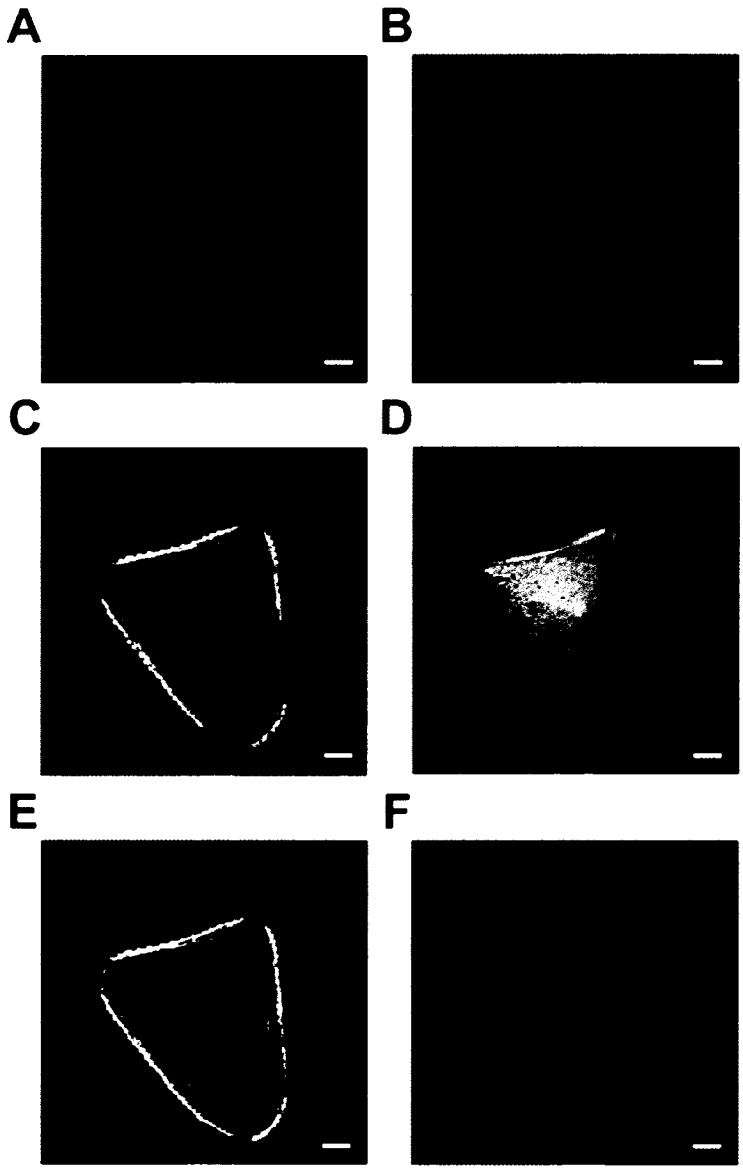

Figure 3.3: Quantitative analysis of actin voxel intensity sum in protrusions. (a) pEGFP-actin cytoskeleton was 3-D reconstructed from Z-stack images, at each time point, in the supass mode of the Imaris software program. (B) The 3-D actin cytoskeleton image was surface rendered by setting a background threshold allowing the quantitation of the AVIS of the entire cell. (C) The cell body was defined at each plane of the cell image in the Z-series. (D) A contoured surface of the cell body was generated. (E) The voxels inside the contoured surface were set to zero. (F) The AVIS in the protrusions was obtained.

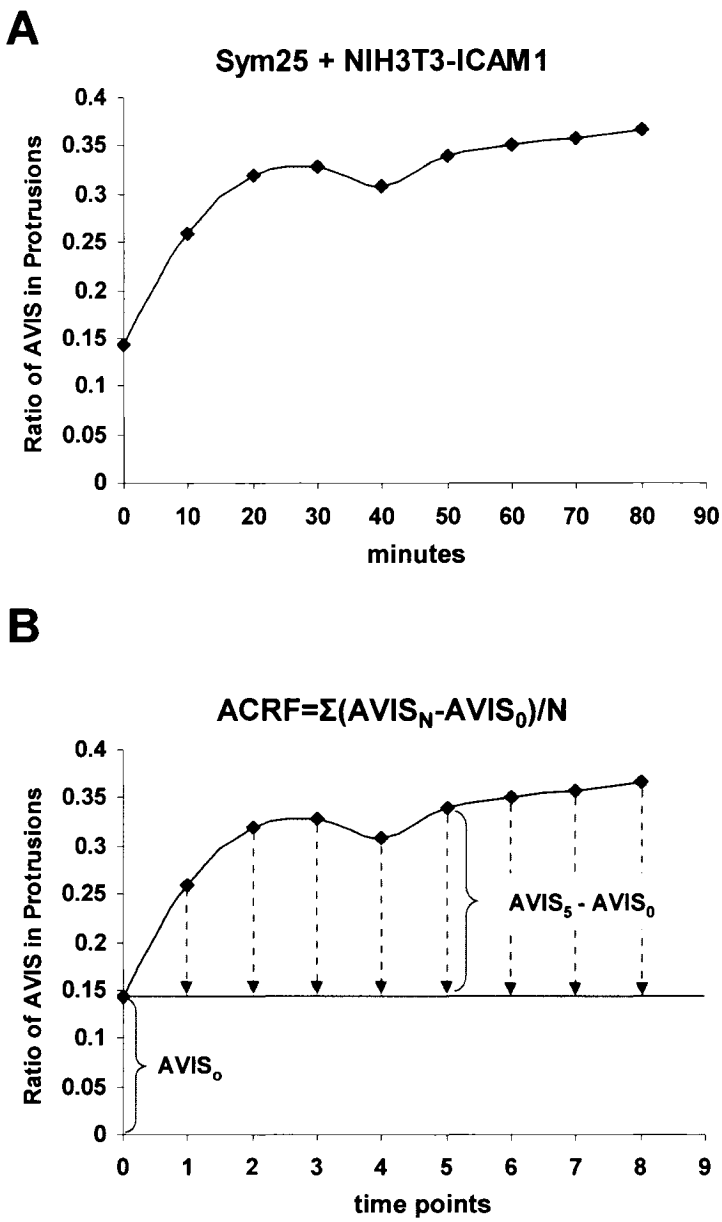

Figure 3.4: Quantitative analysis of cytoskeletal protrusive motility. (A) The cytoskeletal dynamics of one EGFP-actin transfected 293T SYM25 cell were tracked by tracing the proportion of AVIS in protrusions relative to whole cell AVIS, every 10 minutes (each time point), over the trial period. (B) ACRF represents the average of the AVIS changes in protrusions during the cytoskeletal reorganization assays.

3.1.10. Microinjection

Microinjection was performed on a Zeiss Axiovert 100M fluorescent microscope equipped with an Eppendorf microinjection system. The pEGFP-actin transfected T47D or 293T SYM25 cells were plated as described previously for the actin cytoskeletal reorganization assays. 100μg/ml of Rac1-T17N, Cdc42-T17N or RhoA-T19N plasmid was mixed with Dextran-Alexa Fluor 568 in sterilized PBS. The mixture was then centrifuged at 14000 xg for 30 minute at 4°C, and the supernatant was taken for microinjection. The microinjection needles were pulled from aluminosilicate filaments in a P-97 Flaming/Brown Micropipette Puller (Sutter Instrument, Novato, CA). Subsequently, the microinjection needle was loaded with ~2μl of the plasmid-dye mixture and then attached to the control motor, with its blunt end connected to the universal capillary holder of an eppendorf transinjector 5246. The cells were then placed on the microscope and focused under a 40X lens. After the injection parameters including the injection port (I1), holding pressure P_c (50 hPa), injection pressure P_i (~200 hPa), and injection time t_i (0.5s) was set, the needle was lowered over a cell until the tip was seen to slighty indent the cell membrane. The injection Z-limit was set at that height and microinjection was initiated. Following microinjection, the cells were rinsed once with PBS, incubated with fresh media, and then returned to the incubator for another 8-12 hours before the actin cytoskeleton reorganization assay. The successfully injected cells were identified by the fluorescence of Alexa 568 using a Cy3 filter set (Fig. 3.5).

3.1.11. Statistical Analysis

The data was graphed as the average ACRF ± S.E. from at least three individual experiments. Statistical significance was determined using the Student's t-test, $P<0.05$.

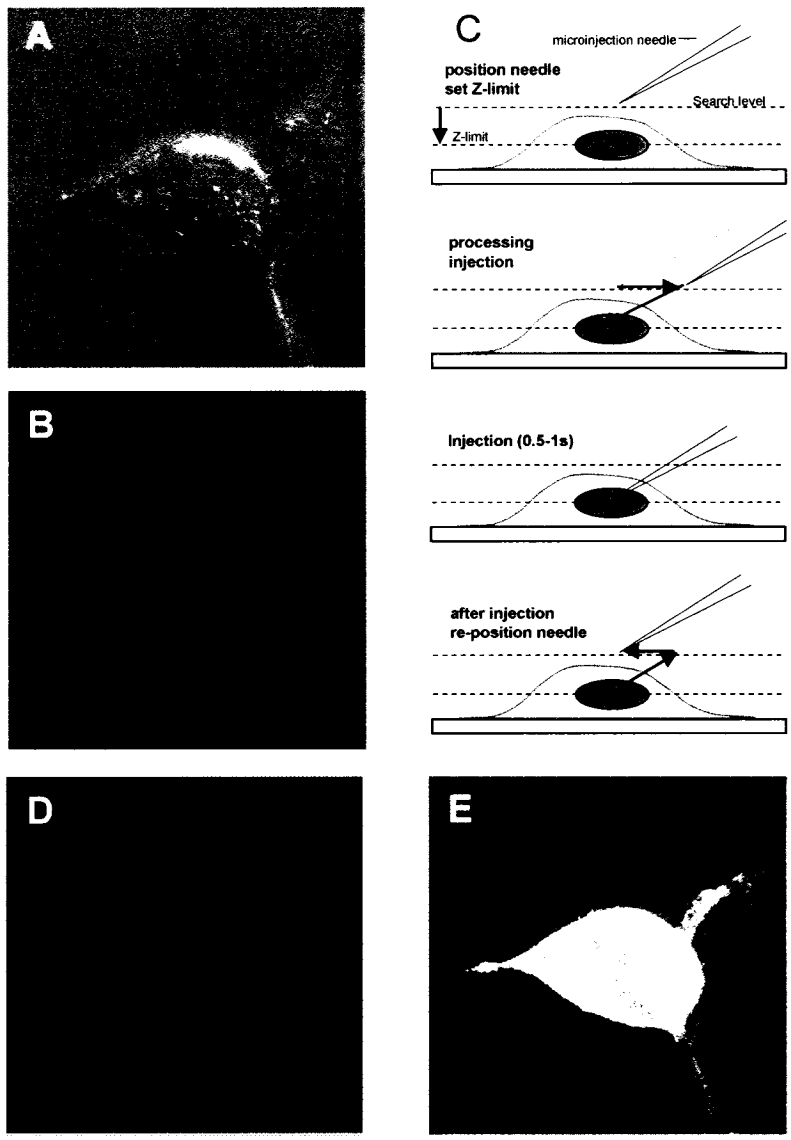

Figure 3.5: Microinjection of dominant negative Rho GTPases. (A) A 293T SYM25 cell was focused with a 40X lens under the DIC channel. (B) GFP-actin signal was identified under a FITC filter. (C) Dominant negative Rho-GTPase/Dextran-Alexa568 mixture was loaded into a microinjection needle and microinjection was performed as described. (D) The successfully microinjected cell was identified by the red fluorescence under a Cy3 filter. (E) The GFP and Alexa 568 Fluor signals were overlapped.

3.2. Results

3.2.1. Human ICAM-1 Initiates Dramatic Actin Cytoskeletal Reorganization in Breast Cancer Cell Lines and MUC1-transfected 293T Cells

To investigate if MUC1 initiates actin cytoskeletal reorganization in response to ICAM-1 ligation, pEGFP-actin expression vector was transfected into three breast cancer cell lines (T47D, MCF-7, and Hs578T) and three MUC1-transfected 293T cell subclones (SYM25, SYM33, and SYM3), which had been used in the studies of chapter 2 and differed in their MUC1 expression levels (Fig. 3.6 A). In this study, we first examined if increased actin cytoskeletal rearrangements could be initiated in MUC1-bearing cells in the presence of human ICAM-1 expressed on NIH3T3 transfectants (Fig. 3.6 B). Using time-lapse confocal microscopy, we found that the exogenous expression of MUC1 on 293T SYM25 and SYM33 cells by itself did not elicit obvious cell morphological changes as compared with the MUC1-negative 293T SYM3 control cells (Fig. 3.7). However, dramatic actin cytoskeletal reorganization and membrane ruffling were provoked in the MUC1-positive breast cancer cells (Fig. 3.8) and 293T transfectants (Fig. 3.9) within 4 minutes after contact with ICAM-1-transfected NIH3T3 cells, and these initial membrane dynamics rapidly developed into continually extending lamellipodial and filopodial protrusions, which preferentially occurred at heterotypic cell-cell contact sites. These protrusions were highly motile, as they frequently migrated out of the focus-plane and were accompanied by forward motion of the cell body (Fig. 3.9 left lane). In marked contrast, if either the plated cells lacked MUC1 or the NIH3T3 transfectants lacked ICAM-1, the breast cancer cells and 293T transfectants exhibited only a low degree of membrane ruffling and minor protrusions, and these membrane events were

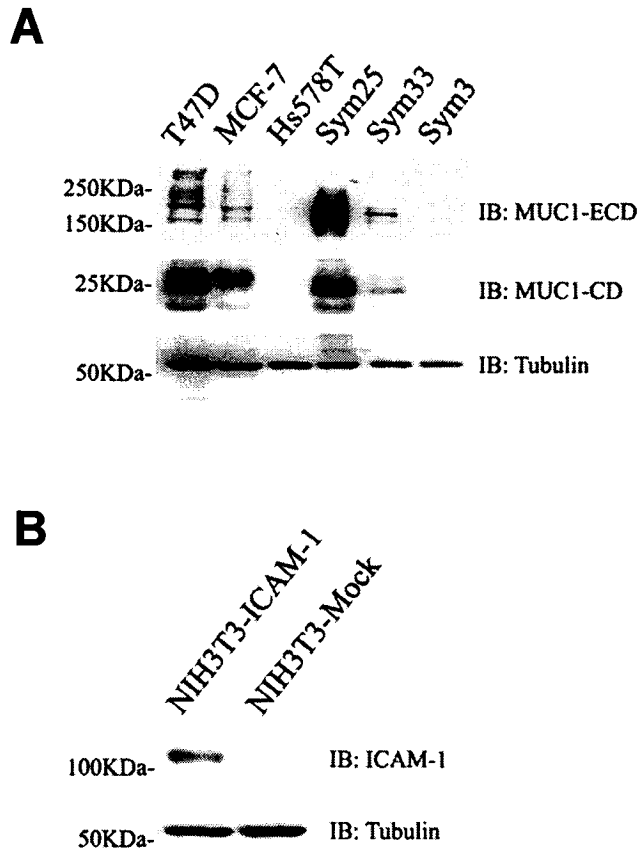

Figure 3.6: Examination of cellular expression of MUC1 and ICAM-1. (A) MUC1 expression was examined in breast cancer cell lines (T47D, MCF-7, and Hs578T) and MUC1-transfected 293T subclones (SYM25, SYM33, and SYM3) with antibodies against MUC1-ECD and MUC1-CD. (B) ICAM-1 expression levels were examined in NIH3T3-ICAM-1 and NIH3T3-Mock transfectants. Tubulin was used as a loading control.

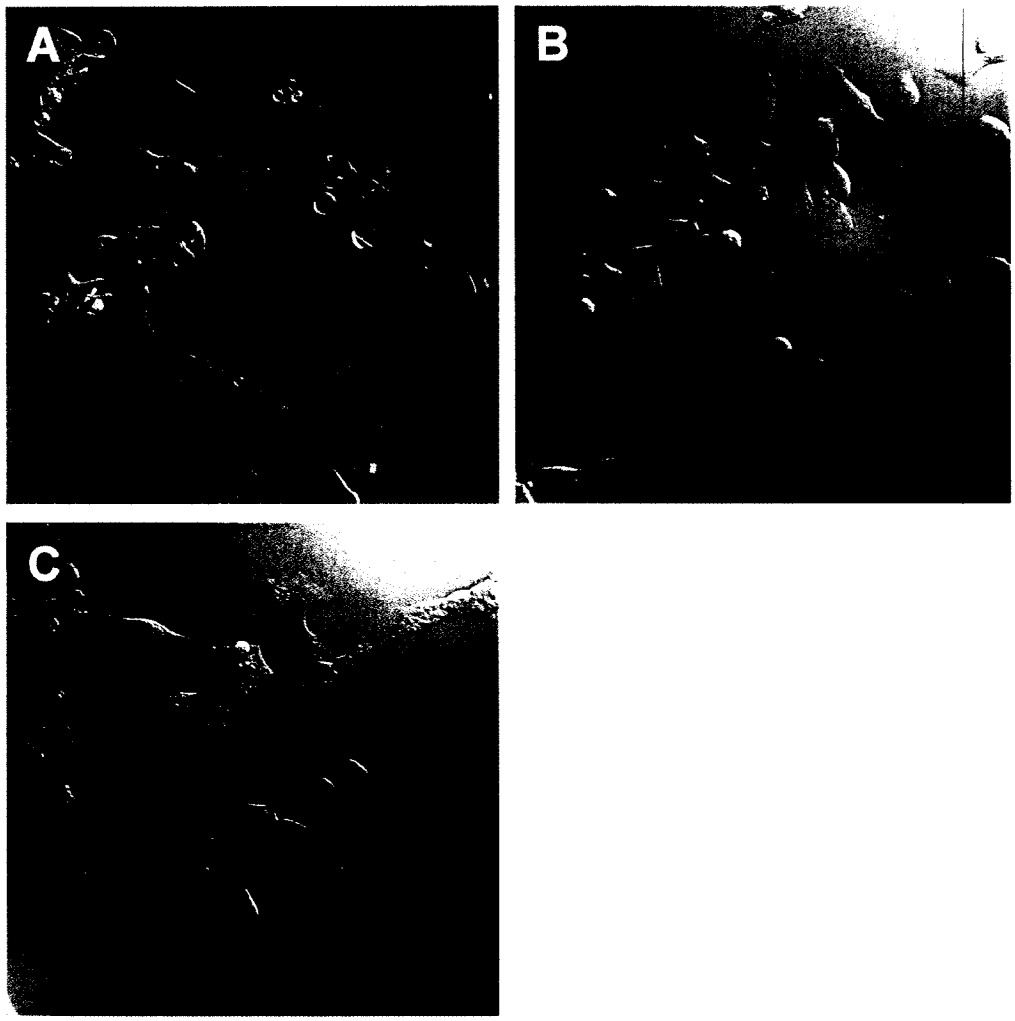

Figure 3.7: Examination of cell morphology of MUC1-transfected 293T subclones. Using laser scanning confocal microscope, the cell morphology of MUC1-transfected 293T SYM3 (A), SYM 25 (B), and SYM33 (C) subclones were examined. Although MUC1 expression levels are different between these cell sublines, no significant morphological changes were observed.

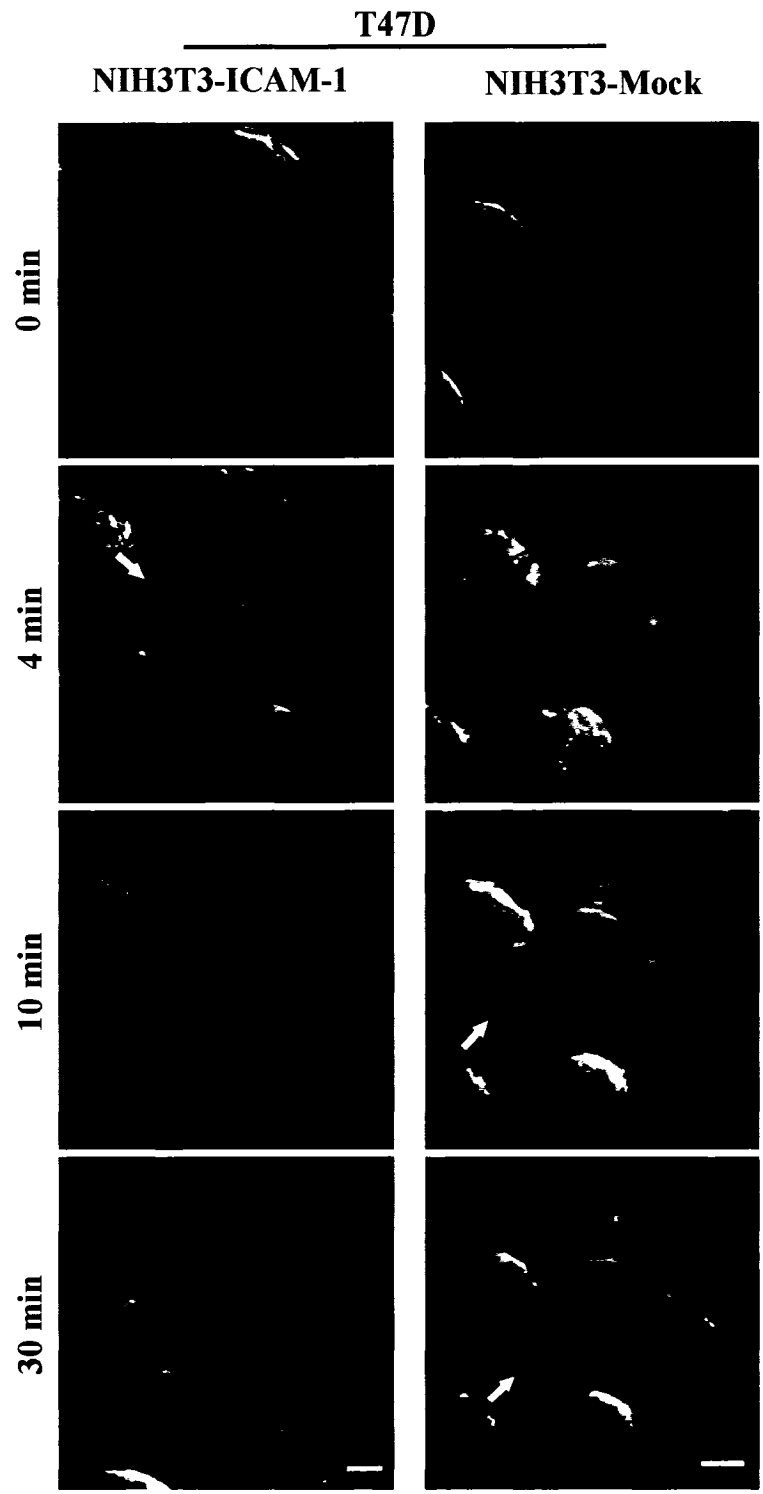

Figure 3.8: MUC1-positive breast cancer cells exhibit dramatic cytoskeletal rearrangements in response to ICAM-1 stimulation. T47D (green cells) were plated

Figure 3.8 continued: on MatTek microwell dishes and then subjected to cytoskeletal reorganization assays upon stimulation by NIH3T3-ICAM-1 (gray cells in the left panel) and NIH3T3-Mock (gray cells in the right panel) transfectants. Membrane ruffling is indicated by white arrows. Membrane lamellipodial-filopodial protrusions are indicated by red arrows. The time "0 min" represents the moment of dropping NIH3T3 tranfectants, and the images at each time point are 3-D reconstructed Z-stacks including all planes of these living cells. Bars, 5μm.

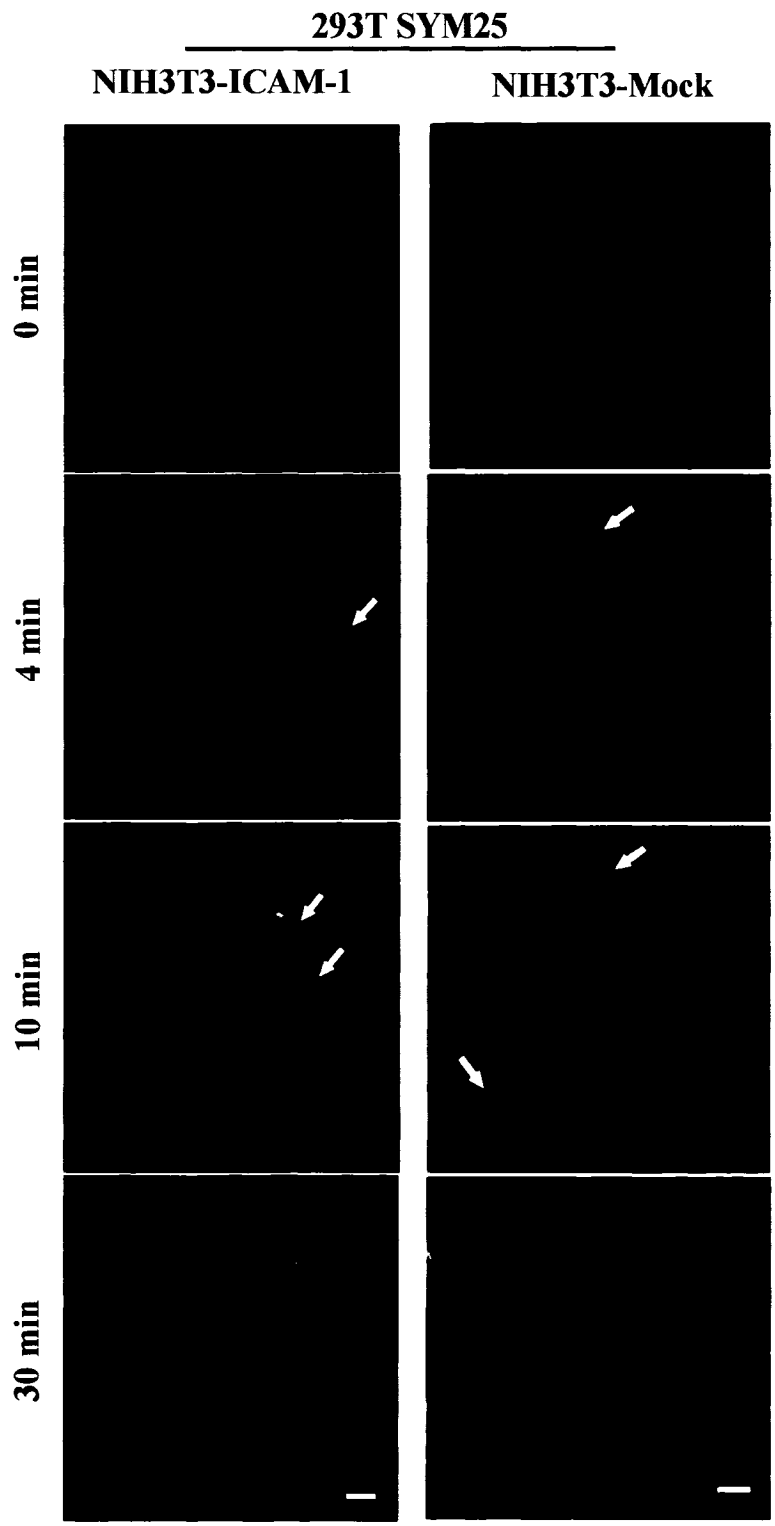

Figure 3.9: MUC1-positive 293T SYM cells exhibit dramatic cytoskeletal rearrangements in response to ICAM-1 stimulation. 293T SYM25 (green cells) were

Figure 3.9 continued: plated on MatTek microwell dishes, and then subjected to cytoskeletal reorganization assays upon stimulation by NIH3T3-ICAM-1 (gray cells in the left panel) and NIH3T3-Mock (gray cells in the right panel) transfectants. Membrane ruffling is indicated by white arrows. Membrane lamellipodial-filopodial protrusions are indicated by red arrows. The time "0 min" represents the moment of dropping NIH3T3 tranfectants, and the images at each time point are 3-D reconstructed Z-stacks including all planes of these living cells. Bars, 5μm

always transient and ceased within minutes, indicating that the presence of both MUC1 and ICAM-1 in this system is critical for the augmented cytoskeletal rearrangements.

To quantitatively analyze the protrusive motility of the actin cytoskeleton, a novel method was developed in this study for quantifying the proportion (%) of actin voxel intensity sum (AVIS) in membrane protrusions as compared to the whole cell (see details in section 3.1.9). Compared with the conventional methods based on the number or area of protrusions, this approach is more precise as it excludes the possible errors caused by the differences in size and thickness of protrusions. Further, by tracing the proportion of AVIS in protrusions over time, we found that the cytoskeletal protrusive motility appears to be a wave-like dynamic process with MUC1-positive cells showing increased but varying amplitude of protrusive activity in the presence of ICAM-1, as compared with the controls (Fig. 3.10). Since there was wide cell-to-cell asynchronization and variation in these dynamic cytoskeletal responses, a quantifiable index - actin cytoskeletal reorganization factor (ACRF), defined as the average of the AVIS changes in protrusions during the trial period was established to facilitate comparisons between experimental conditions (see details in section 3.1.9). For each experimental condition, ACRFs were obtained from four to nine independent trials. Significantly higher levels of cytoskeletal rearrangements were initiated exclusively in the MUC1-positive breast cancer T47D and MCF-7 cells (Fig. 3.11), as well as in 293T SYM25 and SYM33 cells (Fig. 3.12) in response to NIH3T3-ICAM-1 stimulation, as compared with NIH3T3-Mock stimulation or in the MUC1-negative Hs578T and 293T SYM3 cells regardless of the presence or absence of ICAM-1. These findings suggest that MUC1 initiates actin cytoskeletal reorganization and protrusive motility in the presence of ICAM-1.

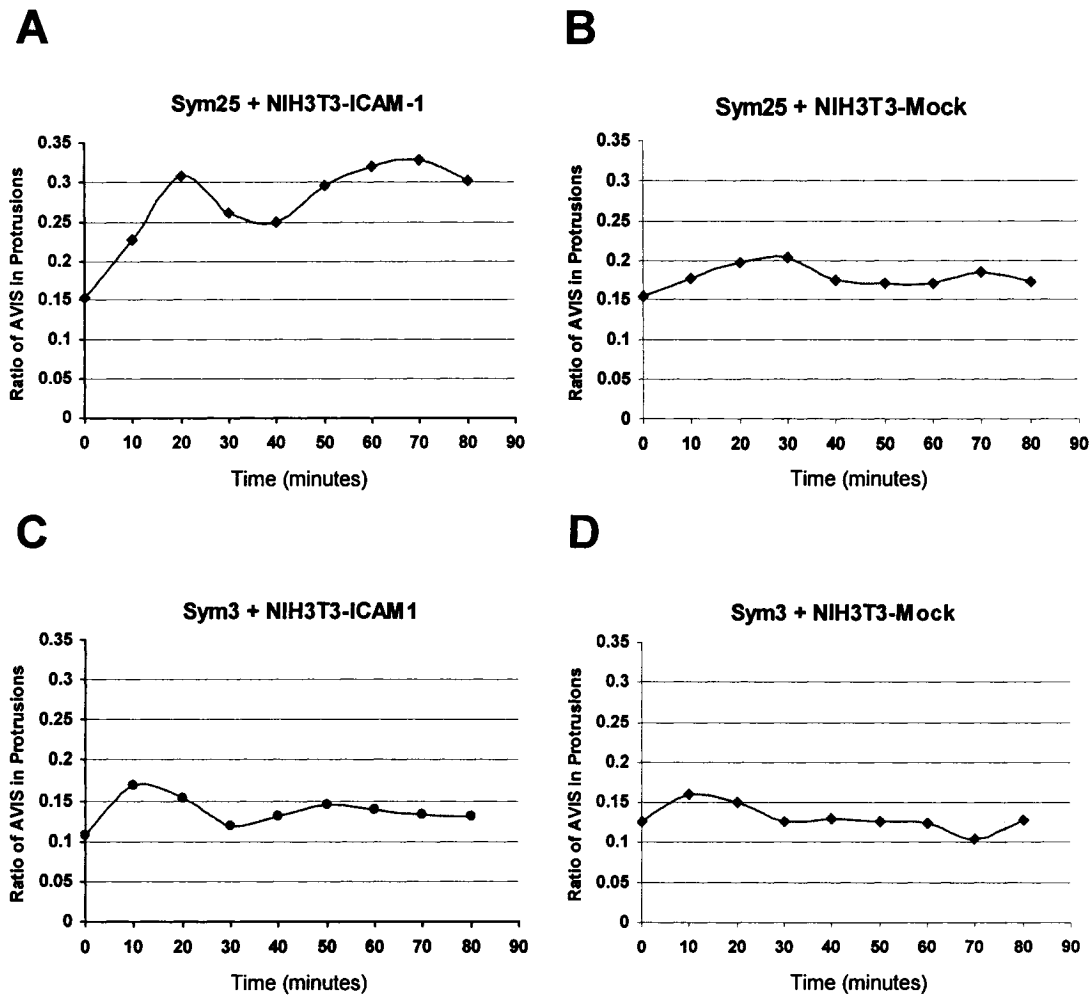

Figure 3.10: Dynamic cytoskeletal protrusive motility in MUC1-positive and negative cells in the presence or absence of ICAM-1 stimulation. The dynamic actin cytoskeletal rearrangements were tracked by tracing the proportion of AVIS in protrusions over time in individual MUC1-positive 293T SYM25 cell in response to (A) NIH3T3-ICAM-1 or (B) NIH3T3-Mock stimulation, as well as in individual MUC1-negative 293T SYM3 cell in response to (C) NIH3T3-ICAM-1 or (D) NIH3T3-Mock stimulation.

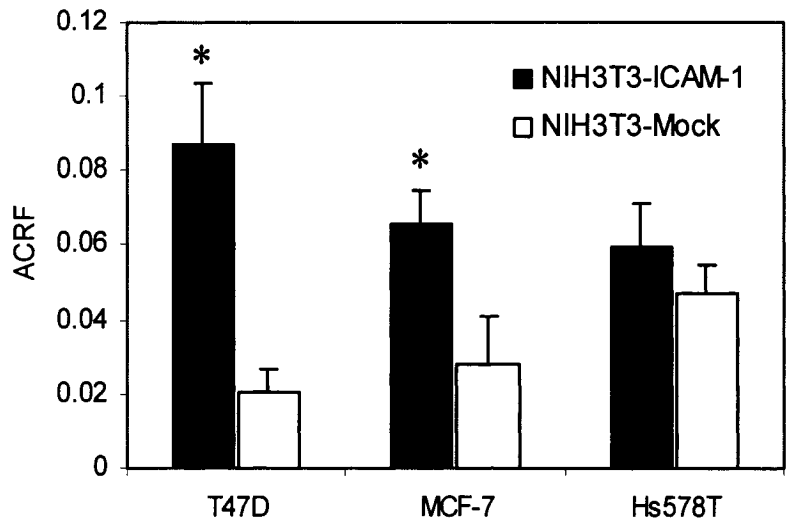

Figure 3.11: Cytoskeletal reorganization in breast cancer cells in the presence or absence of ICAM-1. Data are the average ACRF ± S.E. for breast cancer T47D, MCF-7, and Hs578T cells from at least four independent experiments in the presence or absence of ICAM-1 stimulation. The two MUC1-expressing cell lines, T47D and MCF-7, displayed statistically significant increases in actin cytoskeletal reorganization following ICAM-1 stimulation ($p<0.01$ and $p<0.05$ respectively), as compared with Mock stimulation.

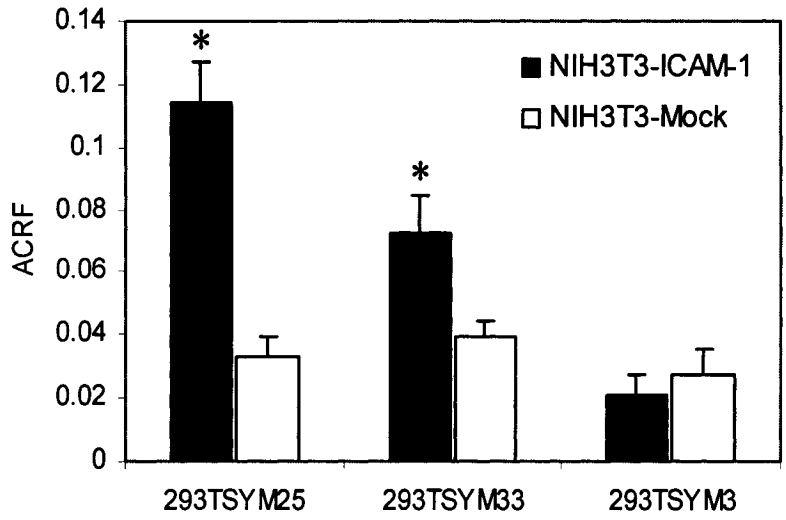

Figure 3.12: Cytoskeletal reorganization in MUC1-transfected 293T cells in the presence or absence of ICAM-1. Data are the average ACRF ± S.E. for the MUC1-transfected 293T SYM25, SYM33, and SYM3 cells from at least four independent experiments in the presence or absence of ICAM-1 stimulation. The two MUC1-expressing subclones, 293T SYM25 and SYM33, displayed statistically significant increases in actin cytoskeletal reorganization following ICAM-1 stimulation ($p<0.0001$ and $p<0.05$ respectively), as compared with Mock stimulation.

3.2.2. MUC1 Initiates Cytoskeletal Rearrangements in Response to ICAM-1 Stimulation

To exclude any possible bias due to unrelated differences in breast cancer cell lines or subclone selection, we generated the Flp-In T-REx 293 MUC1-inducible expression system (see detailed procedures in section 3.1.3 and 3.1.4). In this system, the Tet repressor (tetR) is constitutively expressed and binds to the Tet operator 2 (TetO2) sequences in the pcDNA5/FRT/TO-MUC1 vector, repressing transcription of the downstream *MUC1* gene. Since tetracycline can bind the tetR and release it from the Tet operator sequences thereby allowing gene transcription, by adding or removing tetracycline in the culture medium, MUC1 expression could be induced or inhibited in this system to generate Flp-In T-REx 293 MUC1+ and Flp-In T-REx 293 MUC1- cells (Fig. 3.13 A). Subsequently, the time-lapse confocal microscopy showed results similar to those seen previously, in that the Flp-In T-REx 293 MUC1+ cells exhibited significantly (~3 fold, t-test, $p<0.05$) higher levels of actin cytoskeletal reorganization and cytoskeletal protrusive motility in response to NIH3T3-ICAM-1 stimulation as compared with their counterparts stimulated with NIH3T3-Mock transfectants (Fig. 3.13 B). Conversely, the Flp-In T-REx 293 MUC1- cells showed only minor levels of cytoskeletal protrusive motility regardless of the presence or absence of ICAM-1 on the contacting NIH3T3 transfectants (Fig. 3.13 B). These results, together with the previous findings that ICAM-1 specifically initiated cytoskeletal reorganization in MUC1-positive breast cancer cells and 293T transfectants, demonstrate that MUC1 is the key molecule that induces increased actin cytoskeletal rearrangements upon ICAM-1 stimulation.

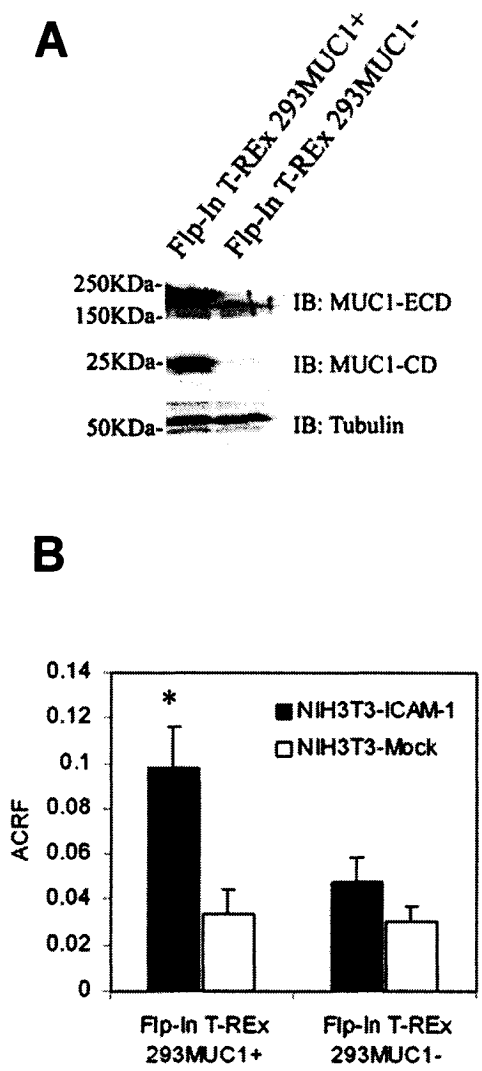

Figure 3.13: Effect of MUC1 on cytoskeletal rearrangements in Flp-In T-REx 293 MUC1 cells. (A) MUC1 expression levels were examined in Flp-In T-REx 293 MUC1+ and Flp-In T-REx 293 MUC1- cells. Tubulin was used as a loading control. (B) Data are the average ACRF ± S.E. for Flp-In T-REx 293 MUC1 cells, from at least four independent experiments, in the presence or absence of ICAM-1 stimulation.

3.2.3. MUC1 Initiates Cytoskeletal Rearrangements by Ligating ICAM-1

To further confirm that this MUC1-initiated cytoskeletal reorganization is specifically induced by the ligation of ICAM-1, anti-ICAM-1 mAb (18E3D or 164B) blockade was introduced prior to the cytoskeletal reorganization assays. Our previous work [3] had demonstrated that mAb 18E3D, but not 164B, could target the MUC1 ligation site on ICAM-1 thereby blocking the MUC1/ICAM-1 interaction. By stimulating the breast cancer cells (T47D and Hs578T) and MUC1-transfected 293T cells (SYM25 and SYM3) with NIH3T3-ICAM-1 cells that had been preincubated with either 18E3D or 164B (see detailed procedures in section 3.1.8), we found that the anti-ICAM-1 mAb 18E3D significantly (>70%, t-test, $p<0.05$) blocked MUC1-initiated actin cytoskeletal rearrangements in the T47D cells, but had no effect on the MUC1-negative Hs578T cells (Fig. 3.14). However, the anti-ICAM-1 mAb 164B pre-treated NIH3T3-ICAM-1 cells showed no significant difference when compared with the T47D cells stimulated with no antibody pretreated NIH3T3-ICAM-1 transfectants (Fig. 3.14).

Similar results were also obtained in 293T SYM25 cells where 18E3D, but not 164B, abrogated the MUC1-induced cytoskeletal dynamics in the presence of ICAM-1 (Fig. 3.15, t-test, $p<0.05$). No significant differences between the pre-treatments of 18E3D and 164B were observed in MUC1-negative 293T SYM3 cells regardless of the presence or absence of ICAM-1 on NIH3T3 transfectants. Collectively, we conclude that MUC1 mediates the increased actin cytoskeletal rearrangements and motile membrane protrusions by ligating ICAM-1.

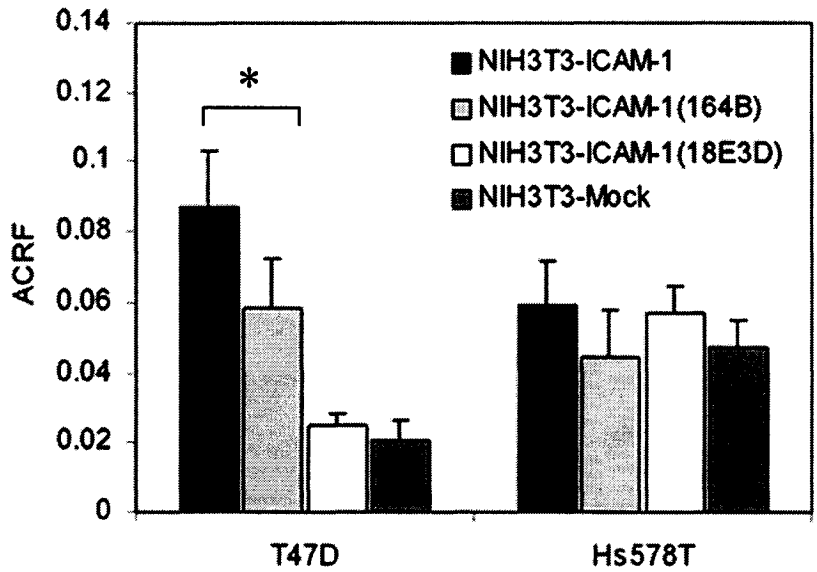

Figure 3.14: MUC1/ICAM-1 ligation is required for increased cytoskeletal dynamics in breast cancer cells. NIH3T3-ICAM-1 cells were pretreated with anti-ICAM-1 mAb, 18E3D or 164B, before stimulating breast cancer cells in the cytoskeletal reorganization assays, using the non-pretreated NIH3T3-ICAM-1 or -Mock cells as controls. Data are the average ACRF ± S.E. for breast cancer cells T47D and Hs578T from at least three independent experiments.

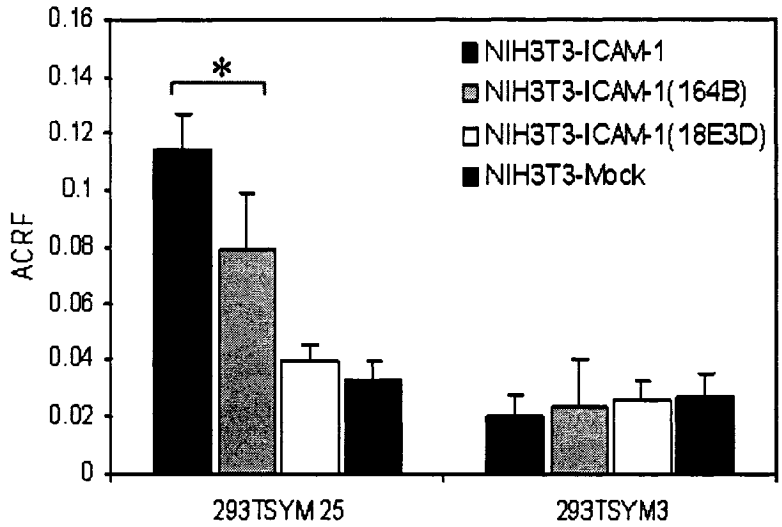

Figure 3.15: MUC1/ICAM-1 ligation is required for increased cytoskeletal dynamics in MUC1-transfected 293T cells. NIH3T3-ICAM-1 cells were pretreated with anti-ICAM-1 mAb, 18E3D or 164B, before stimulating MUC1-transfected 293T cells in the cytoskeletal reorganization assays, using the non-pretreated NIH3T3-ICAM-1 or -Mock cells as controls. Data are the average ACRF ± S.E. for 293T SYM25 and SYM3 from at least three independent experiments.

3.2.4. β1 Integrin is Involved in the MUC1/ICAM-1 Interaction Initiated Cytoskeletal Rearrangements

Compelling evidence has implicated integrins, heterodimeric transmembrane adhesion receptors, in both cytoskeletal rearrangements and focal contact dynamics during cell migration [7]. The β1 subunit-containing integrins represent the major subgroup of this family (see table 1.2), and are present in both breast cancer T47D cells and 293T cells (Fig. 3.16 A). There is circumstantial evidence to suggest that MUC1 may cooperate with integrins in cyoskeletal reorganization. MUC1, similar to integrins, is reported to be localized in lipid rafts [20,21] and concentrated at the leading edge of migrating cells [12]. Also MUC1-CD associates with components, such as ezrin and Src [13,22], both of which are associated with integrins and the actin cytoskeleton. Supporting this hypothesis, we have found that the MUC1-initiated calcium signaling is ECM dependent and, by blocking β1 integrin, both the MUC1/ICAM-1 ligation-induced calcium signaling (unpublished prelimilary data) and transendothelial migration were reduced [23].

To investigate the role of β1 integrin in MUC1/ICAM-1 ligation-initiated cytoskeletal reorganization, the anti-β1 integrin mAb AP-138, which is known to selectively block β1 integrin-mediated cell adhesion [24], and an isotype matched mouse IgG1 control were used to pretreat the plated T47D and 293T SYM25 cells prior to NIH3T3-ICAM-1 or -Mock stimulation in the cytoskeletal reorganization assay (see detail procedures in section 3.1.8). Time-lapse confocal microscopy showed that with AP-138 mAb preincubation, although some membrane ruffling was initiated, the subsequent membrane events were transient and did not develop into extending

lamellipodial or filopodial protrusions. Correspondingly, the ACRFs were significantly (>50%) reduced in the AP-138 mAb pretreated T47D (Fig. 3.16 B) and 293T SYM25 (Fig. 3.16 C) cells in the presence of ICAM-1 stimulation, as compared with their isotype control-mouse IgG1 pretreated counterparts (t-test, $p<0.05$). However, there is no difference between AP-138 and isotype pretreated cells after stimulation with NIH3T3-Mock transfectants (Fig. 3.16 B and C).

Further, to confirm the results generated by anti-β1 integrin mAb, the T47D and 293T SYM25 cells were preincubated with the β1 integrin blocking RGD peptide (GRGDNP) or a control peptide (RGES) (see details in section 3.1.8). Similar to the AP-138 mediated blockade, the GRGDNP pretreated 293T SYM25 cells showed significantly (>60%) decreased cytoskeletal rearrangements in response to NIH3T3-ICAM-1 stimulation as compared with their RGES peptide pretreated counterparts or NIH3T3-Mock stimulated controls (Fig. 3.17 A, t-test, $p<0.05$). Although the GRGDNP peptide-mediated inhibitory effects were also observed on T47D cells (Fig. 3.17 B), the abrogating effect was minor as compared with that on 293T SYM25 cells. This may reflect the different integrin profile expressed on these cells.

Since MUC1/ICAM-1 could not fully initiate cytoskeletal protrusive motility with β1 integrin blockade and conversely, without MUC1/ICAM-1 interaction, no significant cytoskeletal dynamics were observed in the absence of β1 integrin blockade, we conclude that β1 integrins functionally associate with MUC1 and cooperate with MUC1/ICAM-1 interaction-induced cytoskeletal rearrangements. In this system, we propose that the β1 integrins may function as adhesion receptors to stabilize MUC1-initiated membrane protrusions.

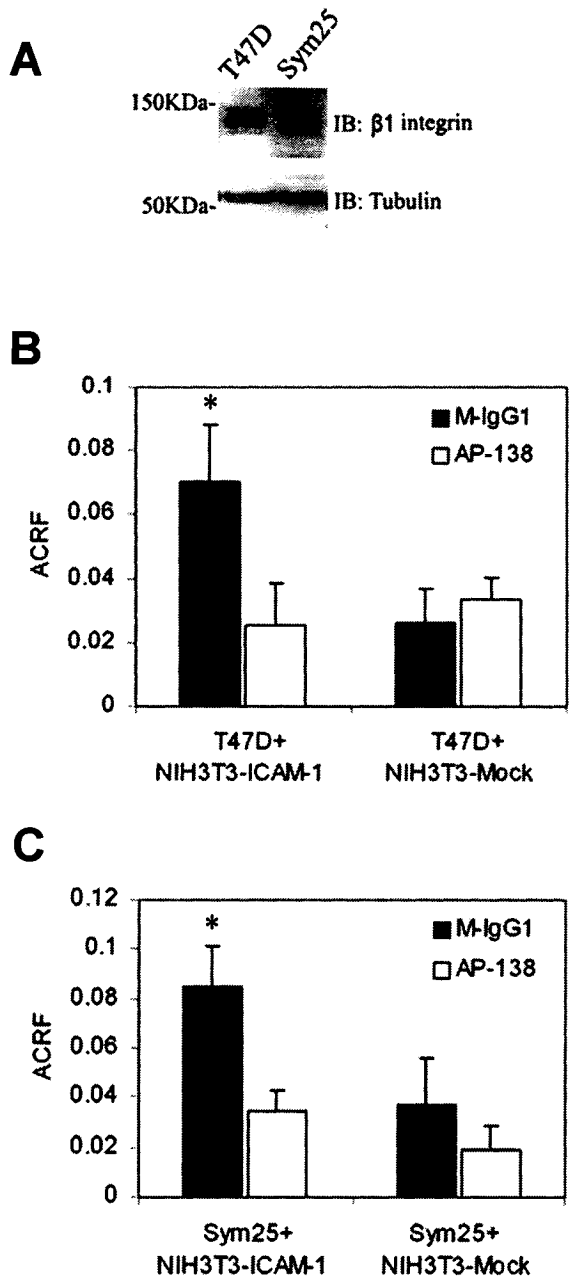

Figure 3.16: Role of β1 integrins in MUC1/ICAM-1 ligation induced cytoskeletal reorganization. (A) Expression of β1 integrin was detected by mAb AP-138 in both T47D and SYM25 cells. (B) T47D cells and (C) 293T SYM25 cells were pretreated with mAb AP-138 or isotype mouse IgG1 (M-IgG1), followed by the cytoskeletal reorganization assay in the presence or absence of ICAM-1 stimulation. Data are the average ACRF ± S.E. from at least three independent experiments.

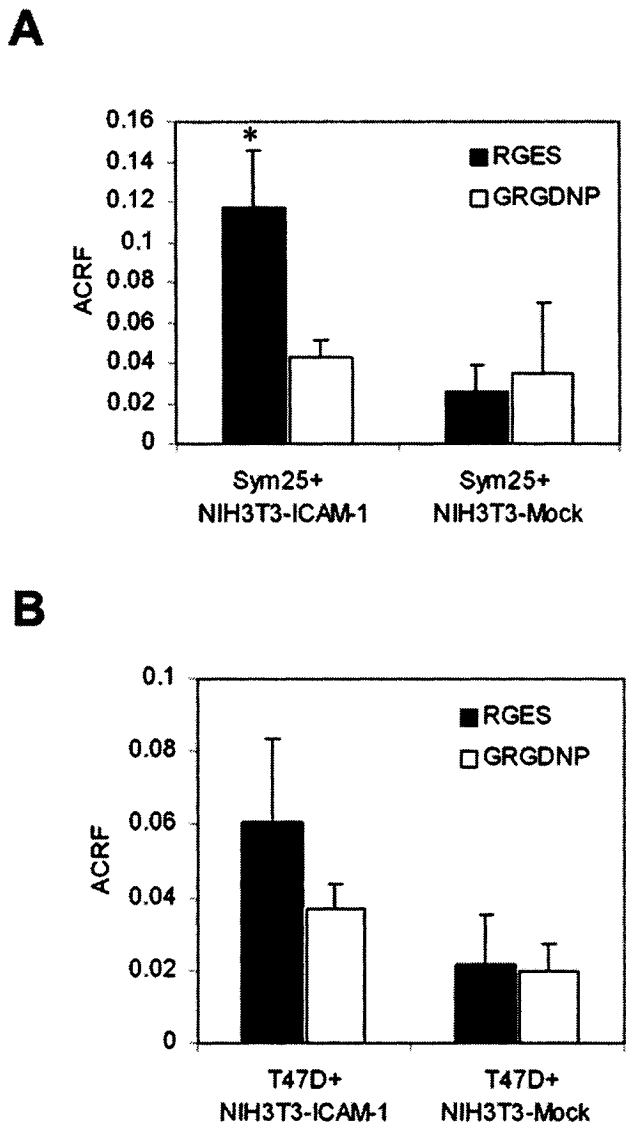

Figure 3.17: Effect of β1 integrin blocking RGD peptide on the MUC1/ICAM-1 ligation induced cytoskeletal responses. (A) SYM25 cells and (B) T47D cells were pretreated with β1 blocking GRGDNP peptide prior to NIH3T3-ICAM-1 or -Mock stimulation and cytoskeletal reorganization assay, using RGES peptide pretreated counterparts as controls. Data are the average ACRF ± S.E. from at least three independent experiments.

3.2.5. Involvement of PI3K, Src Family Kinase and PLC in the MUC1/ICAM-1 Ligation Initiated Cytoskeletal Rearrangements

Next, we investigated the potential downstream mediators of the MUC1/ICAM-1 ligation-induced cytoskeletal migratory response. Our previous work has established that PI3K, Src family kinase, and PLC are involved in the MUC1/ICAM-1 interaction-initiated calcium signal [18]. Significantly, all of these molecules have been implicated in the regulation of cytoskeletal reorganization and cell motility. PI3K is critical in defining the leading edge and maintaining protrusions in cell migration [25,26]. Src family kinase has been implicated in the phosphorylation and regulation of some signaling mediators, such as PI3K, focal adhesion kinase (FAK) and p130CAS, crucial for cytoskeletal reorganization [7]. Also, PLC-mediated cleavage of PtdIns(4,5)P_2 regulates the actin cytoskeleton modulating proteins, profilin, gelsolin and cofilin, resulting in directional actin cytoskeletal rearrangements at the leading edge [9].

In order to characterize the role of these intermediaries in the MUC1/ICAM-1 ligation-induced cytoskeletal response: T47D cells, as well as 293T SYM25 cells, were pretreated with the pharmaceutical inhibitors wortmannin (inhibits PI3K), PP2 (inhibits Src family kinase), U-73122 (inhibits PLC), 2-APB (inhibits calcium release through IP3 receptor) or U-73343 (inactive analogue of U-73122) and compared with untreated control cells in the cytoskeletal reorganization assays (see details in section 3.1.8). For T47D cells (Fig. 3.18), we found that wortmannin, PP2, and 2-APB substantially (~75%, t-test, $p<0.05$) abrogated the MUC1/ICAM-1-induced cytoskeletal protrusive motility, and U-73122 exhibited a moderate (~45%) inhibitory effect, whereas no statistically significant inhibitory effect was observed in the U-73343-pretreated cells.

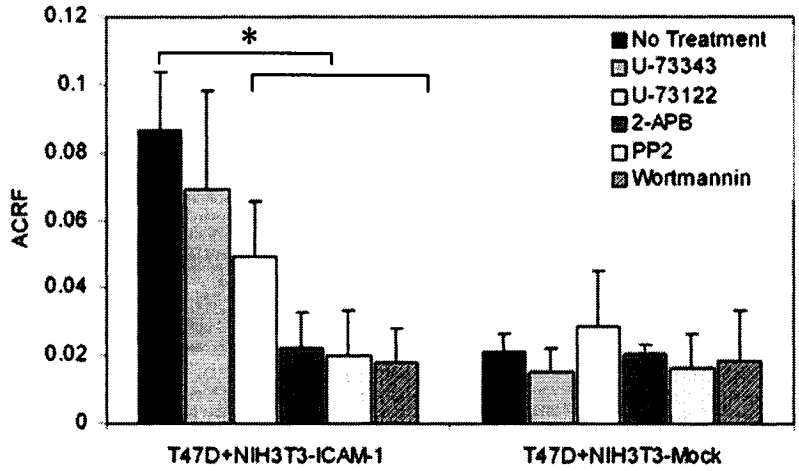

Figure 3.18: Effect of PI3K, Src family kinase, and PLC on the MUC1/ICAM-1 induced cytoskeletal rearrangements in breast cancer cells. T47D cells were treated with inhibitors of PI3K (wortmannin), Src family kinase (PP2), IP3R (2-APB), PLC (U-73122), or the inactive analogue (U-73343) prior to cytoskeletal reorganization assays, in the presence or absence of ICAM-1 stimulation. Data are the average ACRF ± S.E. from at least three independent experiments.

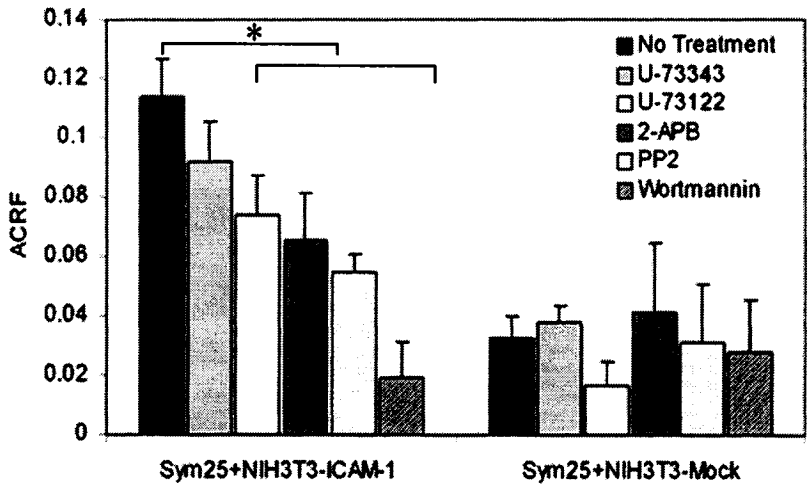

Figure 3.19: Effect of PI3K, Src family kinase, and PLC on the MUC1/ICAM-1 induced cytoskeletal rearrangements in MUC1-transfected 293T Cells. 293T SYM25 cells were treated with inhibitors of PI3K (wortmannin), Src family kinase (PP2), IP3R (2-APB), PLC (U-73122), or the inactive analogue (U-73343) prior to cytoskeletal reorganization assays, in the presence or absence of ICAM-1 stimulation. Data are the average ACRF ± S.E. from at least three independent experiments.

Similar results were also obtained in 293T SYM25 cells (Fig. 3.19). These findings suggest that PI3K, Src family kinase, and PLC may mediate the MUC1-initiated cytoskeletal rearrangements.

3.2.6. Role of Rho Family GTPases in the MUC1/ICAM-1 Interaction Induced Cytoskeletal Rearrangements

Rho family small GTPases Rac1, Cdc42, and RhoA are pivotal regulators of actin cytoskeletal reorganization and formation of motile lamellipodial or filopodial protrusions [15,27]. As MUC1/ICAM-1 ligation initiates actin cytoskeletal protrusive motility, we hypothesized that these GTPases may be involved in the MUC1-induced cytoskeletal rearrangements in response to ICAM-1 ligation. For the purpose of this study, breast cancer T47D and 293T SYM25 cells were microinjected with the Rac1-T17N, Cdc42-T17N or RhoA-T19N expression plasmid which confers the dominant negative phenotype of the corresponding GTPases, using Dextran-Alexa 568 as an injection tracer. Time-lapse confocal microscopy revealed that coexpression of dominant negative Rac1-T17N, as well as Cdc42-T17N, led to complete inhibition of the MUC1-induced protrusive motility (Fig. 3.20 and Fig. 3.21). Moreover, the initial membrane ruffling and cell movement were also totally abrogated in both of these cell lines. In contrast, coexpression of dominant negative RhoA-T19N had no obvious inhibitory effect on the MUC1-induced cytoskeletal activity as compared with the control cells injected only with Dextran-Alexa 568 (Fig. 3.20 and Fig. 3.21). Therefore, we conclude that the Rho family small GTPases Rac1, Cdc42, but not RhoA, are required for the MUC1/ICAM-1 ligation-initiated actin cytoskeletal rearrangements and protrusive motility.

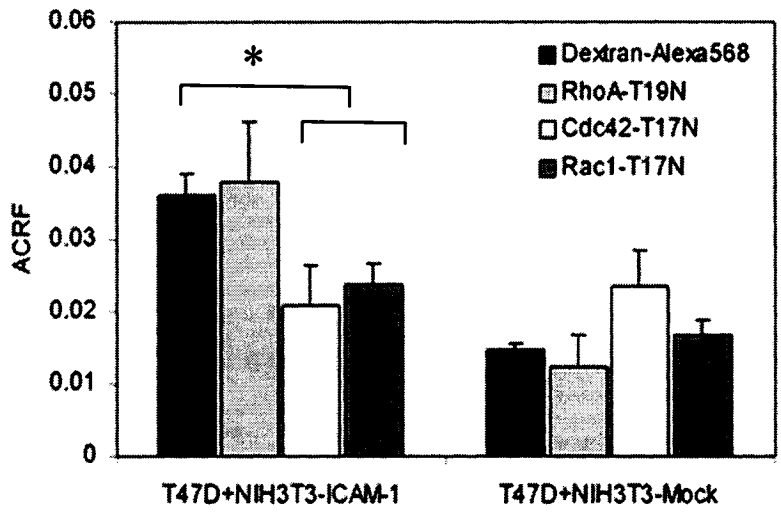

Figure 3.20: Effect of Rho family GTPases on the MUC1/ICAM-1 induced cytoskeletal rearrangements in breast cancer T47D cells. T47D cells were microinjected with dominant negative Rac1-T17N, Cdc42-T17N, or RhoA-T19N and the tracking dye Dextran Alexa568 prior to cytoskeletal reorganization assays in the presence or absence of ICAM-1 stimulation. The cells injected only with Dextran Alexa568 were used as controls. Data are the average ACRF ± S.E. from at least three independent experiments.

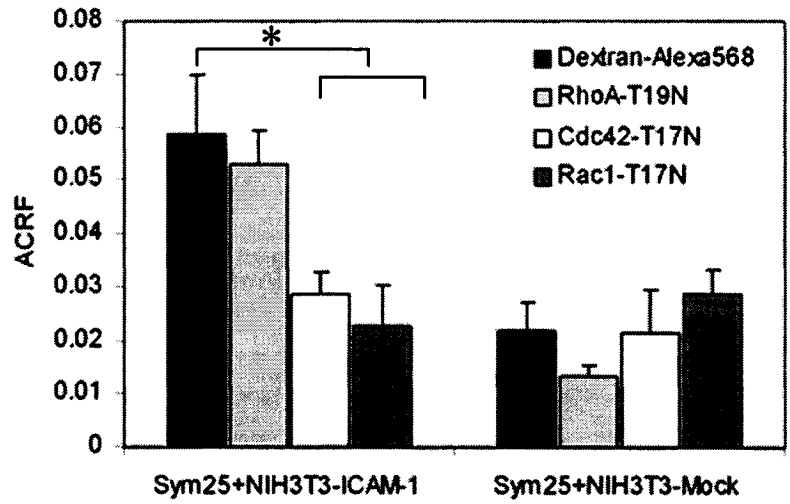

Figure 3.21: Effect of Rho family GTPases on the MUC1/ICAM-1 induced cytoskeletal rearrangements in MUC1-transfected 293T cells. 293T SYM25 cells were microinjected with dominant negative Rac1-T17N, Cdc42-T17N, or RhoA-T19N and the tracking dye Dextran Alexa568 prior to cytoskeletal reorganization assays in the presence or absence of ICAM-1 stimulation. The cells injected only with Dextran Alexa568 were used as controls. Data are average ACRF ± S.E. from at least three independent experiments.

3.3. Discussion

Since cell migration is characterized by directed actin cytoskeletal reorganization and our previous work has demonstrated that MUC1, by ligating ICAM-1, not only mediates heterotypic cell-cell adhesion but also initiates calcium-based pro-migratory signaling, we hypothesized that MUC1/ICAM-1 ligation induces cytoskeletal rearrangements. In this study, we examined the effect of MUC1/ICAM-1 interaction on cytoskeletal protrusive motility. This required the establishment of a novel *in vitro* model that can precisely trace the actin cytoskeletal dynamics in protrusions over time. Thus, the possible errors caused by cell-to-cell asynchronization and variations of protrusions in conventional methods were avoided. Further, by exploring the molecular requirements underlying the MUC1/ICAM-1-induced cytoskeletal reorganization in this model, the crucial role of the MUC1/ICAM-1 interaction was reinforced.

3.3.1. MUC1 Initiates Cytoskeletal Rearrangements and Protrusive Motility by Ligating ICAM-1

In this study, we used live imaging of single cells to show that MUC1 initiates dramatic cytoskeletal rearrangements and increased protrusive motility in response to ICAM-1 ligation. Since these enhanced cytoskeletal responses are only induced in MUC1-expressing cells, including human breast cancer cells, MUC1-transfected 293T cells and Flp-In T-REx 293 MUC1 cells, and exclusively abrogated by the anti-ICAM-1 antibody which specifically blocks the MUC1/ICAM-1 ligation, the results indicate that the MUC1/ICAM-1 ligation is the extracellular event that relays the pro-migratory signaling into cells and directly initiates the dynamic cytoskeletal rearrangements. This is consistent with our previous data showing that MUC1/ICAM-1 ligation initiates

intracellular calcium oscillations [18], providing solid evidence that MUC1 can promote cell motility not only as an adhesion protein but also by functioning as a signaling molecule.

3.3.2. Possible Mechanism of MUC1/ICAM-1 Ligation Initiated Cytoskeletal Rearrangements

Similar to the calcium oscillation data, we found that inhibition of the pathways involving PI3K, Src family kinase, and PLC significantly abrogated the MUC1/ICAM-1 ligation-induced cytoskeletal protrusive motility. Since MUC1-CD lacks intrinsic enzymatic activity, its association with non-receptor tyrosine kinases is crucial to understanding the signal initiation which occurs downstream of the MUC1/ICAM-1 ligation. Src may play a key role in this process, as Src was previously reported to phosphorylate MUC1-CD at $Y^{46}EKV$ generating a consensus binding site for the Src SH2 domain [22,28]. This may directly serve to activate downstream PI3K and PLC [29-31]. Significantly, the SH3 domain of Src has also been shown to interact with MUC1 [22] and increased Src was associated with MUC1 in response to ICAM-1 ligation (see details in section 2.2.5). In this respect, there is evidence that the intracellular targeting of Src is a kinase-independent mechanism that is determined principally by interactions involving the SH3 domain with modulation by the SH2 domain [32]. Others have also suggested [33] that the tumorigenic effect of MUC1 may be due to its association with Src thereby regulating intracellular targeting and thus promoting the association of Src with its substrate proteins (e.g. PI3K).

Our studies provide the first evidence that β1 integrin is required for the MUC1/ICAM-1 ligation-initiated cytoskeletal rearrangements and protrusive motility.

This is consistent with the MUC1/ICAM-1 ligation-induced calcium oscillation and transendothelial migration, where inhibitory effects were also observed by β1 integrin blockade [23]. Since only minor cytoskeletal activity was observed without MUC1/ICAM-1 ligation, regardless of the presence or absence of β1 integrin blockade, there is a synergistic effect between MUC1 and β1 integrin that leads to increased cytoskeletal protrusive motility in response to ICAM-1 stimulation. Although we do not know the exact mechanism(s) by which β1 integrins may synergize with MUC1, there are several possible scenarios. First, β1 integrin may act as an adhesive receptor for the substrate ECM and thereby stabilize the MUC1/ICAM-1-initiated membrane protrusions at the heterotypic cell-cell contact sites, where it can further serve as a contraction site when the newly formed motile protrusions extend forward. Second, since both MUC1 and β1 integrin localize in lipid rafts [20,21,34], which are crucial for cytoskeletal reorganization and cell motility [35,36], MUC1/ICAM-1 ligation-induced association with Src may serve to bring Src in proximity to β1 integrins on lipid rafts. It is well documented that integrins can form a "FAK-Src signaling complex" [7] at newly created focal contact sites and subsequently initiate cell polarization and cytoskeletal protrusive motility through PI3K and p130CAS/Crk/Rac-Cdc42 cascades [37-40]. Significantly, recent work by Al Masri *et al.* demonstrated that MUC1 is directly associated with FAK and facilitates the interaction of Src with its substrate PI3K in MMTV-PyV MT mammary tumors [33]. This suggests that MUC1 may play a critical role in integrin-associated pro-migratory signaling.

The cytoskeleton linker protein ezrin is also associated with the MUC1-CD in breast cancer cells [13], which is significant since ezrin has been implicated in binding

the FAK N-terminal domain and activating FAK independently of cell-matrix adhesion [41]. Thus it is possible that the MUC1/ICAM-1 ligation, by targeting ezrin to sites of heterotypic cell-cell contact, may promote integrin-associated signaling. In this model, MUC1 may play a role similar to platelet-derived growth factor receptor (PDGFR) and epidermal growth factor receptor (EGFR) in cell motility, whereby FAK integrates growth factor receptor and integrin signals to promote cell migration [42]. Further support for the integrative signaling of MUC1 and integrins is the recent discovery that integrins are transcriptionally regulated by MUC1 [43].

Our studies also provide evidence that the MUC1/ICAM-1 ligation-induced cytoskeletal protrusive motility requires activation of both Rho GTPases Rac1 and Cdc42. This is consistent with the known role of Rho family GTPase in the regulation of actin cytoskeletal reorganization. PI3K may mediate this process in response to MUC1/ICAM-1 ligation, since it is well documented that PI3K defines and activates Rac and Cdc42 at the leading edge of polarized cells to initiate and maintain cell protrusive motility [25,44]. The MUC1-associated Src and FAK could also regulate the activity of Rac1 and Cdc42 by directly activating PI3K or p130CAS/Crk cascade. Notably, the MUC1-CD contains two highly conserved YXXP sequences ($Y^{35}VPP^{38}$ and $Y^{60}TNP^{63}$), which represent potential docking sites for the SH2 domain of the adaptor protein Crk [45]. Since Crk has been implicated in activating Rac1 and Cdc42 in cell motility [46,47], MUC1/ICAM-1 ligation may also initiate Rho GTPase-mediated cytoskeletal rearrangements through the Crk pathway.

MUC1 has long been associated with breast cancer metastasis, with the underlying mechanism still elusive. This study provides the first sketch of the

intracellular molecular mechanisms by which MUC1 may promote cell motility during tumor metastasis.

3.4. References

1. Horne GJ, University of Alberta. Dept. of Laboratory Medicine and Pathology.: **The role of breast cancer associated with MUC1 in tumor cell recruitment to vascular endothelium during physiological fluid flow**: 1999.
2. Kam JL, Regimbald LH, Hilgers JH, Hoffman P, Krantz MJ, Longenecker BM, Hugh JC: **MUC1 synthetic peptide inhibition of intercellular adhesion molecule-1 and MUC1 binding requires six tandem repeats.** *Cancer Res* 1998, **58**:5577-5581.
3. Regimbald LH, Pilarski LM, Longenecker BM, Reddish MA, Zimmermann G, Hugh JC: **The breast mucin MUCI as a novel adhesion ligand for endothelial intercellular adhesion molecule 1 in breast cancer.** *Cancer Res* 1996, **56**:4244-4249.
4. Rahn JJ, Chow JW, Horne GJ, Mah BK, Emerman JT, Hoffman P, Hugh JC: **MUC1 mediates transendothelial migration in vitro by ligating endothelial cell ICAM-1.** *Clin Exp Metastasis* 2005, **22**:475-483.
5. Rahn JJ, Hugh JC: **The MUC1/ICAM-1 signal: its potential to trigger tumor cell migration.** *Six Conference on Signaling in Normal and Cancer Cells, IRCM* 2004.
6. Piccolo E, Innominato PF, Mariggio MA, Maffucci T, Iacobelli S, Falasca M: **The mechanism involved in the regulation of phospholipase Cgamma1 activity in cell migration.** *Oncogene* 2002, **21**:6520-6529.
7. Playford MP, Schaller MD: **The interplay between Src and integrins in normal and tumor biology.** *Oncogene* 2004, **23**:7928-7946.
8. Sotsios Y, Ward SG: **Phosphoinositide 3-kinase: a key biochemical signal for cell migration in response to chemokines.** *Immunol Rev* 2000, **177**:217-235.
9. Feldner JC, Brandt BH: **Cancer cell motility--on the road from c-erbB-2 receptor steered signaling to actin reorganization.** *Exp Cell Res* 2002, **272**:93-108.
10. Kumada T, Komuro H: **Completion of neuronal migration regulated by loss of Ca(2+) transients.** *Proc Natl Acad Sci U S A* 2004, **101**:8479-8484.
11. Ridley AJ, Schwartz MA, Burridge K, Firtel RA, Ginsberg MH, Borisy G, Parsons JT, Horwitz AR: **Cell migration: integrating signals from front to back.** *Science* 2003, **302**:1704-1709.
12. Correa I, Plunkett T, Vlad A, Mungul A, Candelora-Kettel J, Burchell JM, Taylor-Papadimitriou J, Finn OJ: **Form and pattern of MUC1 expression on T cells activated in vivo or in vitro suggests a function in T-cell migration.** *Immunology* 2003, **108**:32-41.
13. Bennett R, Jr., Jarvela T, Engelhardt P, Kostamovaara L, Sparks P, Carpen O, Turunen O, Vaheri A: **Mucin MUC1 is seen in cell surface protrusions together with ezrin in immunoelectron tomography and is concentrated at tips of filopodial protrusions in MCF-7 breast carcinoma cells.** *J Histochem Cytochem* 2001, **49**:67-77.
14. Hall A: **Rho GTPases and the actin cytoskeleton.** *Science* 1998, **279**:509-514.
15. Van Aelst L, D'Souza-Schorey C: **Rho GTPases and signaling networks.** *Genes Dev* 1997, **11**:2295-2322.
16. Nobes CD, Hall A: **Rho GTPases control polarity, protrusion, and adhesion during cell movement.** *J Cell Biol* 1999, **144**:1235-1244.

17. Rottner K, Hall A, Small JV: **Interplay between Rac and Rho in the control of substrate contact dynamics.** *Curr Biol* 1999, **9**:640-648.
18. Rahn JJ, Shen Q, Mah BK, Hugh JC: **MUC1 initiates a calcium signal after ligation by intercellular adhesion molecule-1.** *J Biol Chem* 2004, **279**:29386-29390.
19. Oosawa Y, Imada C, Furuya K: **Temperature dependency of calcium responses in mammary tumour cells.** *Cell Biochem Funct* 1997, **15**:113-117.
20. Foster LJ, De Hoog CL, Mann M: **Unbiased quantitative proteomics of lipid rafts reveals high specificity for signaling factors.** *Proc Natl Acad Sci U S A* 2003, **100**:5813-5818.
21. Handa K, Jacobs F, Longenecker BM, Hakomori SI: **Association of MUC-1 and SPGL-1 with low-density microdomain in T-lymphocytes: a preliminary note.** *Biochem Biophys Res Commun* 2001, **285**:788-794.
22. Li Y, Kuwahara H, Ren J, Wen G, Kufe D: **The c-Src tyrosine kinase regulates signaling of the human DF3/MUC1 carcinoma-associated antigen with GSK3 beta and beta-catenin.** *J Biol Chem* 2001, **276**:6061-6064.
23. Rahn JJ, University of Alberta. Dept. of Medical Sciences.: **The role of the MUC1/ICAM-1 interaction in promoting breast cancer cell migration**: 2004.
24. Shaw AR, Domanska A, Mak A, Gilchrist A, Dobler K, Visser L, Poppema S, Fliegel L, Letarte M, Willett BJ: **Ectopic expression of human and feline CD9 in a human B cell line confers beta 1 integrin-dependent motility on fibronectin and laminin substrates and enhanced tyrosine phosphorylation.** *J Biol Chem* 1995, **270**:24092-24099.
25. Hawkins PT, Eguinoa A, Qiu RG, Stokoe D, Cooke FT, Walters R, Wennstrom S, Claesson-Welsh L, Evans T, Symons M, et al.: **PDGF stimulates an increase in GTP-Rac via activation of phosphoinositide 3-kinase.** *Curr Biol* 1995, **5**:393-403.
26. Funamoto S, Meili R, Lee S, Parry L, Firtel RA: **Spatial and temporal regulation of 3-phosphoinositides by PI 3-kinase and PTEN mediates chemotaxis.** *Cell* 2002, **109**:611-623.
27. Ridley AJ: **Rho GTPases and cell migration.** *J Cell Sci* 2001, **114**:2713-2722.
28. Li Y, Ren J, Yu W, Li Q, Kuwahara H, Yin L, Carraway KL, 3rd, Kufe D: **The epidermal growth factor receptor regulates interaction of the human DF3/MUC1 carcinoma antigen with c-Src and beta-catenin.** *J Biol Chem* 2001, **276**:35239-35242.
29. Ozdener F, Dangelmaier C, Ashby B, Kunapuli SP, Daniel JL: **Activation of phospholipase Cgamma2 by tyrosine phosphorylation.** *Mol Pharmacol* 2002, **62**:672-679.
30. Tokmakov AA, Sato KI, Iwasaki T, Fukami Y: **Src kinase induces calcium release in Xenopus egg extracts via PLCgamma and IP3-dependent mechanism.** *Cell Calcium* 2002, **32**:11-20.
31. Shu L, Shayman JA: **Src kinase mediates the regulation of phospholipase C-gamma activity by glycosphingolipids.** *J Biol Chem* 2003, **278**:31419-31425.
32. Kaplan KB, Bibbins KB, Swedlow JR, Arnaud M, Morgan DO, Varmus HE: **Association of the amino-terminal half of c-Src with focal adhesions alters**

their properties and is regulated by phosphorylation of tyrosine 527. *Embo J* 1994, **13**:4745-4756.
33. Al Masri A, Gendler SJ: **Muc1 affects c-Src signaling in PyV MT-induced mammary tumorigenesis.** *Oncogene* 2005, **24**:5799-5808.
34. Pankov R, Markovska T, Hazarosova R, Antonov P, Ivanova L, Momchilova A: **Cholesterol distribution in plasma membranes of beta1 integrin-expressing and beta1 integrin-deficient fibroblasts.** *Arch Biochem Biophys* 2005, **442**:160-168.
35. Golub T, Caroni P: **PI(4,5)P2-dependent microdomain assemblies capture microtubules to promote and control leading edge motility.** *J Cell Biol* 2005, **169**:151-165.
36. Gomez-Mouton C, Lacalle RA, Mira E, Jimenez-Baranda S, Barber DF, Carrera AC, Martinez AC, Manes S: **Dynamic redistribution of raft domains as an organizing platform for signaling during cell chemotaxis.** *J Cell Biol* 2004, **164**:759-768.
37. Chodniewicz D, Klemke RL: **Regulation of integrin-mediated cellular responses through assembly of a CAS/Crk scaffold.** *Biochim Biophys Acta* 2004, **1692**:63-76.
38. Hanks SK, Ryzhova L, Shin NY, Brabek J: **Focal adhesion kinase signaling activities and their implications in the control of cell survival and motility.** *Front Biosci* 2003, **8**:d982-996.
39. Reiske HR, Kao SC, Cary LA, Guan JL, Lai JF, Chen HC: **Requirement of phosphatidylinositol 3-kinase in focal adhesion kinase-promoted cell migration.** *J Biol Chem* 1999, **274**:12361-12366.
40. Mitra SK, Hanson DA, Schlaepfer DD: **Focal adhesion kinase: in command and control of cell motility.** *Nat Rev Mol Cell Biol* 2005, **6**:56-68.
41. Poullet P, Gautreau A, Kadare G, Girault JA, Louvard D, Arpin M: **Ezrin interacts with focal adhesion kinase and induces its activation independently of cell-matrix adhesion.** *J Biol Chem* 2001, **276**:37686-37691.
42. Sieg DJ, Hauck CR, Ilic D, Klingbeil CK, Schaefer E, Damsky CH, Schlaepfer DD: **FAK integrates growth-factor and integrin signals to promote cell migration.** *Nat Cell Biol* 2000, **2**:249-256.
43. Hattrup CL, Gendler SJ: **MUC1 alters oncogenic events and transcription in human breast cancer cells.** *Breast Cancer Res* 2006, **8**:R37.
44. Li Z, Hannigan M, Mo Z, Liu B, Lu W, Wu Y, Smrcka AV, Wu G, Li L, Liu M, et al.: **Directional sensing requires G beta gamma-mediated PAK1 and PIX alpha-dependent activation of Cdc42.** *Cell* 2003, **114**:215-227.
45. Schaller MD, Parsons JT: **pp125FAK-dependent tyrosine phosphorylation of paxillin creates a high-affinity binding site for Crk.** *Mol Cell Biol* 1995, **15**:2635-2645.
46. Cho SY, Klemke RL: **Purification of pseudopodia from polarized cells reveals redistribution and activation of Rac through assembly of a CAS/Crk scaffold.** *J Cell Biol* 2002, **156**:725-736.
47. Fukuyama T, Ogita H, Kawakatsu T, Fukuhara T, Yamada T, Sato T, Shimizu K, Nakamura T, Matsuda M, Takai Y: **Involvement of the c-Src-Crk-C3G-Rap1**

signaling in the nectin-induced activation of Cdc42 and formation of adherens junctions. *J Biol Chem* 2005, **280**:815-825.

Chapter 4: ICAM-1 Potentiates the Invasion of MUC1-expressing Cells

4.0. Introduction

The evidence provided in chapters 2 and 3 has shown that MUC1, by binding ICAM-1, not only induces calcium-based pro-migratory signaling, but also initiates increased cytoskeletal protrusive motility. Since tumor cell migration and invasion are mainly propelled by polarized cytoskeletal rearrangements, these findings strongly suggest a crucial role for the MUC1/ICAM-1 interaction in tumor cell invasive motility. Our previous studies by Rahn *et al.* (2005) have demonstrated that the MUC1/ICAM-1 interaction facilitates transendothelial migration of MUC1-bearing cells in a series of transwell assays [1]. However, little is known about the potential impact of the MUC1/ICAM-1 interaction on stromal invasion, although increased ICAM-1 expression has been observed on the peri-tumoral stromal fibroblasts [2].

In the experiments presented in this chapter, we tested the hypothesis that the human ICAM-1 expressed on fibroblasts also potentiates stromal invasion of MUC1-expressing cells. This was addressed by spatial-temporally tracking the transmigratory and invasive capability of MUC1-bearing epithelial cells through a mouse fibroblast NIH3T3 monolayer, which has been transfected with/without human ICAM-1 and coated on a gelatin matrix. Our previous studies have shown that MUC1-expressing 293T SYM cells could induce mild calcium oscillatory responses in a cell monolayer expressing ICAM-1 [3]. As well, others have reported that leukocytes and MCF-7 breast cancer cells, but not normal mammary epithelial cells, could bind to endothelial cells and trigger an intracellular calcium flux, localized disassembly of focal contacts and partial retraction of endothelial cells [4-8], where endothelial ICAM-1 is believed to play a causative role

[9]. Thus, in this study, morphological responses of the NIH3T3 monolayer were also investigated during the process of transmigration of MUC1-positive cells.

4.1. Materials and Methods

4.1.1. Reagents

The 35mm glass-bottomed microwell dishes were purchased from MatTek Corporation. Gelatin Type A, potassium chloride (KCl), magnesium chloride ($MgCl_2$), calcium chloride ($CaCl_2$), glucose and HEPES were purchased from Sigma-Aldrich (Oakville, ON, Canada). Sodium chloride was purchased from Fisher Ltd (Nepean, ON, Canada). DMEM, FBS, trypsin, G418, and blasticidin S were purchased from Invitrogen, Inc (Carlsbad, CA, USA). Imaging buffer (152mM NaCl, 5.4mM KCl, 0.8mM $MgCl_2$, 1.8mM $CaCl_2$, 10mM HEPES, 5.6 mM glucose, pH 7.2 [10,11]) was prepared in-house.

4.1.2. Cell Culture

The MUC1-transfected 293T SYM25 and SYM3 cells were maintained in DMEM supplemented with 10% FBS and 200μg/ml G418. Mock and ICAM-1 transfected NIH3T3 mouse fibroblast cells (kindly provided by Dr. Ken Dimock, University of Ottawa, ON) were maintained in DMEM supplemented with 10% FBS and 2μg/ml Blasticidin S. All these cell lines are cultured at 37°C in a humidified incubator containing 5% CO_2 (Water-Jacketed Incubator, Forma Scientific, Marietta, OH, USA)

4.1.3. Cell Invasion Assay

The 35mm glass-bottomed MatTek microwell dishes were coated with 100 μl of 2% (w/v) gelatin, which was allowed to gel in the microwell at room temperature. Then,

100 μl of NIH3T3-ICAM-1 or -Mock transfectants at 1 X 10^6/ml were plated on the top of the gelatin matrix overnight to get a confluent NIH3T3 cell monolayer (Fig. 4.1). The day of the experiment, the cell monolayer was washed once gently with Imaging Buffer and placed in a 37°C stage warmer on a Zeiss 2-photon confocal microscope (Zeiss LSM NLO 510). The EGFP signal was excited using a 488 nm laser line of a 25mW Argon laser excitation source with the intensity output was set to 25%. 8-bit images were collected with a 2.56μs dwell time per pixel. The pinhole was set to 2.48 Airy unit and images were collected at 0.64 μm/pixel resolution. The gain and offset were set to expand the signal from the cell being imaged over the 255 grey value scale of the 8-bit data range. Then, Z stacks (~1.5 μm intervals from coverslip bottom of the dish to 10 μm above the surface of NIH3T3 monolayer) were acquired every 20 minutes over the 6 hour experiment under both DIC and a 505 nm long pass filter (EGFP). 3 ml of MUC1-transfected 293T Sym25 or SYM3 cells at 3 x 10^4/ml in Imaging Buffer were added upon the surface of the NIH3T3 cell monolayer immediately after the first stack was taken.

For investigating the processes of cell transmigration and invasion, the spatial-temporally acquired Z-stack images were first retrieved by LSM-FCS software (expert mode). Then, using the orthogonal sections display mode, the processes of cell adhesion, transmigration and invasion were displayed by adjusting the X, Y, and Z orthogonal planes respectively at each time point (Fig. 4.2 A and B). To quantify cell invasion, the Z-stack images were 3-D reconstructed by Imaris Software (Bitplane AG, version 4.2). Further, the DIC channel was deleted and the 3-D GFP images of 293T SYM cells were surface rendered by setting a background cut-off threshold value. Thus, by tracing the cells over time, the proportion (%) of cells that penetrated the cell monolayer, the gelatin

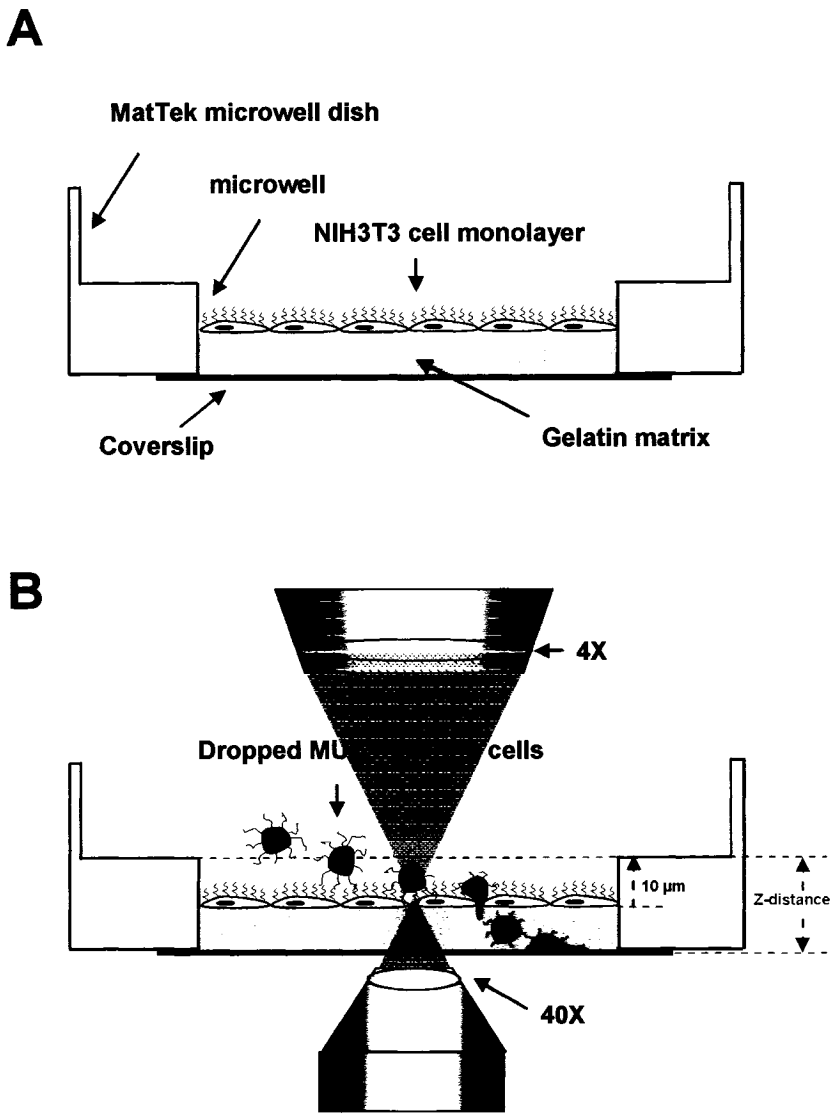

Figure 4.1: The cell invasion assay. (A) NIH3T3-ICAM-1 or -Mock cell monolayer was layered over a gelatin matrix in the microwell of a MatTek dish. (B) pEGFP-actin transfected cells, with/without MUC1 expression, were dropped onto the NIH3T3 cell monolayer, followed by the acquisition of Z-stack images (indicated as red dash lines and arrows) every 20 minutes over the 6 hour experiment using a Zeiss 2-photon confocal microscope.

matrix and reached the glass bottom were counted. The experiment was repeated 3 times under each condition, the average proportions were calculated and used to compare between different experimental conditions.

4.1.4. Statistical Analysis

The proportion of cells that transmigrated through NIH3T3 fibroblast cell monolayer or invaded through gelatin matrix were graphed based on the average % ± S.E., using MS Excel software. Statistical significance was determined using the Student's t-test, $p<0.05$.

4.2. Results

4.2.1. Human ICAM-1 Potentiates Transmigration of MUC1-expressing 293T Cells through a NIH3T3 Cell Monolayer and Subsequent Invasion of a Gelatin Matrix.

To investigate if human ICAM-1 promotes the transmigration and invasion of MUC1-bearing cells, we have examined the invasive process of MUC1-positive 293T SYM25 cells through a NIH3T3-ICAM-1 fibroblast monolayer and compared this with a NIH3T3-Mock monolayer, using the MUC1-negative 293T SYM3 cells as controls. The time-lapse confocal microscopy showed that, typically following the dropping of cells, the 293T SYM25 cells migrated/rolled on the NIH3T3-ICAM-1 cell monolayer a short distant before adhesion (Fig. 4.2 C-E). Then, an invadopodium formed at the heterotypic cell-monolayer contact interface and inserted into the gelatin matrix through an intercellular space of the NIH3T3 cell monolayer (Fig. 4.2 F). This was followed by penetration of the invadopodium to the bottom of matrix (Fig. 4.2 G). Lastly, the cell

completely transmigrated through the monolayer, and spread beneath the NIH3T3-ICAM-1 cell monolayer (Fig. 4.2 H). This process is analogous to leukocytes in the process of transmigration through an endothelium.

Imaris software was used to quantify cell transmigration and invasion through the gelatin matrix during the 6 hour assay. By comparing the percentages of successfully penetrated cells under each condition, it was shown that the MUC1-expressing 293T SYM25 exhibited significantly increased invasive motility when ICAM-1 was present on the NIH3T3 cell monolayer, as compared with the NIH3T3-Mock monolayer and MUC1-negative 293T SYM3 cells (Fig. 4.3). In addition, cell cohort invasion was also frequently observed (data not shown), indicating cell-cell dissociation is not obligatory for cell transmigration and subsequent invasion. Further, by spatial-temporally tracing cell transmigration and invasion at each time point during the invasion assay, we found that transmigration of both 293T SYM25 and SYM3 cells started to reach a plateau 4 hours after cell dropping, under the conditions without MUC1/ICAM-1 interaction (Fig. 4.4 A). However, when the MUC1-expressing 293T SYM25 cells were dropped on NIH3T3-ICAM-1 cell monolayers, they appeared to have a constant migration rate over the period of the invasion assay (Fig. 4.4 A). Thus, as shown in Fig. 4.4 A, a statistically significant difference in cell transmigration began 5 hours after addition of the MUC1-positive cells and continued to increase with time, suggesting that the presence of both MUC1 and ICAM-1 in this co-culture system is crucial for sustained cell transmigration. Moreover, we found the rate of invasion for the 293T SYM25 cells was also significantly higher from the "5 hour" time point, only in the setting of an ICAM-1-positive monolayer

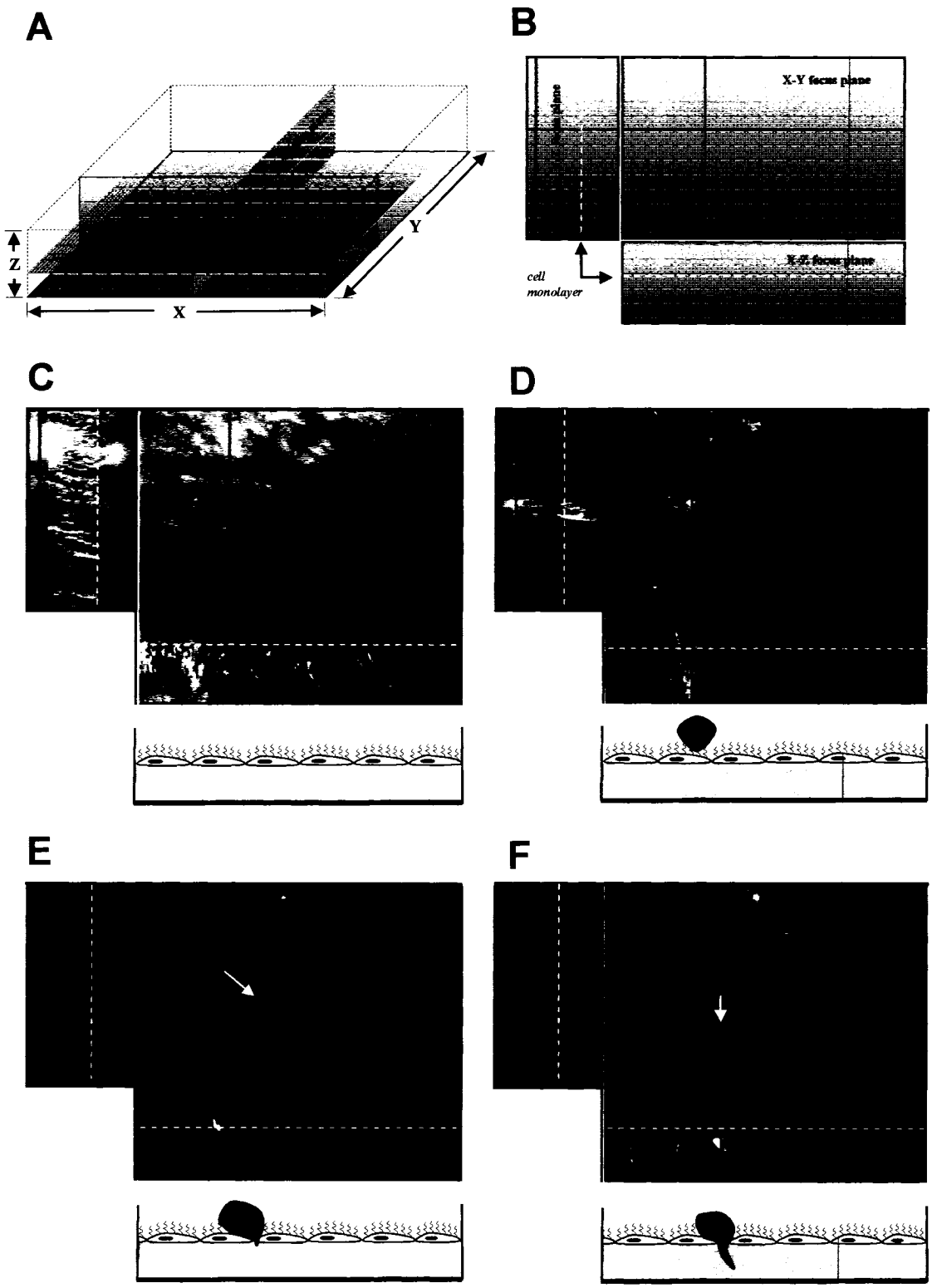

Figure 4.2: 293T SYM25 cell invasion through a NIH3T3-ICAM-1 cell monolayer.

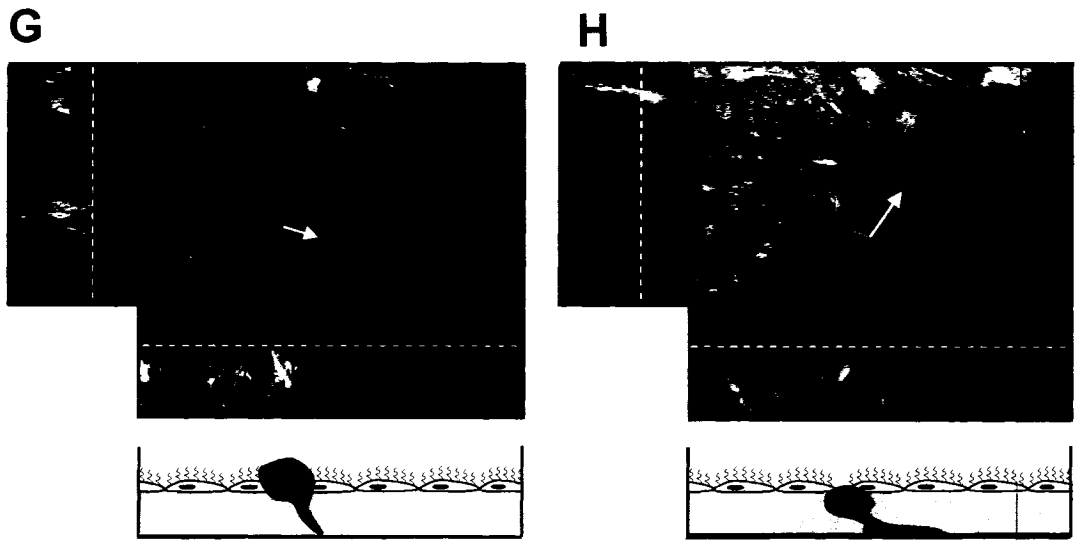

Figure 4.2 continued: (A) Illustration of the 3-D orthogonal sections display mode. (B) Diagram of how the corresponding orthogonal sections were displayed in the LSM-FCS software. (C) Focus plane represents the bottom layer of the Z-stack images. (D) 293T SYM25 cells were dropped on the top of NIH3T3-ICAM-1 cell monolayer. (E) The 293T SYM25 cell migrated/rolled a short distant. (F) An invadopodium was formed and inserted through an intercellular space of the NIH3T3-ICAM-1 cell monolayer. (G) The cell invadopodial protrusion touched the bottom of the gelatin matrix. (H) The 293T SYM25 cell totally invaded through and spread out underneath the NIH3T3-ICAM-1 cell monolayer.

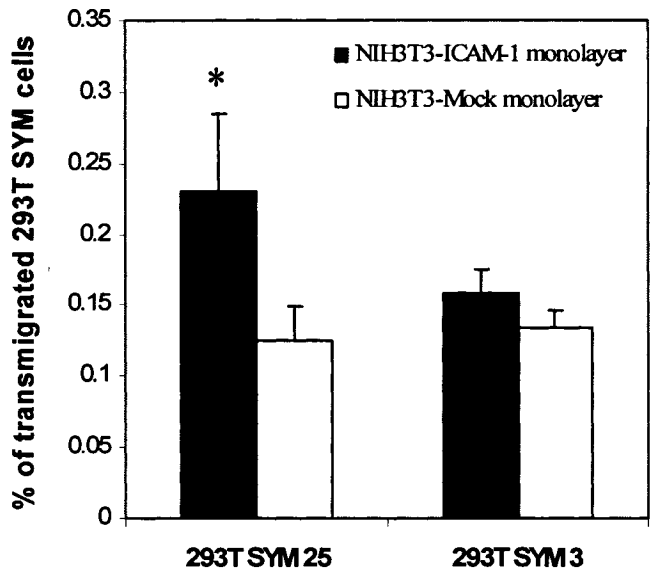

Figure 4.3: Human ICAM-1 promotes MUC1-expressing 293T cell invasive motility. Data are the average percentage (%) ± S.D. of transmigrated 293T SYM 25 and SYM3 cells through the NIH3T3-ICAM-1 or -Mock cell monolayers. MUC1-positive 293T SYM25 cells displayed statistically significant increases in cell invasion (t-test, $p<0.05$), as compared with the controls.

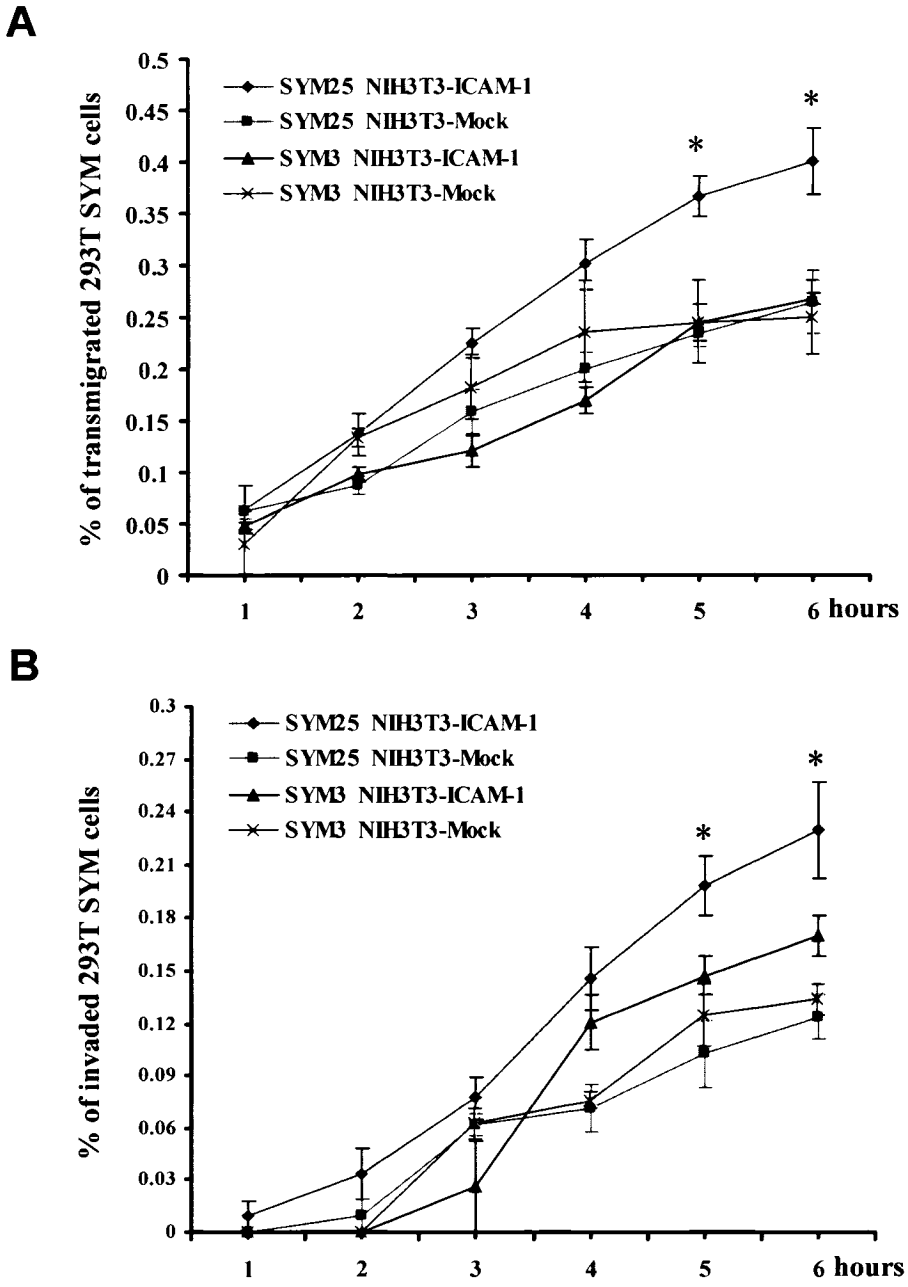

Figure 4.4: Human ICAM-1 promotes MUC1-expressing 293T cells transmigration and subsequent invasion. Data represent the average percentage ± S.E. (n=3) of 293T SYM 25 and SYM3 cells that (A) transmigrated through the NIH3T3-ICAM-1 or -Mock cell monolayers, and (B) successfully penetrated through the gelatin matrix, reaching the bottom, at each time point during the cell invasion assay. MUC1-positive 293T SYM25 cells displayed a statistically significant increase in cell transmigration and invasion, in the presence of ICAM-1 on the NIH3T3 cell monolayer, as compared with the controls.

(Fig. 4.4 B). Based on the above results, we conclude that the MUC1/ICAM-1 interaction may not only promote cell transmigration, but also potentiate cell stromal invasion.

4.2.2. Cellular Retraction of a NIH3T3 Cell Monolayer in Response to MUC1-transfected 293T Cells Invasion.

Using DIC and long-pass 505nm filters on a Zeiss 2-photon confocal microscope (see materials and methods), we investigated the morphological responses of the NIH3T3 cell monolayer following contact with MUC1-transfected 293T SYM25 or SYM3 cells. As shown in Fig. 4.5, both the NIH3T3-ICAM-1 and -Mock transfectants exhibited a flattened and spread appearance forming a confluent cell monolayer on the gelatin matrix. Subsequent to the seeding of MUC1-positive 293T SYM25 cells onto the cell monolayer, the time-lapse microscopy showed that the NIH3T3-ICAM-1 cells retracted within 3 hours, resulting in broad intercellular spaces coinciding with the location of the 293T SYM25 cells (Fig. 4.5 A). In contrast, no obvious cellular retraction was observed in the NIH3T3-Mock cell monolayer after contact with 293T SYM25 cells (Fig. 4.5 B). Similar results were also obtained in both NIH3T3-ICAM-1 and -Mock cell monolayers when the MUC1-negative 293T SYM3 cells were dropped on the top, showing a low degree of morphological response (data not shown). Collectively, these findings suggest that the presence of both MUC1 and ICAM-1 are required for this retraction response in NIH3T3 transfectant monolayers, potentiating transmigration and invasion of MUC1-positive cells.

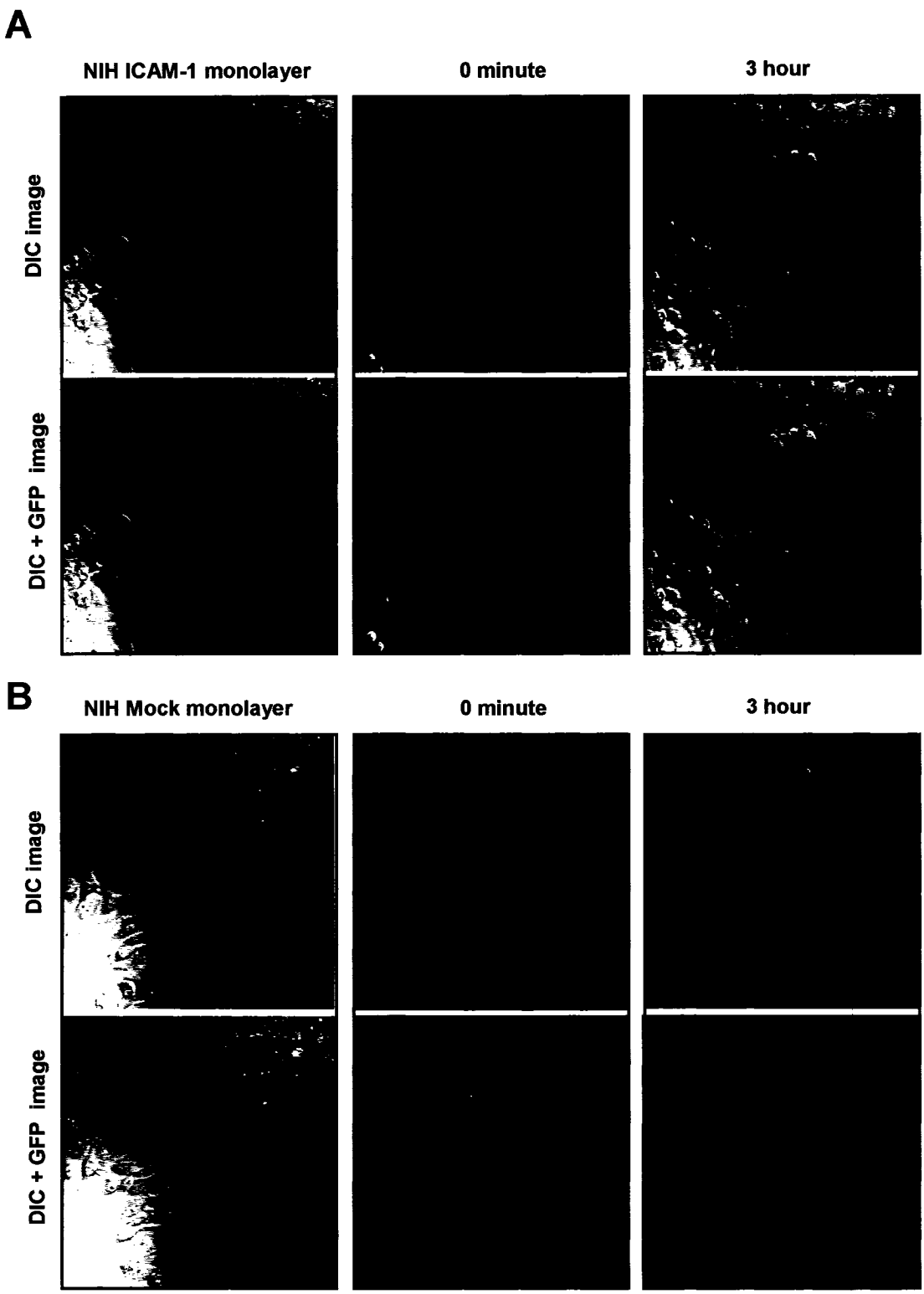

Figure 4.5: 293T SYM25 cells induce NIH3T3-ICAM-1 cellular retraction.

Figure 4.5 continued: (A) NIH3T3-ICAM-1 and (B) NIH3T3-Mock transfectants (gray cells in the DIC images) were plated on the gelatin matrix in MatTek microwell dishes to generate a confluent cell monolayer, and then subjected to cell invasion assays upon addition of the MUC1-transfected 293T SYM cells (green cells in the GFP-DIC overlaied images in the bottom lanes). The images represent the monolayer-focus plane of the Z-stacks.

4.3. Discussion

Tumor cell stromal invasion represents one of the most critical steps in blood-borne metastasis, as the tumor cells in the primary lesion have to invade through their surrounding stroma before commencing intravasation. As well, after transendothelial migration, efficient stromal invasion at the target organs is crucial for successful extravasation and formation of a metastatic focus. Breast cancer cell invasion of the stroma has generally been correlated with ECM protease activity, particularly uPAR [12] and MMP-2 [13]. There is little data on the stromal fibroblast participation in the tumor cell invasive motility even though the peri-tumoral fibroblast acquires an altered phenotype, including increased ICAM-1 expression [2] and is synergistic with the neoplastic process [14,15]. Previous work in this thesis project has demonstrated that the MUC1/ICAM-1 interaction initiates actin cytoskeletal protrusive motility. In the present study using a novel invasion model and live-imaging confocal microscopy, we found that human ICAM-1 expressed on the fibroblast NIH3T3 monolayer also potentiates transmigration and invasion of MUC1-expressing 293T cells. This is consistent with our previous transwell results by Rahn *et al.* (2005) showing that MUC1, by ligating ICAM-1 facilitates transendothelial migration of MUC1-bearing cells through a monolayer of ICAM-1-expressing endothelial cells [1]. The present data suggests an additional critical role of the MUC1/ICAM-1 interaction in stromal invasion. This is significant for fully understanding the biological function of MUC1/ICAM-1 ligation, in the context of tumor-microenvironment interaction, during the process of breast cancer stromal invasion and blood-borne metastasis. As well, the observation of cohort invasion of MUC1-positive 293T SYM25 cells strengthens our hypothesis that MUC1, instead of inhibiting

E-cadherin/integrin-mediated cell-cell/matrix adhesion, is a pro-adhesive molecule crucial for cell invasive motility. The use of a live-imaging invasion model is novel for several reasons: (1) the 3-D matrix is more analogous to the *in vivo* condition when compared to cell motility in 2-D dishes or filters, and (2) this live-imaging model allows direct observation of the dynamic processes of cell invasion. Using this model, a significant difference in cell invasion was shown only after 5 hours of heterotypic cell-cell contact. This is supportive for our previous cytoskeletal reorganization data showing that the MUC1/ICAM-1 interaction-induced migration starts after 1.5 hour. Taken together, these findings suggest that the MUC1/ICAM-1 interaction-induced transmigration and subsequent invasion, parallel to leukocytes, may represent a crucial mechanism for the sustained invasive motility of tumor cells.

Mechanistically, the main motor of cell transmigration and invasion is invadopodia, which involve the Rho family small GTPases Rac/Cdc42 analogous to the lamellipodial protrusions in migrating cells [16,17]. Thus, we propose that the increased invasiveness is induced by the MUC1/ICAM-1 interaction-induced actin cytoskeletal protrusive motility. Moreover, the MUC1/ICAM ligation may also facilitate cell invasion by extracellular protease-mediated ECM degradation, as MMP2 which is involved in hydrolysis of the gelatin matrix can be upregulated via JNK cascade in response to Rac GTPase activation [18-20] and Rac has been implicated in MUC1/ICAM-1 ligation-induced signaling (see details in chapter 3).

The present studies also provide evidence that the MUC1-expressing cells induce cellular retraction of the NIH3T3-ICAM-1 fibroblast monolayer, which is consistent with our previous findings that MUC1-bearing cells could trigger calcium signals in the

accessory cells with ICAM-1 expression [3]. Calcium and calcium-based signaling are crucial for the actin cytoskeletal reorganization and cellular contraction (see mechanisms in section 1.1.3.3). Since leukocytes and breast cancer cells, but not normal mammary epithelial cells, were reported to initiate intracellular calcium flux, focal contact turnover and cellular retraction of endothelial cells [4-8], the cellular retraction in the fibroblast monolayer may serve as another mechanism by which the MUC1/ICAM-1 interaction may facilitate cell invasion. Thus, further studies clarifying the molecular events within the ICAM-1-expressing cells following MUC1 ligation will provide the complete molecular picture of the MUC1/ICAM-1 interaction in cancer metastasis.

4.4. References

1. Rahn JJ, Chow JW, Horne GJ, Mah BK, Emerman JT, Hoffman P, Hugh JC: **MUC1 mediates transendothelial migration in vitro by ligating endothelial cell ICAM-1.** *Clin Exp Metastasis* 2005, **22**:475-483.
2. Vogetseder W, Feichtinger H, Schulz TF, Schwaeble W, Tabaczewski P, Mitterer M, Bock G, Marth C, Dapunt O, Mikuz G, et al.: **Expression of 7F7-antigen, a human adhesion molecule identical to intercellular adhesion molecule-1 (ICAM-1) in human carcinomas and their stromal fibroblasts.** *Int J Cancer* 1989, **43**:768-773.
3. Rahn JJ, University of Alberta. Dept. of Medical Sciences.: **The role of the MUC1/ICAM-1 interaction in promoting breast cancer cell migration**: 2004.
4. Lewalle JM, Bajou K, Desreux J, Mareel M, Dejana E, Noel A, Foidart JM: **Alteration of interendothelial adherens junctions following tumor cell-endothelial cell interaction in vitro.** *Exp Cell Res* 1997, **237**:347-356.
5. Lewalle JM, Cataldo D, Bajou K, Lambert CA, Foidart JM: **Endothelial cell intracellular Ca2+ concentration is increased upon breast tumor cell contact and mediates tumor cell transendothelial migration.** *Clin Exp Metastasis* 1998, **16**:21-29.
6. Burns AR, Bowden RA, MacDonell SD, Walker DC, Odebunmi TO, Donnachie EM, Simon SI, Entman ML, Smith CW: **Analysis of tight junctions during neutrophil transendothelial migration.** *J Cell Sci* 2000, **113(Pt1)**:45-57.
7. Burns AR, Walker DC, Brown ES, Thurmon LT, Bowden RA, Keese CR, Simon SI, Entman ML, Smith CW: **Neutrophil transendothelial migration is independent of tight junctions and occurs preferentially at tricellular corners.** *J Immunol.* 1997, **159**:2893-2903.
8. Phan C, McMahon AW, Nelson RC, Elliott JF, Murray AG: **Activated lymphocytes promote endothelial cell detachment from matrix: a role for modulation of endothelial cell beta 1 integrin affinity.** *J Immunol* 1999, **163**:4557-4563.
9. Etienne S, Adamson P, Greenwood J, Strosberg AD, Cazaubon S, Couraud PO: **ICAM-1 signaling pathways associated with Rho activation in microvascular brain endothelial cells.** *J Immunol* 1998, **161**:5755-5761.
10. Oosawa Y, Imada C, Furuya K: **Temperature dependency of calcium responses in mammary tumour cells.** *Cell Biochem Funct* 1997, **15**:113-117.
11. Rahn JJ, Shen Q, Mah BK, Hugh JC: **MUC1 initiates a calcium signal after ligation by intercellular adhesion molecule-1.** *J Biol Chem* 2004, **279**:29386-29390.
12. Xing RH, Rabbani SA: **Overexpression of urokinase receptor in breast cancer cells results in increased tumor invasion, growth and metastasis.** *Int J Cancer* 1996, **67**:423-429.
13. Munoz-Najar UM, Neurath KM, Vumbaca F, Claffey KP: **Hypoxia stimulates breast carcinoma cell invasion through MT1-MMP and MMP-2 activation.** *Oncogene* 2006, **25**:2379-2392.
14. Lagace R, Grimaud JA, Schurch W, Seemayer TA: **Myofibroblastic stromal reaction in carcinoma of the breast: variations of collagenous matrix and**

structural glycoproteins. *Virchows Arch A Pathol Anat Histopathol* 1985, **408**:49-59.
15. Chiavegato A, Bochaton-Piallat ML, D'Amore E, Sartore S, Gabbiani G: **Expression of myosin heavy chain isoforms in mammary epithelial cells and in myofibroblasts from different fibrotic settings during neoplasia.** *Virchows Arch* 1995, **426**:77-86.
16. Nakahara H, Otani T, Sasaki T, Miura Y, Takai Y, Kogo M: **Involvement of Cdc42 and Rac small G proteins in invadopodia formation of RPMI7951 cells.** *Genes Cells* 2003, **8**:1019-1027.
17. Yamaguchi H, Lorenz M, Kempiak S, Sarmiento C, Coniglio S, Symons M, Segall J, Eddy R, Miki H, Takenawa T, et al.: **Molecular mechanisms of invadopodium formation: the role of the N-WASP-Arp2/3 complex pathway and cofilin.** *J Cell Biol* 2005, **168**:441-452.
18. Playford MP, Schaller MD: **The interplay between Src and integrins in normal and tumor biology**. *Oncogene* 2004, **23**:7928-7946.
19. Hsia DA, Mitra SK, Hauck CR, Streblow DN, Nelson JA, Ilic D, Huang S, Li E, Nemerow GR, Leng J, et al.: **Differential regulation of cell motility and invasion by FAK.** *J Cell Biol* 2003, **160**:753-767.
20. Xu X, Wang Y, Lauer-Fields JL, Fields GB, Steffensen B: **Contributions of the MMP-2 collagen binding domain to gelatin cleavage. Substrate binding via the collagen binding domain is required for hydrolysis of gelatin but not short peptides.** *Matrix Biol* 2004, **23**:171-181.

Chapter 5: Summary and Discussion

5.1. Summary

The research presented in this thesis has focused on the potential role of MUC1/ICAM-1 interaction in promoting breast cancer cell pro-migratory signaling and cell motility. Breast cancer is the most frequently diagnosed malignancy in women and despite the progress in therapeutic strategies, prognosis remains poor for the large majority of patients with advanced stage disease at diagnosis. Similar to other malignancies, a major obstacle to offering curative cancer therapy in breast cancer is metastasis, the process characterized by increased pro-migratory signaling and cell motility, whereby the cancer cells break through restricting boundaries to invade into surrounding tissues and vessels to establish secondary tumors at distant body sites [1-7]. With advances in understanding breast tumorigenesis, the MUC1 transmembrane glycoprotein when aberrantly overexpressed in breast cancer cells is increasingly associated with breast cancer progression and metastasis [8-10]. Regimbald *et al.* (1996) found that breast cancer MUC1 could bind to endothelial ICAM-1 [11], an adhesion molecule involved in leukocyte transendothelial migration [12]. The subsequent work in our laboratory has since demonstrated that this MUC1/ICAM-1 interaction could mediate heterotypic cell-cell adhesion that is strong enough to withstand the shear stresses equivalent to physiologic blood flow [13,14]. These findings strongly suggest a direct role that MUC1 may play in cellular pro-migratory signaling and motility by ligating ICAM-1.

In **chapter 2**, using live imaging fluorescence microscopy, we found that MUC1 specifically induces a series of intracellular calcium oscillatory signals in the MUC1-positive breast cancer cells, as well as in the MUC1-transfected 293T subclones, in

response to ICAM-1 stimulation [15]. This MUC1/ICAM-1 interaction-initiated calcium signaling appears to be different from non-specific cell-cell contact induced transient calcium spike, which may be due to mechanical stress [16]. Subsequently, the selective pharmaceutical inhibition assays demonstrated that the MUC1/ICAM-1-initiated calcium oscillations are mediated by the signaling cascade(s) involving Src family kinase, PI3K, PLC, and IP3R, but not MAPK [15]. Thus, it appears to be different from the previously described MUC1 phosphotyrosine-based signal(s), which generally involve the MAPK cascade [17-25]. Further, as the calcium/calcium-based signaling and the signaling mediators implicated in the MUC1/ICAM-1-induced calcium oscillations are frequently implicated in cell motility [4,26-33], this calcium-based oscillatory signaling may represent a novel MUC1-initiated signaling that is associated with cell motility.

Evidence provided in **chapter 2** also showed that MUC1 (~50%) is localized within lipid rafts in breast cancer cells, as well as in MUC1-transfected 293T cells. This is significant, because lipid rafts are membrane signaling platforms and crucial for both intracellular calcum signaling and cytoskeleton-based cell motility [34-40]. This notion was further strengthened by the lipid raft disruption assays in this study, showing that the MUC1/ICAM-1 interaction-induced calcium oscillations were significantly abrogated by MBCD/nystatin-mediated raft disruption [15]. Moreover, through the lipid raft extraction assays and co-immunoprecipitation, we found that Src was rapidly shifted into lipid rafts and increased Src was associated with MUC1 in both breast cancer cells and MUC1-transfected 293T cells in response to ICAM-1 stimulation, strongly suggesting Src may play a critical role in the MUC1/ICAM-1-initiated calcium signaling, possibly putting Src upstream of PI3K and PLC to induce calcium release from the IP3R on the ER.

To address the questions raised in chapter 2 regarding the consequence(s) of MUC1/ICAM-1 interaction-induced pro-migratory signaling in cell motility, the study described in **chapter 3** shows that MUC1 initiates dramatic cytoskeletal rearrangements and increased protrusive motility in response to ICAM-1 ligation, in a panel of breast cancer cell lines, MUC1-transfected 293T subclones, as well as an inducible Flp-In T-REx 293 MUC1 system. The specificity was further demonstrated by anti-ICAM-1 mAbs, showing only the anti-ICAM-1 antibody (18E3D) which specifically targets the MUC1 binding site, could block the MUC1/ICAM-1-induced actin cytoskeletal protrusive motility. Mechanistically, similar to the calcium oscillation data, we found that inhibition of the pathways involving PI3K, Src family kinase, and PLC significantly abrogated the MUC1/ICAM-1 ligation-induced cytoskeletal protrusive motility. These findings provide solid evidence that MUC1 could promote tumor metastasis not only as an adhesion protein but also by functioning as a pro-migratory signaling molecule to potentiate cell motility. In addition, since both MUC1 and β1 integrins are localized in lipid rafts and associate with cell motility [41-43], we further investigated the relationship between β1 integrin and MUC1 in ICAM-1 ligation-induced cytoskeletal protrusive motility. Using an anti-β1 integrin blocking mAb and RGD peptides in a time-lapse confocal microscopy assay, we showed that β1 integrin is required for the MUC1/ICAM-1 ligation-initiated cytoskeletal rearrangements and protrusive motility. As well, no obvious cytoskeletal dynamics were observed without MUC1/ICAM-1 ligation, regardless of the presence or absence of β1 integrin blockade. Thus, we proposed that there is a synergistic effect between MUC1 and β1 integrin in promoting cytoskeletal protrusive motility in response to ICAM-1 stimulation. Our studies also provide

evidence that the MUC1/ICAM-1 ligation-induced cytoskeletal protrusive motility requires activation of both Rho GTPase Rac1 and Cdc42, but not RhoA. This is consistent with the role of Rho family GTPases previously described in the regulation of actin ctyoskeletal reorganization [7,44,45].

Based on the previous work in this thesis project showing that the MUC1/ICAM-1 interaction not only induces pro-migratory signaling but also initiates actin cytoskeletal protrusive motility, the research presented in **chapter 4** was a follow-up study to investigate the possible role of the MUC1/ICAM-1 interaction in cell transmigration and invasion. Using a novel live cell imaging method, we found that human ICAM-1 expressed on the NIH3T3 fibroblast monolayer significantly potentiates MUC1-expressing 293T cells transmigration and invasion. This is not only consistent with the previous work by Rahn *et al.* (2005) in our laboratory showing that the MUC1/ICAM-1 interaction facilitates transendothelial migration in a transwell model [46], but also provides the first evidence that MUC1/ICAM-1 may be involved in stromal invasion. Further, the evidence presented in this study showed that the MUC1-expressing cells induce cellular retraction of the NIH3T3-ICAM-1 monolayer, as compared with the mock-transfected NIH3T3 cell monolayer, which may serve as another mechanism to facilitate cell transmigration and subsequent invasion.

5.2. General Discussion

Adhesion receptors play critical roles in the oncogenic transformation of normal cells through induction of cancer-specific cellular behaviour and morphology. During metastasis, cancer cells lose their original tissue contacts, invade through the ECM, transit via the lymphatic/blood system, adhere and then extravsate at the secondary

metastatic site [47]. This implies that tumor cells likely upregulate and utilize a distinct set of adhesion receptors to adjust to the changes in these cell-ECM interactions, thereby facilitating the metastatic spread. In this thesis study, we focused on the transmembrane glycoprotein MUC1, which is frequently overexpressed in breast cancer and is increasingly associated with malignant progression [8-10,48-50]. In addition to the potential roles that have been suggested for MUC1 in tumor cell proliferation, scattering and survival [20,23,51,52], we are the first to report that MUC1 is a pro-adhesive molecule and mediates heterotypic cell-cell adhesion by binding endothelial cell ICAM-1. This strongly suggests the MUC1/ICAM-1 interaction may be implicated in tumor cell extravasation, with a mechamism(s) parallel to the leukocytes. Also, contrary to the MUC1 steric hindrance theory that the extreme length and negative charge of the multiple O-glycosylation residues in MUC1's rigid extracellular domain blocks other adhesion molecules (e.g. integrins) from their binding sites [9,53], the evidence provided in this study showed that exogenous or increased MUC1 expression did not alter cellular adhesion or morphology in 293T cells (see section 3.2.1). Moreover, if MUC1 were blocking integrin-mediated cell-ECM adhesion, anti-integrin blockade should not influence the MUC1/ICAM-1 interaction-induced biological activities. However, by blocking integrins, we found that both the MUC1/ICAM-1-initiated calcium signaling (unpublished data) and cytoskeletal protrusive motility (see section 3.2.4) were significantly reduced. Thus, instead of preventing cell-ECM adhesion, we propose that MUC1 synergizes with other adhesion molecules, such as integrin, in mediating cancer cell adhesion and subsequent cell motility.

This study also provided the first evidence that MUC1/ICAM-1 intiates calcium-based pro-migratory signaling and cytoskeletal protrusive motility (see chapter 2 and 3). These findings demonstrate that cellular adhesion is not the only input contributed by the MUC1/ICAM-1 interaction in cell motility. Mechanistically, we found Src family kinase, PI3K, and PLC were involved in both the MUC1/ICAM-1 interaction-induced migratory signaling and motility. Since the MUC1-CD lacks intrinsic enzymatic activity, the evidence of the rapid translocation of Src non-receptor tyrosine kinase into lipid rafts and increased MUC1-Src association following MUC1/ICAM-1 interaction (see section 2.2.4 and 2.2.5) is crucial to understanding the signal initiation which occurs downstream of the MUC1/ICAM-1 ligation. Thus, we propose that on contact with ICAM-1, Src is recruited by MUC1 into lipid rafts, thereby activating downstream PI3K and PLC to induce calcium oscillations through the IP3R. Further, the signaling mediators together with calcium and calcium-based signals initiate actin cytoskeletal protrusive motility. This model is supported by the research of Al Masri *et al.* (2005) showing that the MUC1-Src interaction facilitated the association of Src with its substrate proteins, such as PI3K [54]. Since the previous studies by Li *et al.* (2001) demonstrated that Src can interact with MUC1-CD (Y^{46}EKV or Y^{35}VPP) via either its SH2 or SH3 domain [18,19], the ICAM-1-induced MUC1-Src association could be a kinase-independent mechanism determined principally by interactions involving the SH3 domain with modulation by the SH2 domain [55]. Site-directed mutagenesis experiments are currently underway to determine which binding motif(s) of the MUC1-CD is crucial in the MUC1/ICAM-1-induced migratory activities (work of Yan Tang).

Significantly, as described above, we found that β1 integrin synergizes with the MUC1/ICAM-1 interaction in the MUC1-initiated calcium-based pro-migratory signaling and cytoskeletal protrusive motility. In the cytoskeletal reorganization assays, as the NIH3T3 transfectants were dropped on top of the pEGFP-actin transfected cells, we proposed that β1 integrin may function as an adhesive receptor for the ECM substrate to stabilize the MUC1/ICAM-1-initiated membrane protrusions at the heterotypic cell-cell contact sites. Further, since β1 integrin is also localized in lipid rafts [34,43], an alternative hypothesis is that the MUC1/ICAM-1 interaction may serve to bring Src in proximity to β1 integrins on lipid rafts, where by forming a "FAK-Src signaling complex" to initiate calcium oscillatory signaling and cytoskeletal protrusive motility through PI3K/PLC and p130CAS/Crk/Rac-Cdc42 cascades (Fig. 5.1). Strengthening this hypothesis, FAK has recently been reported to be associated with MUC1 in MMTV-PyV MT mammary tumors [54]. However, since no FAK-binding domain has identified at MUC1-CD, we suggest that this MUC1-FAK association is an indirect interaction through Ezrin. MUC1 was reported to be associated with the cytoskeleton linker protein - ezrin [56], which has been implicated in binding the FAK N-terminal domain and activating FAK independently of cell-matrix adhesion [57]. Thus, it is possible that the MUC1/ICAM-1 interaction initiates Src-FAK complex formation by the MUC1-CD, where FAK bridges MUC1 and β1 integrin so as to integrate their signals to promote cell motility (Fig. 5.1). A follow-up study based on this hypothesis is being planned in our laboratory to further clarify the MUC1/ICAM-1 ligation-initiated migratory signaling.

Moreover, as we expected, both Rho GTPases Rac1 and Cdc42 are required for the MUC1/ICAM-1 interaction-induced cytoskeletal protrusive motility. This may be

mediated by PI3K-associated signaling in response to MUC1/ICAM-1 interaction (Fig. 5.1). The PI3K-generated PtdIns(3,4,5)P3 has been implicated in recruiting PH domain-containing GEFs to the plasma membrane, thereby facilitating GEF-mediated GTP-loading on Rac/Cdc42 GTPases and their subsequent activation [58-61]. Also, in response to ICAM-1 ligation, the MUC1-associated Src and FAK signaling may also regulate the Rac/Cdc42-mediated cytoskeletal protrusive motility through the PI3K and/or p130CAS/Crk pathway (see details in section 1.1.3.2, and Fig. 5.1). Moreover, since the MUC1-CD contains two highly conserved YXXP docking sequences ($Y^{35}VPP^{38}$ and $Y^{60}TNP^{63}$) for the SH2 domain of Crk, which can activate Rac1 and Cdc42 to initiate cell lamellipodial/filopodial protrusions [34,62], it is possible that the MUC1/ICAM-1 ligation may induce the Rac/Cdc42-mediated cytoskeletal dynamics directly via the Crk pathway.

Lastly, evidence provided by live cell imaging transmigration-invasion assays showed that human ICAM-1, expressed on NIH3T3 fibroblasts, potentiates MUC1-bearing cells transmigration and invasion. This is consistent with our previous cytoskeletal reorganization data (see chapter 2) as well as the transendothelial migration data by Rahn *et al.* (2005) [46], and further suggests that the MUC1/ICAM-1 interaction potentiates MUC1-positive cells stromal invasion. This represents an additional step in understanding the critical role of MUC1 in tumor cell migration and metastasis. As well, the MUC1/ICAM-1-induced cell monolayer retraction and the possible effect(s) of MUC1/ICAM-1 interaction on the MMPs-mediated gelatin matrix degradation may also facilitate this process.

5.3. Closing Remarks

The work in this thesis has demonstrated that the MUC1/ICAM-1 interaction initiates calcium-based signaling and cytoskeletal protrusive motility, which are mediated by pathways involving a Src family kinase, PI3K, PLC, and IP3R. Additionally, we found that MUC1 synergizes with β1 integrins in the ICAM-1 ligation-induced cytoskeletal protrusive motility. Further, we demonstrated that the MUC1/ICAM-1 interaction-induced cytoskeletal rearrangements require Rho family GTPases Rac1 and Cdc42, but not RhoA, and is accompanied by increased cell transmigration and invasion. These data offer functional evidence that implicates MUC1 overexpression as a key molecular event in the aggressive tumor phenotype, and provides an insight into the mechanisms that tumor cells may use following the heterotypic MUC1/ICAM-1 interaction to facilitate cell metastasis (Fig. 5.2).

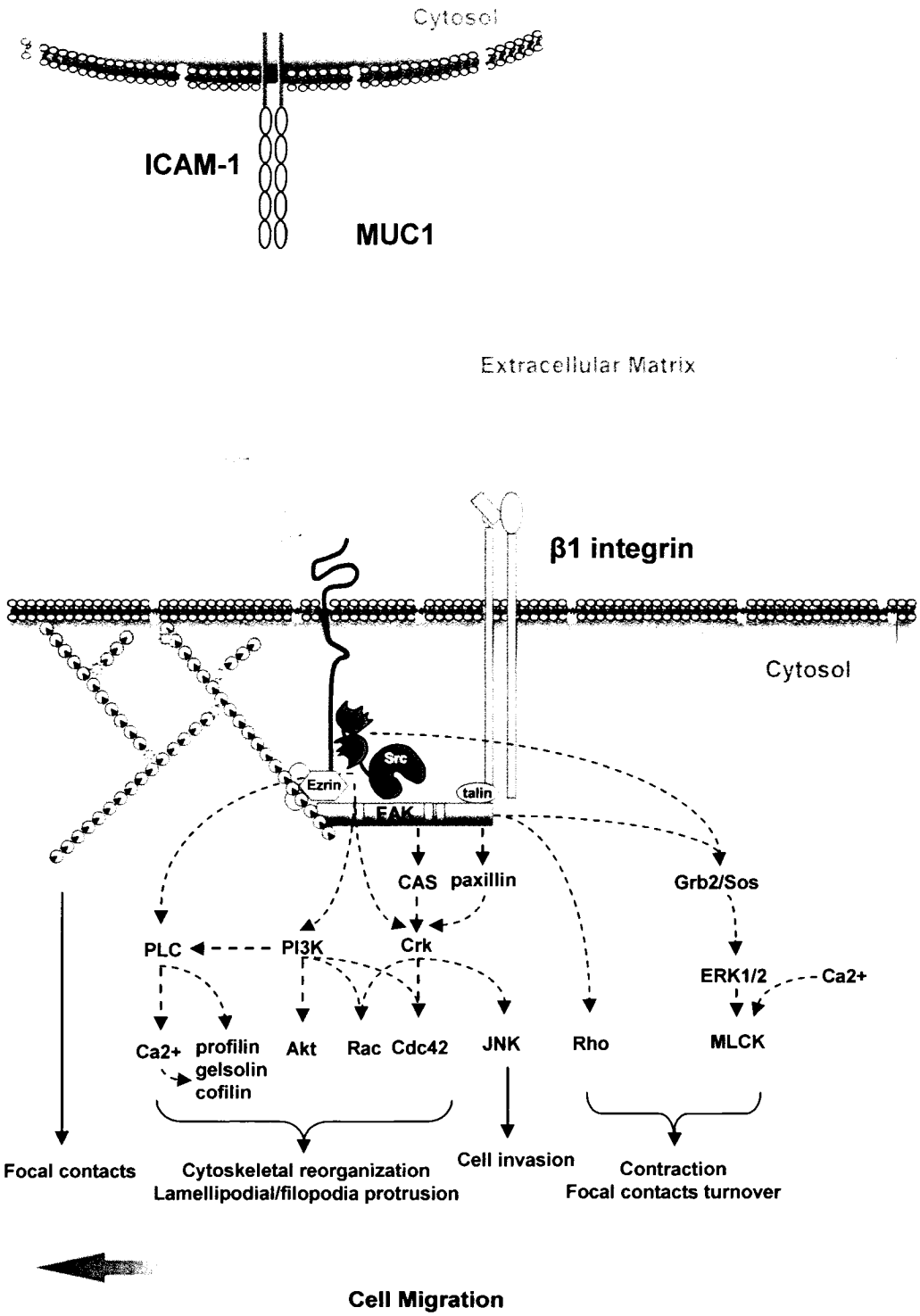

Figure 5.1: Hypothetical model of how the MUC1/ICAM-1 interaction synergizes with β1 integrins and promotes pro-migratory signaling and cell motility.

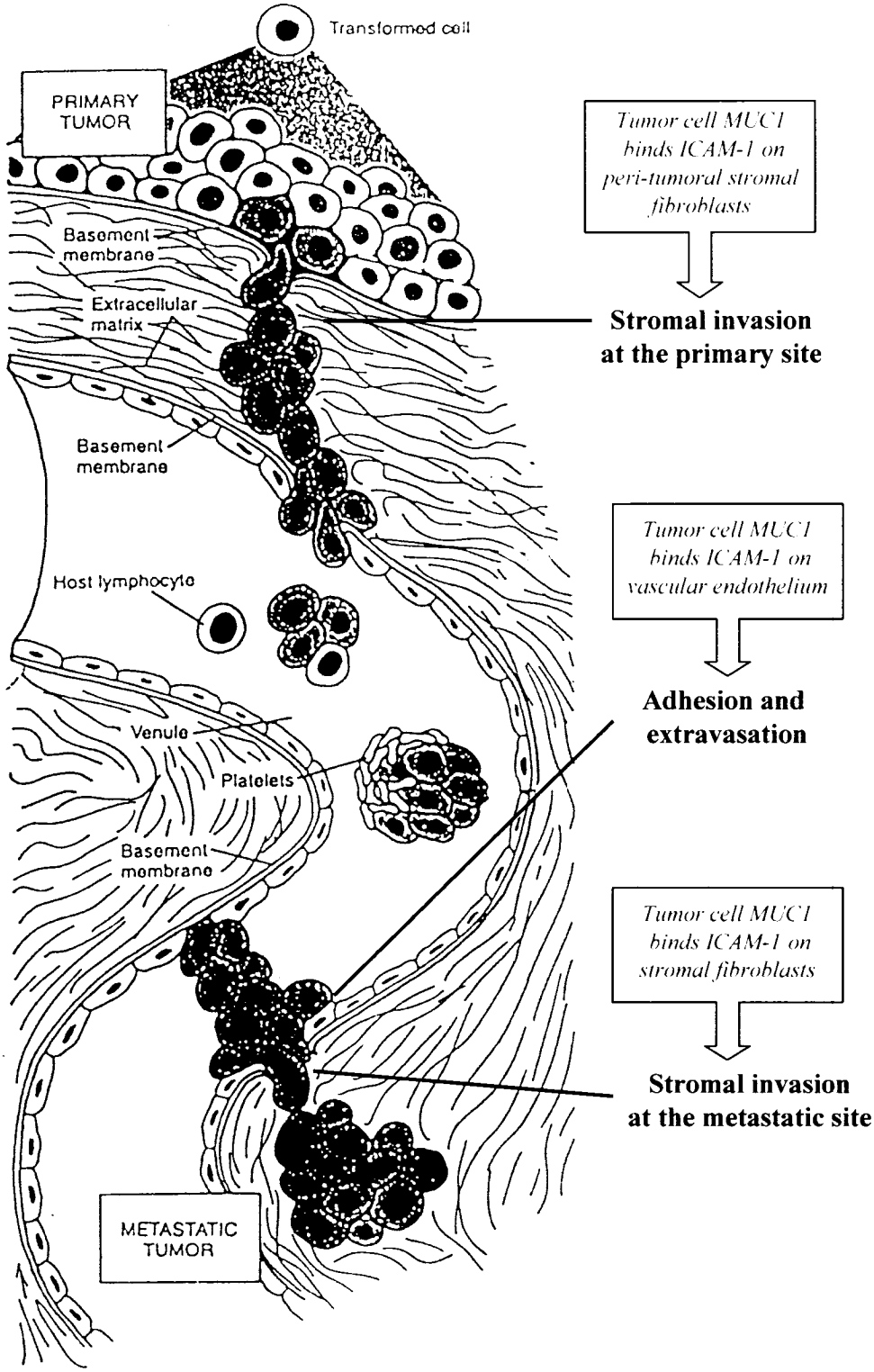

Figure 5.2: Hypothetical role of the MUC1/ICAM-1 interaction in breast cancer metastasis. Based on evidence in this study and [11,13,14,46,47]

5.4. References

1. Patanaphan V, Salazar OM, Risco R: **Breast cancer: metastatic patterns and their prognosis.** *South Med J* 1988, **81**:1109-1112.
2. Fidler IJ: **Critical factors in the biology of human cancer metastasis: twenty-eighth G.H.A. Clowes memorial award lecture.** *Cancer Res* 1990, **50**:6130-6138.
3. Friedl P, Brocker EB, Zanker KS: **Integrins, cell matrix interactions and cell migration strategies: fundamental differences in leukocytes and tumor cells.** *Cell Adhes Commun* 1998, **6**:225-236.
4. Playford MP, Schaller MD: **The interplay between Src and integrins in normal and tumor biology.** *Oncogene* 2004, **23**:7928-7946.
5. Kamby C: **[Pattern of metastases in breast cancer].** *Ugeskr Laeger* 1984, **146**:2615-2620.
6. Suetsugu S, Takenawa T: **Regulation of cortical actin networks in cell migration.** *Int Rev Cytol* 2003, **229**:245-286.
7. Ridley AJ: **Rho proteins and cancer.** *Breast Cancer Res Treat* 2004, **84**:13-19.
8. Rahn JJ, Dabbagh L, Pasdar M, Hugh JC: **The importance of MUC1 cellular localization in patients with breast carcinoma: an immunohistologic study of 71 patients and review of the literature.** *Cancer* 2001, **91**:1973-1982.
9. Hilkens J, Vos HL, Wesseling J, Boer M, Storm J, van der Valk S, Calafat J, Patriarca C: **Is episialin/MUC1 involved in breast cancer progression?** *Cancer Lett* 1995, **90**:27-33.
10. Gendler SJ, Spicer AP, Lalani EN, Duhig T, Peat N, Burchell J, Pemberton L, Boshell M, Taylor-Papadimitriou J: **Structure and biology of a carcinoma-associated mucin, MUC1.** *Am Rev Respir Dis* 1991, **144**:S42-47.
11. Regimbald LH, Pilarski LM, Longenecker BM, Reddish MA, Zimmermann G, Hugh JC: **The breast mucin MUCI as a novel adhesion ligand for endothelial intercellular adhesion molecule 1 in breast cancer.** *Cancer Res* 1996, **56**:4244-4249.
12. Kuby J: *Immunology* edn 3rd. New York: W.H. Freeman; 1997.
13. Kam JL, Regimbald LH, Hilgers JH, Hoffman P, Krantz MJ, Longenecker BM, Hugh JC: **MUC1 synthetic peptide inhibition of intercellular adhesion molecule-1 and MUC1 binding requires six tandem repeats.** *Cancer Res* 1998, **58**:5577-5581.
14. Horne GJ, University of Alberta. Dept. of Laboratory Medicine and Pathology.: **The role of breast cancer associated with MUC1 in tumor cell recruitment to vascular endothelium during physiological fluid flow**: 1999.
15. Rahn JJ, Shen Q, Mah BK, Hugh JC: **MUC1 initiates a calcium signal after ligation by intercellular adhesion molecule-1.** *J Biol Chem* 2004, **279**:29386-29390.
16. Sigurdson WJ, Sachs F, Diamond SL: **Mechanical perturbation of cultured human endothelial cells causes rapid increases of intracellular calcium.** *Am J Physiol* 1993, **264**:H1745-1752.
17. Li Y, Bharti A, Chen D, Gong J, Kufe D: **Interaction of glycogen synthase kinase 3beta with the DF3/MUC1 carcinoma-associated antigen and beta-catenin.** *Mol Cell Biol* 1998, **18**:7216-7224.

18. Li Y, Kuwahara H, Ren J, Wen G, Kufe D: **The c-Src tyrosine kinase regulates signaling of the human DF3/MUC1 carcinoma-associated antigen with GSK3 beta and beta-catenin.** *J Biol Chem* 2001, **276**:6061-6064.
19. Li Y, Ren J, Yu W, Li Q, Kuwahara H, Yin L, Carraway KL, 3rd, Kufe D: **The epidermal growth factor receptor regulates interaction of the human DF3/MUC1 carcinoma antigen with c-Src and beta-catenin.** *J Biol Chem* 2001, **276**:35239-35242.
20. Pandey P, Kharbanda S, Kufe D: **Association of the DF3/MUC1 breast cancer antigen with Grb2 and the Sos/Ras exchange protein.** *Cancer Res* 1995, **55**:4000-4003.
21. Quin RJ, McGuckin MA: **Phosphorylation of the cytoplasmic domain of the MUC1 mucin correlates with changes in cell-cell adhesion.** *Int J Cancer* 2000, **87**:499-506.
22. Ren J, Li Y, Kufe D: **Protein kinase C delta regulates function of the DF3/MUC1 carcinoma antigen in beta-catenin signaling.** *J Biol Chem* 2002, **277**:17616-17622.
23. Schroeder JA, Thompson MC, Gardner MM, Gendler SJ: **Transgenic MUC1 interacts with epidermal growth factor receptor and correlates with mitogen-activated protein kinase activation in the mouse mammary gland.** *J Biol Chem* 2001, **276**:13057-13064.
24. Wang H, Lillehoj EP, Kim KC: **Identification of four sites of stimulated tyrosine phosphorylation in the MUC1 cytoplasmic tail.** *Biochem Biophys Res Commun* 2003, **310**:341-346.
25. Meerzaman D, Shapiro PS, Kim KC: **Involvement of the MAP kinase ERK2 in MUC1 mucin signaling.** *Am J Physiol Lung Cell Mol Physiol* 2001, **281**:L86-91.
26. Marks PW, Hendey B, Maxfield FR: **Attachment to fibronectin or vitronectin makes human neutrophil migration sensitive to alterations in cytosolic free calcium concentration.** *J Cell Biol* 1991, **112**:149-158.
27. Feldner JC, Brandt BH: **Cancer cell motility--on the road from c-erbB-2 receptor steered signaling to actin reorganization.** *Exp Cell Res* 2002, **272**:93-108.
28. Thomas SM, Brugge JS: **Cellular functions regulated by Src family kinases.** *Annu Rev Cell Dev Biol* 1997, **13**:513-609.
29. Kumada T, Komuro H: **Completion of neuronal migration regulated by loss of Ca(2+) transients.** *Proc Natl Acad Sci U S A* 2004, **101**:8479-8484.
30. Hiscox S, Morgan L, Green TP, Barrow D, Gee J, Nicholson RI: **Elevated Src activity promotes cellular invasion and motility in tamoxifen resistant breast cancer cells.** *Breast Cancer Res Treat* 2006, **97**:263-274.
31. Lodish HF: *Molecular cell biology* edn 4th. New York: W.H. Freeman; 2000.
32. Reiske HR, Kao SC, Cary LA, Guan JL, Lai JF, Chen HC: **Requirement of phosphatidylinositol 3-kinase in focal adhesion kinase-promoted cell migration.** *J Biol Chem* 1999, **274**:12361-12366.
33. Berridge MJ, Lipp P, Bootman MD: **The versatility and universality of calcium signalling.** *Nat Rev Mol Cell Biol* 2000, **1**:11-21.
34. Zajchowski LD, Robbins SM: **Lipid rafts and little caves. Compartmentalized signalling in membrane microdomains.** *Eur J Biochem* 2002, **269**:737-752.

35. Simons K, Toomre D: **Lipid rafts and signal transduction.** *Nat Rev Mol Cell Biol* 2000, **1**:31-39.
36. Higgs HN, Pollard TD: **Activation by Cdc42 and PIP(2) of Wiskott-Aldrich syndrome protein (WASp) stimulates actin nucleation by Arp2/3 complex.** *J Cell Biol* 2000, **150**:1311-1320.
37. Rozelle AL, Machesky LM, Yamamoto M, Driessens MH, Insall RH, Roth MG, Luby-Phelps K, Marriott G, Hall A, Yin HL: **Phosphatidylinositol 4,5-bisphosphate induces actin-based movement of raft-enriched vesicles through WASP-Arp2/3.** *Curr Biol* 2000, **10**:311-320.
38. Golub T, Caroni P: **PI(4,5)P2-dependent microdomain assemblies capture microtubules to promote and control leading edge motility.** *J Cell Biol* 2005, **169**:151-165.
39. van Rheenen J, Achame EM, Janssen H, Calafat J, Jalink K: **PIP2 signaling in lipid domains: a critical re-evaluation.** *Embo J* 2005, **24**:1664-1673.
40. Sato K, Fukami Y, Stith BJ: **Signal transduction pathways leading to Ca(2+) release in a vertebrate model system: Lessons from Xenopus eggs.** *Semin Cell Dev Biol* 2006, **17**:285-292.
41. Foster LJ, De Hoog CL, Mann M: **Unbiased quantitative proteomics of lipid rafts reveals high specificity for signaling factors.** *Proc Natl Acad Sci U S A* 2003, **100**:5813-5818.
42. Handa K, Jacobs F, Longenecker BM, Hakomori SI: **Association of MUC-1 and SPGL-1 with low-density microdomain in T-lymphocytes: a preliminary note.** *Biochem Biophys Res Commun* 2001, **285**:788-794.
43. Pankov R, Markovska T, Hazarosova R, Antonov P, Ivanova L, Momchilova A: **Cholesterol distribution in plasma membranes of beta1 integrin-expressing and beta1 integrin-deficient fibroblasts.** *Arch Biochem Biophys* 2005, **442**:160-168.
44. Ridley AJ: **Rho GTPases and cell migration.** *J Cell Sci* 2001, **114**:2713-2722.
45. Hall A: **Rho GTPases and the actin cytoskeleton.** *Science* 1998, **279**:509-514.
46. Rahn JJ, Chow JW, Horne GJ, Mah BK, Emerman JT, Hoffman P, Hugh JC: **MUC1 mediates transendothelial migration in vitro by ligating endothelial cell ICAM-1.** *Clin Exp Metastasis* 2005, **22**:475-483.
47. Tannock I, Hill RP: *The basic science of oncology* edn 3rd. New York: McGraw-Hill, Health Professions Division; 1998.
48. Nakamori S, Ota DM, Cleary KR, Shirotani K, Irimura T: **MUC1 mucin expression as a marker of progression and metastasis of human colorectal carcinoma.** *Gastroenterology* 1994, **106**:353-361.
49. McGuckin MA, Walsh MD, Hohn BG, Ward BG, Wright RG: **Prognostic significance of MUC1 epithelial mucin expression in breast cancer.** *Hum Pathol* 1995, **26**:432-439.
50. Szpak CA, Johnston WW, Lottich SC, Kufe D, Thor A, Schlom J: **Patterns of reactivity of four novel monoclonal antibodies (B72.3, DF3, B1.1 and B6.2) with cells in human malignant and benign effusions.** *Acta Cytol* 1984, **28**:356-367.

51. Raina D, Kharbanda S, Kufe D: **The MUC1 oncoprotein activates the anti-apoptotic phosphoinositide 3-kinase/Akt and Bcl-xL pathways in rat 3Y1 fibroblasts.** *J Biol Chem* 2004, **279**:20607-20612.
52. Schroeder JA, Adriance MC, Thompson MC, Camenisch TD, Gendler SJ: **MUC1 alters beta-catenin-dependent tumor formation and promotes cellular invasion.** *Oncogene* 2003, **22**:1324-1332.
53. Wesseling J, van der Valk SW, Vos HL, Sonnenberg A, Hilkens J: **Episialin (MUC1) overexpression inhibits integrin-mediated cell adhesion to extracellular matrix components.** *J Cell Biol* 1995, **129**:255-265.
54. Al Masri A, Gendler SJ: **Muc1 affects c-Src signaling in PyV MT-induced mammary tumorigenesis.** *Oncogene* 2005, **24**:5799-5808.
55. Kaplan KB, Bibbins KB, Swedlow JR, Arnaud M, Morgan DO, Varmus HE: **Association of the amino-terminal half of c-Src with focal adhesions alters their properties and is regulated by phosphorylation of tyrosine 527.** *Embo J* 1994, **13**:4745-4756.
56. Bennett R, Jr., Jarvela T, Engelhardt P, Kostamovaara L, Sparks P, Carpen O, Turunen O, Vaheri A: **Mucin MUC1 is seen in cell surface protrusions together with ezrin in immunoelectron tomography and is concentrated at tips of filopodial protrusions in MCF-7 breast carcinoma cells.** *J Histochem Cytochem* 2001, **49**:67-77.
57. Poullet P, Gautreau A, Kadare G, Girault JA, Louvard D, Arpin M: **Ezrin interacts with focal adhesion kinase and induces its activation independently of cell-matrix adhesion.** *J Biol Chem* 2001, **276**:37686-37691.
58. Hawkins PT, Eguinoa A, Qiu RG, Stokoe D, Cooke FT, Walters R, Wennstrom S, Claesson-Welsh L, Evans T, Symons M, et al.: **PDGF stimulates an increase in GTP-Rac via activation of phosphoinositide 3-kinase.** *Curr Biol* 1995, **5**:393-403.
59. Li Z, Hannigan M, Mo Z, Liu B, Lu W, Wu Y, Smrcka AV, Wu G, Li L, Liu M, et al.: **Directional sensing requires G beta gamma-mediated PAK1 and PIX alpha-dependent activation of Cdc42.** *Cell* 2003, **114**:215-227.
60. Srinivasan S, Wang F, Glavas S, Ott A, Hofmann F, Aktories K, Kalman D, Bourne HR: **Rac and Cdc42 play distinct roles in regulating PI(3,4,5)P3 and polarity during neutrophil chemotaxis.** *J Cell Biol* 2003, **160**:375-385.
61. Welch HC, Coadwell WJ, Stephens LR, Hawkins PT: **Phosphoinositide 3-kinase-dependent activation of Rac.** *FEBS Lett* 2003, **546**:93-97.
62. Fukuyama T, Ogita H, Kawakatsu T, Fukuhara T, Yamada T, Sato T, Shimizu K, Nakamura T, Matsuda M, Takai Y: **Involvement of the c-Src-Crk-C3G-Rap1 signaling in the nectin-induced activation of Cdc42 and formation of adherens junctions.** *J Biol Chem* 2005, **280**:815-825.

Appendix: Regulating Effect of TGF-β on MUC1 Expression in Breast Cancer MCF-7 Cells

A.1. Introduction and Objective

Transforming Growth Factor-beta (TGF-β) has been demonstrated to be a multifunctional cytokine with both tumor suppressor and pro-oncogenic activities. Unlike other tumor suppressors or proto-oncogenes which usually function in a simple "On/Off" manner, TGF-β always appears to be functional and utilized by different cells in various biological processes, regardless of whether it is mutated, upregulated or downregulated. In normal tissues and early stages of cancer, TGF-β normally has dominant suppressor effects, however it switches function to act as a tumor promoter in advanced cancers [1], with the mechanism of this alteration still obscure.

The Smads pathway is the mainstay of the signals initiated by TGF-β through activation of its cell surface receptor (TβRI/II) serine-threonine kinase [1] (Fig A.1). Following phosphorylation of R-Smad (Smad 2 and 3) by the activated TβRI/II complex, R-Smad forms an oligomeric complex with Co-Smad (Smad 4), and then translocates into the nucleus [1], where both R-Smads (except Smad2) and Co-Smads can bind directly to Smad binding elements (SBE) in the promoter regions of target genes via a highly conserved β-hairpin loop in the MH1 domain [2]. In addition, Smad3 and Smad 4 have also been shown to bind to the GC-rich sequence motifs of certain genes [3], suggesting that the DNA binding specificity of Smads is not restricted. Recently, the TGF-β inhibitory/activated elements (TIE/TAE) were found in the promoter region of several genes (e.g. c-Myc). These are thought to be responsible for TGF-β induced down/upregulation, but it is still not clear whether Smads can bind directly to these elements [4,5]. The transactivation properties of Smads are mediated by their MH2 domains, which allows direct association with certain transcription activators, such as

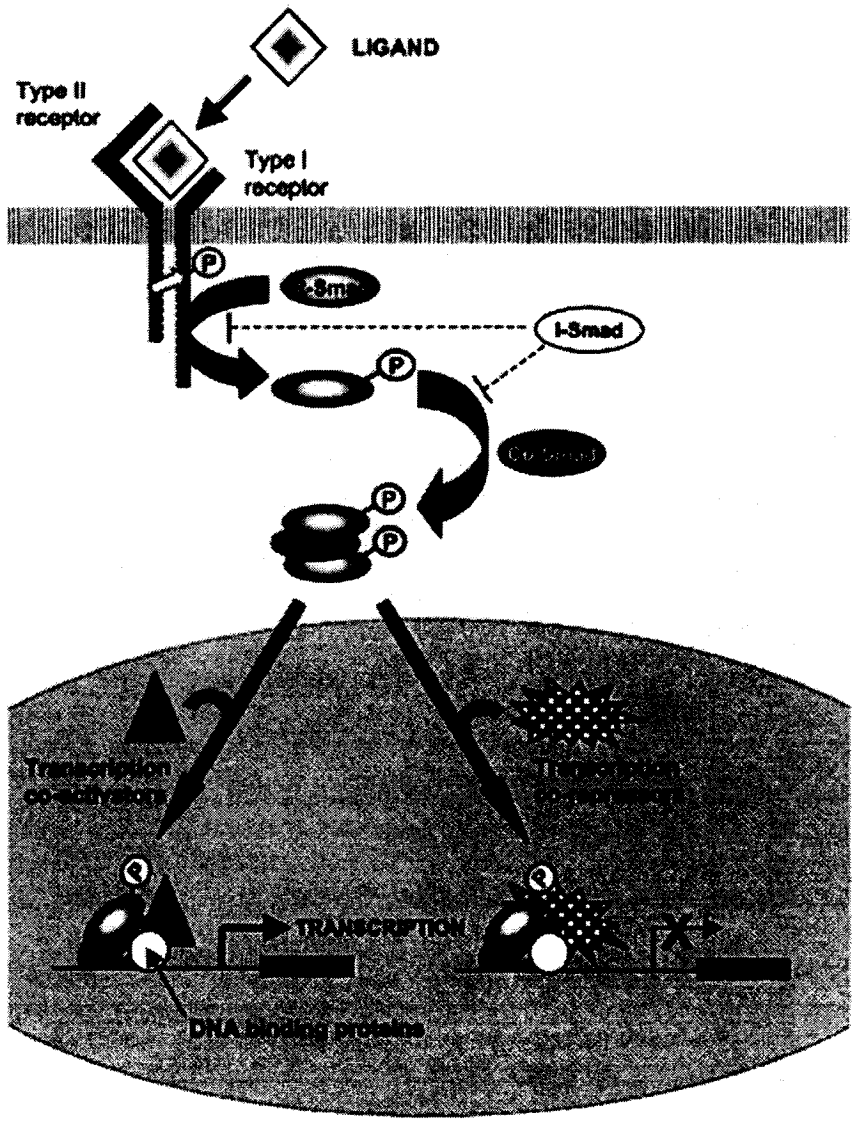

Figure A.1: Transcriptional effect of TGF-β signals through Smad pathways. TGF-β binds its cell surface receptor (TβRI/II) serine-threonine kinase, resulting in activation of a receptor-activated Smad (R-Smad). The R-Smad subsequently forms a complex with common-mediator Smad (Co-Smad) and then translocates into the nucleus, where they can regulate transcription by association with DNA binding proteins and recruitment of transcriptional co-activators or co-repressors to the promoters of targets genes. Adapted from [1]

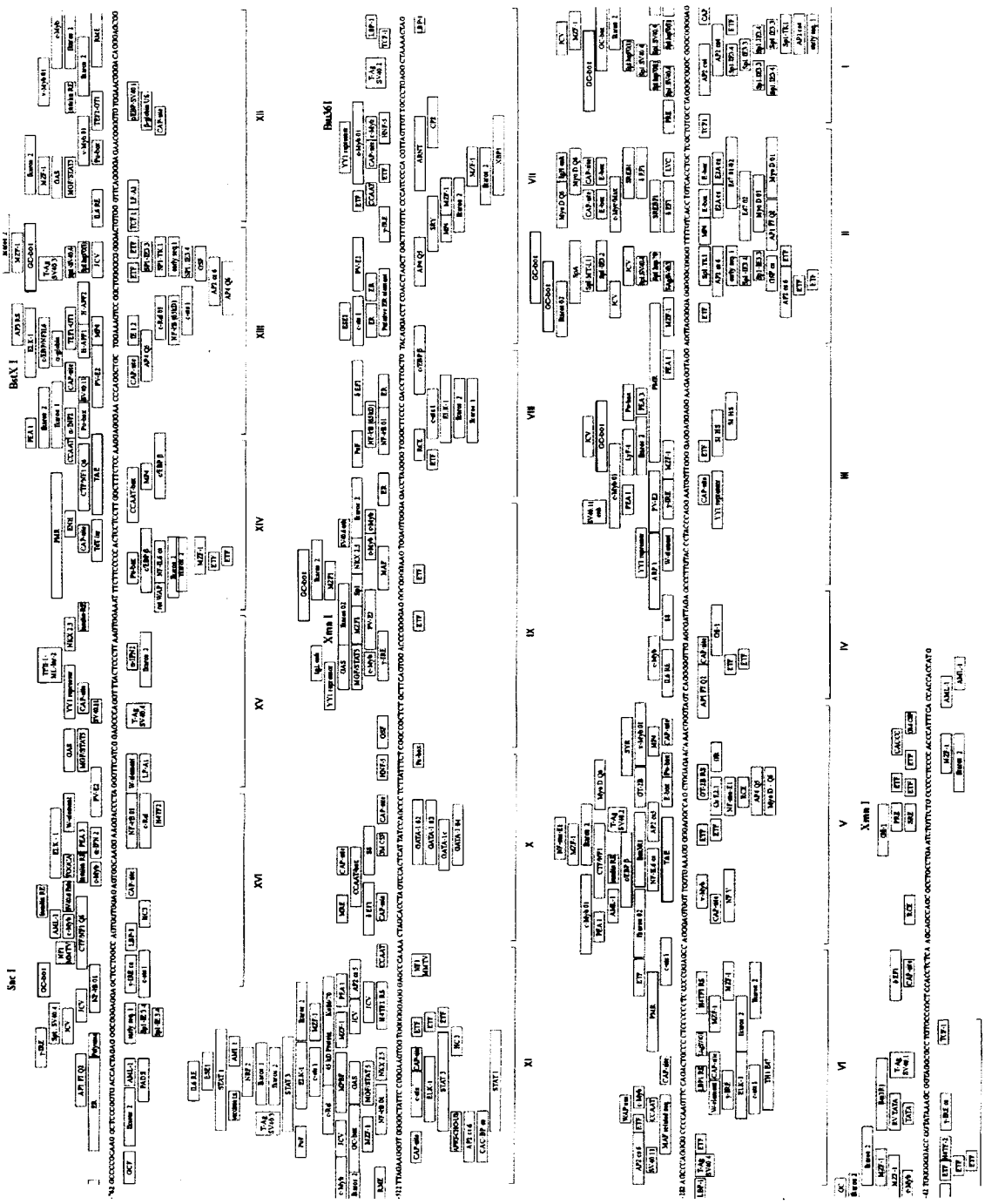

Figure A.2: The map of potential transcriptional *cis*-elements present in the MUC1 promoter region. Nine potential TGF-β regulatory sites are high-lighted by colored boxes. Adapted from [6]

p300/CBP and MSG1 [1]. In contrast to this activation effect, Smads can also repress gene transcription. The MH2 domain has been demonstrated to associate with co-repressors which then recruit histone deacetylase (HDAC) to induce transcriptional repression [1]. In addition to the effects on gene transcription, TGF-β can also initiate oncogenic signal cascades involving MAPK [1].

MUC1, as previously described, is overexpressed in breast cancer and associated with an aggressive phenotype and metastasis. Notably, it was found that the MUC1 promoter region contains nine potential TGF-β regulatory sites (Fig. A.2). Thus, we hypothesized that TGF-β may be involved in the regulation of MUC1 expression. In this study, we investigated the regulatory effect of TGF-β on MUC1 expression in MCF-7 cells, which has been shown to retain a high sensitivity to TGF-β [7] and express abundant MUC1 (see section 2.2.1, Fig 2.4).

A.2. Materials and Methods

A.2.1. Reagents

The B27.29 mAb against MUC1-ECD was kindly provided by Biomira, Inc (Edmonton, AB, Canada). The CT2 mAb against MUC1-CD was kindly provided by Dr. Sandra Gendler, Mayo Clinic, Scottsdale, AZ, USA. Anti-tubulin B-5-1-2 antibody, protease inhibitor cocktail, phosphatase inhibitor cocktail II, deoxycholic acid, Tris-Base, Nonidet P-40, diamidinophenylindole (DAPI) and Tween-20 were purchased from Sigma-Aldrich (Oakville, ON, Canada). The goat anti-mouse or anti-Armenian hamster alkaline phosphatase (AP) conjugated secondary antibodies, and the goat anti-mouse Cy3 conjugated secondary antibody were purchased from Jackson ImmunoResearch

Laboratories, Inc (West Grove, PA, USA). The goat anti-mouse phycoerythrin secondary antibody was purchased from Southern Biotechnology Associates, Inc (Birmingham, AL, USA). NBT/BCIP stock solution was purchased from Roche Diagnostics (Indianapolis, IN, USA). TGF-β was purchased from R&D Systems, Inc (Minneapolis, MN, USA). SDS was purchased from Pierce Biotechnology (Rockford, IL, USA). NaCl, ammonium persulfate, 40% (w/v) acrylamide stock solution, BSA and methanol were purchased from Fisher Scientific International (Nepean, ON, Canada). Bromophenol blue was purchased from Bio-Rad Laboratories Ltd (Hercules, CA, USA). DMEM, FBS, EDTA, and trypsin were purchased from Invitrogen, Inc (Carlsbad, CA, USA).

A.2.2. Cell Culture and TGF-β Treatment

Breast cancer cell line MCF-7 was from ATCC and maintained in DMEM supplemented with 10% FBS and 60μg/ml insulin. The cells were cultured at 37°C in a humidified incubator containing 5% CO_2. To investigate the effect of TGF-β on MUC1 expression, MCF-7 cells were seeded on 10cm cell culture dishes (Corning Inc.) until ~90% confluency, and then treated with TGF-β at 200pM for 4 hours, 9 hours, 16 hours, 24 hours, and 48 hours respectively. The MCF-7 cells without TGF-β treatment were used as controls.

A.2.3. SDS-PAGE and Western Blot Analysis

Cells were lysed in RIPA buffer, and then analyzed with a Bio-Rad DC assay and Bio-Rad Mini-PROTEIN II gel (15% resolving with 4% stacking) electrophoresis. The separated proteins were then transferred to an Immobilon-P membrane using Bio-Rad Mini Trans-Blot system (see detailed procedures in section 2.1.3). After immunoblotting,

the membrane was incubated with 10ml of NBT/BCIP solution until the desired level of staining was attained. The Membrane was then rinsed with copious amounts of water, scanned, and processed with NIH Scion-Image software for quantification.

A.2.4. Flow Cytometry

The MCF-7 cells with or without TGF-β treatment were trypsinized from culture dishes, washed 1X in Flow Cytometry Buffer (FCB, see details in section 3.1.6), and then divided into 3 aliquots, each of which was incubated with FCB only (unlabeled control), 5μg/mL MOPC 31C in FCB (isotype control), or 5μg/ml B27.29 in FCB, on ice for 1 hour in a volume of 300μl. The cells were then washed 3X in ice cold FCB, resuspended in 300μl FCB (unlabeled control) or 300μl of phycoerythrin secondary (2μg/ml in FCB) for 1 hour on ice, in dark. Then, the cells were again washed 3X in FCB, and resuspended in 300μl FCB supplemented with 120U/ml DNase I and 4.2mM $MgCl_2$. Samples were stored at 4°C in the dark until analysed by flow cytometry. At least 10,000 events were recorded on the FL2 (phycoerythrin) channel.

A.2.5. Immunofluorescence Staining

The MCF-7 cells were seeded onto coverslips placed in a 24-well plate (Corning Inc.) until ~90% confluency, and then treated with TGF-β at 200pM for 4, 9, 16, 24, and 48 hours respectively. The MCF-7 cells without TGF-β treatment were used as controls. Following TGF-β treatment, culture media was aspirated; the cells were rinsed once with ice cold PBS, and then were incubated with 3.7% formaldehyde in PBS for 15 minutes. Then, the cells were blocked with 500μl/well of 2% BSA, 0.02% Tween-20 in PBS (BTP buffer) for 1 hour, followed by incubation with 200μl/well of B27.29 (5μg/ml) in BTP

buffer for 1 hour. The cells were then washed 3X in BTP buffer, and incubated with 200μl/well of goat anti-mouse Cy3 conjugated secondary antibody (5μg/ml) in BTP for a further 1 hour, followed by counterstaining with DAPI (0.5μg/ml). Lastly, the cells were rinsed once with BTP buffer, inverted before mounting on slides and then stored in the dark at 4°C until imaged by fluorescence microscopy.

A.3. Results and Discussion

To investigate the regulating effects of TGF-β on the expression of MUC1 in MCF-7 cells, we first treated the MCF-7 cells with TGF-β at 200pM for various time courses (0, 4, 9, 16, 24, and 48 hours), and then examined the expression levels of MUC1 by SDS-PAGE/Western blots. As shown in Fig A.3, MUC1 expression (both the MUC1-ECD and CD) was decreased within 4 hours of TGF-β treatment. After 48 hours, the MCF-7 exhibited ~30-50% reduction in MUC1 expression as compared with the cells without TGF-β treatment (Fig. A.3), suggesting TGF-β has an inhibitory effect on MUC1 expression in breast cancer MCF-7 cells. To confirm these results, MCF-7 cells with or without TGF-β treatment (200pM, 48 hours) were subjected B27.29, phycoerythrin secondary antibody labelling, and flow cytometry analysis. We found results similar to that shown with Western blotting, i.e. cell surface MUC1 was significantly decreased after 48 hours of TGF-β treatment, as compared with cells without TGF-β treatment, using unlabeled and isotypic control antibody-treated cells as controls (Fig. A.4). This inhibitory effect was also corroborated in the anti-MUC1 mAb B27.29-mediated immunofluorescence staining assay (Fig. A.5). Based on these findings, we conclude that TGF-β represses MUC1 expression in breast cancer MCF-7 cells, although the underlying mechanism(s) is still obscure.

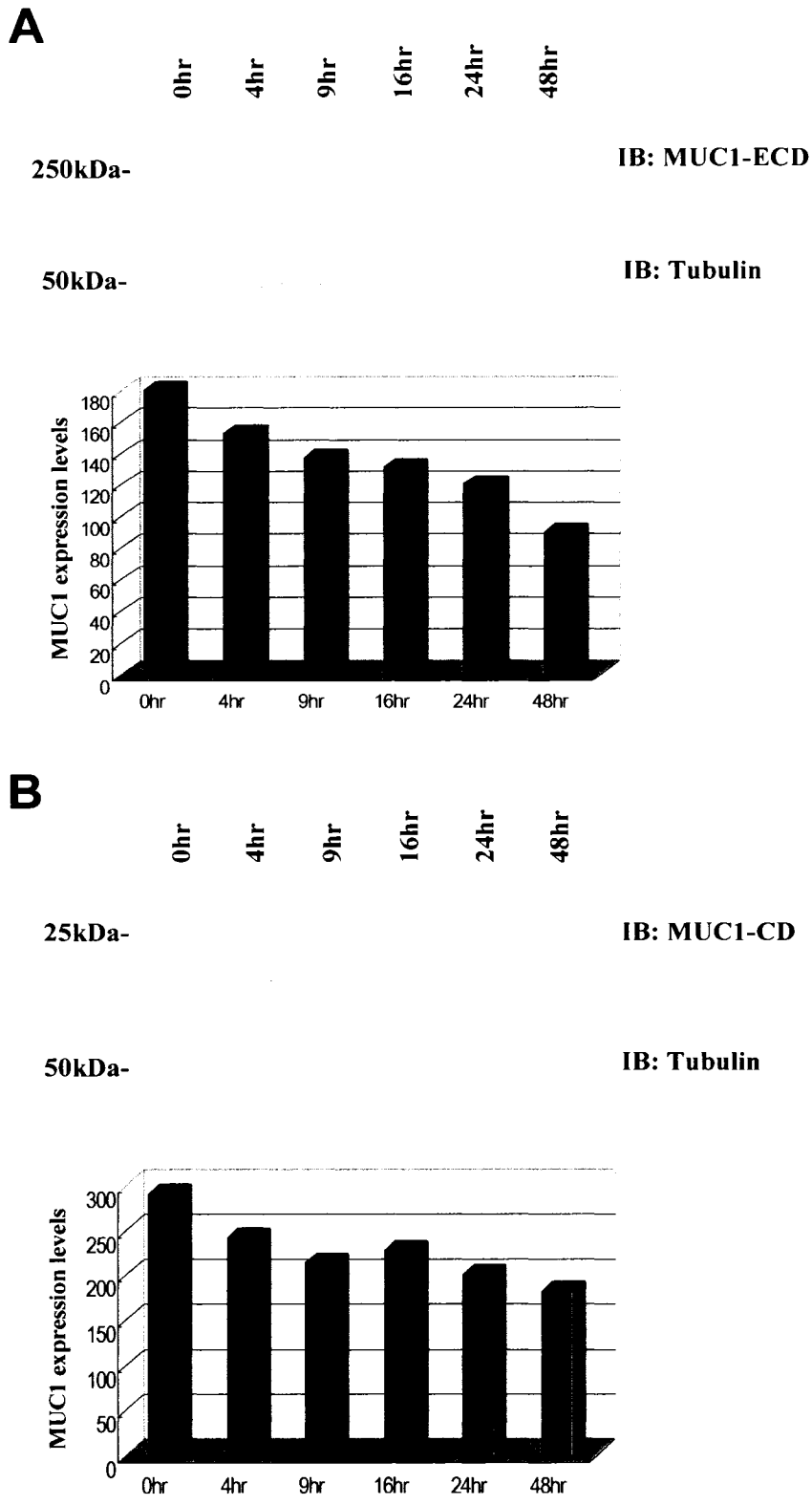

Figure A.3: TGF-β decreases the expression levels of MUC1 on MCF-7 cells.

Figure A.3 Continued: MCF-7 cells were treated with TGF-β at 200pM for various time courses as indicated, and then examined for the expression levels of MUC1, using tubulin as a loading control. (A) MUC1 extracellular domain (MUC1-ECD) was probed with B27.29 mAb (top lane). Using tubulin as a loading control (middle lane) to normalize the expression levels of MUC1 following TGF-β treatment, the column graph shows that the relative pixel density of MUC1 was decreased ~50% after 48 hours. (B) MUC1 cytoplasmic domain (MUC1-CD) was probed with CT2 mAb (top lane). Using tubulin as a loading control (middle lane) to normalize the expression levels of MUC1 following TGF-β treatment, the column graph shows that the relative pixel density of MUC1 was decreased ~30% after 48 hours.

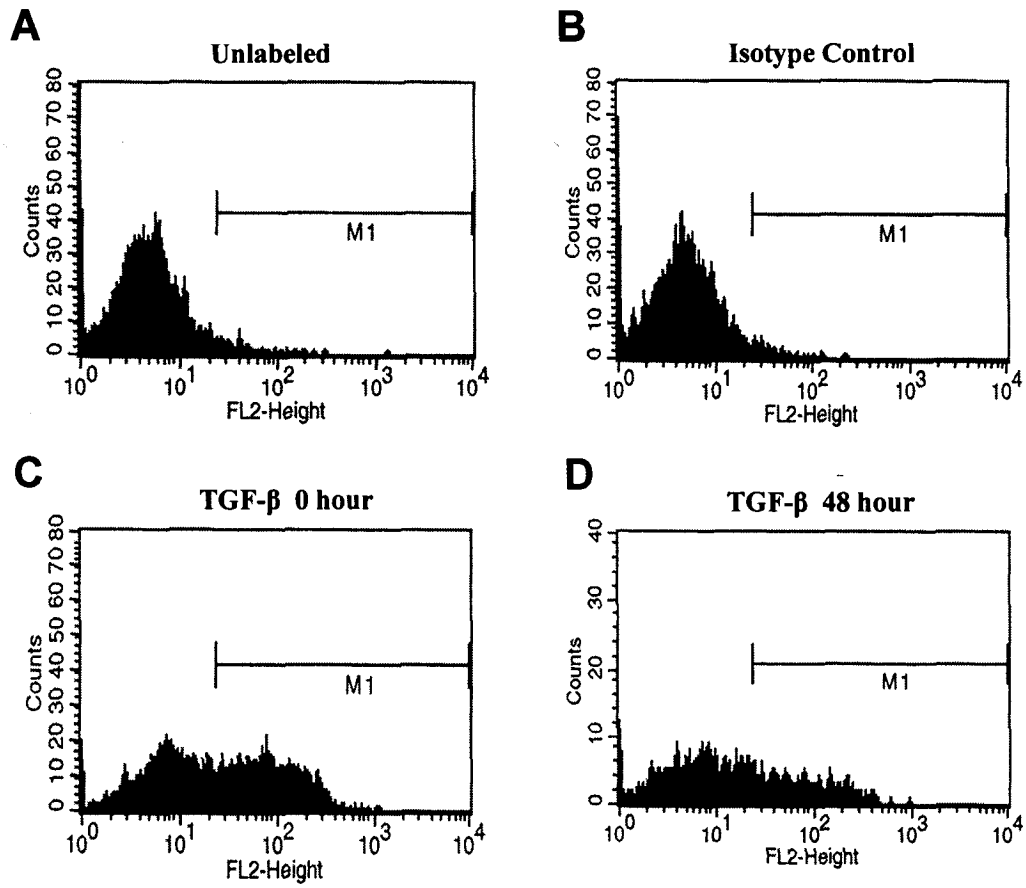

Figure A.4: Flow cytometry measurements of MUC1 expression on MCF-7 cells following TGF-β treatment. MCF-7 cells with or without TGF-β treatment (200pM, 48 hours) were incubated with FCB (unlabeled), isotype control antibody or B27.29, and then subjected to phycoerythrin secondary antibody. Flow cytometry showed that as compared with the (A) unlabeled, (B) isotype, (C) non-TGF-β treated controls, cell surface MUC1 was significantly decreased after 48 hours of TGF-β treatment.

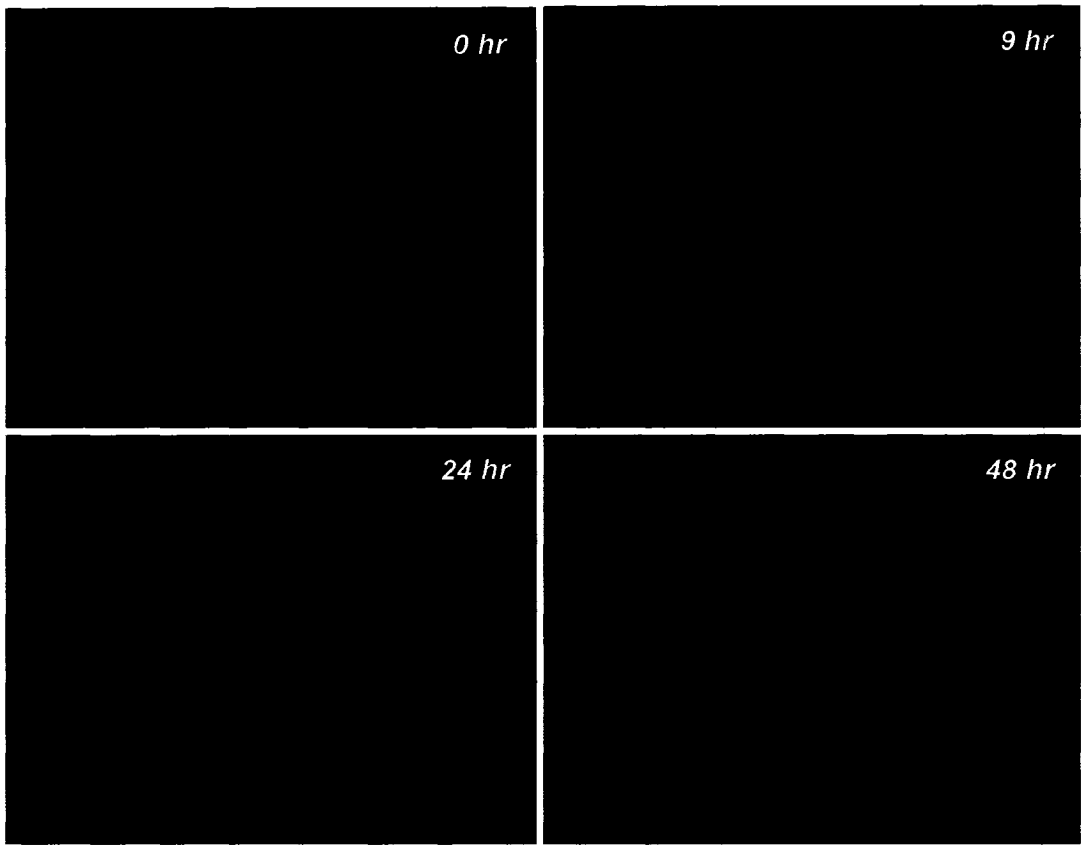

Figure A.5: Immunofluorescence staining measurements of MUC1 expression on MCF-7 cells following TGF-β treatment. MCF-7 cells were treated with TGF-β (200pM) for time intervals as indicated, and then subjected to a MUC1 immunofluorescence stain using Cy3 and a nulear counter stain using DAPI. Fluorescent microscopy confirmed that MUC1 expression level was decreased followed TGF-β treatment.

Previous evidence showed that aberrantly overexpressed MUC1 is correlated with breast cancer metastasis and poor prognosis [8]. Thus, the results of this study are perhaps inconsistent with the theory that expression of TGF-β is associated with breast cancer malignant progression [1]. It has been suggested that the expression of TβRs has a "dosage effect" on the paradoxical role of TGF-β in tumorigenesis. It was demonstrated that when signaling from TβRII is decreased, as widely seen in multiple cancers [7,9,10], the growth inhibitory responses of cancer cells to TGF-β are selectively lost [11], while its oncogenic effects (e.g. EMT) were not only retained but also enhanced [12,13]. This is significant, as studies by Arteaga *et al.* showed that ER-positive breast cancer cells (e.g. T47D) were generally resistant to the inhibitory effects of TGF-β [14], with the exception for MCF-7 [15]. This is believed to be due to inadequate TβRII expression, and stable transfection of the TβRII restored the sensitivity of T47D cells to TGF-β [16]. Therefore, we suggest that in normal epithelial cells and in breast cancer cells with TβRII expression (e.g. MCF-7), TGF-β exhibits a dominant inhibitory effect on MUC1 expression. However, the repressing effect is released in ER-positive/TβRII-negative breast cancer cells, resulting in tipping the balance of TGF-β signal in favour of its oncogenic activities, such as MUC1 expression. This is supported by Zaretskey's studies [6], showing that TGF-β facilitates MUC1 expression on T47D cells. Conversely, MUC1 has been reported to stabilize and activate ER signaling [17], suggesting that MUC1 expression may be implicated in restraining the inhibitory effect of TGF-β, thereby constructing a positive feedback loop to promote malignant progression of breast cancer.

A.4. References

1. Wakefield LM, Piek E, Bottinger EP: **TGF-beta signaling in mammary gland development and tumorigenesis.** *J Mammary Gland Biol Neoplasia* 2001, **6**:67-82.
2. Kusanagi K, Kawabata M, Mishima HK, Miyazono K: **Alpha-helix 2 in the amino-terminal mad homology 1 domain is responsible for specific DNA binding of Smad3.** *J Biol Chem* 2001, **276**:28155-28163.
3. Labbe E, Silvestri C, Hoodless PA, Wrana JL, Attisano L: **Smad2 and Smad3 positively and negatively regulate TGF beta-dependent transcription through the forkhead DNA-binding protein FAST2.** *Mol Cell* 1998, **2**:109-120.
4. Chen CR, Kang Y, Massague J: **Defective repression of c-myc in breast cancer cells: A loss at the core of the transforming growth factor beta growth arrest program.** *Proc Natl Acad Sci U S A* 2001, **98**:992-999.
5. Feng XH, Zhang Y, Wu RY, Derynck R: **The tumor suppressor Smad4/DPC4 and transcriptional adaptor CBP/p300 are coactivators for smad3 in TGF-beta-induced transcriptional activation.** *Genes Dev* 1998, **12**:2153-2163.
6. Zaretsky JZ, Sarid R, Aylon Y, Mittelman LA, Wreschner DH, Keydar I: **Analysis of the promoter of the MUC1 gene overexpressed in breast cancer.** *FEBS Lett* 1999, **461**:189-195.
7. Brattain MG, Ko Y, Banerji SS, Wu G, Willson JK: **Defects of TGF-beta receptor signaling in mammary cell tumorigenesis.** *J Mammary Gland Biol Neoplasia* 1996, **1**:365-372.
8. Rahn JJ, Dabbagh L, Pasdar M, Hugh JC: **The importance of MUC1 cellular localization in patients with breast carcinoma: an immunohistologic study of 71 patients and review of the literature.** *Cancer* 2001, **91**:1973-1982.
9. Franchi A, Gallo O, Sardi I, Santucci M: **Downregulation of transforming growth factor beta type II receptor in laryngeal carcinogenesis.** *J Clin Pathol* 2001, **54**:201-204.
10. Markowitz S, Wang J, Myeroff L, Parsons R, Sun L, Lutterbaugh J, Fan RS, Zborowska E, Kinzler KW, Vogelstein B, et al.: **Inactivation of the type II TGF-beta receptor in colon cancer cells with microsatellite instability.** *Science* 1995, **268**:1336-1338.
11. Lu SL, Kawabata M, Imamura T, Miyazono K, Yuasa Y: **Two divergent signaling pathways for TGF-beta separated by a mutation of its type II receptor gene.** *Biochem Biophys Res Commun* 1999, **259**:385-390.
12. Han G, Lu SL, Li AG, He W, Corless CL, Kulesz-Martin M, Wang XJ: **Distinct mechanisms of TGF-beta1-mediated epithelial-to-mesenchymal transition and metastasis during skin carcinogenesis.** *J Clin Invest* 2005, **115**:1714-1723.
13. Portella G, Cumming SA, Liddell J, Cui W, Ireland H, Akhurst RJ, Balmain A: **Transforming growth factor beta is essential for spindle cell conversion of mouse skin carcinoma in vivo: implications for tumor invasion.** *Cell Growth Differ* 1998, **9**:393-404.
14. Arteaga CL, Tandon AK, Von Hoff DD, Osborne CK: **Transforming growth factor beta: potential autocrine growth inhibitor of estrogen receptor-negative human breast cancer cells.** *Cancer Res* 1988, **48**:3898-3904.

15. Wu G, Fan RS, Li W, Srinivas V, Brattain MG: **Regulation of transforming growth factor-beta type II receptor expression in human breast cancer MCF-7 cells by vitamin D3 and its analogues.** *J Biol Chem* 1998, **273**:7749-7756.
16. Kalkhoven E, Roelen BA, de Winter JP, Mummery CL, van den Eijnden-van Raaij AJ, van der Saag PT, van der Burg B: **Resistance to transforming growth factor beta and activin due to reduced receptor expression in human breast tumor cell lines.** *Cell Growth Differ* 1995, **6**:1151-1161.
17. Wei X, Xu H, Kufe D: **MUC1 oncoprotein stabilizes and activates estrogen receptor alpha.** *Mol Cell* 2006, **21**:295-305.